The Dissertation Committee for Zheng Lu certifies that this is the approved version of the following dissertation.

Synthesis and Characterization of Group 13 & 15 Complexes Supported by N,N′-Bidentate Ligands

Committee:

_____

Alan H. Cowley, SUPERVISOR

_____

Richard A. Jones

_____

John T. McDevitt

_____

Ben A. Shoulders

_____

John G. Ekerdt

Synthesis and Characterization of Group 13 & 15 Complexes Supported by N,N´-Bidentate Ligands

by

Zheng Lu, B.S.; M.Sc.

Dissertation

Presented to the Faculty of the Graduate School of
The University of Texas at Austin
in Partial Fulfillment
of the Requirements
for the Degree of
Doctor of Philosophy

The University of Texas at Austin
December 2007

Dedicate to my beloved family

Acknowledgements

First of all I would like to thank my supervisor, Professor Alan H. Cowley, for his intellectual guidance and support. It has been a great honor to work with him during my PhD study.

I wish to express my appreciation to the past and present Cowley group members for their help and friendship: Dr. Robert Wiacek, Dr. Jeff Pietryga, Dr. Piyush Shukla, Lucy Mullins, Dr. Dragoslav Vidovic, Kalyan Vasudevan, Clint Hoberg and Adam Powell.

Special thanks go to Dr. Jamie Jones, Dr. Jennifer Moore, Dr. Nicholas Hill, Dr. Gregor Reeske and Michael Findlater for their tireless work on the X-ray crystallography.

I thank Julie Campos for her great help during my graduate study. I also thank the gentlemen of the NMR facility and Mass Spectroscopy for their helpful discussion.

My deepest gratitude goes to my parents, my wife, Changli Yuan, and my son, Boting Lu. Their endless love and care are the greatest for me.

Synthesis and Characterization of Group 13 & 15 Complexes Supported by N,N´-Bidentate Ligands

Publication No._____

Zheng Lu, Ph.D.

The University of Texas at Austin

Supervisor: Alan H. Cowley

The first example of an N,N'-chelated β-diketiminato phosphenium salt has been isolated by careful tuning of both the ligand architecture and the electronic characteristics of the phosphorus containing moiety. Using a two-electron reduction approach, the first example of a phosphinidene valence isomer has been isolated and structurally characterized. The mechanism of formation of this valence isomer was elucidated via Density Functional Theory (DFT) calculations. These calculations revealed that the formation of this valence isomer involves the intermediacy of a triplet diradical. In turn, the triplet diradical decays by two further steps to generate the observed product. A cationic phosphinous acid has been prepared via the hydrolysis of a cationic

phosphenium complex in basic solution. DFT calculations reveals that the introduction of a positive charge stabilizes the phosphinous acid form. Two N,C-bonded phosphenium cation salts have also been obtained, the crystal structures of which reveal that the formation of these compounds involves C-H activation of a methyl group on the β–diketiminate ligand.

Three synthetic methods, namely halide abstraction, aluminum/boron halide exchange process and salt metathesis, have been explored for the preparation of boron cations supported by β-diketiminate ligands. The first structurally characterized boron cation supported by a β-diketiminate ligand has been isolated as its $[Al_2Cl_7]^-$ salt. A Ga-Fe organometallic complex supported by a β-diketiminate ligand has also been synthesized via salt metathesis reaction and fully characterized.

Finally, several bisamidinate supported boron complexes have been synthesized and structurally characterized. Such complexes may have applications as bifunctional catalysts or as building blocks for novel polymers.

Table of Contents

List of Tables

List of Figures

Index of Compounds

Chapter 1

21. [{MeC(MeC)$_2$N(Dipp)}$_2$H]

22. [MeC(H)(CMe)2(NDipp)]

23. [MeC(CMe)$_2$(NDipp)$_2$]Li

24. [MeC(CMe)$_2$(NDipp)$_2$]K·Et$_2$O

25. "[MeC(CMe)$_2$(NDipp)$_2$]PPhCl"

26. "[MeC(CMe)$_2$(NDipp)$_2$]PPh$_2$"

27. "[MeC(CMe)$_2$(NDipp)$_2$]PCl$_2$"

28. [{MeC(CMe)$_2$(NDipp)$_2$}PCl][OTf]

29. [{MeC(CMe)$_2$(NDipp)$_2$}PCl][B(C$_6$F$_5$)$_4$]

30. [{MeC(CMe)$_2$(NDipp)$_2$}PBr][OTf]

33. [MeCC(Me)C(CH$_2$)N(Dipp)PN(Dipp)H]

37. [{MeC(MeCN(Dipp))$_2$}P(OH)][OTf]

40. [MeC(H)(MeCN(Dipp)(H))$_2$] OTf$_2$

41. [{MeC(MeCN(Dipp))$_2$}P(OH)]Br

44. [CH$_2$N(Ar)(CMe)$_2$N(Ar)PPh][AlCl$_4$]

46. [CH$_2$N(Ar)C(H)C(Me) N(Ar)PCl] OTf

Chapter 2

25. $[HC(CMe)_2(NDipp)_2]\ BF_2$

26. $[MeC(CMe)_2(NDipp)_2]AlMe_2$

27. $[MeC(CMe)_2(NDipp)_2]AlCl_2$

28. $[\{HC(CMe)_2(NDipp)_2\}B(Ph)Cl]$

30. $[\{HC(CMe)_2(NDipp)_2\}BPh][Al_2Cl_7]$

31. [(NDipp)C(Me)C(H)C(Me)(NDipp)B(Cp*)Cl]

32. $[\{HC(CMe)_2(NDipp)_2\}BCp^*][AlCl_4]$

33. $[\{MeC(CMe)_2(NDipp)_2\}BPh][AlCl_4]$

34. $[\{HC(CMe)_2(NDipp)_2\}BF][B(C_6F_5)_4]$

36. $1,4\text{-}C_6H_4[BBr\{(NDipp)_2(CMe)_2CMe\}]_2$)

37. $1,4\text{-}C_6H_4[B(OH)\{(NDipp)_2(CMe)_2CMe\}]_2$

39. $[\{HC(CMe)_2(NDipp)_2\}Ga(Cl)Fe(C_5H_5)(CO)_2]$

42. $[\{HC(CMe)_2(NDipp)_2\}H_2][AlBr_4]$

50. $1,3\text{-}C_6H_4[C\{N(SiMe_3)\}_2BCl_2]_2$

51. $1,4\text{-}C_6H_4[C\{N(SiMe_3)\}_2BCl_2]_2$

52. $1,4\text{-}C_6H_4[C\{N(SiMe_3)\}_2B(Ph)Cl]_2$.

53. $1,4\text{-}C_6H_4[BrB\{N(SiMe_3)\}_2CPh]_2$.

54. $1,4\text{-}C_6H_4[C\{NCy\}_2BCl_2]_2$

55. $1,4\text{-}C_6H_4[C\{NCy\}_2B(Ph)Cl]_2$

CHAPTER 1

β-Diketiminate-Supported Phosphorus Complexes

Introduction

Phosphine ligands are used extensively in transition metal chemistry for the support of a wide range of highly active and versatile catalysts. The widespread use of phosphines is due to the ease with which the steric and electronic properties of this ligand class can be tuned. Examples of important catalytic processes that involve the support of phosphine ligands include hydrogenaton[1], olefin metathesis[2], cross-coupling[3], and asymmetric transformations[4].

Phosphenium cations (R_2P^+) represent a more recent addition to the family of phosphorus ligands. Interest in such cations has been prompted by the fact that they can serve as both σ-donors and π-acceptors depending on the substituents, R.[5] Special interest is associated with the N-heterocyclic phosphenium cations (**3** in Figure 1.1) due to their isovalent relationship to N-heterocyclic carbenes (**1**) and silylenes (**2**). However, in contrast to N-heterocyclic carbenes, which function primarily as σ-donors,[6] N-heterocyclic phosphenium cations are beginning to find use as strong π-acceptor ligands, particularly for transition metal catalysts based on platinum[7] and rhodium[8]. As a further example, Sakakibaka *et al.*[7a] reported a dramatic improvement in yield for the carboxylation of arenes by the addition of a phosphenium salt to a Pd(II)-based catalyst.

An additional advantage of precious metal phosphenium cation complexes is that they have the potential to serve as bifunctional catalysts in the sense that they can employ the Lewis acid functionality at phosphorus within the coordination sphere of the metal.[9]

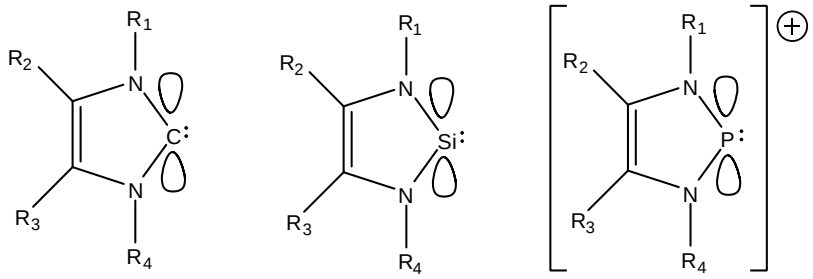

1 **2** **3**

Figure 1.1. General structures of N-heterocyclic carbenes (**1**), silylenes (**2**) and phosphenium cations (**3**).

Interestingly, a structurally authenticated phosphenium cation (**4** in Figure 1.2) was reported[10] prior to the isolation of the first stable N-heterocyclic carbene.[11] This particu-

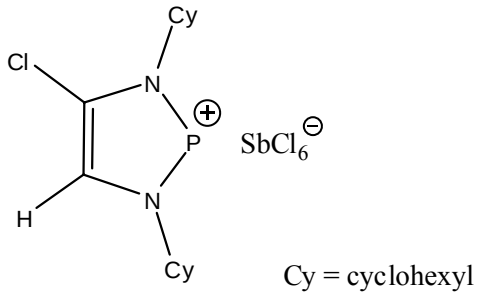

4

Cy = cyclohexyl

Figure 1.2. Structure of the first structurally characterized phosphenium cation.

lar cation was isolated as the hexachloroantimonate salt by treatment of the precursor phosphorus(III) chloride with $SbCl_5$ which, in turn, had been synthesized in 73% yield *via* the reaction of CyN=CHCH=NCy with PCl_3 in the presence of Et_3N.[12] Halide ion abstraction has also been effected by several other Lewis acids such as $AlCl_3$[5] and $GaCl_3$[13]. Typically, these halide ion abstraction reactions result in >90% yields of the desired salts. However, recent work from the Cowley group[14] has shown that N-heterocyclic phosphenium salts can be prepared *via* a one-step redox route involving the redox reaction of α-diimines with PI_3. Analogous 1,2-bis(arylimino)acenaphthene (aryl-

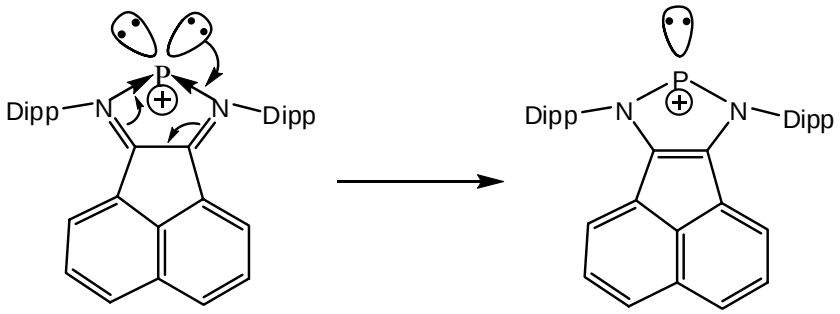

Dipp = 2,6-diisopropylphenyl

5 **6**

Scheme 1.1. Mechanism for the formation of a BIAN phosphenium cation.

BIAN) phosphenium cation salts can also be obtained *via* this self-redox route by treatment of the appropriate BIAN ligand with PI_3 or $SnCl_2/PCl_3$ (Scheme 1.1). [15] For both the α-diimine and the BIAN reactions, the resulting phosphenium cations (**6**) are formed *via* the intramolecular charge transfer of two electrons from a phosphorus(I)

moiety (**5**) into the low-lying LUMO of the α-diimine or BIAN ligand as illustrated in Scheme 1.1.

To date, most of the examples of structurally authenticated phosphenium cations involve the incorporation of the cationic center in a five-membered ring.[5] However, acyclic phosphenium cations such as **7** are also known[16] and typically isolated as their $[AlCl_4]^-$ salts. More recently, six-membered phosphenium cation systems such as **8**, which involve the electron-rich 1,8-bis(alkylamido)naphthalene framework, have begun to emerge.[8a]

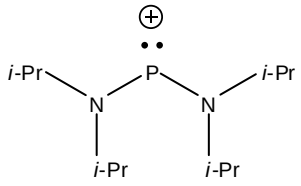

7

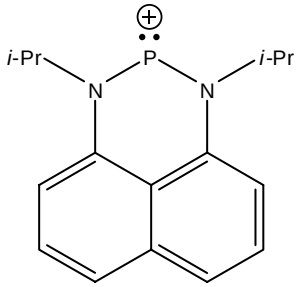

8

Figure 1.3. Acyclic and six-membered ring phosphenium cations.

Although β-diketiminates (Figure 1.4) were first employed as ligands in the mid- to late-1960s, it is only since the mid-1990s that their use has become extensive due in part to the ease of tuning the electronic and steric properties by the choice of the nitrogen substituents, R and R'. In fact, N,N'-chelated β-diketiminate complexes are now known for a large number of the elements in the Periodic Table.[17] Several β-diketiminate

complexes have found useful applications, particularly in the field of catalysis. For example, in 1994, Lappert *et al.*[18] found that a β-diketiminate-supported zirconium com-

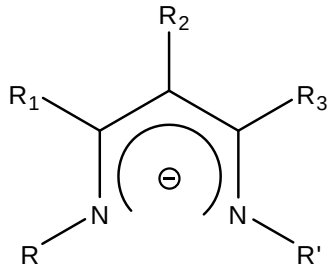

Figure 1.4. General structure of a β-diketiminate ligand.

plex is an effective catalyst for ethylene and propylene polymerization, and in 2004 Tolman *et al.*[19] reported the preparation of a β-diketiminate copper(I) complex (**9**) that can activate O_2 at a single copper site in a 1:1 Cu-O_2 adduct (**10**). Since then, β-diketiminate complexes have been reported for an increasingly large number of transition

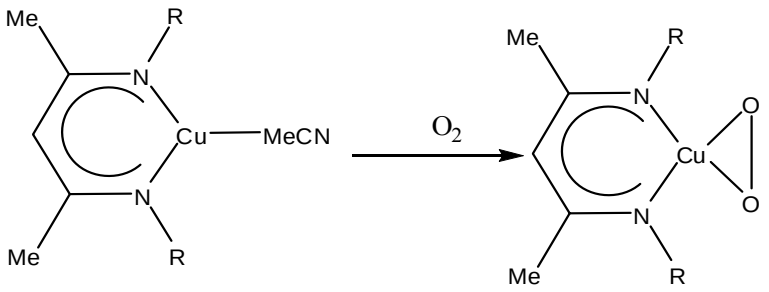

9 **10**

R = 2,6-diisopropylphenyl

Scheme 1.2. Single point activation of O_2 on a β-diketiminate Cu complex.

metal, lanthanide and main group elements. These developments were summarized in an important review by Lappert and co-workers in 2002. [17]

In terms of main group chemistry, β-diketiminate ligands have been used effectively for the stabilization of unusual oxidation states and novel bonding arrangements. Some important developments since the publication of the 2002 Lappert *et al.* review include the isolation of an interesting indium(I) monomer (**11**), dimer (**12**) and hexamer by Hill *et al.*[20]. In 2005, the Cowley group[21] reported the synthesis and X-ray crystal structure of the first β-diketiminate-supported oxoborane (**13**). Given the highly reactive nature of the B=O moiety, it was necessary to stabilize the oxoborane by attachment of the Lewis

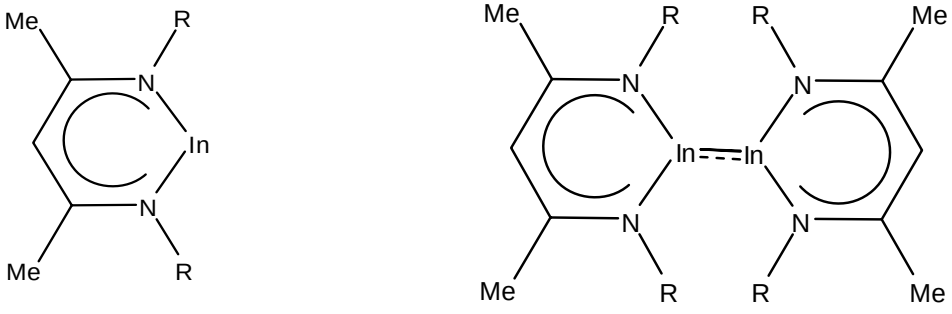

11

R = 2,6-diisopropylphenyl

12

R = 2,4,6-$Me_3C_6H_2$

Figure 1.5. The steric effect and the dimerization of on the In(I) β-diketiminate complexes.

acid $AlCl_3$. Nevertheless, the boron-oxygen distance indicated that considerable double bond character remained in **13**. This view was supported by DFT calculations.[21]

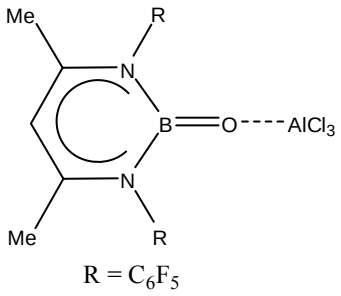

13

Figure 1.6. Structure of the first B=O complex.

Despite the considerable progress that has been made in β-diketiminate main group chemistry, there was a very obvious gap in this area of research in the sense that, prior to the present work, there were no examples of uncoordinated N,N'-chelated β-diketiminate complexes of the electron-rich elements from group 15, 16 and 17 of the Periodic Table. Accordingly, the synthesis of such compounds became a focal point of this part of the dissertation work. The challenge was both of intrinsic interest and, if successful, could provide new types of supporting ligands for use in *d*- and *f*-block chemistry.

Previous attempts to prepare β-diketiminates that incorporate phosphorus-containing moieties resulted in the γ-substituted derivatives **14**[22] and **15**[23]. Several other acyclic phosphorus-substituted β-diketiminate derivatives (**16**) have also been prepared by treatment of malodinitriles with phosphines in the presence of $[Cp_2ZrClH]$[24].

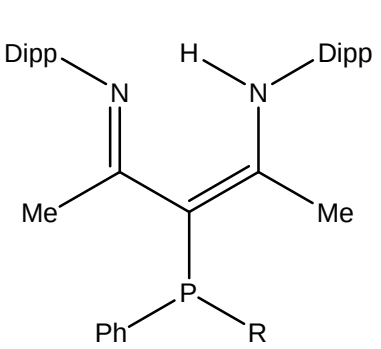

14: R = Cl
15: R = Ph

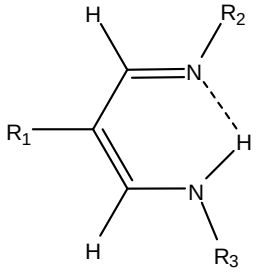

16

R_1 = H, R_2 = P(N-*i*-Pr_2)$_2$, R_3 = PEt_2 or Ph
R_1 = PPh_2, R_2 = R_3 = P(N-*i*-Pr_2)$_2$ or Ph
R_1 = PPh_2, R_2 = P(N-*i*-Pr_2)$_2$, R_3 = Me

Figure 1.7. Examples of non-chelated β-diketiminate phosphorus complexes.

Also by way of introduction, it is worth pointing out that the most widely used β-diketiminate ligand is **17** (Figure 1.8).[25] Indeed, the availability of this ligand has played

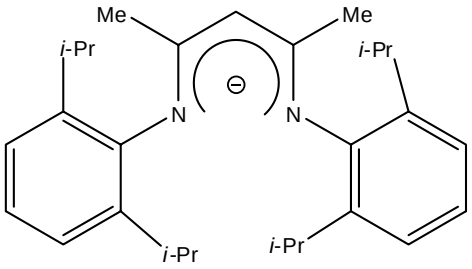

17

Figure 1.8. Structure of the Dipp-substituent β-diketiminate ligand **17**.

an important role in the successful development of β-diketiminate chemistry. The reason for this relates to the fact that the bulky 2,6-diisopropylphenyl (Dipp) substituents

provide a sterically protected pocket at the nitrogen atoms. In turn, this kinetically stabilizing environment permits the isolation of otherwise very reactive N,N'-chelated entities. Examples of unprecedented structures stabilized by the Dipp-substituted β-diketiminate ligand include the carbene analogous complexes **18** and **19** (Figure 1.9) in

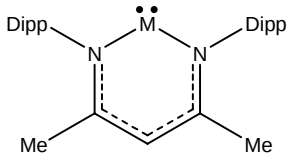

18: M = Al
19: M = Ga

Figure 1.9. Structures of carbene analogous aluminum (I) and gallium (I) derivatives.

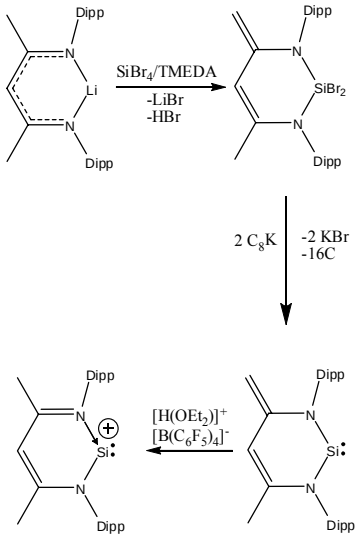

Scheme 1.3. Preparation of a silylene and a silyliumlidene supported by the Dipp-substituted β-diketiminate ligand.

which the group 13 element is present in the +1 oxidation state[26]. Ligand **17** has also been used to stabilize a rare example of a Zn-Zn bond[27]. Furthermore, and of particular relevance to the present work, the Dipp-substituted β-diketiminate ligand has been used for the support of both a silylene[28] and a silicon cation[29] as summarized in Scheme 1.3. Even though the Dipp-substituted β-diketiminate ligand **17** has proved very useful, it did not seem appropriate for the support of the targeted N,N'-chelated phosphorus derivative, because, as pointed out above, previous attempts to use this ligand resulted in attack of γ-CH bond and formation of the acyclic products **14** and **15**. The most obvious remedy was to block this γ position with a methyl group. In turn, this involved the synthesis of

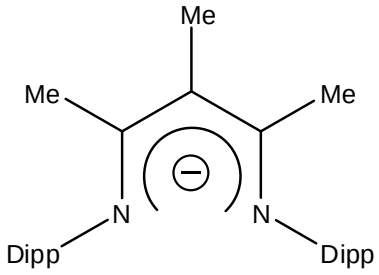

20

Figure 1.10. Structure of the proposed new β-diketiminate ligand **20**.

the new β-diketiminate ligand **20**. It will be shown that ligand **20** can be successfully employed for the synthesis of the first example of N,N'-chelated group 15 compounds. Furthermore, it will be shown that under certain circumstances, the β-methyl groups of **20** can be activated. As a consequence, it was possible to isolate the first example of an

N,C-bonded β-diketiminate phosphorus compound. Another novel development was the isolation and structural characterization of the first valence isomer of a phosphinidene.

Results and Discussions

As pointed out in the Introduction, prior to the present work there were no examples of N,N'-chelated β-diketiminate complexes of the group 15, 16 or 17 elements. Of these elements, phosphorus is the most convenient to work with because reactions are easy to follow by NMR due to the fact that the ^{31}P nucleus has a spin of one half and a natural abundance of 100%.

Several factors were considered in terms of developing a strategy for the preparation of the first phosphorus compounds of the desired type:

(i) As pointed out in the Introduction, it was necessary to block the γ-position of the β-diketiminate ring to avoid the occurrence of phosphorus substitution at this site that had been reported earlier by Burford *et al.*[22] and Lappert *et al.*[23]. Accordingly, the first task was to synthesize the new ligand **20**.

(ii) Since the region between the β-diketiminate nitrogen atoms is electron rich and sterically encumbered by the bulky Dipp substituents, it was logical to select a phosphorus-containing fragment that is both small and electronegative. A $[P\text{-halogen}]^+$ entity seemed ideal for this purpose and also offered the possibility of substitution reactions at phosphorus center.

*Preparation of the New β-Diketiminate Ligand $[MeC(CMe)_2(NDipp)_2]^-$ (**20**)*

The iminoamine $[MeC(CMe)_2(NDipp)_2]H$ (**21**) was prepared by treatment of 3-methyl-2,4-pentanedione with 2,6-diisopropylphenylaniline ($DippNH_2$) in toluene

solution in the presence of *p*-toluenesulfonic acid (Eq. 1) following the procedure of Power *et al.*[30]. Colorless, crystalline **21** was obtained in *ca.* 40 % yield and characterized

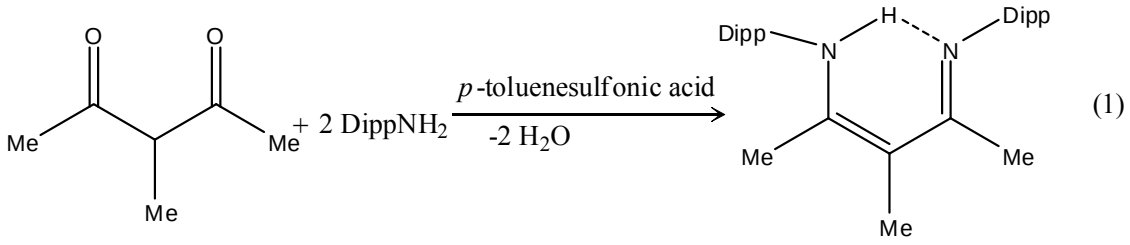

(1)

21

by HRMS and single-crystal X-ray diffraction (Figure 1.11). Although the X-ray crystal structure of **21** is not of sufficient quality to permit a detailed discussion of metrical parameters, it is clear that it exists in the iminoamine form in the solid state because of

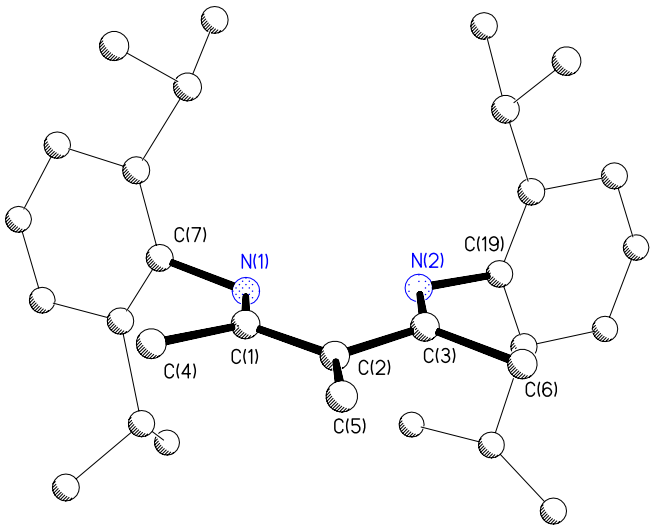

Figure 1.11. X-ray crystal structure of **21**.

the planar conformation of the N_2C_3 skeleton. Interestingly, however, examination of a benzene solution of this product by ^1H NMR spectroscopy revealed the existence of tautomerism (Eq. 2). The observed ^1H chemical shift of δ 13.69 ppm is diagnostic of the presence of an N-H group and therefore indicative of the persistence of the iminoamine form **21** in solution. The evidence for the presence of the diimine form **22** stems from de-

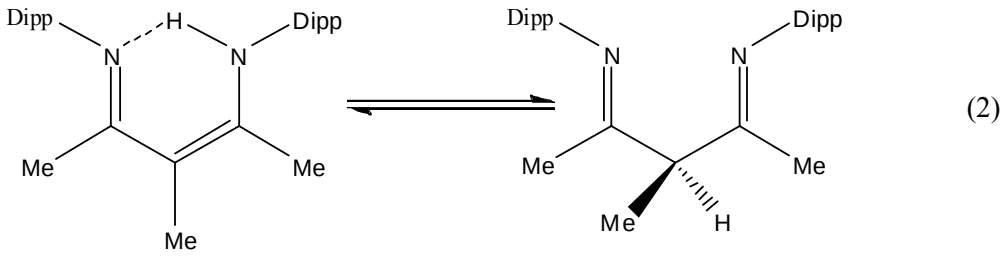

21 **22** (2)

tection of a doublet signal at δ 1.52 ppm (J = 6.9 Hz) which is attributable to the γ-methyl group and a quartet at δ 3.44 ppm (J = 6.9 Hz) due to the presence of a hydrogen in the γ-position. Integration of the ^1H spectra revealed that the tautomers are present in approximately equimolar quantities at 25°C. It is worth noting that the free diimine form of this ligand system is rarely observed[31].

*Preparation of Alkali Metal Salts of the New β-diketiminate Ligand $[MeC(CMe)_2(NDipp)_2]^-$ (**20**)*

The lithium and potassium salts of ligand **20** were prepared in anticipation that they would prove to be useful reagents for the syntheses of the desired phosphorus compounds.

Both salts were prepared by metallation of **21** as summarized in Eq. 3. The lithium derivative **23** was isolated as a white powder in virtually quantitative yield following the treatment of **21** with *n*-BuLi in hexane solution for 3 h at 25°C. This compound was characterized by LRMS (M^+, *m/z* = 439) and ^1H NMR spectroscopy. The proposed delocalized structure is consistent with the detection of the methyl groups resonances in a 2:1 intensity ratio.

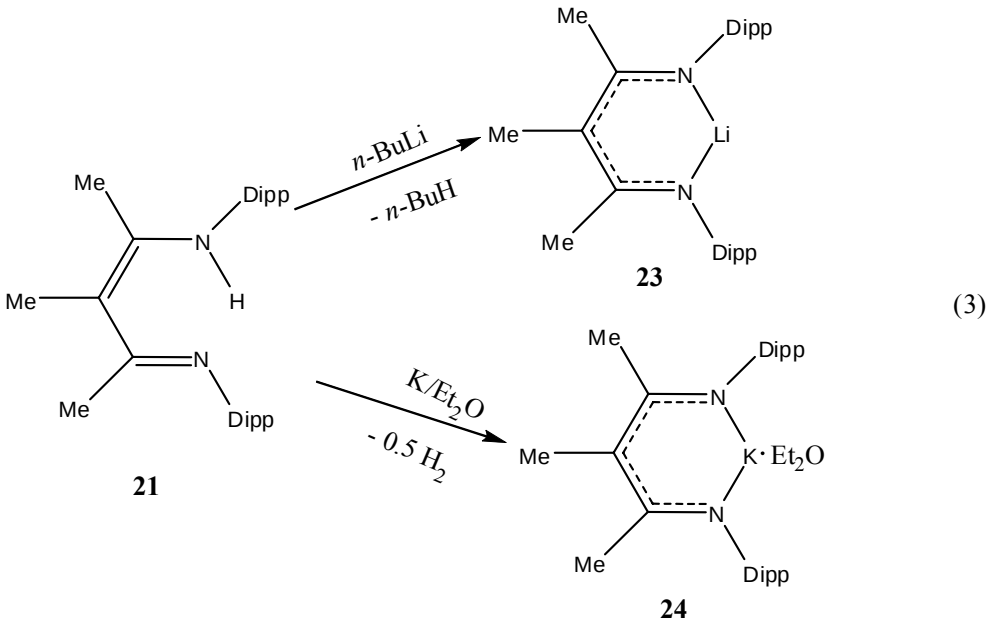

(3)

The corresponding potassium derivative **24** was isolated as a colorless mono-etherate in 72% yield following workup of the reaction mixture resulting from the treatment of **21** with potassium metal in Et_2O solution at ambient temperature. The ^1H and $^{13}C\{^1H\}$ NMR spectra of **24** showed the presence of equivalent Dipp groups and ring methyl groups in a 2:1 intensity ratio. The CI^+ mass spectrum evidenced the M^+ ion at *m/z* 471

which corresponds to the formula $[MeC(CMe)_2(NDipp)_2]K$. Crystals of **24** suitable for single-crystal X-ray diffraction were obtained by cooling a saturated toluene solution to -40°C for 2 d. Compound 24 crystallizes in the monoclinic space group $P2_1/c$ with Z = 4.

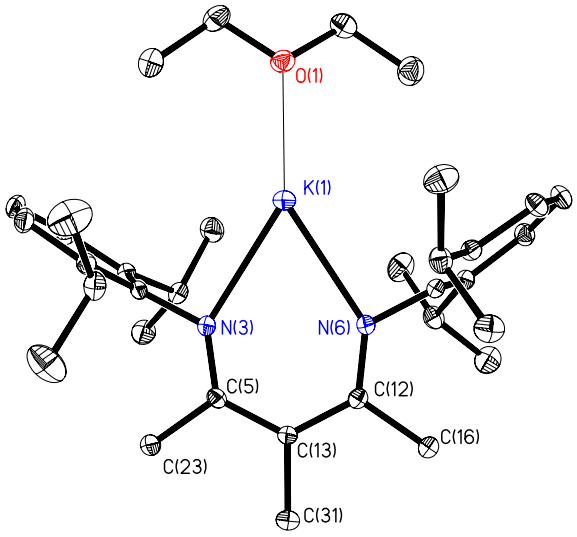

Figure 1.12. ORTEP view of **24**. The thermal ellipsoids are drawn at 30% probability. All hydrogen atoms have been omitted for clarity.

The X-ray crystal structure of **24** confirmed the presence of a coordinated Et_2O molecule and revealed that the cyclic potassium salt (Figure 1.12) consists of an N,N'-chelated six-membered β-diketiminate ring. The metrical parameters for the six-membered KN_2C_3 ring indicate that the geometry tends toward an alternating, somewhat localized distribution of electron density as reflected by the differences of ~ 0.2 Å between the C–C, C–N and N–K distances on either side of the ring. The geometry of the KN_2C_3 ring is

almost planar as shown by the fact that the sum of bond angles is 718.72(5)°. The average N–K bond distance of 2.651 (2) Å is slightly shorter than that of the corresponding potassium salt of $[HC(CMe)_2(NDipp)_2]K$ [2.690(2) Å].[32]

Attempted Syntheses of Neutral N,N′-Chelated Phosphorus (III) compounds

Several attempts were made to synthesize neutral N,N′-chelated phosphorus compounds by treatment of **23** with chlorophosphines following the same procedure that described for the syntheses of **14** [22] and **15** [23].

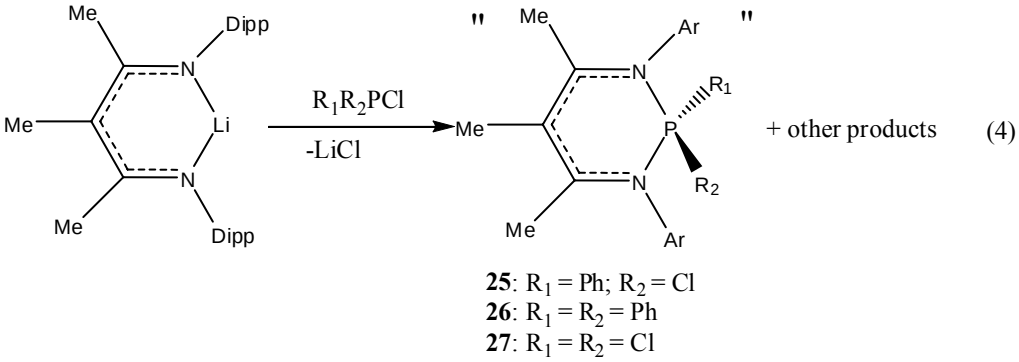

25: R_1 = Ph; R_2 = Cl
26: $R_1 = R_2$ = Ph
27: $R_1 = R_2$ = Cl

The $^{31}P\{^1H\}$ NMR chemical shifts of the products resulting from these reactions are listed in Table 1.1. In each case, multiple $^{31}P\{^1H\}$ NMR signals were detected, which

Table 1.1. $^{31}P\{^1H\}$ NMR chemical shifts of product mixture **25**, **26** and **27**

Reaction mixture	$^{31}P\{^1H\}$ NMR chemical shifts (ppm)
25	94.99, 93.39, 88.42
26	6.35, -14.76, -15.39
27	Multiple signals of ~ 167.57 and between 12.85 to 8.22
14	-11
15	94.12

implies the presence of several species in the reaction mixture. Despite several attempts, it was not possible to isolate a pure product from any of these reactions. However, the $^{31}P\{^{1}H\}$ NMR chemical shifts of one peak in reaction mixture **25** and one peak in reaction mixture **26** are similar to those reported for **14** and **15**, respectively, hence it is likely that γ-substituted β-diketiminate compounds were formed. In the particular case of reaction mixture **27**, the intensities of the various $^{31}P\{^{1}H\}$ resonances changed with time and no product identification was possible.

Given the above results, it was clear that the metathetical reaction of the β-diketiminato lithium reagent **22** was not a viable synthetic route to the desired N,N'-chelated phosphorus compounds.

Synthesis and Characterization of N,N'-Chelated β-Diketiminato Phosphenium Cation Salts

Since neutral N,N′-chelated phosphorus derivatives could not be isolated from the product mixtures, attention was turned to tuning the steric and electronic properties of the phosphorus moiety to be incorporated in the β-diketiminate ring. As noted above, the region between the β-diketiminate nitrogen atoms is electron rich and sterically encumbered. To accommodate to both factors, it was decided to use $[P\text{-}Cl]^{+}$ and $[P\text{-}Br]^{+}$ fragments, as the N,N'-chelated entities. Even though the reaction of the lithium reagent

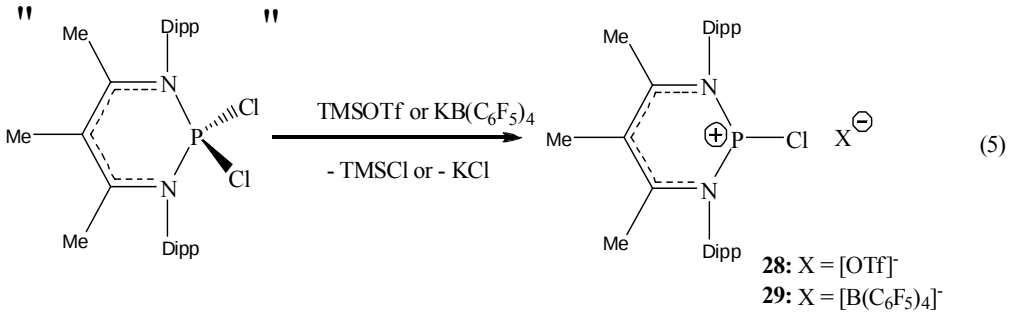

(5)

23 with PCl_3 gave several products, it was found that the initially formed material was primarily $[MeC(CMe)_2(NDipp)_2]PCl_2$ (**27**). Accordingly, **27** was treated with TMSOTf or $K[B(C_6F_5)_4]$ in CH_2Cl_2 solution *in situ* as soon as possible after its formation. After workup of the reaction mixtures and recrystallization from pentane/CH_2Cl_2 solution, $[\{MeC(CMe)_2(NDipp)_2\}PCl][OTf]$ (**28**) and $[\{MeC(CMe)_2(NDipp)_2\}PCl][B(C_6F_5)_4]$ (**29**) were isolated in yields of ~ 50%. The NMR spectra of both compounds are very similar. In both cases, the ^1H and $^{13}C\{^1H\}$ spectra are consistent with the presence of an N,N'-chelated β-diketiminate ring system and the $^{31}P\{^1H\}$ NMR chemical shifts of δ 97.24 and δ 96.61 ppm fall in the region anticipated for phosphenium cation. The presence of the $[OTf]^-$ and $[B(C_6F_5)_4]^-$ anions in **28** and **29**, respectively, was also confirmed by ^{19}F and $^{11}B\{^1H\}/^{19}F$ NMR spectroscopy. The elemental composition of both phosphenium cations was confirmed by HRMS.

*X-ray Crystal Structure of [{MeC(CMe)$_2$(NDipp)$_2$}PCl][OTf] (**28**)*

A crystalline sample of **28** suitable for single-crystal X-ray diffraction was obtained by recrystallization from pentane/CH_2Cl_2 solution. Compound **28** crystallizes in the

monoclinic space group $P2_1/c$ with Z = 2. The X-ray crystal structure of **28** reveals an ensemble of chlorophosphenium cations and triflate anions. The closest cation–anion contact is 3.312 (7) Å between Cl(1) and a triflate fluorine atom. The cyclic cation (Figure 1.13) consists of a PCl^+ moiety which is N,N'-chelated by the β-diketiminate ligand, **20**. The metrical parameters for the six-membered PN_2C_3 ring indicate that the geometry tends toward an alternating, somewhat localized distribution of electron density as reflected by the 0.02–0.03 Å differences in the C–C, C–N and N–P distances. The geometry of the PN_2C_3 ring is non-planar [sum of bond angles = 708.6(2)°]. However, the atoms N(1), C(1), C(2), C(3) and N(2) are approximately coplanar and P(1) deviates

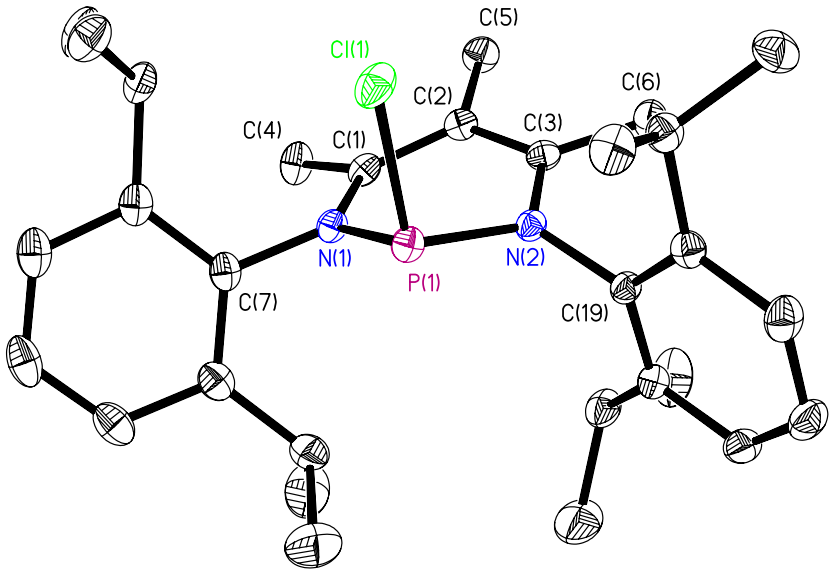

Figure 1.13. ORTEP view of the cation $[\{MeC(CMe)_2(NDipp)_2\}PCl]^+$ in **28**. The thermal ellipsoids are drawn at 30% probability. All hydrogen atoms have been omitted for clarity.

from this plane by 0.549(3) Å. The average N–P bond distance is 1.716(2) Å. Due to the presence of a stereochemically active lone pair at P(1), the chloride ligand is approximately orthogonal to the PN_2C_3 ring. [The Cl(1)–P(1)–N(1) and Cl(1)–P(1)–N(2) angles are 97.41(9) and 102.65(9)°, respectively]. Overall, the structure of the cation of **28** bears a close resemblance to that of the neutral germanium (II) β-diketiminate $[HC(CMe)_2(NDipp)_2]GeCl$ with which it is isovalent.[32]

*X-ray Crystal Structure of $[\{MeC(CMe)_2(NDipp)_2\}PCl][B(C_6F_5)_4]$ (**29**)*

A suitable single crystal of compound **29** was obtained in the same way as that described for compound **28**. Compound **29** crystallizes in the space group C2/c with Z = 4. The conformation and metrical parameters for **29** are very similar to those of **28**. However, the differences between the C–C, C–N and N–P distances on either side of the β-diketiminate ring are larger for compound **29** (0.04 - 0.05 Å) than for those of compound **28** (0.02 – 0.03 Å), which means that the electron density in the backbone of compound **29** is more localized than that of **28**. Since the $[B(C_6F_5)_4]^-$ anion is less coordinating than the $[OTf]^-$ anion, the P···Cl distance in **29** [2.079(2) Å] is shorter than in **28** [2.092(1) Å]. A superimposed view of the phosphenium cations of **28** and **29** is presented in Figure 1.15.

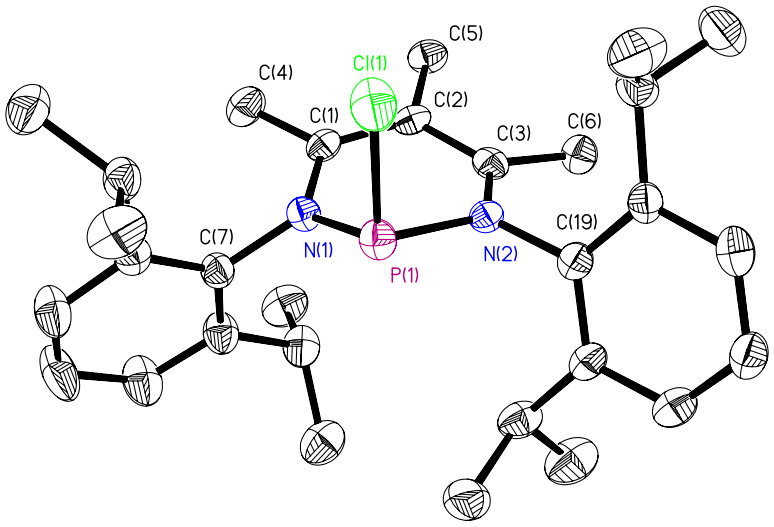

Figure 1.14. ORTEP view of the cation $[\{MeC(CMe)_2(NDipp)_2\}PCl]^+$ in **29**. The thermal ellipsoids are drawn at 30% probability. All hydrogen atoms have been omitted for clarity.

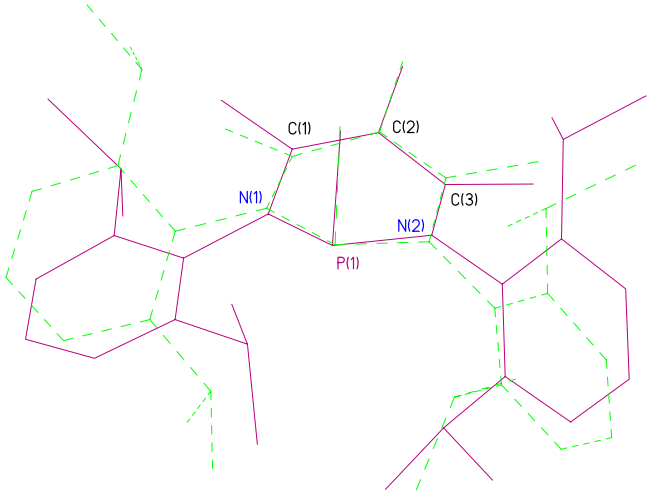

Figure 1.15. Superimposed view of the phosphenium cations in **29** (solid lines) and **28** (dashed lines).

*X-ray Crystal Structure of [{MeC(CMe)$_2$(NDipp)$_2$}PBr][OTf] (**30**)*

The bromophosphenium salt [{MeC(CMe)$_2$(NDipp)$_2$}PBr][OTf] (**30**) was obtained in exactly the same way as compound **28** by using PBr_3 instead of PCl_3. Compound **30** was isolated as a pale yellow crystalline solid. The ^1H and $^{13}C\{^1H\}$ NMR spectra for **30** are very similar to those for **28**. As expected, the $^{31}P\{^1H\}$ NMR chemical shift for compound **30** (δ 102.16) falls in the same region as those for phosphenium cations **28** (δ 97.24 ppm) and **29** (δ 96.61 ppm). The single-crystal X-ray structure revealed that this compound has a very similar crystal and molecular structure to compound **28**. A superimposed view of the cations of **28** and **30** is presented in Figure 1.17.

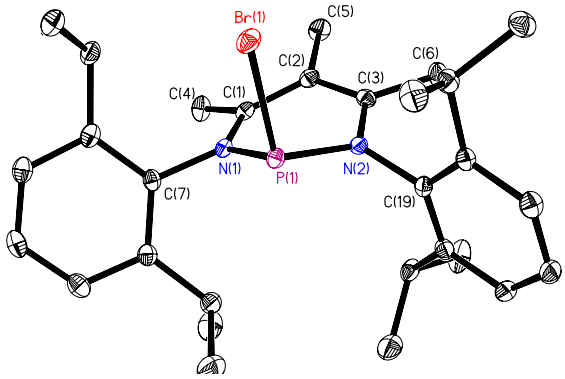

Figure 1.16. ORTEP view of the cation [{MeC(CMe)$_2$(NDipp)$_2$}PBr]$^+$ in **30**. The thermal ellipsoids are drawn at 30% probability. All hydrogen atoms have been omitted for clarity.

Important insights into the mechanism of formation of the β-diketiminate-substituted phosphenium cations **28**, **29** and **30** are provided by the work of my former colleague, Dr. Dragoslav Vidovic, on an analogous system[34]. Dr. Vidovic was able to isolate the bis-

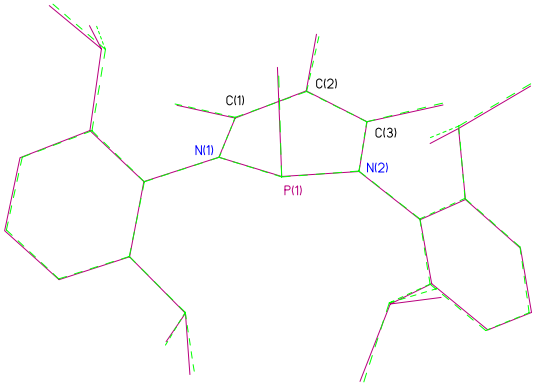

Figure 1.17. Superimposed view of the phosphenium cations in **28** (dashed lines) and **30** (solid lines).

imine compound **31** from the reaction of $[HC(CMe)_2(NC_6F_5)_2]Na$ with PCl_3 in hexane solution. As shown in Figure 1.18. One of the interesting features of the X-ray crystal structure of **31** relates to the short P(1)···N(1) and P(1)···N(2) contacts of 2.690 (4) and 2.894 (4) Å, respectively. Both of these distances are apparently shorter than the sum of

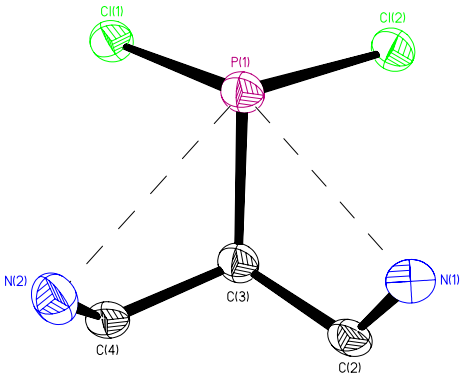

Figure 1.18. View of the skeleton of **31** showing the short N···P contacts.

van der Waals radii for P and N (3.40 Å)[35]. This structure feature may provide an important clue regarding the mechanism of conversion of $[MeC(CMe)_2(NDipp)_2]PCl_2$ into **28**, **29** and **30**. Phosphenium ion formation can be envisaged as occurring by a concerted process in which P(1)-N(1) and P(1)-N(2) bond formation is accompanied by concomitant rupture of the P(1)-C(3) bond as a chloride anion is abstracted from P(1). Alternatively, P(1)-N(1) formation and P(1)-C(3) cleavage could occur in a first step, followed by rotation of the C(4)-N(2) imine group around the C(3)-C(4) bond to effect ring closure.

Density Functional Theory (DFT) Calculations on Phosphenium Cation $[\{MeC(CMe)_2(NDipp)_2\}PCl]^+$ *(**28**$^+$)*

Density Functional Theory (DFT) calculations have been performed on phosphenium cation **28**$^+$ at the B3LYP level of theory using the 6-31+G(d) basis set. The input parameters for the geometry optimization were generated from the X-ray crystallographic data set for **28**. In general, the computed metrical parameters lie within 2.5% of the experimental values as listed in Table 1.2.

The HOMO and LUMO for **28**$^+$ are aryl ring bonding and β-diketiminate π* in character, respectively, and the HOMO–LUMO gap is 362 kJ·mol^{-1}. As shown in Figure 1.20, the orbital that features the most phosphorus lone pair character is the HOMO–5.

Table 1.2. Selected bond distances (Å) and bond angles (°) for phosphenium cation $[\{MeC(CMe)_2(NDipp)_2\}PCl]^+$ (**28**$^+$)

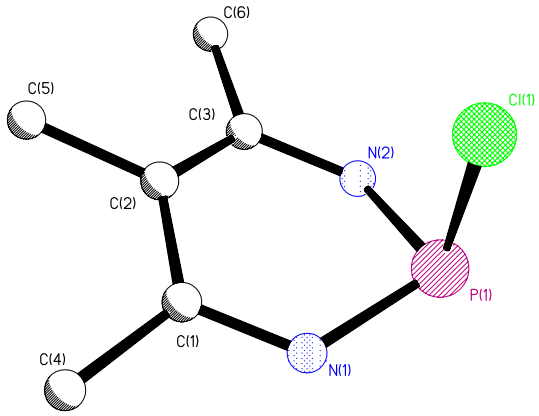

	Experimental	Theoretical
P(1)-N(1)	1.70	1.74
P(1)-N(2)	1.73	1.77
C(3)-N(2)	1.38	1.37
C(1)-N(1)	1.36	1.35
C(1)-C(2)	1.38	1.40
C(2)-C(3)	1.41	1.42
P(1)-Cl(1)	2.09	2.13
N(1)-P(1)-N(2)	97.5	97.6
P(1)-N(2)-C(3)	122.8	122.4
P(1)-N(1)-C(1)	124.0	123.6
N(2)-C(3)-C(2)	121.2	121.4
N(1)-C(1)-C(2)	121.4	122.3
C(1)-C(2)-C(3)	121.7	121.6
N(1)-P(1)-Cl(1)	97.5	98.2
N(2)-P(1)-Cl(1)	102.7	102.4

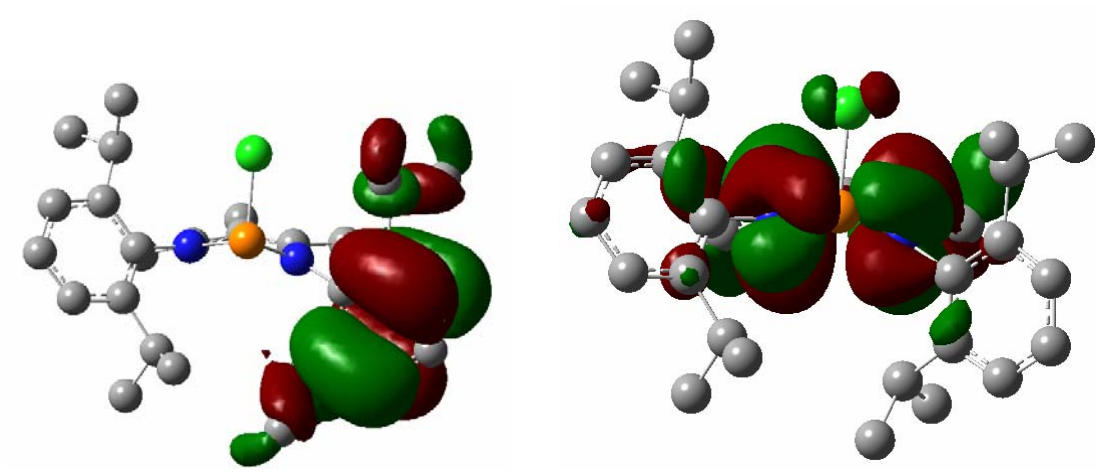

HOMO LUMO

Figure 1.19. HOMO and LUMO of phosphenium cation $[\{MeC(CMe)_2(NDipp)_2\}PCl]^+$ (**28**$^+$).

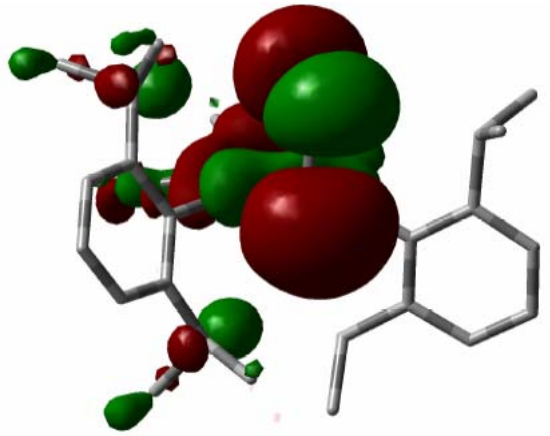

Figure 1.20. The HOMO–5 orbital of phosphenium cation of **28**$^+$ showing the phosphorus lone pair.

Reactivity of β-Diketiminate-Supported Phosphenium Cations

Valence Isomer of a β-diketiminate-Supported Phosphinidene: a Case of C-H Activation and Ring Contraction

The availability of N,N´-chelated phosphenium complexes raised the prospect that they might prove useful as precursors to the corresponding phosphinidenes (Figure 1.21).

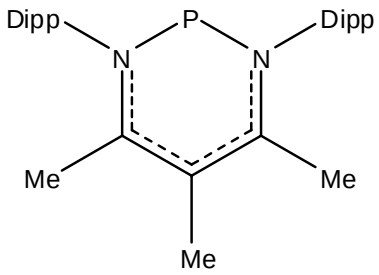

Figure 1.21. Proposed phosphinidene structure.

Phosphinidenes, the phosphorus analogues of carbenes, have attracted the attention of both the experimental and theoretical communities for several years. However, despite the presentation of convincing evidence for the intermediacy of such species[36] and the development of a fruitful phosphinidene coordination chemistry[36,37], the only example of a non-ligated phosphinidene is (mesityl)P which was isolated in a glassy methylcyclohexane matrix at 77 K by UV irradiation of *trans*-2,3-dimethyl-1-

mesitylphosphirane. This phosphinidene was shown to possess a triplet ground state.[38] No such compounds have been isolated at ambient temperature.

Treatment of **28** with two equivalents of potassium metal in toluene solution at 25 ºC for 8 h resulted, after workup of the reaction mixture and recrystallization from hexane, in ~ 30% yields of pale yellow crystalline **32** (Eq. 6). Although the low-resolution mass spectrum of **32** exhibits a peak at *m/z* 462 corresponding to the molecular ion of the targeted phosphinidene, examination of the ^{1}H NMR and IR spectrum revealed the presence of a methylene group and an N-H moiety. The $^{31}P\{^{1}H\}$ NMR spectrum also indicated a more shielded phosphorus center in **32** than that anticipated for a phosphinidene. It was therefore necessary to appeal to X-ray crystallography to gain further insight into the molecular structure.

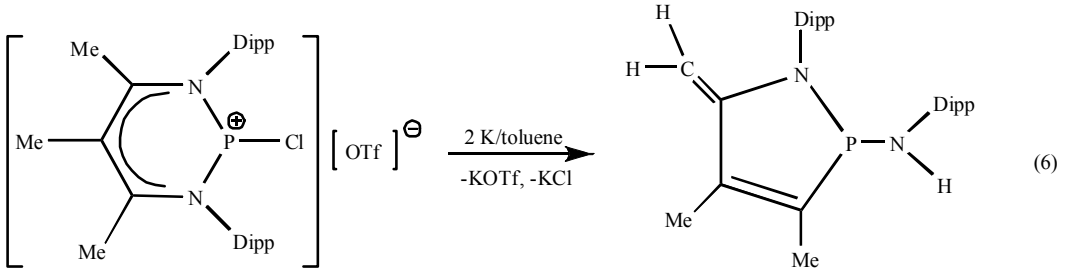

28 **32** (6)

Compound **32** crystallizes in the trigonal space group $R\bar{3}$ with Z = 18. The crystalline state of **32** comprises an ensemble of individual molecules of a valence isomer of the desired phosphinidene (Figure 1.22); there are no unusually short intermolecular contacts. The five-membered NCCCP ring is planar (sum of bond angles = 539.9(2)º)

and the ring bond angles range from 88.61(11)º for N(1)–P(1)–C(3) to 115.94(17)º for C(1)–N(1)–P(1). Two carbon-carbon double bonds are evident in the structure, namely C(2)–C(3) (1.333(4) Å) and C(1)–C(4) (1.340 (4) Å) and the geometries at C(2), C(3) and N(1) are trigonal planar as evidenced by the sums of bond angles at these centers.

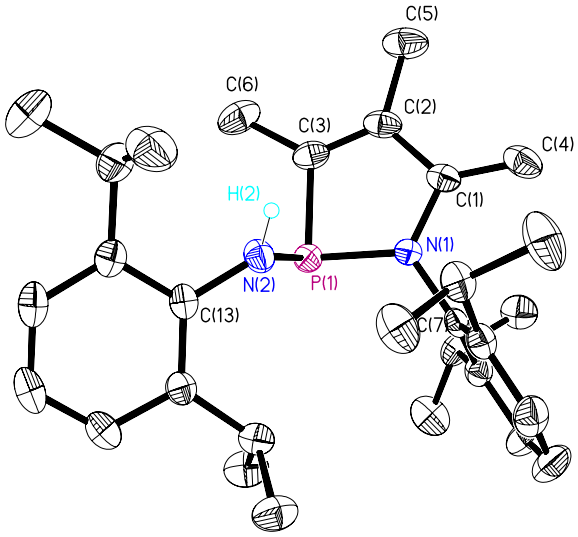

Figure 1.22. ORTEP view of phosphinidene valence isomer **32**. The thermal ellipsoids are drawn at 40% probability.

There is considerable current interest in the reductive C-N bond cleavage of the NCCCN backbone of β-diketiminate complexes of Ti, Zr and Hf since this transformation results in the formation of group 4 terminal imides supported by an azabutadienyl ligand system.[39] Although reductive C-N bond cleavage of the NCCCN backbone also takes place in the conversion of **28** to **32**, the outcome of this process is distinct from that reported for group 4 β-diketiminates[39] in the sense that an amido

derivative of a 1,2-azaphospholine ring system is produced rather than an imido azabutadienyl derivative. A search of the literature revealed that there is only one reference to the 1,2-azaphospholine ring system, namely 2-(dimethylamino)-1,2-dimethyl-5-methylene-Δ^3-1,2-azaphospholine-2-oxide.[40] However, no X-ray crystal structure for this particular ring system was available previously. Moreover, it is worth noting that, although there are prior reports concerning the C-H activation of a β-methyl group of main group β-diketiminates[28,29,41], there was no previous example of the occurrence of *both* β-methyl activation and NCCCN ligand backbone cleavage.

DFT calculations were carried out at the B3LYP level of theory in conjunction with the 6-31 G* basis set in an effort to gain some insight into the mechanism of formation of the phosphinidene valence isomer, **32**. In the interest of computational efficiency, the bulky Dipp substituents were replaced by Ph groups. Comparison of the energies of the idealized phosphinidene **33** with that of its valence isomer **32** reveals that the latter is more stable by 254 kJ·mol^{-1}.

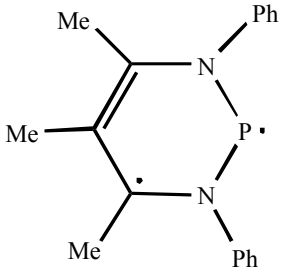

33

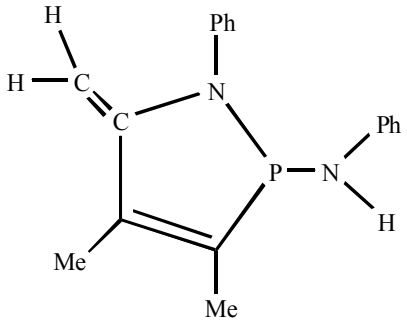

32

Interestingly, **33** is computed to adopt a triplet ground state (note that only one canonical form is depicted; the other form is obtained by interchanging the unpaired electron and the double bond). The triplet-singlet gap is computed to be 68 $kJ \cdot mol^{-1}$. This result contrasts with a similar type of calculation on the all-hydrogen-substituted β-diketiminato phosphinidene, $[HC(CH)_2(NH)_2]P$, by Ellis and Macdonald[42] which revealed a singlet ground state. This calculation was repeated and the results were found to be in excellent agreement with those of these authors. Inferentially, the nature of the ground state of β-diketiminato phosphinidenes is dependent upon the nature of the ring substituents. A similar conclusion has been reached in the case of β-diketiminate-substituted boranediyls.[43] A plausible, albeit speculative, mechanism for the formation of the phosphinidene valence isomer is summarized in Scheme 1.4.

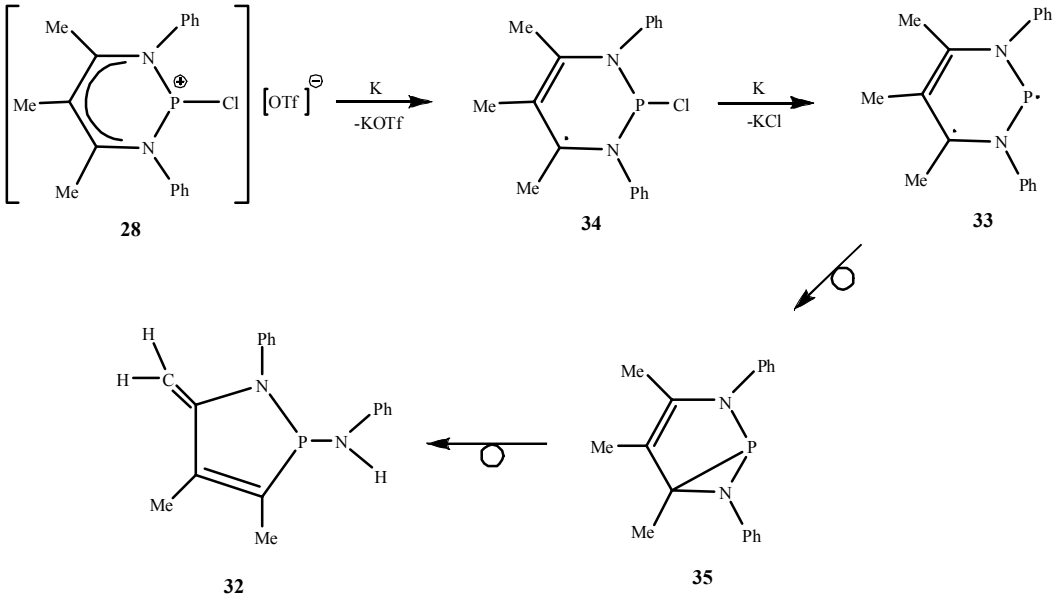

Scheme 1.4. Proposed mechanism for the conversion of the β-diketiminato phosphenium salt **28** into phosphinidene valence isomer **32**.

Assuming that the two-electron reduction of the idealized chlorophosphenium ion **28** proceeds in two steps, addition of the first electron would generate the monoradical **34** (as in the case of **33**, only one canonical form is shown). The SOMO of monoradical **34** is shown in Figure 1.23. It is evident that the unpaired electron is mainly located in the $^{2}P_{z}$ orbitals of the β-carbon atoms.

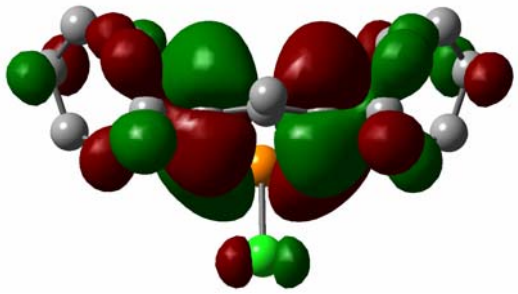

Figure 1.23. SOMO of compound cholorophosphenium radical **34**.

Addition of the second electron would then generate the triplet state of phosphinidene diradical **33**. Figure1.24 shows the two SOMOs of this diradical. One of the unpaired electrons is the same as that in monoradical **34**, while the other is located mainly on the phosphorus $^{3}P_{z}$ orbital.

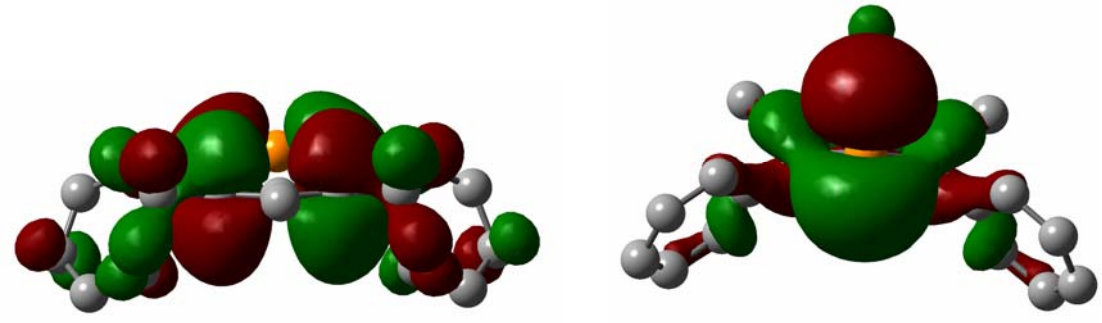

Figure 1.24. SOMOs of phosphinidene diradical **33**.

The conversion of **33** to **35** takes place by intramolecular P-C bond formation to afford the bicylic diamagnetic derivative **35**, thereby liberating 103 kJ·mol^{-1}. Finally, the phosphinidene valence isomer **32** is formed by N-C bond cleavage and hydrogen transfer from a β-methyl group to the nascent imido nitrogen center. The latter rearrangement is computed to be exothermic by 151 kJ·mol^{-1}.

Table 1.3. Selected experimental and calculated bond lengths (Å) and bond angles (°) for a model phosphinidene valence isomer

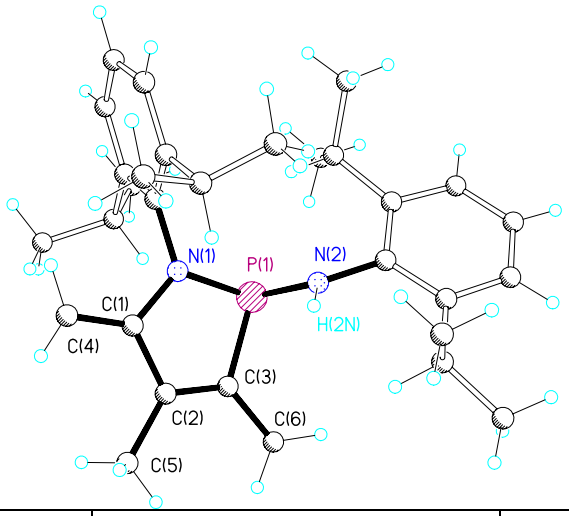

	Experimental	Calculated
P(1)-N(1)	1.713	1.752
P(1)-N(2)	1.704	1.736
P(1)-C(3)	1.816	1.836
N(1)-C(1)	1.399	1.409
C(1)-C(2)	1.470	1.481
C(2)-C(3)	1.337	1.354
C(1)-C(4)	1.343	1.351
N(1)-P(1)-N(2)	104.00	106.53
N(1)-P(1)-C(3)	88.68	88.86
P(1)-C(3)-C(2)	112.57	112.18
C(1)-C(2)-C(3)	113.55	114.03
N(1)-C(1)-C(2)	109.25	109.83
C(1)-N(1)-P(1)	115.89	115.11
C(3)-P(1)-N(2)	102.81	98.03

Attempted Preparation of a Phosphorus Dication

Mononuclear main group dicationic complexes are extremely rare. In fact, the only examples of such a cation supported by a β-diketiminate ligand is the boron complex, $[\{HC(CMe)_2(NC_6F_5)_2\}B(bipy)][OTf]_2$[44] (bipy = 2,2'-bipyridine). DFT calculations on the model N,N′-chelated β-diketiminate phosphorus dication **36** revealed that this species should be stable.[42]

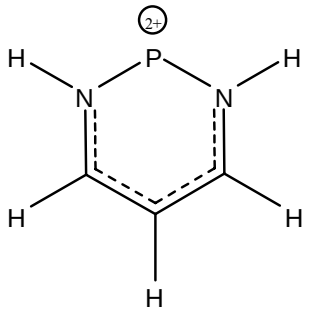

Figure 1.25. DFT computed structure for the model phosphorus dication **36**.[42]

Several attempts were made to generate such a β-diketiminatophosphorus dication using salt metathesis and halide anion abstraction methodologies. All these reactions were performed in NMR tubes and the outcomes were monitored by ^{31}P NMR spectroscopy. The reagents employed for the salt metathesis reactions included $K[B(C_6F_5)_4]$, AgOTf and $Ag[B(C_6F_5)_4]$, while halide anion abstractions were attempted with $AlCl_3$, $B(C_6F_5)_3$, $[Et_3Si][B(C_6F_5)_4]$. However, none of these experiments provided any evidence for reaction after a 12 h reaction time. Evidently, the positive charge on the

phosphorus center strengthens the phosphorus-halogen bond making it difficult to heterolyze.

*Hydrolysis of [{MeC(CMe)$_2$(NDipp)$_2$}PBr][OTf] (**30**)*

The reactions of NaCp* and KH with compound **30** were investigated in an effort to form the corresponding P-Cp* and P-H derivatives, respectively. However, in both cases, the outcome of the reaction was the production of the P-OH derivative [{MeC(CMe)$_2$(NDipp)$_2$}POH][OTf] (**37**). Evidently, the salt **37** resulted from hydrolysis of the desired P-Cp* and P-H compounds. A diagnostic feature of the hydroxyphosphenium cation **37**$^+$ is the detection of a ^{31}P NMR singlet at δ 70 ppm. The ^{1}H NMR data were consistent with the presence of an N,N'-chelated β-diketiminate ring. The triflate anion was detected by ^{19}F NMR. However, in order to confirm the spectroscopic data, a single-crystal X-ray diffraction study of **37** was undertaken.

The C_3N_2P ring of compound **37** is very similar to that of the bromophosphenium salt **30**. A superimposed view of the two β-diketiminato phosphenium cations is shown in Figure 1.27.

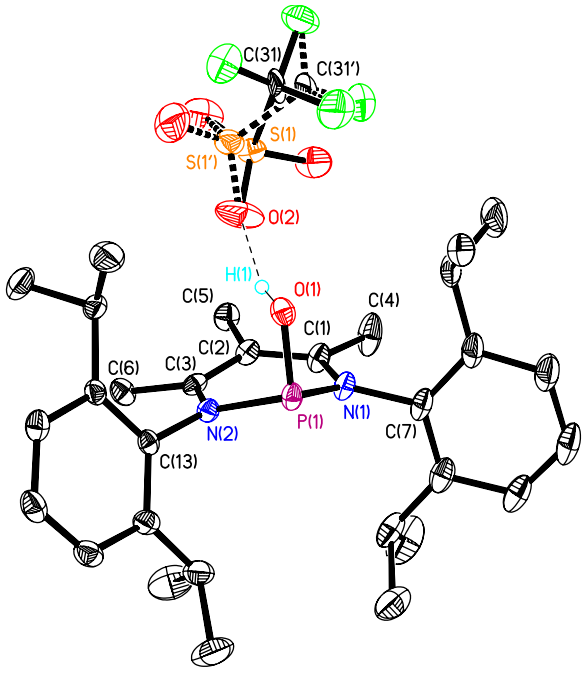

Figure 1.26. ORTEP view of compound **37**. The thermal ellipsoids are drawn at 30% probability.

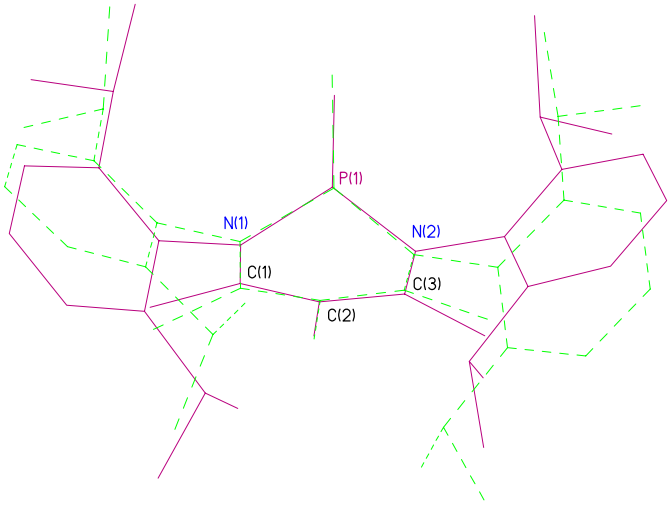

Figure 1.27. Superimposed view of the cations $[\{MeC(CMe)_2(NDipp)_2\}POH]^+$ (**37**$^+$) (solid lines) and $[MeC(CMe)_2(NDipp)_2]PBr]^+$ (**30**$^+$) (dashed lines).

Phosphinous acids and secondary phosphine oxides can undergo tautomerism as shown in Scheme 1.5. Normally this equilibrium is shifted almost completely to the secondary phosphine oxide side[45].

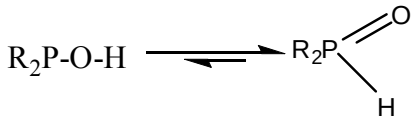

Scheme 1.5. Tautomerism of a phosphinous acid and a secondary phosphine oxide.

In the case of complex **37**, it was difficult to determine whether the product is a phosphinous acid or a secondary phosphine oxide based solely on X-ray crystallographic data. However, even though the hydrogen atom in question could not be located accurately, the relatively short distance between O(1) and O(2) (Figure 1.26) was suggestive of the presence of a hydrogen bond between these oxygen atoms. Proof of the presence of this hydrogen bond was provided by an IR spectroscopic experiment which evidenced a peak in the O-H stretching region (3364.2 cm^{-1}). Additional evidence was provided by performing molecular orbital calculations on a phosphinous acid model (**38**) and a secondary phosphine oxide model (**39**) using the B3LYP method and the 6-31+G(d) basis set. It was found that the energy of **38** is approximately 38.95 $kJ \cdot mol^{-1}$ lower than that of **39** thus indicating that **38** is the more thermodynamically stable form. This energy difference is even larger than that between $(CF_3)_2P(O)H$ and $(CF_3)_2POH$.[45] The latter compound represents the only previous case in which the phosphinous acid form is more stable than the secondary phosphine oxide tautomer.

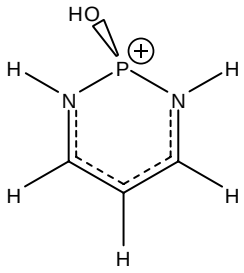

38

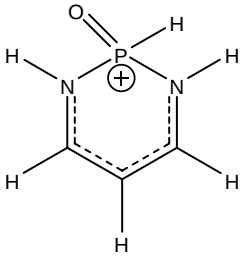

39

Given the above results, it was of interest to investigate the deliberate hydrolysis of the bromophosphenium salt [{MeC(CMe)$_2$(NDipp)$_2$}PBr][OTf] (**30**). Treatment of **30** with an excess of water at ambient temperature resulted, after workup of the reaction mixture, in the isolation of few crystals of the protonated form of the neutral β-diketiminate ligand, *i.e.* [{MeC(CMe)$_2$(NDipp)$_2$}H$_2$][OTf]$_2$ (**40**). This compound was characterized solely on the basis of a single-crystal X-ray diffraction study. Compound

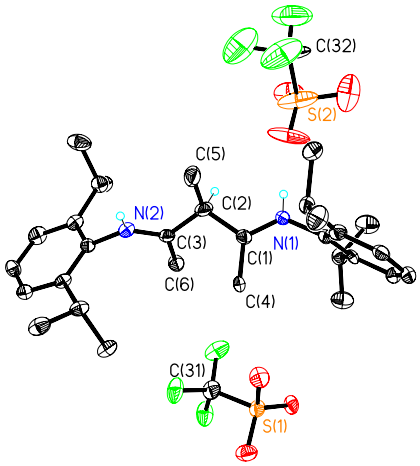

Figure 1.28. ORTEP view of compound **40**. The thermal ellipsoids are drawn at 30% probability.

40 crystallizes in the triclinic space group $P\bar{1}$ with Z = 2. The molecular structure of **40** is shown in Figure 1.28. The C(1)-N(1) and C(3)-N(2) bond distances of 1.279 (9) Å and 1.285 (8) Å, respectively and the C(1)-C(2) and C(3)-C(2) bond distances of 1.516 (10) Å and 1.503 (9) Å, respectively are indicative of a diimine structure for this molecule. Overall the molecular structure is similar to that of 2,2,6,6-tetramethyl-3,5-bis(2,6-diisopropylphenylimino) heptane.[31]

The use of solid NaOH instead of H_2O for the hydrolysis reaction gave a different result, namely a mixture of the hydroxyl phosphenium salts [{$MeC(CMe)_2(NDipp)_2$} POH][OTf] (**37**) and [{$MeC(CMe)_2(NDipp)_2$}POH]Br (**41**) (Eq. 7). Due to the insolubility of NaOH in organic solvents, both complexes were obtained in poor yields. Since compound **41** was isolated in a very small yield, it was characterized solely by single-crystal X-ray diffraction. The structure of this salt is shown in Figure 1.29. As expected, the structures of the cation of **37** and **41** are very similar as shown by the superimposed view in Figure 1.30.

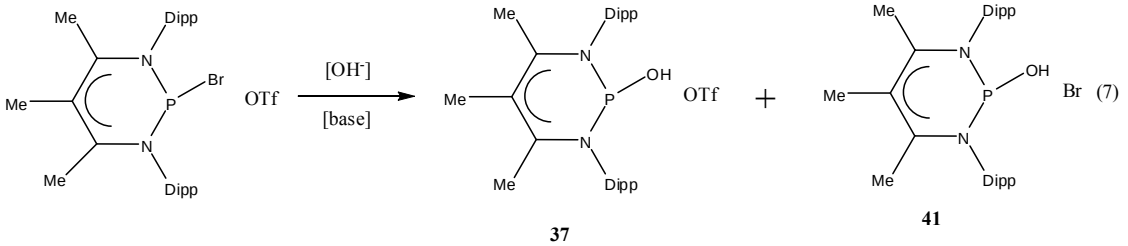

(7)

37 **41**

Compounds **37** and **41** represent first examples of structurally characterized β-diketiminate-supported phosphinous acid derivatives. As noted earlier, $(CF_3)_2P$-O-H is

the only previous example of a thermally stable uncoordinated phosphinous acid. Presumably, the reason for this structural preference in this case relates to the strong electron-withdrawing nature of the CF_3 substituents.

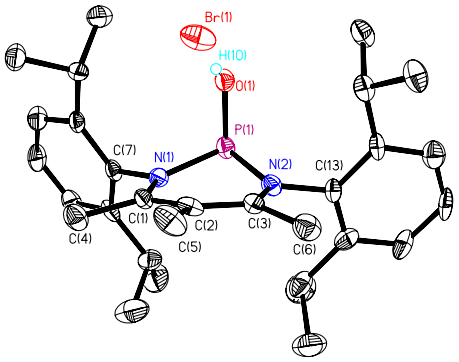

Figure 1.29. ORTEP view of compound **41**. The thermal ellipsoids are drawn at 30% probability.

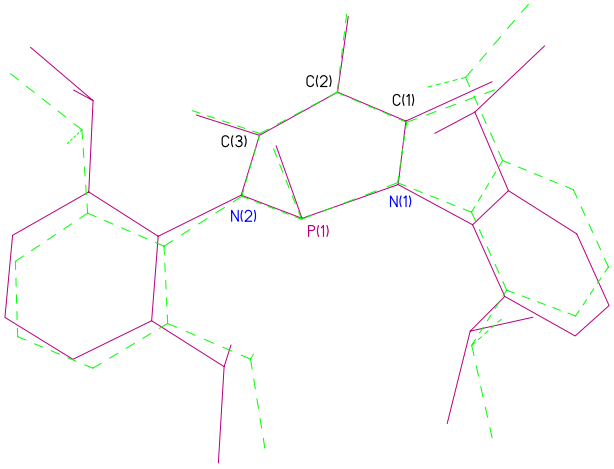

Figure 1.30. Superimposed view of the cations in [{MeC(CMe)$_2$(NDipp)$_2$}POH][OTf] (**37**) (solid lines) and in [{MeC(CMe)$_2$(NDipp)$_2$}POH]Br (**41**) (dashed lines).

A further DFT calculation on a model α-diimine ligand supported phosphinous acid (**42**) and a phosphine oxide (**43**) was performed using the B3LYP method and the 6-31+G(d) basis set. Interestingly, the total energy of the phosphinous acid (**42**) is approximately 22.16 kJ·mol^{-1} higher than that of phosphine oxide (**43**). Evidently, the positive charge on the phosphorus center of the β-diketiminate-supported phosphinous acid helps to stabilize this form, which is analogous to the electron-withdrawing effect of a CF_3 substituent.

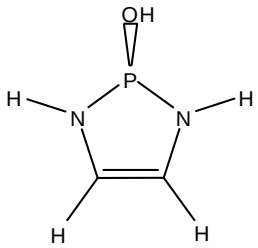

42

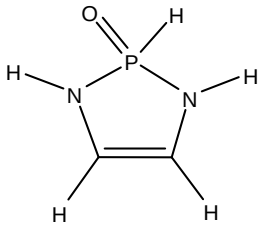

43

*DFT Calculations on the Phosphenium Cation [{MeC(CMe)$_2$(NDipp)$_2$}POH]$^+$ (**37**$^+$)*

DFT calculations have been performed on the phosphenium cation **37**$^+$ at the B3LYP level of theory using the 3-21G basis set. The input parameters for the geometry optimization were generated from the X-ray crystallographic data set for **37**. In general, the computed metrical parameters lie within 3% of the experimental values as listed in Table 1.4.

Table 1.4. Selected bond distances (Å) and bond angles (°) for the phosphenium cation $[\{MeC(CMe)_2(NDipp)_2\}POH]^+$ (**37**$^+$)

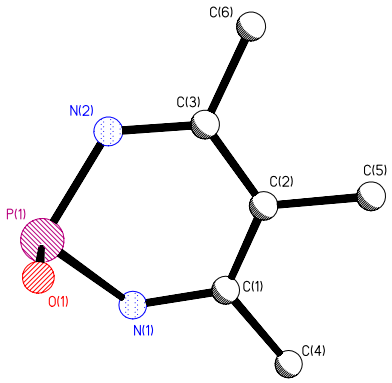

	Experimental	Theoretical
P(1)-N(1)	1.74	1.77
P(1)-N(2)	1.76	1.77
C(3)-N(2)	1.34	1.36
C(1)-N(1)	1.36	1.36
C(1)-C(2)	1.39	1.41
C(2)-C(3)	1.41	1.41
P(1)-O(1)	1.58	1.63
N(1)-P(1)-N(2)	95.5	95.2
P(1)-N(2)-C(3)	125.3	127.6
P(1)-N(1)-C(1)	124.4	127.6
N(2)-C(3)-C(2)	121.9	122.4
N(1)-C(1)-C(2)	122.2	122.4
C(1)-C(2)-C(3)	103.9	121.6
N(1)-P(1)-O(1)	121.3	102.9
N(2)-P(1)-O(1)	102.7	102.9

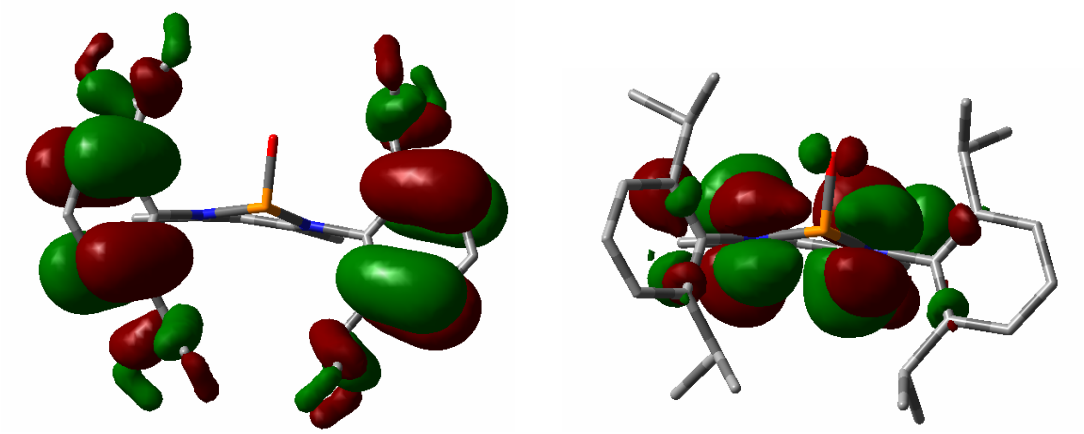

HOMO LUMO

Figure 1.31. HOMO and LUMO of phosphenium cation **37**$^{+}$.

The HOMO and LUMO for **7** are aryl ring bonding and β-diketiminate π* in character, respectively, and the HOMO–LUMO gap is 189 kJ·mol^{-1}. As shown in Figure 1.32, the orbital that features the most phosphorus lone pair character is the HOMO–5.

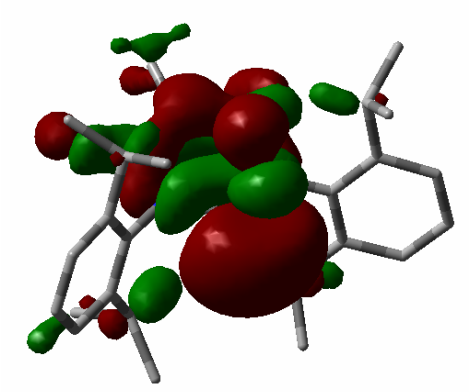

Figure 1.32. The HOMO–5 orbital of phosphenium cation **37**$^{+}$ showing the phosphorus lone pair.

N,C-Chelated β-Diketiminate-Supported Phosphenium Salts

The successful isolation of compounds **28**, **29** and **30** encouraged the search for β-diketiminato phosphenium compounds other than the halo-substituted derivatives.

Initial effort was focused on the use of ligand **21** in the expectation that the presence of a γ-methyl group would disfavor substitution at this site. Accordingly, a toluene solution of $[MeC(CMe)_2(NDipp)_2]K{\cdot}Et_2O$ (**24**) was treated with an equimolar quantity of neat $PhPCl_2$, following which the resulting yellow solution was added to one equivalent of $AlCl_3$ in toluene solution. After work-up of the reaction mixture and recrystallization from hexane/CH_2Cl_2, a yellow crystalline product (**44**) was isolated in 46% yield. Collectively, the NMR and MS data for **44** were consistent with the formation of the $[AlCl_4]^-$ salt of an N,C-bonded β-diketiminato phosphenium cation (**44**). Unfortunately,

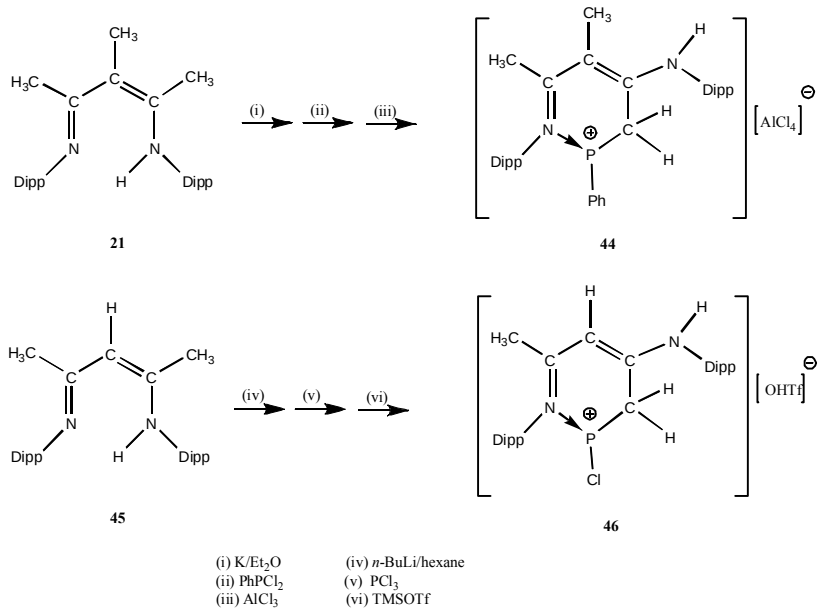

21 44 45 46

Scheme 1.6. Preparation of N,C-bonded β-diketiminato phosphenium cations.

the X-ray crystallographic data for this product were not of sufficient quality to allow a detailed discussion of metrical parameters. Nevertheless, the atom connectivities were clear (Figure 1.33) and unequivocally establish that the structure of **44** corresponds to the one shown in Scheme 1.6.

From the standpoint of the phosphorus center, **44** can be regarded as an imine donor-stabilized phosphenium ion. Phosphenium ions with only two P-C bonds are not isolable because they lack sufficient π-donor stabilization. However, it is known that such cations can be isolated when coordinated to *e.g.* phosphorus donors.[46]

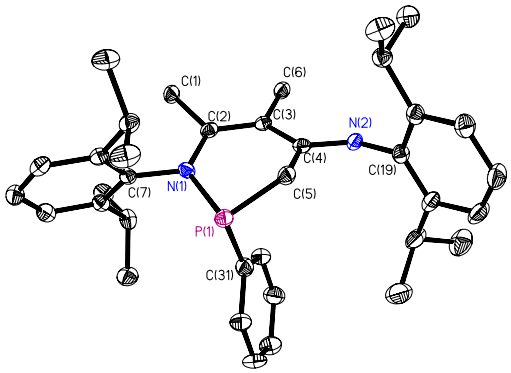

Figure 1.33. ORTEP view of the N,C-bonded β-diketiminato phosphenium cation in **44**. The thermal ellipsoids are drawn at 30% probability. All hydrogen atoms have been omitted for clarity.

Attention was turned next to the use of the $[HC(CMe)_2(NDipp)_2]H$ ligand (**45**) with a view to obtaining a phosphenium salt with improved crystallinity. It was thought that the use of this ligand might provide some insight into the necessity or otherwise of blocking the *γ*-position. As summarized in Scheme 1.6, the synthesis of **46** was carried out in a

very similar fashion to that described for **44**, the main difference being the use of TMSOTf rather than $AlCl_3$ for chloride ion abstraction. Colorless, crystalline **45** was isolated in 42% yield. The ^{1}H NMR spectral data for **46** are similar to those for **45**, suggesting an analogous N,C mode of ligation for the β-diketiminate ligand. The presence of the triflate anion was evident from the ^{19}F NMR spectrum. The $^{31}P\{^{1}H\}$ chemical shifts for **45** (δ 162.7 ppm) and **46** (δ 149.4 ppm) are similar and fall in the phosphenium cation region.

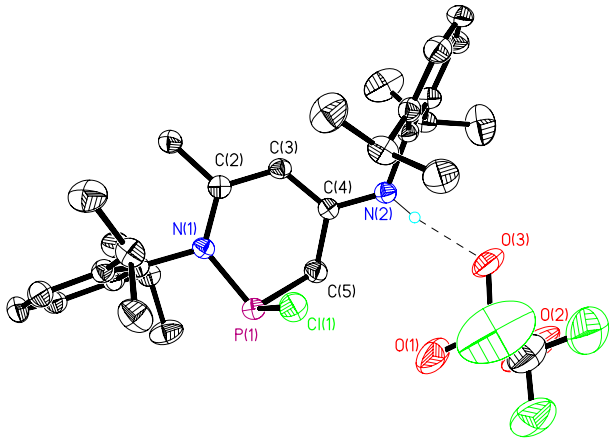

Figure 1.34. ORTEP view of the N,C-bonded β-diketiminato phosphenium cation in **46**. The thermal ellipsoids are drawn at 30% probability.

Confirmation of the structural assignment for **46** shown in Scheme 1.6 was provided by a single-crystal X-ray diffraction study. Compound **46** crystallizes in the triclinic space group $P\bar{1}$ with Z = 2. The crystalline state of **46** consists of an ensemble of phosphenium cations and triflate anions. For each ion pair, one of the triflate oxygen atoms [O(3)] is hydrogen bonded to the unligated nitrogen atom of the β-diketiminate

ligand [N(2)]. The presence of this hydrogen bond is also evidenced by the detection of an IR-active vibration at 3215 cm^{-1} and a ^{1}H NMR signal at δ 9.05 ppm. The six-membered PNCCCC ring adopts an envelope conformation. The atoms P(1), N(1), C(2), C(3) and C(4) are planar within experimental error and the "flap" of the envelope forms an angle of 45.99° with respect to said plane. The P(1)-C(5) and C(4)-C(5) distances of 1.821(4) and 1.495(5) Å, respectively, correspond to single bonds and the N(1)-P(1) distance of 1.718(3) Å falls in the range observed for N→P donor-acceptor bonding[47]. Although N(1)-C(2) and C(3)-C(4) are shown as double bonds in the canonical form depicted in Scheme 1.6 there is, in fact, considerable delocalization across the N(1)-C(2)-C(3)-C(4) fragment. Moreover, the C(4)-N(2) bond distance of 1.310(4) Å is indicative of partial double bond character. Finally, there is a wide scatter of bond angles within the PNCCC ring which range from 97.90(15)º for N(1)-P(1)-C(5) to 125.7(2)º for P(1)-N(1)-C(2).

DFT calculations have been performed on phosphenium ion **46** at the B3LYP level of theory using the 6-31+G(d) basis set. The input parameters for the geometry optimization were generated from the X-ray crystallographic data set for **46**. In general, the computed metrical parameters lie within 3% of the experimental values.

Table 1.5. Computed bond distances (Å) and bond angles (°) for the N,C-bonded β-diketiminato phosphenium cation **46**$^{+}$.

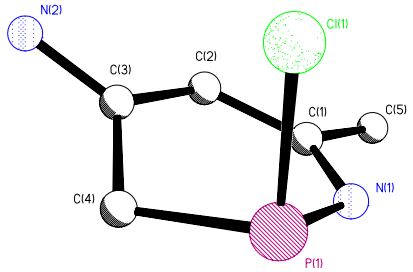

	Experimental	Theoretical
N(1)-P(1)	1.72	1.76
N(1)-C(2)	1.39	1.37
C(2)-C(3)	1.39	1.40
C(3)-C(4)	1.40	1.40
C(4)-C(5)	1.50	1.50
C(4)-N(2)	1.31	1.33
C(5)-P(1)	1.82	1.86
P(1)-Cl(1)	2.10	2.12
C(5)-P(1)-N(1)	97.9	97.4
P(1)-N(1)-C(2)	125.7	124.5
N(1)-C(2)-C(3)	121.9	123.8
C(2)-C(3)-C(4)	123.7	124.4
C(3)-C(4)-N(2)	122.8	122.6
C(3)-C(4)-C(5)	119.3	119.9
C(4)-C(5)-P(1)	112.7	114.6
C(5)-P(1)-Cl(1)	96.7	96.7
N(1)-P(1)-Cl(1)	102.8	103.1

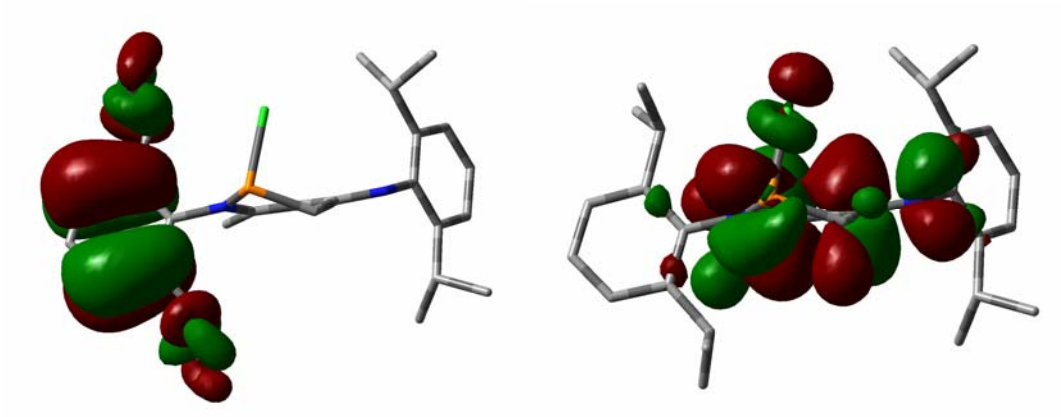

HOMO LUMO

Figure 1.35. HOMO and LUMO of the N,C-bonded β-diketiminato phosphenium cation **46**$^{+}$.

The HOMO and LUMO for **46**$^{+}$ are aryl ring bonding and β-diketiminate π* in character, respectively, and the HOMO–LUMO gap is 349 kJ·mol^{-1}. As shown in Figure 1.36, the orbital that features the most phosphorus lone pair character is the HOMO–5.

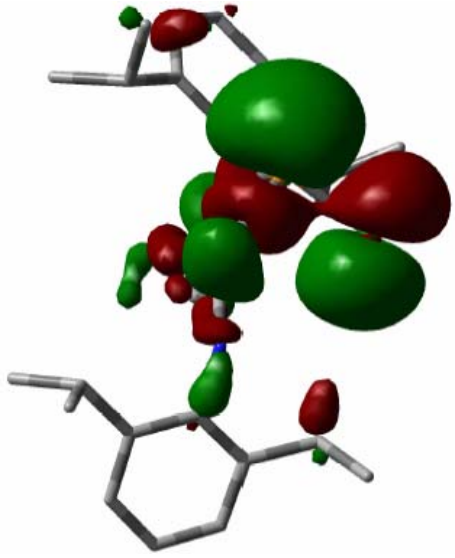

Figure 1.36. HOMO-5 of the N,C-bonded β-diketiminato phosphenium cation **46**$^{+}$.

DFT calculations were used to determine the difference in energy between the N,N′-chelated and the N,C-bonded phosphenium cations. To minimize the calculation time, phenyl groups were used as the nitrogen substituents in the model compounds **47** and **48**. The two structures were optimized using the B3LPY method and the 3-21G basis set. The total energies of **47** and **48** were calculated using the MP2 method and the 6-31+G(d) basis set. These calculations revealed that the N,C-bonded cation **48** is only 35.64 $kJ \cdot mol^{-1}$ less stable than the N,N'-chelated cation **47**. This result indicates that the two structures are of comparable energy and that the observed structural preference largely depends on steric effects and the electronegativity of the phosphorus fragment.

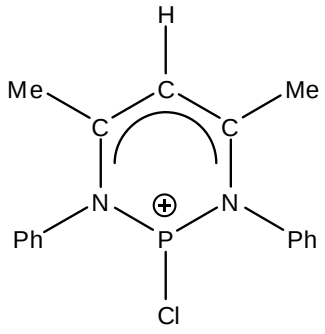

47

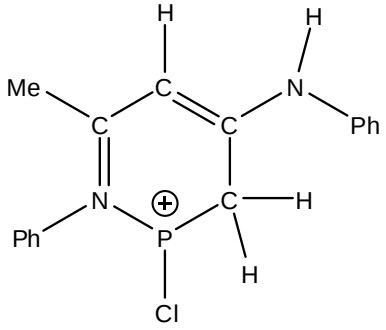

48

Conclusions

The new β-diketiminate ligand [{MeC(CMe)$_2$(NDipp)$_2$}H] has been prepared which features the γ-position blocked with a methyl group. An NMR study revealed that this ligand exists as tautomeric forms in solution at room temperature. However, only the iminoamine form is isolable in solid state. The formation of the metallated derivatives [{MeC(CMe)$_2$(NDipp)$_2$}M] (M = Li, K) indicates that this new ligand behaves in a similar fashion to the widely used ligand [{HC(CMe)$_2$(NDipp)$_2$}H].

Neutral phosphorus compounds supported by the new ligand have not been obtained in pure state due to the complexity of the product mixture. However, a series of N,N′-chelated halophosphenium complexes supported by this γ-methylated β-diketiminate ligand have been successfully synthesized and structurally characterized.

Two-electron reduction of a β-diketiminate-supported halophosphenium complex gave the first example of a valence isomer of phosphinidene. DFT calculations showed that the formation of this valence isomer occurs via the intermediacy of a triplet diradical phosphinidene.

Hydrolysis of the N,N′-chelated phosphenium cations in basic solution produces a thermally stable cationic β-diketiminato phosphinous acid, while treatment with neutral water results in formation of the diprotonated diimine form of the ligand.

The first examples of N,C-bonded phosphenium complexes have been isolated as their triflate or tetrachloroaluminate salts, both of which were structurally characterized.

Experimental Section

General Procedures

Unless specified otherwise, all manipulations were carried out in a dry box or under a dry, oxygen-free argon atmosphere using standard Schlenk techniques. The solvents toluene, diethyl ether, hexanes, benzene and pentane were dried over sodium benzophenone ketyl and freshly distilled prior to use. Dichloromethane was dried and distilled from CaH_2. The phosphorus reagents, trimethylsilyl triflate, 3-methyl-2,4-petanedione, 2,6-diisopropylphenylaniline, *p*-toluenesulfonic acid, aluminum trichloride, potassium metal, and *n*-butyl lithium solution were obtained commercially and used without further purification.

Low-resolution CI mass spectra were obtained on a Finnigan MAT TSQ-700 mass spectrometer and high-resolution CI mass spectra recorded on a VG Analytical ZAB-VE sector instrument. ^{1}H, $^{13}C\{^{1}H\}$, $^{31}P\{^{1}H\}$, ^{19}F, $^{27}Al\{^{1}H\}$ and $^{11}B\{^{1}H\}$ NMR spectra were recorded at 295K on a Varian Unity +300 instrument (^{1}H, 300 MHz; ^{13}C, 75 MHz; ^{11}B, 96 MHz; ^{27}Al, 78.14 MHz; ^{31}P, 121.50 MHz; ^{19}F, 282.41 MHz). ^{1}H and $^{13}C\{^{1}H\}$ chemical shift values are reported in parts per million (ppm) relative to $SiMe_4$ (δ 0 ppm). $^{31}P\{^{1}H\}$ NMR data are referenced to 85% H_3PO_4 (δ 0 ppm). ^{19}F NMR are referenced to $CFCl_3$ (δ 0 ppm). $^{27}Al\{^{1}H\}$ NMR are referenced to $AlCl_3$ in D_2O solution (δ 0 ppm). $^{11}B\{^{1}H\}$ NMR are referenced to $BF_3{\cdot}Et_2O$ (δ 0 ppm).

X-ray Crystallography

Suitable single crystals were removed from a Schlenk flask under a positive pressure of argon, placed on a glass slide, covered immediately with degassed hydrocarbon oil and mounted on a thin glass fiber. The X-ray diffraction data were collected at 153 K on a Nonius Kappa CCD diffractometer equipped with an Oxford Cryostream low-temperature device and a graphite-monochromated Mo Kα radiation source (λ = 0.71073 Å). Corrections were applied for Lorentz and polarization effects. All structures were solved by direct methods and refined by full-matrix least-squares cycles on F^2.[48] All non-hydrogen atoms were allowed anisotropic thermal motion, and hydrogen atoms were placed in fixed, calculated positions using a riding model (C-H 0.96 Å).

*Preparation of [{MeC(CMe)$_2$(NDipp)$_2$}H] (**21**)*

3-Methyl-2,4-pentanedione (5 mL), 2,6-diisopropylphenylaniline (16 mL), toluene (200 mL) and *p*-toluenesulfonic acid (9.0 g) were added to a 250 mL round bottom flask equipped with a Dean-Stark apparatus. The reaction mixture was refluxed for 36 h, following which the toluene was removed under reduced pressure, and the resulting residue was re-dissolved in 200 mL of $CHCl_3$. A saturated aqueous solution of Na_2CO_3 was then added and the resulting mixture was allowed to stir approximately 2 h. The aqueous layer was discarded and the organic layer was washed with 150 mL of water, then dried over anhydrous $MgSO_4$. After removal of the $CHCl_3$ under reduced pressure, 5-10 mL of methanol was added to the resulting dark-brown oil, and the mixture was maintained at –40 °C overnight. Several crops of the colorless crystalline product were

isolated in a total yield of approximately 10 g (ca. 50%). ^{1}H NMR (C_6D_6): δ, 13.69 (s,1H, N*H*), 7.42-7.89 (m, 6H, Ar), 2.98 (quartet, J = 6.9 Hz, 2H, C*H*Me$_2$), 2.88 (quartet, J = 6.9 Hz, 2H, C*H*Me$_2$), 1.82 (s, 3H, C*H$_3$*), 1.75 (s, 3H, C*H$_3$*), 1.66 (s, 3H, C*H$_3$*), 1.57-1.14 (m, 24H, CH*Me$_2$*); For diimine tautomer (**22**), 7.42-7.89 (m, 6H, Ar), 3.44 (quartet, J = 6.9 Hz, 1H, C*H*Me), 3.30 (quartet, J = 6.9 Hz, 4H, C*H*Me$_2$), 1.57 (s, 6H, C*H$_3$*), 1.52 (d, J = 6.9 Hz, 3H, CH*Me*), 1.57-1.14 (m, 24H, CH*Me$_2$*). HRMS, calcd. for $[M+H]^+$ $C_{30}H_{45}N_2$ 433.3583, found 433.3592.

*Preparation of [MeC(CMe)$_2$(NDipp)$_2$]Li (**23**)*

An equimolar quantity of a hexane solution of *n*-BuLi was added to a hexane solution of **21** at ambient temperature. The reaction mixture was allowed to stir for 3 h, following which all volatiles were removed under reduced pressure, leaving **23** as a white powdery residue. ^{1}H NMR (C_6D_6) δ 7.32-7.11 (m, 6H, Ar), 3.02 (quartet, J = 6.9 Hz, 4H, C*H*Me$_2$), 2.02 (s, 3H, C*H$_3$*), 1.89 (s, 6H, C*H$_3$*), 1.22-1.11 (m, 24H, CH*Me$_2$*). Mass Spectrum (CI^+, CH_4): M^+ 439.

*Preparation of [MeC(CMe)$_2$(NDipp)$_2$]K·Et$_2$O (**24**)*

Diethyl ether (100 mL) was added to a mixture of 0.01 g (0.26 mmol) of finely cut potassium metal and 0.1 g (0.23 mmol) of **21**. The reaction mixture was allowed to stir overnight. The unreacted potassium metal was filtered off and the filtrate was concentrated to a volume of approximately 5 mL. Cooling of this solution to –40 °C overnight resulted in the formation of 0.09 g (72% yield) of colorless crystalline **24**. ^{1}H

NMR (C_6D_6) δ 7.17-7.02 (m, 6H, Ar), 3.30 (quartet, J = 6.9 Hz, 4H, C*H*Me_2), 1.82 (s, 3H, CH_3), 1.75 (s, 6H, CH_3), 1.21-1.12 (m, 24H, CHMe_2). $^{13}C\{^1H\}$ NMR (C_6D_6): δ 161.16 (*C*N), 142.78, 141.42, 125.47, 123.18 (Ar), 95.47 (*C*Me), 28.49 (*C*HMe_2), 24.31, 23.53 (CHMe_2), 18.64 (*C*H_3), 15.82 (*C*H_3).

*Attempted Preparation of[{MeC(CMe)$_2$(NDipp)$_2$}]PPhCl (**25**), [{MeC(CMe)$_2$(NDipp)$_2$}]PPh$_2$ (**26**) and [{MeC(CMe)$_2$(NDipp)$_2$}]PCl$_2$ (**27**)*

To a freshly prepared solution of **21** in hexane, an equimolar quantity of the corresponding chloro-phosphine was added. After the reaction mixture had been stirred overnight, the resulting precipitate was removed by filtration. Removal of the solvent under reduced pressure resulted in the formation of **25**, **26** and **27** as oily residues.

*Preparation of [{MeC(CMe)$_2$(NDipp)$_2$}PCl][OTf] (**28**)*

A solution of *n*-BuLi (0.46 mL of 2.5 M in hexanes, 1.14 mmol) was added dropwise to a solution of **21** (0.5 g, 1.14 mmol) in 30 mL of hexane at room temperature. The reaction mixture was stirred for 3 h, after which PCl_3 (0.16 g, 1.14 mmol) was added dropwise. After being stirred overnight, the reaction mixture was filtered through Celite® and the solvent was stripped from the filtrate to afford a pale yellow oily residue. This residue was re-dissolved in 30 mL of CH_2Cl_2, followed by the addition of trimethylsilyl trifluoromethanesulfonate (0.46 g, 2.28 mmol). The reaction mixture was then allowed to stir for 3 days, after which the solvent was removed under reduced pressure. The resulting yellow residue was washed twice with 10 mL portions of pentane.

Recrystallization of this yellow residue from a dichloromethane/pentane solution afforded 0.4 g yellow crystals of **28**. The yield was 54 % yield based on the consumption of **21**. ^{1}H NMR (CD_2Cl_2, 300 MHz): δ 7.64-7.41 (m, 6H, Ar), 2.90 (sept, 2H, J = 6.6 Hz, C*H*Me$_2$), 2.71 (sept, 2H, J = 6.6 Hz, C*H*Me$_2$), 2.44 (s, 3H, CH_3), 2.43 (s, 6H, CH_3), 1.34 (d, 6H, J = 6.6 Hz, CH(CH_3)$_2$), 1.32 (d, 6H, J = 6.6 Hz, CH(CH_3)$_2$), 1.29 (d, 6H, J = 6.6 Hz, CH(CH_3)$_2$), 1.10 (d, 6H, J = 6.6 Hz, CH(CH_3)$_2$). ^{13}C{^{1}H} NMR (CD_2Cl_2,): δ 169.82 (*C*N), 147.83, 145.37, 127.35, 126.50 (Ar), 132.55 (*C*F$_3$), 116.89 (*C*CH$_3$), 30.46, 29.67 (*C*Me$_2$), 26.18, 25.22, 24.34, 23.77 (C*Me$_2$*), 22.56 (*C*H$_3$), 17.12 (*C*H$_3$). ^{19}F NMR (CD_2Cl_2, 282.41 MHz): δ -79.27. ^{31}P{^{1}H} NMR (CD_2Cl_2, 121.50 MHz): δ 97.24. HRMS (CI, CH_4): calcd for $C_{30}H_{43}N_2PCl$ 497.2852, found 497.2848.

*Preparation of [{MeC(CMe)$_2$(NDipp)$_2$}PCl][B(C$_6$F$_5$)$_4$] (**29**)*

The same procedure was employed as that described above for **28** except that $KB(C_6F_5)_4$ was used instead of TMSOTf (60% yield based on the consumption of **21**). ^{1}H NMR (CD_2Cl_2, 300 MHz): δ 7.64-7.32 (m, 6H, Ar), 2.87 (sept, 2H, J = 6.6 Hz, C*H*Me$_2$), 2.68 (sept, 2H, J = 6.6 Hz, C*H*Me$_2$), 2.38 (s, 6H, CH_3), 2.23 (s, 3H, CH_3), 1.35 (d, 6H, J = 6.6 Hz, CH(CH_3)$_2$), 1.31 (d, 6H, J = 6.6 Hz, CH(CH_3)$_2$), 1.29 (d, 6H, J = 6.6 Hz, CH(CH_3)$_2$), 1.07 (d, 6H, J = 6.6 Hz, CH(CH_3)$_2$). ^{19}F NMR (CD_2Cl_2, 282.41 MHz): δ –133.51 (m, 8F), -164.05 (t, 4F), -167.93(t, 8F). ^{31}P{^{1}H} NMR (CD_2Cl_2, 121.50 MHz): δ 96.61. ^{11}B{^{1}H} NMR (CD_2Cl_2,) δ –16.92. Mass Spectrum (CI$^-$): $[B(C_6F_5)_4]^-$ *m/z* 679.

*Preparation of [{MeC(CMe)$_2$(NDipp)$_2$}PBr][OTf] (**30**)*

The same procedure was employed as that described above for **28** using PBr_3 instead of PCl_3 (62% yield based on the consumption of **21**). ^{1}H NMR (CD_2Cl_2, 300 MHz): δ 7.64-7.40 (m, 6H, Ar), 2.96 (sept, 2H, J = 6.6 Hz, C*H*Me$_2$), 2.65 (sept, 2H, J = 6.6 Hz, C*H*Me$_2$), 2.46 (s, 3H, C*H*$_3$), 2.44 (s, 6H, C*H*$_3$), 1.32 (d, 6H, J = 6.6 Hz, CH(C*H*$_3$)$_2$), 1.26 (d, 6H, J = 6.6 Hz, CH(C*H*$_3$)$_2$), 1.24 (d, 6H, J = 6.6 Hz, CH(C*H*$_3$)$_2$), 1.09 (d, 6H, J=6.6 Hz, CH(C*H*$_3$)$_2$). ^{13}C{^{1}H} NMR (CD_2Cl_2, 75.47 MHz): δ 170.13 (*C*N), 147.58, 145.56, 127.35, 126.51 (Ar), 132.45 (*C*F$_3$), 117.89 (*C*CH$_3$), 30.37, 29.80 (*C*Me$_2$), 26.66, 25.31, 24.27, 23.74 (C*Me$_2$*), 22.98, 22.51 (*C*H$_3$), 17.18 (*C*H$_3$). ^{19}F NMR (CD_2Cl_2, 282.41 MHz): δ -79.27. ^{31}P{^{1}H} NMR (CD_2Cl_2, 121.50 MHz): δ 102.16. HRMS (CI^+, CH_4): calcd for $C_{30}H_{43}N_2PBr$ 541.2347, found 541.2343.

*Preparation of [MeCC(Me)C(CH$_2$)N(Dipp)PN(Dipp)H] (**33**)*

Toluene (30 mL) was added to a mixture of [{MeC(CMe)$_2$(NDipp)$_2$}PCl][OTf] (**28**) (0.2 g, 0.3 mmol) and potassium metal (0.047 g, 0.6 mmol). The reaction mixture was allowed to stir overnight, during which time the potassium metal was completely consumed. The reaction mixture was then filtered and all the volatiles were removed under reduced pressure. The resulting residue was extracted with 20 mL hexane, and recrystallized by slow solvent evaporation. Yield 0.05 g (36%). ^{1}H NMR (299.89 MHz, C_6D_6): δ 0.99-1.34 (m, 24 H, CH*Me$_2$*), 1.78 (d, 3H, C*H*$_3$), 1.82 (s, 3H, C*H*$_3$, $^3J_{PH}$ = 1.2 Hz), 3.01-3.77 (m, 4H, C*H*Me$_2$), 4.18 (d, 1H, N*H*, $^2J_{PH}$ = 3.3 Hz), 4.22 (s, 2H, C*H*$_2$), 6.98-7.29 (m, 6H, Ar); ^{13}C{^{1}H} NMR (74.97 MHz, C_6D_6): δ 15.82 (CH$_3$), 17.80 (CH$_3$), 23.67,

24.54, 24.98, 26.21 (C*Me*$_2$), 28.73, 29.35 (C*Me*$_2$), 85.34 (C*C*H$_3$), 109.78, 123.51, 123.80, 124.26, 142.78, 143.35, 147.82, 148.81, 149.56, 150.34 (Ar + C=C), 161.16 (*C*CH$_2$); ^{31}P{^{1}H} NMR (121.50 MHz, C_6D_6): δ 46.27 (s). HRMS (CI, CH_4): calcd for $C_{30}H_{44}N_2P$ $[M + H]^+$ 463.3242; found 463.3238. IR (cm^{-1}): 1363 (=CH$_2$), 1635, 1647, 1653 (C=C), 3397 (NH).

*Preparation of [{MeC(CMe)$_2$(NDipp)$_2$}POH][OTf] (**37**)*

Equimolar quantities of NaCp* and [{MeC(CMe)$_2$(NDipp)$_2$}PBr][OTf] (**30**) were mixed in toluene solution. The reaction mixture was allowed to stir overnight. The reaction mixture was then filtered and the volatiles were removed under reduced pressure. Recrystallization of the resulting yellow powder by slow evaporation of the toluene solution afforded a pale yellow crystalline product (ca. 20%). ^{1}H NMR (CD_2Cl_2, 300 MHz): δ 7.62-7.31 (m, 6H, Ar), 4.38 (s, 1H, O*H*), 3.07 (sept, 2H, *J* = 6.6 Hz, C*H*Me$_2$), 2.82 (sept, 2H, *J* = 6.6 Hz, C*H*Me$_2$), 2.23 (s, 6H, C*H*$_3$), 2.21 (s, 3H, C*H*$_3$), 1.34-1.05 (m, 24H, CH(C*H*$_3$)$_2$). ^{31}P{^{1}H} NMR (C_6D_6, 121.50 MHz): δ 71.11 (s). ^{19}F NMR (CD_2Cl_2, 282.41 MHz) δ -79.25. FTIR (CH_2Cl_2): 3364.16 cm^{-1} (O-H). HRMS (CI, CH_4): calcd for $C_{30}H_{44}N_2OP$ 479.3191; found 479.3187.

*Preparation of [{MeC(CMe)$_2$(NDipp)$_2$}H$_2$][OTf]$_2$ (**40**)*

Equimolar quantities of water and compound **30** were placed in an NMR tube that contained toluene. A few crystals of **40** were obtained after the NMR tube had been allowed to stand at 25°C for several days. Due to the limited amount of the product, this

compound was characterized solely on the basis of a single-crystal X-ray diffraction experiment.

*Preparation of [{MeC(CMe)$_2$(NDipp)$_2$}POH]Br (**41**)*

On one occasion few crystals of **41** were collected along with compound **37** (see above). Due to the limited amount of product, this compound was characterized solely on the basis of a single-crystal X-ray diffraction experiment.

*Preparation of [$\overline{CH_2N(Ar)(CMe)_2N(Ar)}$PPh][AlCl$_4$] (**44**)*

Diethyl ether (100 mL) was added to a mixture of 0.01 g (0.26 mmol) finely cut potassium metal and 0.1 g (0.23 mmol) of **21**. The reaction mixture was allowed to stir overnight. All insoluble material was filtered off, and the volatiles were removed under reduced pressure. The resulting residue was re-dissolved in 20 mL of toluene, and an equimolar quantity of $PPhCl_2$ was added. The reaction mixture was once again stirred overnight. The insoluble material that had formed was filtered off, and an equimolar quantity of solid $AlCl_3$ solid was added. After the filtrate had been stirred for 3 h, the solid material that had formed was filtered off and the volatiles were removed under reduced pressure. Compound **44** was obtained as a yellow powder in a yield of ca. 46%. ^{1}H NMR (CD_2Cl_2, 300 MHz): δ 7.40-7.32 (m, 11H, Ar), 2.68-2.75 (m, 4H, C*H*Me$_2$), 2.30 (s, 3H, C*H*$_3$), 2.29 (s, 3H, C*H*$_3$), 2.23 (s, 2H, C*H*$_2$), 0.88-1.36 (m, 24H, CH(C*H*$_3$)$_2$). ^{31}P{^{1}H} NMR (CD_2Cl_2, 121.50 MHz): δ 162.68. ^{27}Al{^{1}H} NMR (CD_2Cl_2, 78.14 MHz) δ 103.33 (s, $AlCl_4^-$). HRMS (CI, CH_4): calcd for $C_{36}H_{47}N_2P$: 538.3677; found 538.3481.

*Preparation of [$CH_2N(Ar)C(H)C(Me)\ N(Ar)PCl$] OTf (**46**)*

A solution of *n*-BuLi (0.48 mL of 2.5 M solution in hexane, 1.2 mmol) was added dropwise to a solution of [{$HC(CMe)_2(NDipp)_2$}H] (**45**) (0.5 g, 1.2 mmol) in 30 mL of hexane at room temperature. The reaction mixture was stirred for 3 h, following which neat PCl_3 (0.17 g, 1.2 mmol) was added dropwise. After being stirred overnight, the reaction mixture was filtered through Celite® and the solvent was stripped from the filtrate to afford a pale yellow oily residue. This residue was re-dissolved into 30 mL of CH_2Cl_2, followed by the addition of trimethylsilyl trifluoromethanesulfonate (0.53 g, 2.4 mmol). The reaction mixture was allowed to stir overnight, after which the solvent was removed under reduced pressure, and the resulting yellow residue was washed twice with 10 mL of pentane. Recrystallization of the resulting yellow residue from benzene solution afforded a crop of colorless crystals of **46** (0.33 g, 42% yield based on the consumption of **45**). ^{1}H NMR (CD_2Cl_2, 300 MHz): δ 9.05 (s, 1H, NH), 7.30-7.00 (m, 6H, Ar), 4.39 (s, 1H, C*H*), 2.90 (sept, 2H, J = 6.6 Hz, C*H*Me_2), 2.63-2.58 (m, 7H, C*H*Me_2 + C*H*$_3$ + C*H*$_2$), 1.33-0.82 (m, 24H, CH*Me$_2$*). ^{19}F NMR (CD_2Cl_2, 282.41 MHz): δ -79.34 (s, 3F, OTf). ^{31}P{^{1}H} NMR (CD_2Cl_2, 121.50 MHz): δ 149.40. HRMS (CI, CH_4): calcd for $C_{29}H_{40}N_2P$: 447.2929, found 447.2931. IR (CH_2Cl_2): 3215 cm^{-1} (N-H stretch).

Table of Crystallographic Data

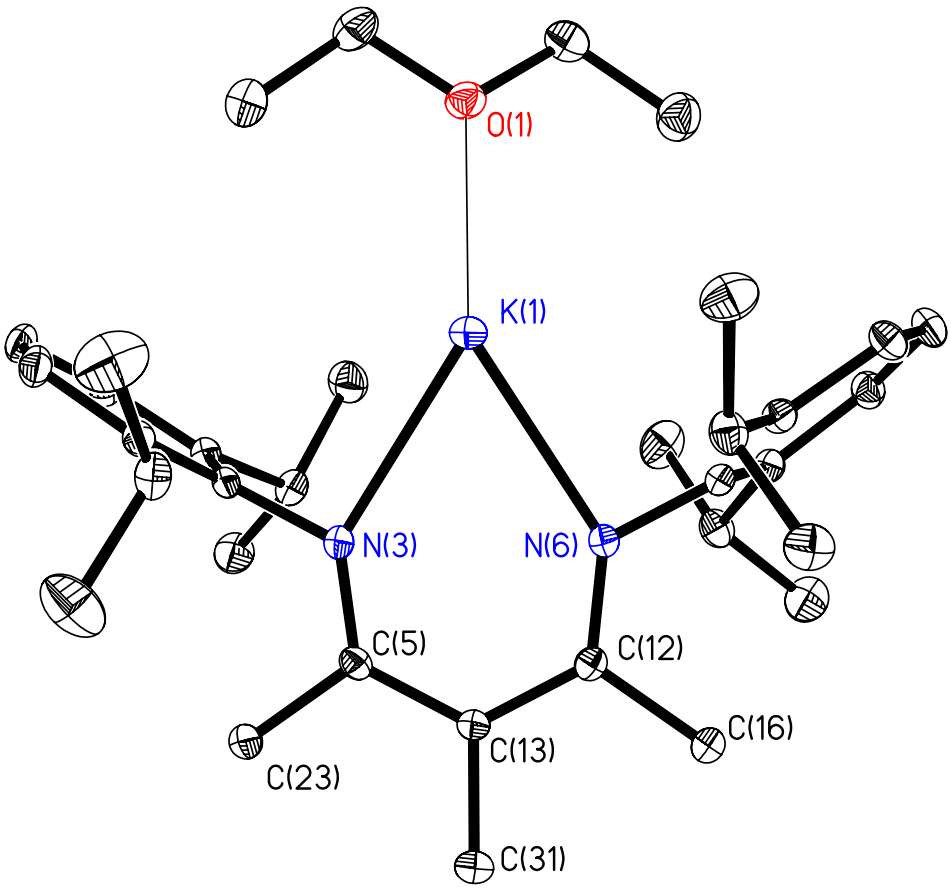

ORTEP diagram of compound **24** at 30% probability. All hydrogen atoms have been omitted for clarity.

Table 1.6. Crystal data and structure refinement for **24**.

Identification code	**24**	
Empirical formula	C34 H53 K N2 O	
Formula weight	544.88	
Temperature	153(2) K	
Wavelength	0.71069 Å	
Crystal system	monoclinic	
Space group	p21/c	
Unit cell dimensions	a = 13.154(5) Å	α= 90.000(5)°.
	b = 14.943(5) Å	β= 99.010(5)°.
	c = 17.002(5) Å	γ = 90.000(5)°.
Volume	3300.7(19) $Å^3$	
Z	4	
Density (calculated)	1.097 Mg/m^3	
Absorption coefficient	0.187 mm^{-1}	
F(000)	1192	
Crystal size	0.20 x 0.20 x 0.20 mm^3	
Theta range for data collection	2.98 to 27.50°.	
Index ranges	-17<=h<=17, -19<=k<=19, -22<=l<=22	
Reflections collected	14084	
Independent reflections	7532 [R(int) = 0.0338]	
Completeness to theta = 27.50°	99.3 %	
Absorption correction	None	
Max. and min. transmission	0.9635 and 0.9635	
Refinement method	Full-matrix least-squares on F^2	
Data / restraints / parameters	7532 / 0 / 556	
Goodness-of-fit on F^2	1.015	
Final R indices [I>2sigma(I)]	R1 = 0.0483, wR2 = 0.0958	
R indices (all data)	R1 = 0.0836, wR2 = 0.1112	
Extinction coefficient	0.0038(6)	
Largest diff. peak and hole	0.281 and -0.496 $e.Å^{-3}$	

Table 1.7. Selected Bond lengths [Å] and angles [°] for **24**.

K(1)-N(3)	2.6478(15)
K(1)-N(6)	2.6537(15)
K(1)-O(1)	2.7065(14)
O(1)-C(26)	1.428(2)
O(1)-C(25)	1.432(2)
N(3)-C(5)	1.322(2)
N(3)-C(9)	1.416(2)
N(6)-C(12)	1.322(2)
N(6)-C(7)	1.409(2)
C(5)-C(13)	1.427(2)
C(5)-C(23)	1.521(2)
C(12)-C(13)	1.419(2)
C(12)-C(16)	1.523(2)
C(13)-C(31)	1.519(2)
N(3)-K(1)-N(6)	64.56(4)
N(3)-K(1)-O(1)	137.87(4)
N(6)-K(1)-O(1)	139.01(5)
C(26)-O(1)-C(25)	111.93(15)
C(26)-O(1)-K(1)	122.11(11)
C(25)-O(1)-K(1)	125.92(11)
C(12)-N(6)-C(7)	123.14(14)
C(12)-N(6)-K(1)	140.65(11)
N(3)-C(5)-C(13)	123.93(14)
N(3)-C(5)-C(23)	118.92(15)
C(13)-C(5)-C(23)	117.15(15)
N(6)-C(12)-C(13)	123.80(15)
N(6)-C(12)-C(16)	118.76(15)
C(13)-C(12)-C(16)	117.44(14)
C(12)-C(13)-C(5)	125.01(15)
C(12)-C(13)-C(31)	117.44(15)

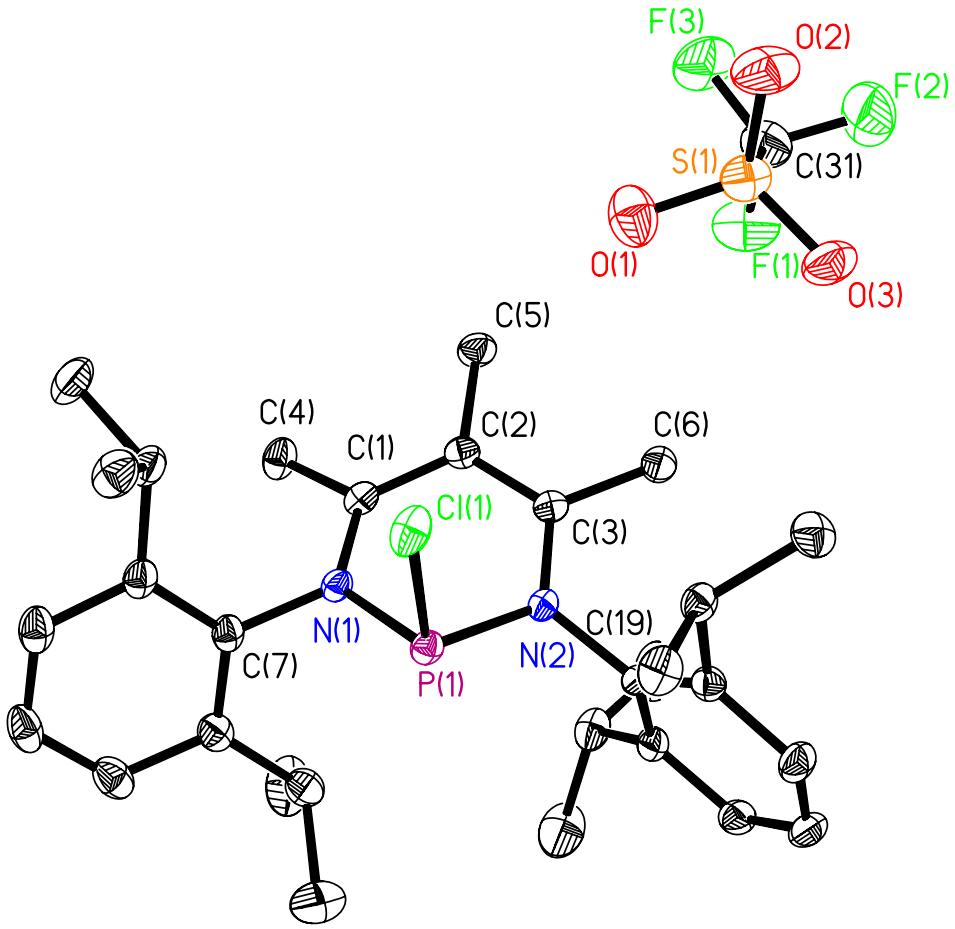

ORTEP diagram of compound **28** at 30% probability. All hydrogen atoms have been omitted for clarity.

Table 1.8. Crystal data and structure refinement for **28**.

Identification code	**28**	
Empirical formula	C62 H86 Cl2 F6 N4 O6 P2 S2	
Formula weight	1294.31	
Temperature	293(2) K	
Wavelength	0.71073 Å	
Crystal system	monoclinic	
Space group	p21/c	
Unit cell dimensions	a = 14.742(3) Å	α= 90°.
	b = 12.911(3) Å	β= 110.87(3)°.
	c = 18.370(4) Å	γ = 90°.
Volume	3267.0(11) $Å^3$	
Z	2	
Density (calculated)	1.316 Mg/m^3	
Absorption coefficient	0.281 mm^{-1}	
F(000)	1368	
Crystal size	0.2 x 0.2 x 0.2 mm^3	
Theta range for data collection	1.97 to 27.47°.	
Index ranges	-19<=h<=19, -16<=k<=16, -23<=l<=23	
Reflections collected	13840	
Independent reflections	7433 [R(int) = 0.0474]	
Completeness to theta = 27.47°	99.3 %	
Absorption correction	None	
Refinement method	Full-matrix least-squares on F^2	
Data / restraints / parameters	7433 / 0 / 390	
Goodness-of-fit on F^2	1.034	
Final R indices [I>2sigma(I)]	R1 = 0.0633, wR2 = 0.1554	
R indices (all data)	R1 = 0.1213, wR2 = 0.1834	
Largest diff. peak and hole	1.180 and -0.653 $e.Å^{-3}$	

Table 1.9. Selected Bond lengths [Å] and angles [°] for **28**.

C(1)-N(1)	1.359(4)
C(1)-C(2)	1.405(4)
C(1)-C(4)	1.490(4)
C(2)-C(3)	1.377(4)
C(2)-C(5)	1.520(4)
C(3)-N(2)	1.381(4)
C(3)-C(6)	1.491(4)
C(7)-N(1)	1.470(4)
N(1)-P(1)	1.731(2)
N(2)-P(1)	1.701(2)
P(1)-Cl(1)	2.0923(11)
N(1)-C(1)-C(2)	121.4(2)
N(1)-C(1)-C(4)	117.7(3)
C(2)-C(1)-C(4)	120.9(3)
C(3)-C(2)-C(1)	121.7(3)
C(3)-C(2)-C(5)	118.6(3)
C(1)-C(2)-C(5)	119.0(2)
C(2)-C(3)-N(2)	121.2(3)
C(2)-C(3)-C(6)	120.9(3)
N(2)-C(3)-C(6)	117.9(2)
C(1)-N(1)-C(7)	122.9(2)
C(1)-N(1)-P(1)	123.96(19)
C(7)-N(1)-P(1)	112.87(18)
C(3)-N(2)-C(19)	121.3(2)
C(3)-N(2)-P(1)	122.80(18)
C(19)-N(2)-P(1)	115.82(18)
N(2)-P(1)-N(1)	97.51(12)
N(2)-P(1)-Cl(1)	102.65(9)
N(1)-P(1)-Cl(1)	97.41(9)

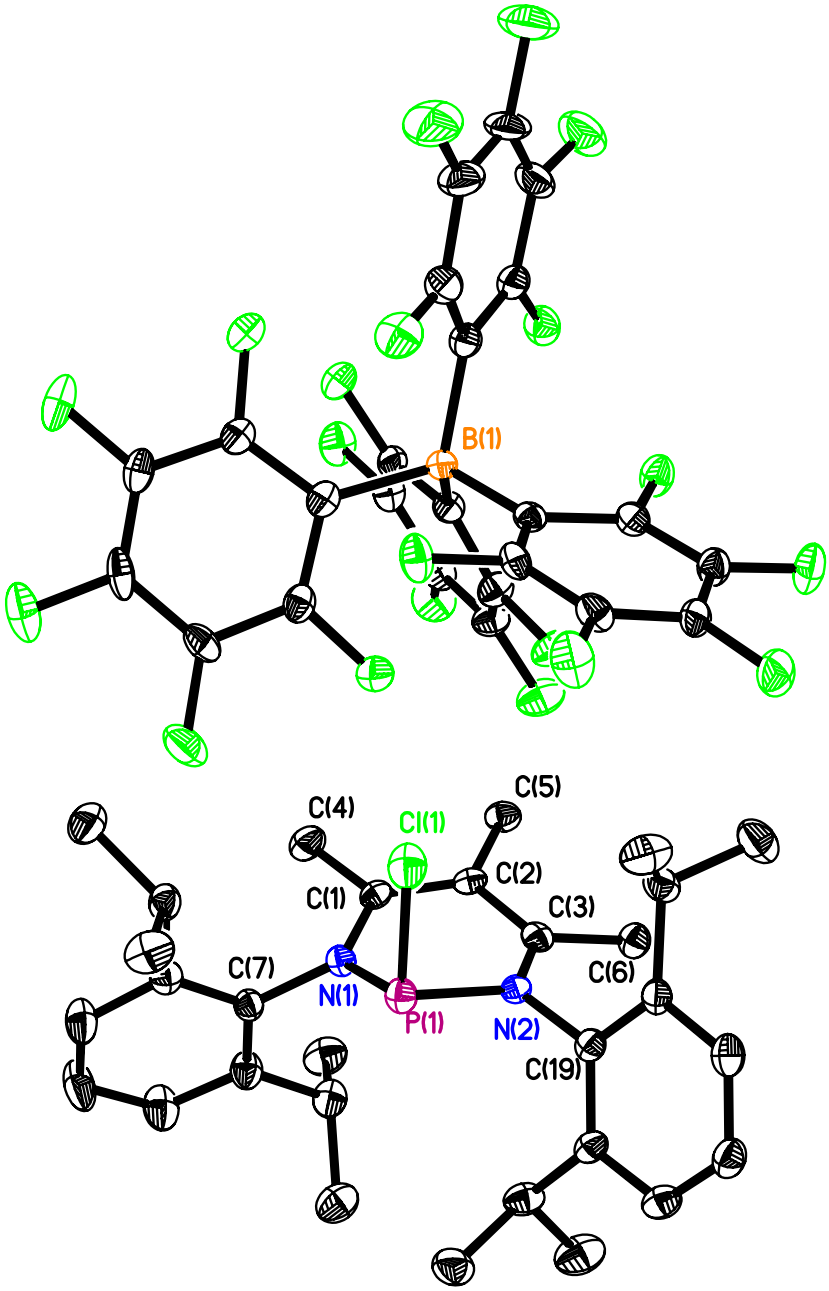

ORTEP diagram of compound **29** at 30% probability. All hydrogen atoms have been omitted for clarity.

Table 1.10. Crystal data and structure refinement for **29**.

Identification code	**29**	
Empirical formula	C108 H86 B2 Cl2 F40 N4 P2	
Formula weight	2354.27	
Temperature	153(2) K	
Wavelength	0.71069 Å	
Crystal system	monoclinic	
Space group	c2/c	
Unit cell dimensions	a = 30.278(5) Å	α= 90.000(5)°.
	b = 12.345(5) Å	β= 96.905(5)°.
	c = 28.441(5) Å	γ = 90.000(5)°.
Volume	10554(5) $Å^3$	
Z	4	
Density (calculated)	1.482 Mg/m^3	
Absorption coefficient	0.213 mm^{-1}	
F(000)	4784	
Crystal size	0.2 x 0.2 x 0.2 mm^3	
Theta range for data collection	1.35 to 27.46°.	
Index ranges	-39<=h<=39, -15<=k<=11, -36<=l<=36	
Reflections collected	20632	
Independent reflections	11813 [R(int) = 0.1130]	
Completeness to theta = 27.46°	97.9 %	
Absorption correction	None	
Refinement method	Full-matrix least-squares on F^2	
Data / restraints / parameters	11813 / 0 / 713	
Goodness-of-fit on F^2	0.885	
Final R indices [I>2sigma(I)]	R1 = 0.0616, wR2 = 0.1208	
R indices (all data)	R1 = 0.2150, wR2 = 0.1802	
Extinction coefficient	0.00108(10)	
Largest diff. peak and hole	0.528 and -0.468 $e.Å^{-3}$	

Table 1.11. Selected Bond lengths [Å] and angles [°] for **29**.

C(1)-C(2)	1.378(5)
C(1)-N(1)	1.383(5)
C(1)-C(4)	1.497(5)
C(2)-C(3)	1.422(5)
C(2)-C(5)	1.510(5)
C(3)-N(2)	1.339(5)
C(3)-C(6)	1.491(5)
C(19)-N(2)	1.471(5)
C(7)-N(1)	1.474(5)
N(1)-P(1)	1.697(3)
N(2)-P(1)	1.740(3)
P(1)-Cl(1)	2.0794(17)
C(2)-C(1)-N(1)	121.1(3)
C(2)-C(1)-C(4)	121.4(4)
N(1)-C(1)-C(4)	117.4(3)
C(1)-C(2)-C(3)	121.2(4)
C(1)-C(2)-C(5)	120.0(3)
C(3)-C(2)-C(5)	118.4(3)
N(2)-C(3)-C(2)	122.0(3)
N(2)-C(3)-C(6)	118.9(3)
C(2)-C(3)-C(6)	119.0(4)
C(1)-N(1)-C(7)	119.1(3)
C(1)-N(1)-P(1)	122.7(3)
C(7)-N(1)-P(1)	118.1(3)
C(3)-N(2)-C(19)	122.1(3)
C(3)-N(2)-P(1)	124.5(3)
C(19)-N(2)-P(1)	113.3(2)
N(1)-P(1)-N(2)	97.57(15)
N(1)-P(1)-Cl(1)	102.79(13)
N(2)-P(1)-Cl(1)	97.43(12)

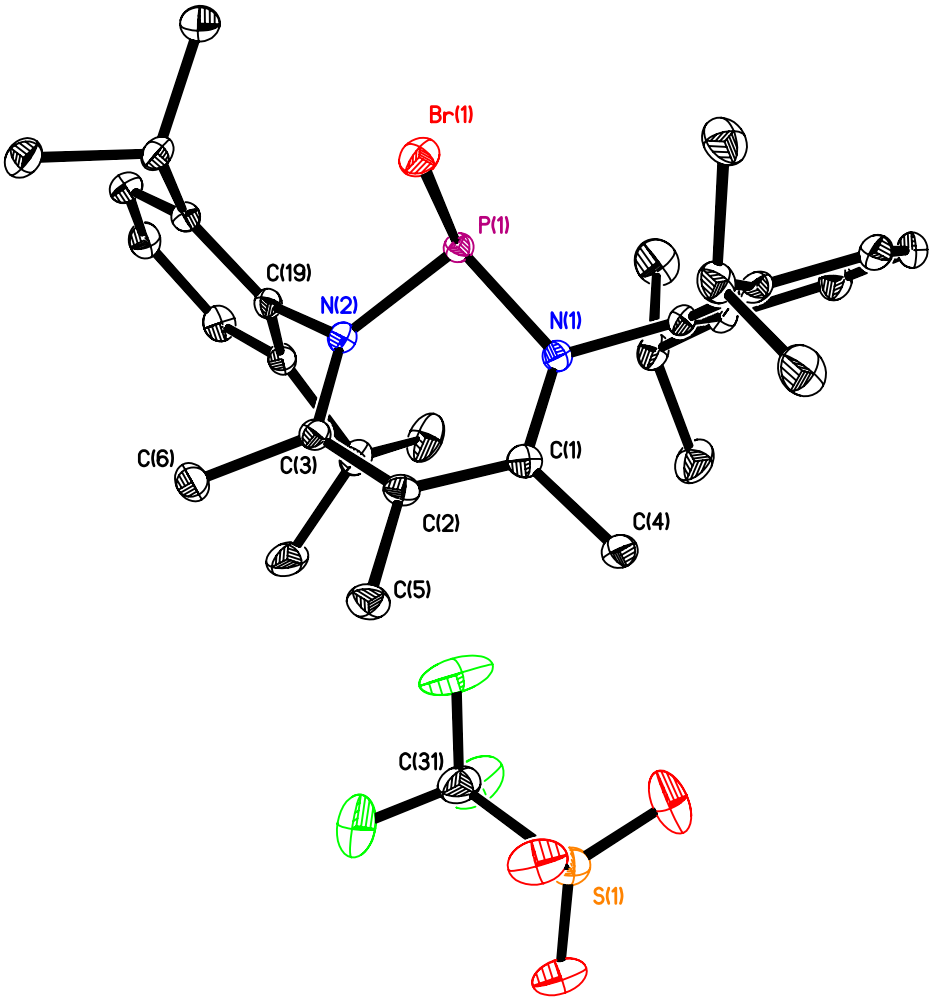

ORTEP diagram of compound **30** at 30% probability. All hydrogen atoms have been omitted for clarity.

Table 1.12. Crystal data and structure refinement for **30**.

Identification code	**30**	
Empirical formula	C31 H43 Br F3 N2 O3 P S	
Formula weight	691.61	
Temperature	153(2) K	
Wavelength	0.71069 Å	
Crystal system	Monoclinic	
Space group	p21/c	
Unit cell dimensions	a = 14.568(5) Å	α= 90.000(5)°.
	b = 12.712(5) Å	β= 110.769(5)°.
	c = 18.815(5) Å	γ = 90.000(5)°.
Volume	3257.9(19) $Å^3$	
Z	4	
Density (calculated)	1.410 Mg/m^3	
Absorption coefficient	1.426 mm^{-1}	
F(000)	1440	
Crystal size	0.12 x 0.09 x 0.08 mm^3	
Theta range for data collection	2.19 to 27.44°.	
Index ranges	-18<=h<=18, -16<=k<=13, -24<=l<=24	
Reflections collected	13329	
Independent reflections	7428 [R(int) = 0.0380]	
Completeness to theta = 27.44°	99.9 %	
Absorption correction	Semi-empirical from equivalents	
Max. and min. transmission	0.8944 and 0.8475	
Refinement method	Full-matrix least-squares on F^2	
Data / restraints / parameters	7428 / 0 / 390	
Goodness-of-fit on F^2	1.033	
Final R indices [I>2sigma(I)]	R1 = 0.0427, wR2 = 0.1003	
R indices (all data)	R1 = 0.0828, wR2 = 0.1303	
Largest diff. peak and hole	0.541 and -0.615 $e.Å^{-3}$	

Table 1.13. Selected Bond lengths [Å] and angles [°] for **30**.

C(1)-N(1)	1.349(4)
C(1)-C(2)	1.409(4)
C(1)-C(4)	1.483(4)
C(2)-C(3)	1.384(4)
C(2)-C(5)	1.518(4)
C(3)-N(2)	1.383(4)
C(3)-C(6)	1.489(4)
C(7)-N(1)	1.473(4)
C(19)-N(2)	1.475(4)
N(1)-P(1)	1.740(2)
N(2)-P(1)	1.706(2)
P(1)-Br(1)	2.2640(10)
N(1)-C(1)-C(2)	121.3(3)
N(1)-C(1)-C(4)	119.0(3)
C(2)-C(1)-C(4)	119.7(3)
C(3)-C(2)-C(1)	121.6(3)
C(3)-C(2)-C(5)	119.8(3)
C(1)-C(2)-C(5)	117.9(3)
N(2)-C(3)-C(2)	120.7(3)
N(2)-C(3)-C(6)	117.5(3)
C(2)-C(3)-C(6)	121.8(3)
C(1)-N(1)-C(7)	122.6(2)
C(1)-N(1)-P(1)	123.8(2)
C(7)-N(1)-P(1)	113.37(18)
C(3)-N(2)-C(19)	121.0(2)
C(3)-N(2)-P(1)	122.5(2)
C(19)-N(2)-P(1)	116.36(18)
N(2)-P(1)-N(1)	97.40(11)
N(2)-P(1)-Br(1)	103.93(9)
N(1)-P(1)-Br(1)	97.59(9)

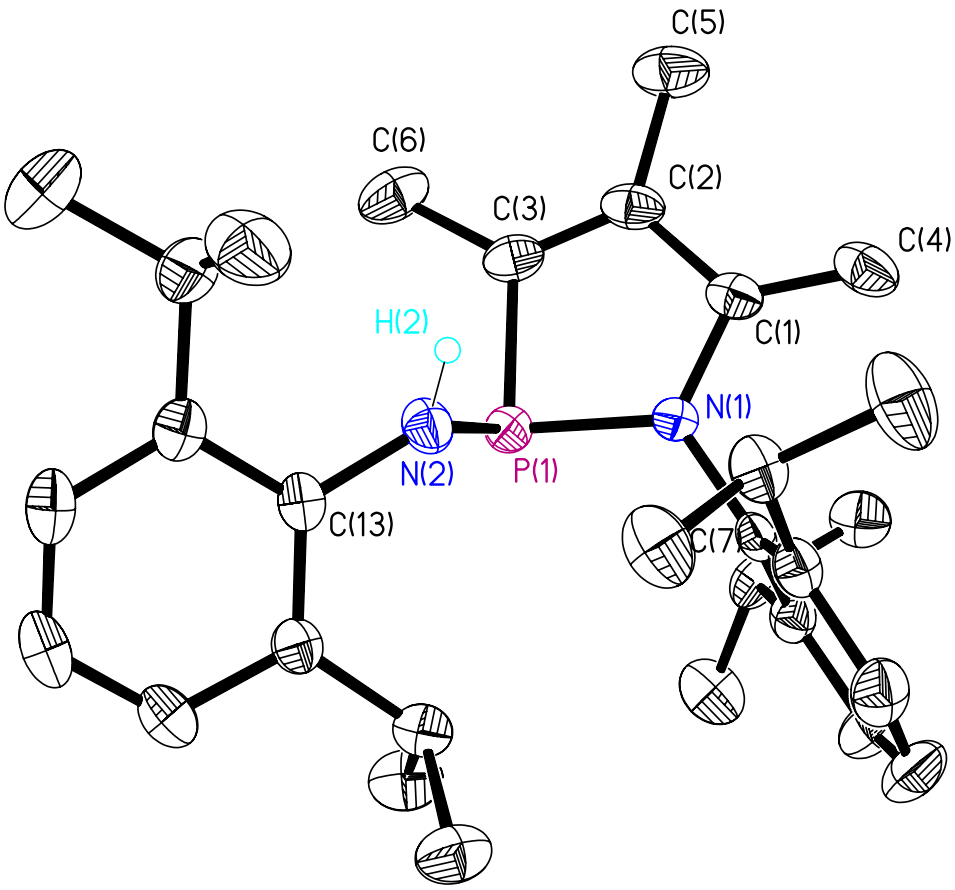

ORTEP diagram of compound **32** at 40% probability.

Table 1.14. Crystal data and structure refinement for **32**.

Identification code	**32**	
Empirical formula	C30 H43 N2 P	
Formula weight	462.63	
Temperature	153(2) K	
Wavelength	0.71069 Å	
Crystal system	Trigonal	
Space group	r-3	
Unit cell dimensions	a = 38.7640(10) Å	α= 90°.
	b = 38.764(2) Å	β= 90°.
	c = 10.065(3) Å	γ = 120°.
Volume	13098(4) $Å^3$	
Z	18	
Density (calculated)	1.056 Mg/m^3	
Absorption coefficient	0.113 mm^{-1}	
F(000)	4536	
Crystal size	0.20 x 0.20 x 0.20 mm^3	
Theta range for data collection	2.98 to 27.49°.	
Index ranges	-50<=h<=50, -46<=k<=50, -12<=l<=13	
Reflections collected	31685	
Independent reflections	6673 [R(int) = 0.0826]	
Completeness to theta = 27.49°	99.8 %	
Absorption correction	Semi-empirical from equivalents	
Max. and min. transmission	0.9778 and 0.9778	
Refinement method	Full-matrix least-squares on F^2	
Data / restraints / parameters	6673 / 0 / 310	
Goodness-of-fit on F^2	1.025	
Final R indices [I>2sigma(I)]	R1 = 0.0645, wR2 = 0.1720	
R indices (all data)	R1 = 0.1324, wR2 = 0.1955	
Extinction coefficient	0.00000(10)	
Largest diff. peak and hole	0.371 and -0.369 $e.Å^{-3}$	

Table 1.15. Selected Bond lengths [Å] and angles [°] for **32**.

C(1)-C(4)	1.341(4)
C(1)-N(1)	1.400(3)
C(1)-C(2)	1.471(4)
C(2)-C(3)	1.334(4)
C(2)-C(5)	1.512(3)
C(3)-C(6)	1.501(4)
C(3)-P(1)	1.817(3)
C(7)-N(1)	1.441(3)
C(13)-N(2)	1.425(3)
N(1)-P(1)	1.714(2)
N(2)-P(1)	1.702(2)
N(2)-H(2N)	0.99(3)
C(4)-C(1)-N(1)	124.3(3)
C(4)-C(1)-C(2)	126.7(3)
N(1)-C(1)-C(2)	109.1(2)
C(3)-C(2)-C(1)	113.8(2)
C(3)-C(2)-C(5)	126.5(3)
C(1)-C(2)-C(5)	119.6(2)
C(2)-C(3)-C(6)	127.6(3)
C(2)-C(3)-P(1)	112.5(2)
C(6)-C(3)-P(1)	120.0(2)
C(1)-N(1)-C(7)	121.11(19)
C(1)-N(1)-P(1)	115.90(16)
C(7)-N(1)-P(1)	122.31(15)
C(13)-N(2)-P(1)	123.69(17)
C(13)-N(2)-H(2N)	120.2(16)
P(1)-N(2)-H(2N)	114.4(16)
N(2)-P(1)-N(1)	103.95(10)
N(2)-P(1)-C(3)	102.90(11)
N(1)-P(1)-C(3)	88.69(11)

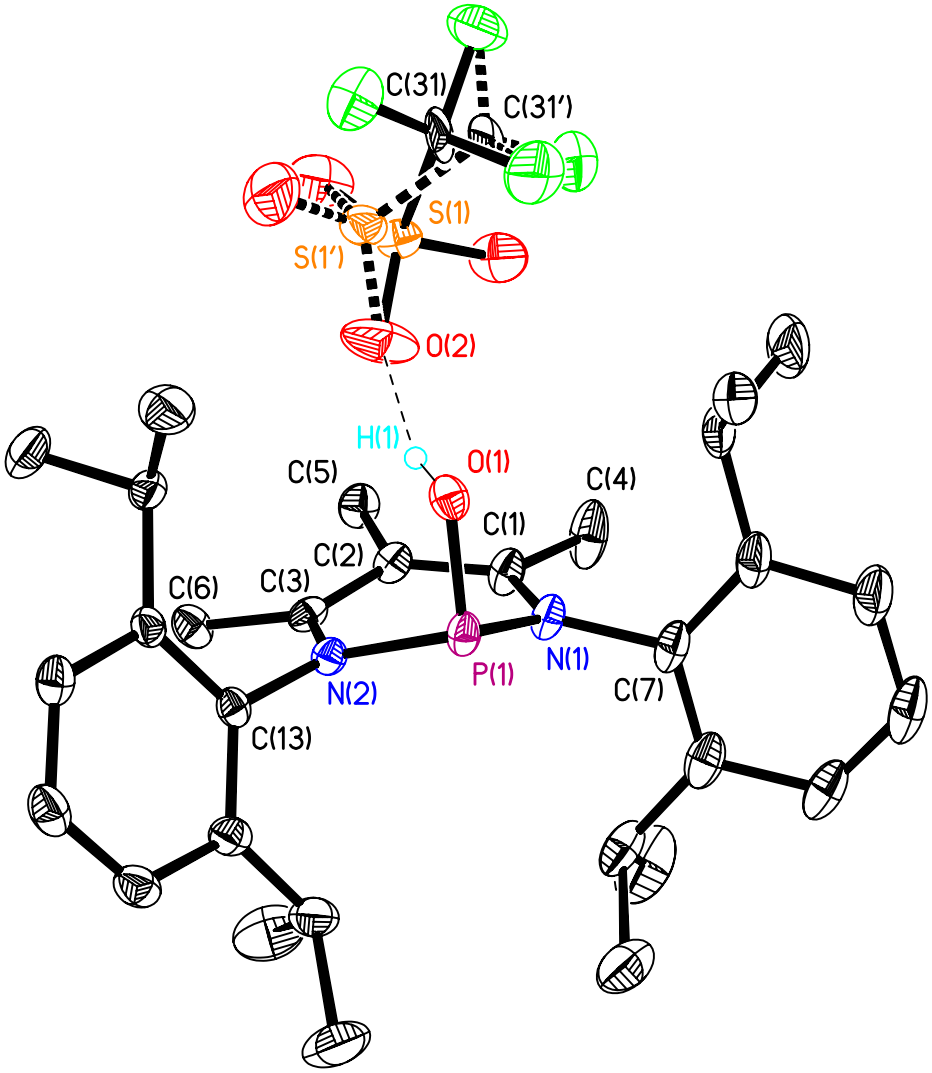

ORTEP diagram of compound **37** at 30% probability.

Table 1.16. Crystal data and structure refinement for **37**.

Identification code	**37**	
Empirical formula	C31 H44 F3 N2 O4 P S	
Formula weight	628.71	
Temperature	153(2) K	
Wavelength	0.71073 Å	
Crystal system	orthorhombic	
Space group	p212121	
Unit cell dimensions	a = 8.9393(18) Å	α= 90°.
	b = 12.215(2) Å	β= 90°.
	c = 30.199(6) Å	γ = 90°.
Volume	3297.5(11) $Å^3$	
Z	4	
Density (calculated)	1.266 Mg/m^3	
Absorption coefficient	0.200 mm^{-1}	
F(000)	1336	
Crystal size	0.2 x 0.2 x 0.2 mm^3	
Theta range for data collection	1.80 to 25.00°.	
Index ranges	-10<=h<=10, -14<=k<=14, -35<=l<=35	
Reflections collected	5512	
Independent reflections	5512 [R(int) = 0.0000]	
Completeness to theta = 25.00°	98.3 %	
Absorption correction	None	
Refinement method	Full-matrix least-squares on F^2	
Data / restraints / parameters	5512 / 0 / 416	
Goodness-of-fit on F^2	1.103	
Final R indices [I>2sigma(I)]	R1 = 0.0531, wR2 = 0.1294	
R indices (all data)	R1 = 0.0658, wR2 = 0.1406	
Absolute structure parameter	0.00	
Extinction coefficient	0.042(3)	
Largest diff. peak and hole	0.502 and -0.470 $e.Å^{-3}$	

Table 1.17. Bond lengths [Å] and angles [°] for **37**.

C(1)-N(1)	1.360(4)
C(1)-C(2)	1.391(4)
C(1)-C(4)	1.507(4)
C(2)-C(3)	1.410(4)
C(2)-C(5)	1.501(4)
C(3)-N(2)	1.344(3)
C(3)-C(6)	1.491(4)
N(1)-P(1)	1.741(2)
N(2)-P(1)	1.755(2)
O(1)-P(1)	1.584(2)
O(1)-H(1)	0.8200
N(1)-C(1)-C(2)	122.2(3)
N(1)-C(1)-C(4)	118.2(3)
C(2)-C(1)-C(4)	119.6(3)
C(1)-C(2)-C(3)	121.2(3)
C(1)-C(2)-C(5)	119.5(3)
C(3)-C(2)-C(5)	119.2(3)
N(2)-C(3)-C(2)	121.9(3)
N(2)-C(3)-C(6)	119.2(3)
C(2)-C(3)-C(6)	119.0(2)
C(1)-N(1)-C(7)	121.8(2)
C(1)-N(1)-P(1)	124.2(2)
C(7)-N(1)-P(1)	113.74(18)
C(3)-N(2)-C(13)	122.6(2)
C(3)-N(2)-P(1)	125.3(2)
C(13)-N(2)-P(1)	110.91(17)
P(1)-O(1)-H(1)	109.5
O(1)-P(1)-N(1)	104.02(11)
O(1)-P(1)-N(2)	102.51(11)
N(1)-P(1)-N(2)	95.68(11)

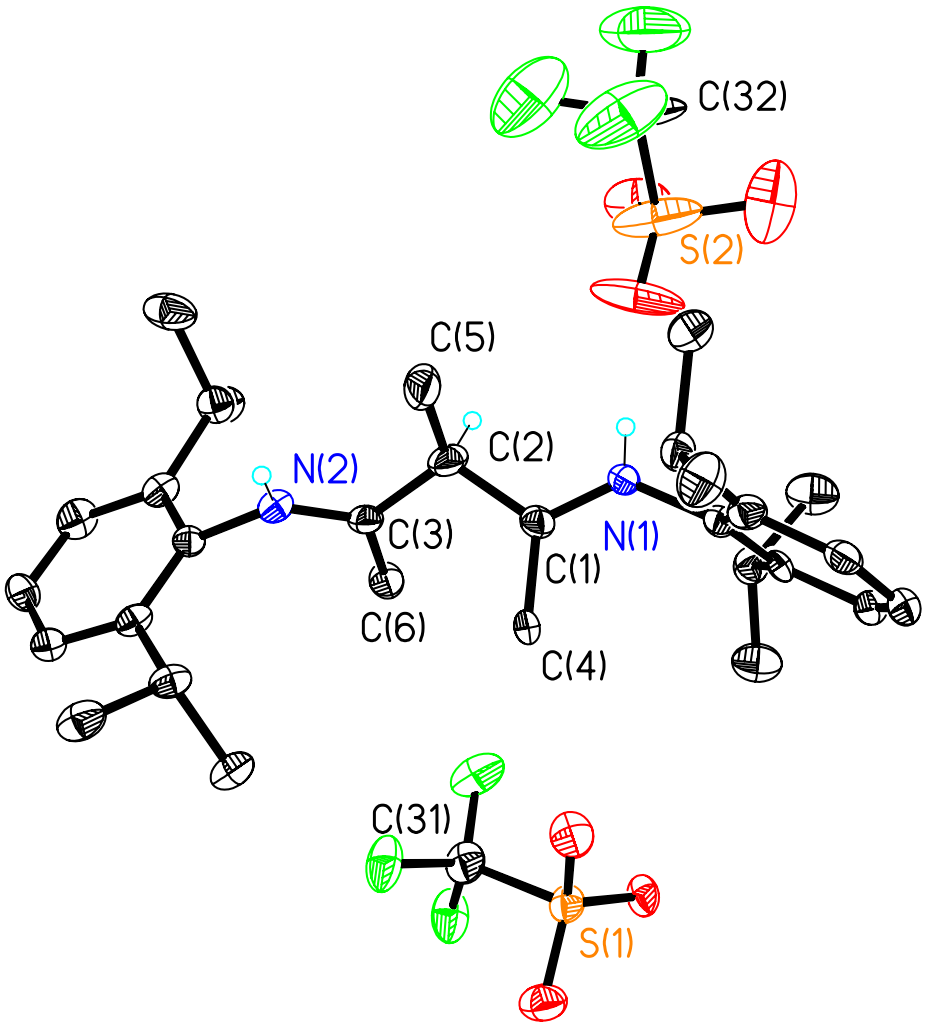

ORTEP diagram of compound **40** at 30% probability.

Table 1.18. Crystal data and structure refinement for **40**.

Identification code	**40**	
Empirical formula	C32 H46 F6 N2 O6 S2	
Formula weight	732.83	
Temperature	153(2) K	
Wavelength	0.71073 Å	
Crystal system	triclinic	
Space group	p-1	
Unit cell dimensions	a = 10.274(2) Å	α= 66.63(3)°.
	b = 13.708(3) Å	β= 87.55(3)°.
	c = 14.967(3) Å	γ = 70.97(3)°.
Volume	1819.9(6) $Å^3$	
Z	2	
Density (calculated)	1.337 Mg/m^3	
Absorption coefficient	0.220 mm^{-1}	
F(000)	772	
Crystal size	0.31 x 0.20 x 0.16 mm^3	
Theta range for data collection	2.11 to 27.33°.	
Index ranges	-13<=h<=10, -17<=k<=17, -19<=l<=18	
Reflections collected	12244	
Independent reflections	8130 [R(int) = 0.0531]	
Completeness to theta = 27.33°	98.9 %	
Absorption correction	None	
Max. and min. transmission	0.9656 and 0.9349	
Refinement method	Full-matrix least-squares on F^2	
Data / restraints / parameters	8130 / 0 / 442	
Goodness-of-fit on F^2	1.080	
Final R indices [I>2sigma(I)]	R1 = 0.1156, wR2 = 0.3055	
R indices (all data)	R1 = 0.2528, wR2 = 0.3908	
Extinction coefficient	0.022(5)	
Largest diff. peak and hole	1.544 and -0.688 $e.Å^{-3}$	

Table 1.19. Selected Bond lengths [Å] and angles [°] for **40**.

N(2)-C(3)	1.285(8)
N(2)-C(13)	1.456(8)
N(2)-H(2)	0.81(7)
N(1)-C(1)	1.279(9)
N(1)-C(7)	1.441(9)
N(1)-H(1)	0.73(10)
C(3)-C(6)	1.476(9)
C(3)-C(2)	1.503(9)
C(1)-C(4)	1.482(9)
C(1)-C(2)	1.516(10)
C(2)-C(5)	1.477(10)
C(2)-H(2A)	1.0000
C(3)-N(2)-C(13)	126.0(6)
C(3)-N(2)-H(2)	117(5)
C(13)-N(2)-H(2)	117(5)
C(1)-N(1)-C(7)	124.9(7)
C(1)-N(1)-H(1)	115(9)
C(7)-N(1)-H(1)	120(9)
N(2)-C(3)-C(6)	121.6(6)
N(2)-C(3)-C(2)	119.4(6)
C(6)-C(3)-C(2)	118.6(6)
N(1)-C(1)-C(4)	121.5(6)
N(1)-C(1)-C(2)	116.9(6)
C(4)-C(1)-C(2)	121.4(6)
C(5)-C(2)-C(3)	117.0(7)
C(5)-C(2)-C(1)	109.2(6)
C(3)-C(2)-C(1)	114.6(6)

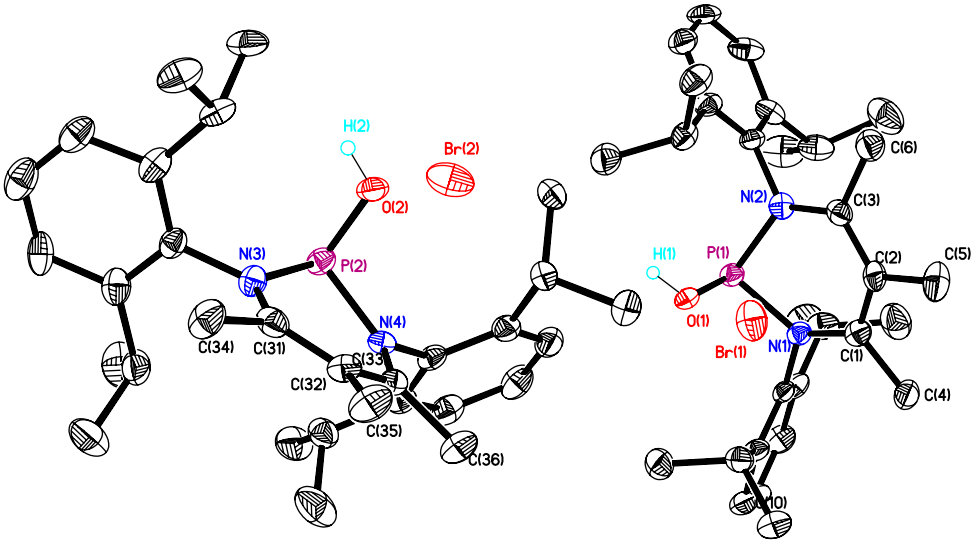

ORTEP diagram of compound **41**at 30% probability.

Table 1.20. Crystal data and structure refinement for **41**.

Identification code	**41**	
Empirical formula	C30 H44 Br N2 O P	
Formula weight	559.55	
Temperature	153(2) K	
Wavelength	0.71073 Å	
Crystal system	monoclinic	
Space group	p21/c	
Unit cell dimensions	a = 16.119(3) Å	α= 90°.
	b = 14.615(3) Å	β= 90.62(3)°.
	c = 25.530(5) Å	γ = 90°.
Volume	6014(2) $Å^3$	
Z	8	
Density (calculated)	1.236 Mg/m^3	
Absorption coefficient	1.444 mm^{-1}	
F(000)	2368	
Crystal size	0.21 x 0.3 x 0.2 mm^3	
Theta range for data collection	1.26 to 27.51°.	
Index ranges	-20<=h<=20, -17<=k<=18, -33<=l<=33	
Reflections collected	22127	
Independent reflections	13636 [R(int) = 0.1666]	
Completeness to theta = 27.51°	98.7 %	
Absorption correction	None	
Refinement method	Full-matrix least-squares on F^2	
Data / restraints / parameters	13636 / 0 / 632	
Goodness-of-fit on F^2	0.840	
Final R indices [I>2sigma(I)]	R1 = 0.0822, wR2 = 0.1586	
R indices (all data)	R1 = 0.3151, wR2 = 0.2343	
Extinction coefficient	0.0105(5)	
Largest diff. peak and hole	0.957 and -0.701 $e.Å^{-3}$	

Table 1.21. Selected Bond lengths [Å] and angles [°] for **41**.

O(1)-P(1)	1.600(5)
O(1)-H(1)	0.8200
O(2)-P(2)	1.588(4)
O(2)-H(2)	0.8200
C(1)-N(1)	1.368(9)
C(1)-C(2)	1.388(10)
C(1)-C(4)	1.509(9)
C(2)-C(3)	1.390(10)
C(2)-C(5)	1.527(10)
C(3)-N(2)	1.350(9)
C(3)-C(6)	1.525(9)
C(31)-N(3)	1.359(9)
C(31)-C(32)	1.369(10)
C(31)-C(34)	1.538(9)
C(32)-C(33)	1.394(9)
C(32)-C(35)	1.529(10)
C(33)-N(4)	1.347(8)
C(33)-C(36)	1.511(9)
N(1)-P(1)	1.750(6)
N(2)-P(1)	1.757(6)
N(3)-P(2)	1.754(6)
N(4)-P(2)	1.743(6)
P(1)-O(1)-H(1)	109.5
P(2)-O(2)-H(2)	109.5
N(1)-C(1)-C(2)	121.3(7)
N(1)-C(1)-C(4)	117.8(6)
C(2)-C(1)-C(4)	120.9(7)
C(1)-C(2)-C(3)	121.5(7)
C(1)-C(2)-C(5)	119.7(7)
C(3)-C(2)-C(5)	118.8(7)
N(2)-C(3)-C(2)	123.4(7)
N(2)-C(3)-C(6)	117.3(7)
C(2)-C(3)-C(6)	119.3(7)
N(3)-C(31)-C(32)	123.8(7)
N(3)-C(31)-C(34)	116.7(7)
C(32)-C(31)-C(34)	119.5(7)
C(31)-C(32)-C(33)	121.4(7)
C(31)-C(32)-C(35)	118.4(7)
C(33)-C(32)-C(35)	120.2(7)
N(4)-C(33)-C(32)	121.9(7)
N(4)-C(33)-C(36)	119.2(6)
C(32)-C(33)-C(36)	118.9(7)
C(1)-N(1)-C(7)	120.4(6)
C(1)-N(1)-P(1)	125.7(5)
C(7)-N(1)-P(1)	113.1(4)
C(3)-N(2)-C(13)	122.2(6)
C(3)-N(2)-P(1)	123.9(5)
C(13)-N(2)-P(1)	113.6(5)
C(31)-N(3)-C(37)	122.7(6)

C(31)-N(3)-P(2)	123.6(5)
C(37)-N(3)-P(2)	113.4(5)
C(33)-N(4)-C(43)	120.6(6)
C(33)-N(4)-P(2)	126.1(5)
C(43)-N(4)-P(2)	112.5(4)
O(1)-P(1)-N(1)	103.1(3)
O(1)-P(1)-N(2)	103.5(3)
N(1)-P(1)-N(2)	95.6(3)
O(2)-P(2)-N(4)	102.7(3)
O(2)-P(2)-N(3)	103.3(3)
N(4)-P(2)-N(3)	95.7(3)

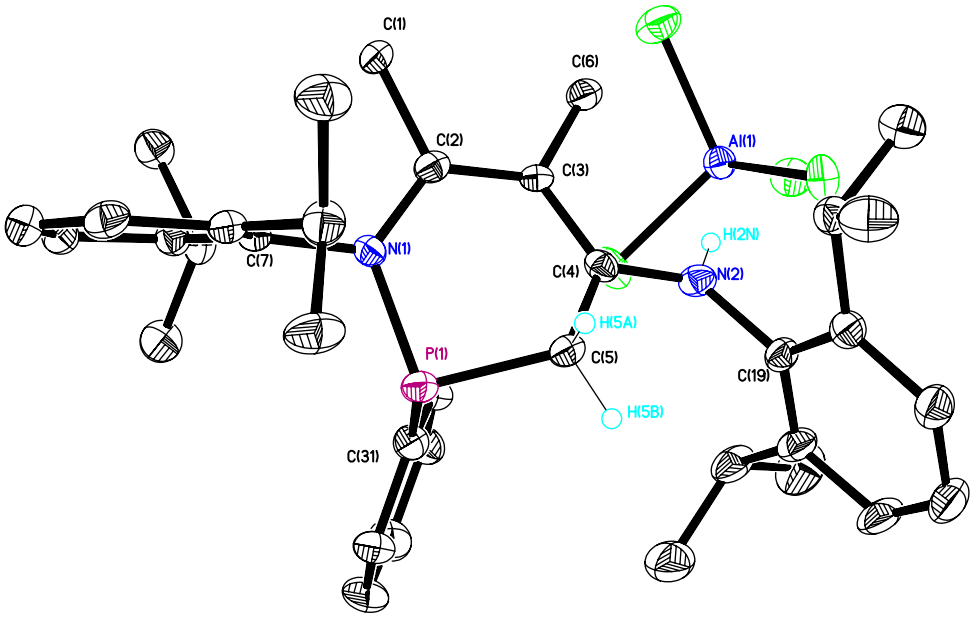

ORTEP diagram of compound **44** at 30% probability.

Table 1.22. Crystal data and structure refinement for **44·CH_2Cl_2**.

Identification code	**44·CH_2Cl**	
Empirical formula	C37 H50 Al Cl6 N2 P	
Formula weight	793.44	
Temperature	153(2) K	
Wavelength	0.71069 Å	
Crystal system	Monoclinic	
Space group	P21/c	
Unit cell dimensions	a = 13.640(5) Å	α= 90.000(5)°.
	b = 13.086(5) Å	β= 97.133(5)°.
	c = 23.778(5) Å	γ = 90.000(5)°.
Volume	4211(2) $Å^3$	
Z	4	
Density (calculated)	1.251 Mg/m^3	
Absorption coefficient	0.494 mm^{-1}	
F(000)	1664	
Crystal size	0.30 x 0.20 x 0.10 mm^3	
Theta range for data collection	3.02 to 27.50°.	
Index ranges	-17<=h<=17, -13<=k<=16, -30<=l<=30	
Reflections collected	30020	
Independent reflections	9608 [R(int) = 0.1703]	
Completeness to theta = 27.50°	99.3 %	
Absorption correction	None	
Max. and min. transmission	0.9522 and 0.8659	
Refinement method	Full-matrix least-squares on F^2	
Data / restraints / parameters	9608 / 0 / 438	
Goodness-of-fit on F^2	0.987	
Final R indices [I>2sigma(I)]	R1 = 0.0743, wR2 = 0.1608	
R indices (all data)	R1 = 0.2296, wR2 = 0.2099	
Largest diff. peak and hole	0.634 and -0.881 e.$Å^{-3}$	

Table 1.23. Selected Bond lengths [Å] and angles [°] for **44·CH_2Cl_2**.

C(1)-C(2)	1.513(6)
C(2)-N(1)	1.358(6)
C(2)-C(3)	1.386(6)
C(3)-C(4)	1.392(6)
C(3)-C(6)	1.515(6)
C(4)-N(2)	1.337(6)
C(4)-C(5)	1.492(6)
C(5)-P(1)	1.824(5)
C(5)-H(5A)	0.9900
C(5)-H(5B)	0.9900
C(7)-N(1)	1.449(5)
C(31)-P(1)	1.817(5)
N(1)-P(1)	1.763(4)
N(2)-H(2N)	0.78(4)
N(1)-C(2)-C(3)	124.4(4)
N(1)-C(2)-C(1)	116.0(4)
C(3)-C(2)-C(1)	119.5(4)
C(2)-C(3)-C(4)	121.0(4)
C(2)-C(3)-C(6)	121.0(4)
C(4)-C(3)-C(6)	117.8(4)
N(2)-C(4)-C(3)	122.6(4)
N(2)-C(4)-C(5)	115.9(4)
C(3)-C(4)-C(5)	121.4(4)
C(4)-C(5)-P(1)	114.5(3)
C(2)-N(1)-C(7)	123.0(4)
C(2)-N(1)-P(1)	124.5(3)
C(7)-N(1)-P(1)	112.1(3)
C(4)-N(2)-C(19)	126.3(4)
C(4)-N(2)-H(2N)	116(3)
N(1)-P(1)-C(31)	103.8(2)
N(1)-P(1)-C(5)	96.85(19)
C(31)-P(1)-C(5)	104.1(2)

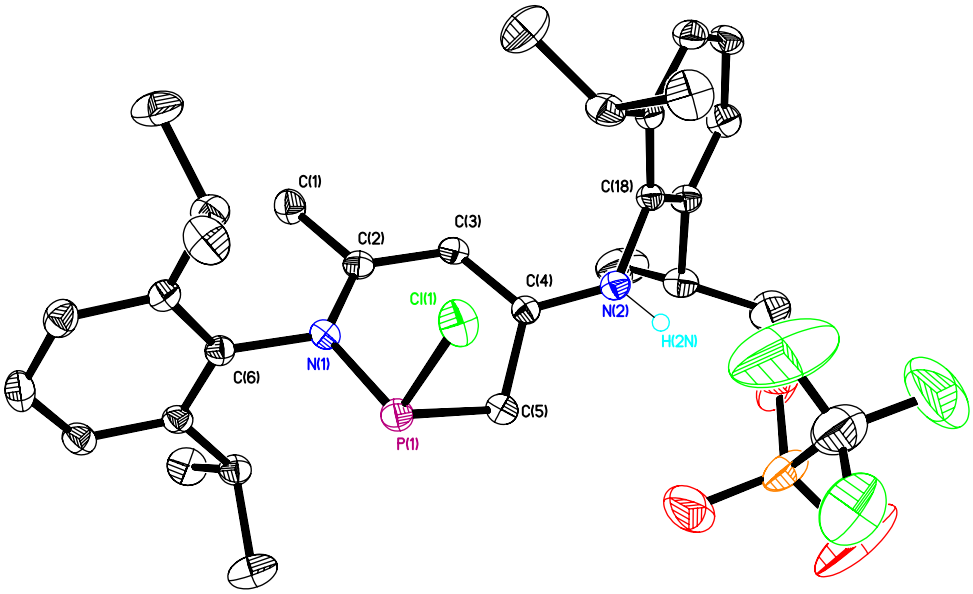

ORTEP diagram of compound **46** at 30% probability.

Table 1.24. Crystal data and structure refinement for **46**.

Identification code	**46**	
Empirical formula	C30 H41 Cl F3 N2 O3 P S	
Formula weight	633.13	
Temperature	153(2) K	
Wavelength	0.71073 Å	
Crystal system	Triclinic	
Space group	p-1	
Unit cell dimensions	a = 10.356(2) Å	α= 100.40(3)°.
	b = 12.553(3) Å	β= 90.53(3)°.
	c = 14.756(3) Å	γ = 110.49(3)°.
Volume	1761.9(8) $Å^3$	
Z	2	
Density (calculated)	1.193 Mg/m^3	
Absorption coefficient	0.259 mm^{-1}	
F(000)	668	
Crystal size	0.15 x 0.13 x 0.12 mm^3	
Theta range for data collection	2.03 to 27.49°.	
Index ranges	-13<=h<=11, -15<=k<=16, -17<=l<=19	
Reflections collected	11412	
Independent reflections	7893 [R(int) = 0.0431]	
Completeness to theta = 27.49°	97.5 %	
Absorption correction	Semi-empirical from equivalents	
Max. and min. transmission	0.970 and 0.962	
Refinement method	Full-matrix least-squares on F^2	
Data / restraints / parameters	7893 / 0 / 383	
Goodness-of-fit on F^2	0.962	
Final R indices [I>2sigma(I)]	R1 = 0.0722, wR2 = 0.1841	
R indices (all data)	R1 = 0.1463, wR2 = 0.2103	
Largest diff. peak and hole	0.632 and -0.462 e.$Å^{-3}$	

Table 1.25. Selected Bond lengths [Å] and angles [°] for **46**.

C(1)-C(2)	1.461(5)
C(2)-N(1)	1.385(4)
C(2)-C(3)	1.385(5)
C(3)-C(4)	1.396(4)
C(4)-N(2)	1.310(4)
C(4)-C(5)	1.495(5)
C(5)-P(1)	1.821(4)
C(6)-N(1)	1.466(4)
N(1)-P(1)	1.718(3)
N(2)-O(3)	2.738(4)
N(2)-H(2N)	0.85(4)
P(1)-Cl(1)	2.0955(15)
N(1)-C(2)-C(3)	121.9(3)
N(1)-C(2)-C(1)	117.7(3)
C(3)-C(2)-C(1)	120.3(3)
C(2)-C(3)-C(4)	123.7(3)
N(2)-C(4)-C(3)	122.8(3)
N(2)-C(4)-C(5)	117.9(3)
C(3)-C(4)-C(5)	119.3(3)
C(4)-C(5)-P(1)	112.7(2)
C(2)-N(1)-C(6)	120.8(3)
C(2)-N(1)-P(1)	125.7(2)
C(6)-N(1)-P(1)	113.5(2)
C(4)-N(2)-C(18)	126.0(3)
C(4)-N(2)-O(3)	129.2(2)
C(18)-N(2)-O(3)	104.6(2)
C(4)-N(2)-H(2N)	122(3)
C(18)-N(2)-H(2N)	112(3)
O(3)-N(2)-H(2N)	8(3)
N(1)-P(1)-C(5)	97.90(15)
N(1)-P(1)-Cl(1)	102.82(10)
C(5)-P(1)-Cl(1)	96.74(12)

References

(1). (a) Osborn, J. A.; Jardine, F. H.; Young, J. F.; Wilkinson, G. *J. Chem. Soc. A,* **1966**, 1711; (b) Birch, A. J.; Williamson, D. H.; *Org. React.* **1976**, *24*, 1; (c) James, B.R. *Homogeneous Hydrogenation*, John Wiley & Sons, New York, **1973**; (d) Evans, D. A.; Fu, G. C.; Hoveyda, A. H. *J. Am. Chem. Soc* **1988**. *110*, 6917; (e) Ojima, I.; Kogure, T.; Nagai, Y. *Tetrahedron Lett.* **1972**, 5035

(2). a) Grubbs, R. H. *Handbook of Metathesis*; Wiley-VCH, Germany, **2003**; (b) Grubbs, R.H.; Trnka, T.M.: *Ruthenium-Catalyzed Olefin Metathesis* in *Ruthenium in Organic Synthesis* Murahashi, S.-I. ed., Wiley-VCH, Germany, **2004**. (c) Trnka, T. M.; Grubbs, R. H. *Acc. Chem. Res.* **2001**, *34*, 18; (d) Scholl, M.; Ding, S.; Lee, C. W.; Grubbs, R. H. *Org. Lett.* **1999**, *1*, 953; (e) Schwab, P.; Grubbs, R. H.; Ziller, J. W. *J. Am. Chem. Soc.* **1996**, *118* , 100; (f) Hong, S. H.; Grubbs, R. H. *J. Am. Chem. Soc.* **2006**, *128*, 3508; (g) White, S. R.; Sottos, N. R.; Geubelle, P. H.; Moore, J. S.; Kessler, M. R.; Sriram, S. R.; Brown, E. N.; Viswanathan, S. *Nature* **2001**, *409,* 794

(3). (a) Tamao, K.; Sumitani, K.; Kumada, M. *Bull. Chem. Soc. Jpn.* **1976**, *49*, 1958; (b) Valentine, D. H., Jr.; Hillhouse, J. H. *Synthesis* **2003**, 2437.; (c) Tsuji, J.; *Palladium Reagents and Catalysts*; Wiley, Chichester, U. K., **2004**; (d) *Metal-Catalyzed Cross-Coupling Reactions*; Diederich, F.; Stang, P. J., Eds.; Wiley-VCH, 1998; (e) *Metal-Catalyzed Cross-Coupling Reactions*; de Meijere, A.; Diederich, F.; Eds.; Wiley-VCH, **2004**

(4). (a) Knowles, W. S. *Angew. Chem. Int. Ed.* **2002**, *41*, 1998; (b) Noyori, R. *Angew. Chem. Int. Ed.* **2002**, *41*, 2008; (c) Hayashi, T. Kumada, M. *Acc. Chem. Res.* **1982**, *15*, 395; (d) Noyori, R.; *Asymmetric Catalysis in Organic Synthesis*; Wiley, New York, 1994

(5). (a) Cowley, A. H.; Kemp, R. A. *Chem. Rev.* **1985**, *85*, 367; (b) Gudat, D. *Coord. Chem. Rev.* **1997**, *163*, 71

(6). (a) Herrmann, W.A.; Kocher, C. *Angew. Chem. Int. Ed. Engl.* **1997**, *36*, 2162; (b) Herrmann, W.A. *Angew. Chem. Int. Ed. Engl.* **2002**, *41*, 1290; (c) Carmalt, C. J.; Cowley, A. H. *Adv. Inorg. Chem.* **2000**, *50*, 1

(7). (a) Sakakibara, K.; Yamashita, M.; Nozaki, K. *Tetrahedron Lett.* **2005**, *46(6)*, 959; (b) Hardman, N. J.; Abrams, M. B.; Pribisko, M. A.; Gilbert, T. M.; Martin, R. L.; Kubas, G. J.; Baker, R. T. *Angew. Chem. Int. Ed.* **2004**, *43*, 1955

(8). (a) Spinney, H. A.; Yap, G. P. A.; Korobkov, I.; DiLabio, G.; Richeson, D. S. *Organometallics* **2006**, *25*, 3541; (b) Abrams, M. B.; Scott, B. L.; Baker, R. T. *Organometallics* **2000**, *19*, 4944; (c) Breit, B. *J. Mol. Catal. A* **1999**, *143*, 143

(9). Keaton, R. J.; Cross, J. L.; Baker, R. T. *Abstract of Papers, 232nd ACS national Meeting*, San Francisco, CA, United States, Sept. 10-14, **2006**

(10). Litvinov, I. A.; Naumov, V. A.; Gryaznova, T. V.; Pudovik, A. N.; Kibardin, A. M. *Dokl. Akad. Nauk SSSR* **1990**, *312*, 623

(11). Arduengo, A. J.; Harlow, R. L.; Kline, M. *J. Am. Chem. Soc.* **1991**, *113*, 361

(12). Kibardin, A. M.; Litvinov, I. A.; Naumov, V. A.; Struchkov, Yu. T.; Gryaznova, T. V.; Mikhailov, Yu. B.; Pudovik, A. N. *Dokl. Akad. Nauk SSSR* **1988**, *298*, 369.

(13). (a) Denk, M. K.; Gupta, S.; Ramachandran, R. *Tetrahedron Lett.* **1996**, *37*, 9025; (b) Denk, M. K.; Gupta, S.; Lough, A. *Eur. J. Inorg. Chem.* **1999**, 41; (c) Burford, N.; Clyburne, J. A. C.; Losier, P.; Parks, T. M. in *Synthetic Methods Organometallic. and Inorganic Chemistr*y, Vol. 3, pg. 21, Herrmann, W. A. ed., Georg Thieme Verlag, Stuttgart, **1996**

(14). Reeske, G.; Cowley, A. H.; *Inorg. Chem.* **2007**, *46 (4)*, 1426

(15). Reeske, G.; Hoberg, C. R.; Hill, N. J.; Cowley, A. H.; *J. Am. Chem. Soc.* **2006**, *128*, 2800

(16). Cowley, A. H.; Cushner, M. C.; Szobota, J. S. *J. Am. Chem. Soc.* **1978**, *100*, 7784

(17). Bourget-Merle, L.; Lappert, M. F.; Severn, J. R.; *Chem. Rev.* **2002**, *102*, 3031

(18). Hitchcock, P. B.; Lappert, M. F.; Lui, D.–S. *J. Chem. Soc., Chem. Commum.* **1994**, 2637

(19). Aboelella, N. W.; Kryatov, S. V.; Gherman, B. F.; Brennessel, W. W.; Young, V. G., Jr.; Sarangi, R.; Rybak-Akimova, E. V.; Hodgson, K. O.; Hedman, B.; Solomon, E. I.; Cramer, C. J.; Tolman, W. B.; *J. Am. Chem. Soc.* **2004**, *126*, 16896

(20). (a) Hill, M. S.; Hitchcock, P. B. *Chem. Commun.* **2004**, 1818; (b) Hill, M. S.; Hitchcock, P. B.; Pongtavornpinyo, R. *Angew. Chem. Int. Ed.* **2005**, *44*, 4231; (c) Hill, M. S.; Hitchcock P. B.; Pongtavornpinyo R.; *Science* **2006**, *5769(311)*, 1904

(21). Vidovic D.; Moore J. A.; Jones J. N.; Cowley A. H. *J. Am Chem Soc.* **2005**, *127*, 4566

(22). (a) Ragogna, P. J.; Burford, N.; D'eon, M.; McDonald, R. *Chem. Commun.* **2003**, 1052; (b) Burford, N.; D'eon, M.; Ragogna, P.; McDonald, R.; Ferguson, M. J. *Inorg. Chem.* **2004**, *43*, 734

(23). Hitchcock, P. B.; Lappert, M. F.; Nycz, J. E. *Chem. Commun. 2003*, 1142

(24). Maraval, A.; Owsianik, K.; Arquier, D.; Igau, A.; Coppel, Y.; Donnadieu, B.; Zablocka, M.; Majoral, J. –P. *Eur. J. Inorg. Chem.* **2003**, 960

(25). Feldman, J.; McLain, S. J.; Parthasarathy, A.; Marshall, W. J.; Calabrese, C. J.; Arthur, S. D. *Organometallics* **1997**, *16*, 1514

(26). (a) Cui, C.; Roesky, H. W.; Schmidt, H.-G.; Noltemeyer, M.; Hao, H.; Cimpoesu, F. *Angew. Chem. Int. Ed.* **2000**, *39*, 4274; (b) Hardman, N. J.; Eichler, B. E.; Power, J. J. *Chem. Commun.* **2000**, 1991

(27). Wang, Y.; Quillian, B.; Wei, P.; Wang, H.; Yang, X. –J.; Xie, Y.; King, B. R.; Scheyer, P. V. R.; Schaefer, III, F. H.; Robinsong, G. H. *J. Am Chem. Soc.* **2005**, *127*, 11944

(28). Driess, M.; Yao, S.; Brym, M.; van Wüllen, C.; Lentz, D. *J. Am. Chem. Soc.* **2006**, *128*, 9628

(29). Driess, M.; Yao, S.; Brym, M.; van Wüllen, C. *Angew. Chem. Int. Ed.* **2006**, *45*, 6730

(30). Panda, A.; Stender, M.; Wright, R. J.; Olmstead, M. M.; Klavins, P.; Power, P. P. *Inorg. Chem.* **2002**, *41*, 3909

(31). Bailey, P. J.; Liddle, S. T.; Parsons, S. *Acta Cryst.* **2001**, *E57*, o865

(32). Clegg, W.; Cope, E. K.; Edwards, A. J.; Mair, F. S. *Inorg. Chem.* **1998**, *37*, 2317

(33). Ding, Y.; Roesky, H. W.; Noltemeyer, M.; Schmidt, H.-G. *Organometallics* **2001**, *20*, 1190

(34). Vidovic, D.; Lu, Z.; Reeske, G.; Moore, J. A.; Cowley, A. H. *Chem. Commun.* **2006**, 3501.

(35). Bondi, A *J. Phys. Chem.* **1964**, *68*, 441

(36). Lammertsma,K. *Top. Curr. Chem.,* **2003**, *229*, 95

(37). (a) Mathey, F.; Tran Huy, N. H.; Marinetti, A. *Helv. Chim. Acta*, **2001**, *84*, 2938; (b) Cowley, A. H. *Acc. Chem. Res.* **1997**, *30*, 445.

(38). Li, X.; Weissmann, S. I.; Lin, T. S.; Gaspar, P. P.; Cowley, A. H.; Smirnov, A. I. *J. Am. Chem. Soc.* **1994**, *116*, 7899

(39). (a) Basuli, F.; Kilgore, U. J.; Brown, D.; Huffman, J. C.; Mindiola, D. J. *Organometallics*, **2004**, *23*, 6166; (b) Hamaki, H.; Takeda, N.; Tokitoh, N. *Organometallics*, **2006**, *25*, 2457; (c) Bai, G.; Wei, P.; Stephan, D. W. *Organometallics*, **2006**, *25*, 2649; (d) Basuli, F.; Huffman, J. C.; Mindiola, D. J. *Inorg. Chim. Acta,* **2007**, *360*, 246.

(40). Mukhametov, F. S.; Eliseenkova, R.M.; and Korshin, E. E. *Zh. Obshch. Khim.*, **1989**, *59*, 321

(41). (a) Ding, Y.; Roesky, H. W.; Noltemeyer, M.; Schmidt, H.-G. *Organometallics*, **2001**, *20*, 4806; (b) Qian, B.; Baek, S. W.; Smith III, M. R. *Polyhedron*, **1999**, *18*, 2405; (c) Lesikar, L. A.; and Richards, A. F. *J. Organomet. Chem.*, **2006**, *691*, 4250

(42). Ellis, B. D.; Macdonald, C. L. B. *Inorg. Chim. Acta*, **2007**, *360*, 329

(43). Clyburne, J. A. C.; McKenzie, I.; Moore, J. A.; Cowley, A. H. to be published

(44). Vidovic, D.; Findlater, M.; Cowley, A. H. *J. Am. Chem. Soc.* **2007**, *129*, 8436

(45). (a) Hoge, B.; Garcia, P.; Willner, H.; Oberhammer, H. *Chem. Eur. J.,* **2006**, *12*, 3567; (b) Corbridge, D. E. C. *Phosphorus: An Outline of its Chemistry, Biochemistry and Uses*, Elsevier, Amsterdam, **1995**, 5th ed., p.336; (c) Hoge, B.; Wiebe, W.; Hettl, S.; Neufeind, S.; Thösen, C. *J. Organomet. Chem.* **2005**, *690*, 2382

(46). Burford, N.; Herbert, D. E.; Ragogna, R. J.; McDonald, R.; Ferguson, M. J. *J. Am. Chem. Soc.* **2004**, *126*, 17067

(47). Burford, N.; Phillips, A. D.; Spinney, H. A.; Lumsden, M.; Werner-Zwanziger, U.; Ferguson, M. J.; McDonald, R. *J. Am. Chem. Soc.* **2005**, *127*, 3921

(48). Sheldrick, G. M. SHELL-PC Version 5;03, Siemens Analytical X-ray Instruments, Inc., Madison, WI, USA, 1994

CHAPTER 2

PART I

β-Diketiminate Supported Group 13 Compounds

Introduction

The presence of six rather than eight valence electrons at the central atom of group 13 compounds results in the exceptional Lewis acidity of such compounds. This property enables neutral three-coordinate group 13 species to accommodate two additional valence electrons resulting in the facile coordination of anionic and neutral bases, such as hydride, halide, alkyl, and aryl functional groups to give anionic four-coordinate products. This characteristic acceptor property has spawned a wide variety of uses for group 13 compounds ranging from reagents for the synthesis of pharmaceuticals and other valuable products[1] to activators/initiators for a variety of catalytic polymerization processes[2].

Compared with these neutral Lewis acids, the corresponding cationic species have been found to be even more reactive due to the presence of a formal positive charge and, in some cases, greater electronic deficiency. Several cations of the group 13 elements (aluminum, gallium and indium) have been reported.[3] For example, the cationic aluminum complex **1** has been used as a catalyst for the polymerization of oxiranes.[4] The

polymerization of ethylene using low-coordinate aluminum derivatives has also been disclosed.[5]

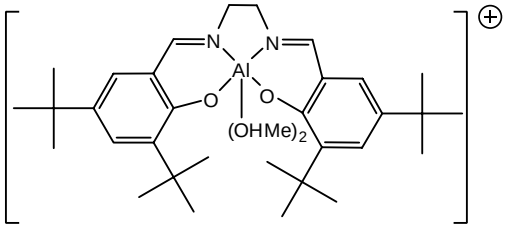

1

As summarized in review articles[6], three types of boron monocations have been identified namely borinium (**2**), borenium (**3**) and boronium (**4**) (Figure 2.1).

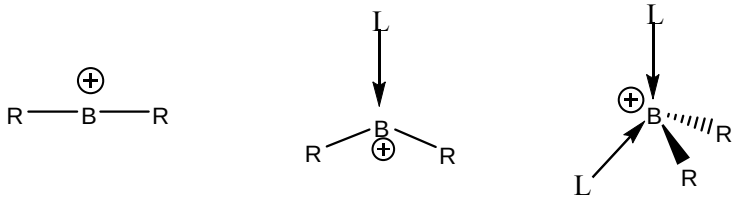

2 **3** **4**

Figure 2.1. Three types of boron monocations.

Several different synthetic methods have been reported for the synthesis of boron cations **2**, **3** and **4**. The most commonly employed methods include B-X bond heterolysis (where X is a hydrogen or halogen atom). Other methods include protic and electrophilic attack of B-N bonds, nucleophilic displacement of halides, and metathesis reactions.[6a]

Since borinium cations are two coordinate, the boron atom features only four valence electrons. As a consequence, borinium cations are highly reactive and usually studied in the gas phase. However, borinium cations are isolable at ambient temperature provided

that they are kinetically stabilized by the use of bulky amido (**5**)[7] or phosphinimide ligands (**6**)[8] (Figure 2.2) and non-reactive anion are present.

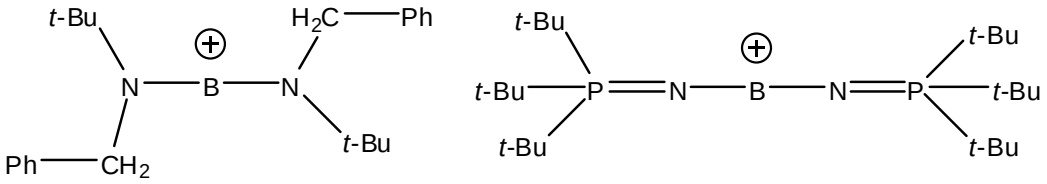

5 **6**

Figure 2.2. Examples of isolable borinium cations.

Prior to 1985, only three structurally authenticated borenium cations had been reported. In each case, a bulky base capable of donor stabilization was required to form a

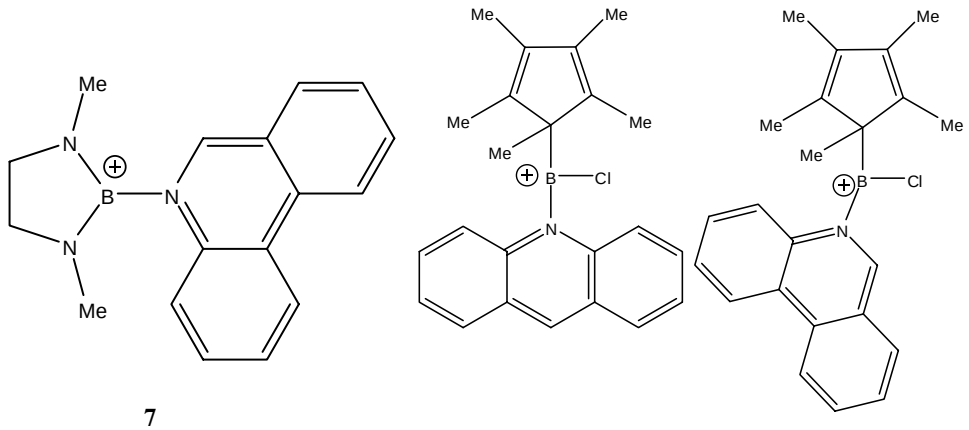

7 **8**

five-membered nitrogen based boracycle (**7**).[9] In 1987, Jutzi *et al.*[10] reported the synthesis of borenium complexes via the reactions of dichloro(η^1-pentamethyl-

cyclopentadienyl)borane with the bulky nitrogen-based donors acridine and phenanthridine (**8**). Several cyclic borenium cations have been reported in the recent years. For example, Manners *et al.*[11] showed that a halide anion could be abstracted from a precursor boratophosphazene to yield the hybrid borazine-phosphazene cation **9**. Piers *et al.*[12] demonstrated that it is possible to use a non-nitrogen based boracycle to stabilize a borenium cation with the help of a pyridine base (**10**).

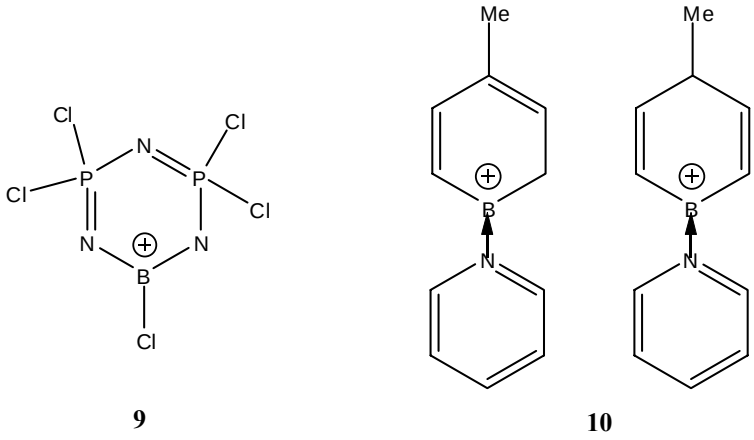

9 **10**

Figure 2.3. Examples of cyclic borenium cation.

Boronium cations have received the most attention thus far because the presence of a complete octet of electrons at boron and the coordinative saturation at this center render these cations particularly stable. In almost all cases, boronium cations feature two covalently bonded ligands and two σ-donors that occupy the unfilled orbitals on the boron centers. A large numbers of such cations have been reported.[6]

β-diketiminate-supported group 13 complexes are now receiving increased attention, particular those that feature aluminum and gallium, and a variety of synthetic strategies

have emerged for such compounds. For example, β-diketiminato aluminum and gallium dimethyl derivatives have been synthesized in good yields by treatment of the conjugate acid of a β-diketiminate ligand with trimethylalane or trimethylgallane.[13] β-diketiminate aluminum and gallium dihalides can be conveniently produced by the reactions of the appropriate β-diketiminate reagent with the metal trihalides.[13b,14] The corresponding diiodoalanes can be prepared in good yields by treatment of the dimethyl derivatives with molecular iodine.[13a] Some dichloro β-diketiminate-supported derivatives of aluminum and gallium have also been synthesized, but in low yields, by treatment of the conjugate acids of the β-diketiminate ligands with metal trichlorides in the presence of Et_3N.[15] The availability of the extreme bulky Dipp ligand **11** has permitted the isolation of novel monomeric compounds of Al(I)[13a], Ga(I)[16], In(I)[17] and Tl(I)[18].

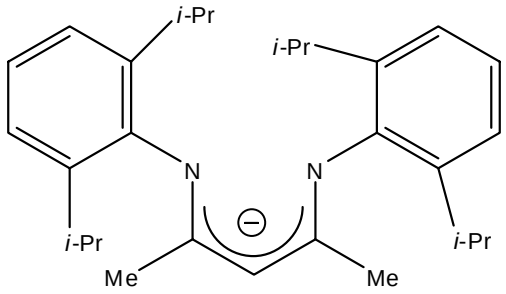

Figure 2.4. The Dipp-substituted β-diketiminate ligand **11**.

Although the first boron-substituted complexes were reported several years ago by treatment of a β-diketimine with $BF_3 \cdot OEt_2$,[19] or by heating a mixture of a trialkylborane

and a nitrile in an autoclave[20], much less is known about β-diketiminato compounds of born than those of the heavier congeners.

Of the reported β-diketiminate-supported boron dihalide complexes the boron difluorides are the most common (Figure 2.5). Several routes have been devised for the preparation of these difluroboranes. For example, Compound **12** was prepared *via* the

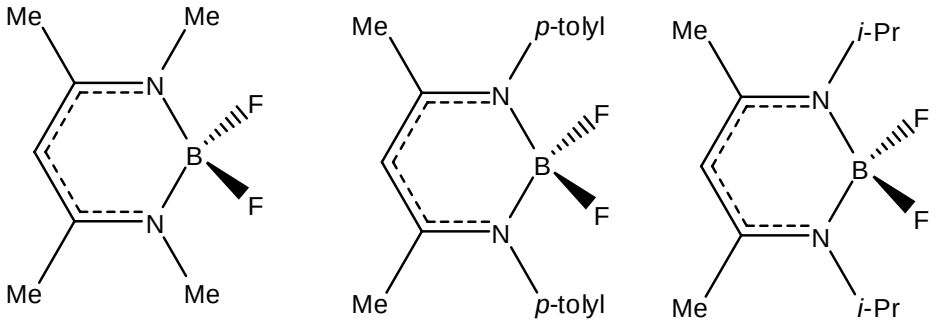

12 **13** **14**

Figure 2.5. Examples of β-diketiminate-boron difluorides.

reaction of the conjugate acid of the corresponding β-diketiminate ligand with $BF_3 \cdot Et_2O$ in the presence of triethylamine.[21] However, the yield of this reaction was low. Compound **13** was prepared via the metathetical reaction of the lithium salt of the diketiminate ligand with $BF_3 \cdot Et_2O$.[22] The third difluroborane, compound **14**, was formed by treatment of N-(isopropylidene)-isopropylamine with *t*-BuLi, followed by the addition of N-methylacetonitrilium tetrafluoroborate.[23] Prior to the present work, compound **15** (Scheme 2.1) was the only example of a β-diketiminate-substituted boron dihalide other than the above mentioned difluorides.[24] Scheme 2.1 summarizes the series of steps

involved in the preparation of compound **15**. On the basis of ^{11}B NMR evidence, it was claimed that **15** is in equilibrium with the chloroborenium chloride salt, **16**.

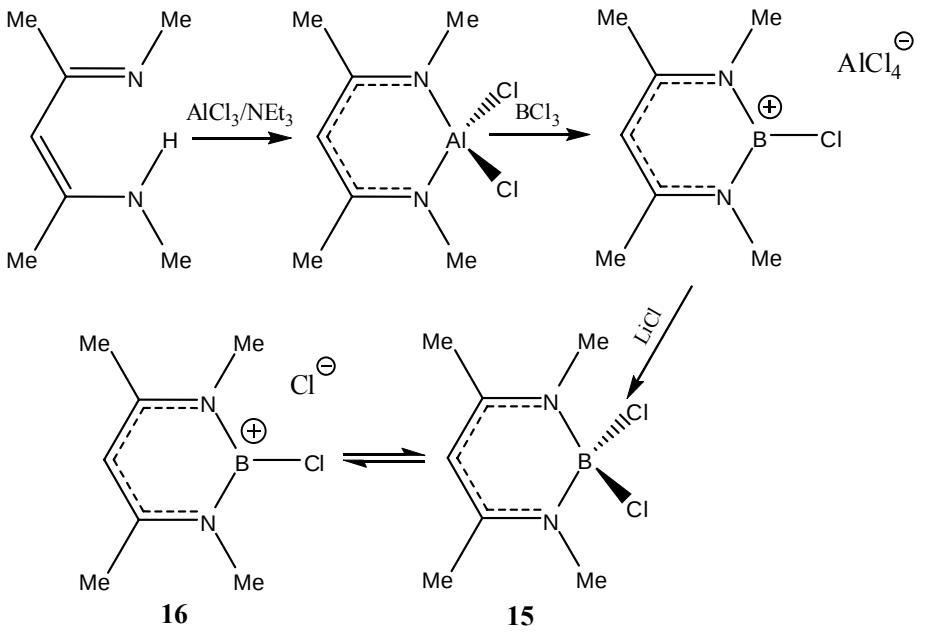

Scheme 2.1. Preparation of a β-diketiminate-supported boron dichloride.

These boron difluoride complexes **12**, **13** and **14** provide facile access to the corresponding alkyl complexes, which in turn, are useful for generation of boron cations. However, some caution has to be exercised in the choice of alkylating agent. For example, compound **13** reacts with alkyllithium reagents to give products that arise from ligand deprotonation or nucleophilic attack at the imine carbon atoms of the β-diketiminate ligand, while treatment of **13** with alkyl Grignard reagents cleanly affords the dialkyl products.[22]

Although β-diketiminate-supported boron cations had been reported previously, [22,24] no X-ray crystallographic data were available for such cations prior to the present work.

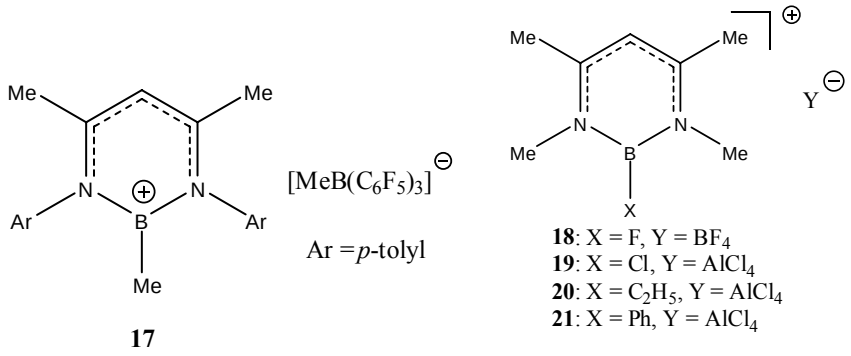

17

Figure 2.6. Examples of β-diketiminate-supported boron cations.

In the case of compound **17**, NMR data suggested that the anion and cation are weakly associated in solution.[22] Two methods employed for the generation of these β-diketiminatoboron cations have been reported, namely fluoride anion abstraction from a precursor boron difluoride using $BF_3{\cdot}Et_2O$ and the metal exchange/chloride anion abstraction process that takes place when a β-diketiminate-supported aluminum dichloride is treated with boron halides (Scheme 2.2).[24]

A further point of interest in neutral β-diketiminate-supported group 13 compounds concerns their ability to serve as ligands for transition metal complexes. Several such compounds have been reported, namely, $[\{HC(CMe)_2(NDipp)_2\}GaFe(CO)_4]$ (**22**), $[\{HC(CMe)_2(NDipp)_2\}Ga(Cl)Rh(PPh)_3]$ (**23**) and $[(\{HC(CMe)_2(NDipp)_2\}Ga)_2Au]^+$ (**24**)

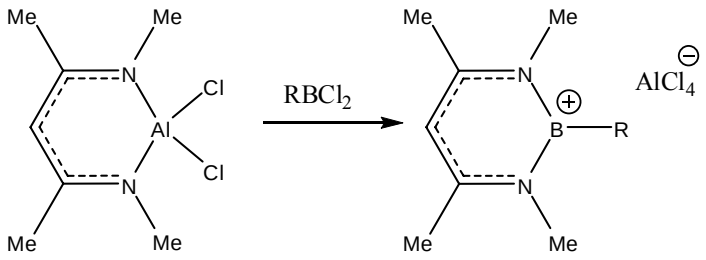

R = Cl, C_2H_5, Ph

Scheme 2.2. Generation of a boron cation by a metal exchange/halide ion abstraction process.

as summarized in Scheme 2.3.[25] The iron complex **22** was prepared by displacement of one carbonyl group of $Fe(CO)_5$ with the more nucleophilic gallium (I) derivative [{$HC(CMe)_2(NDipp)_2$}Ga] complex. Complexes **23** and **24** were synthesized by the insertion of [{$HC(CMe)_2(NDipp)_2$}Ga] into a metal-chlorine bond of $(Ph_3P)_2RhCl$ and AuCl, respectively. Both complexes were found to be very electrophilic despite the fact that they are coordinated to electron-rich Rh(I) and Au(I) centers. Some analogous Al-Pd complexes have also been reported.[26] All of these organometallic complexes require the availability of Al(I) or Ga(I) β-diketiminate starting materials. In these reactions the Al(I) and Ga(I) β-diketiminates play a similar role to that of the corresponding pentamethylcyclopentadienyl-substituted Al(I) and Ga(I) derivatives $(Cp^*Al)_4$ and $(Cp^*Ga)_6$ (Cp^* = pentamethylcyclopentadienyl). Complexes such as [$Ni(AlCp^*)_3$], [$Fe(AlCp^*)_n$] and [$RhCp^*(CH_3)_2(GaCp^*)$] are electron rich[27] and promote C-H, C-C or Si-H activation reactions[28].

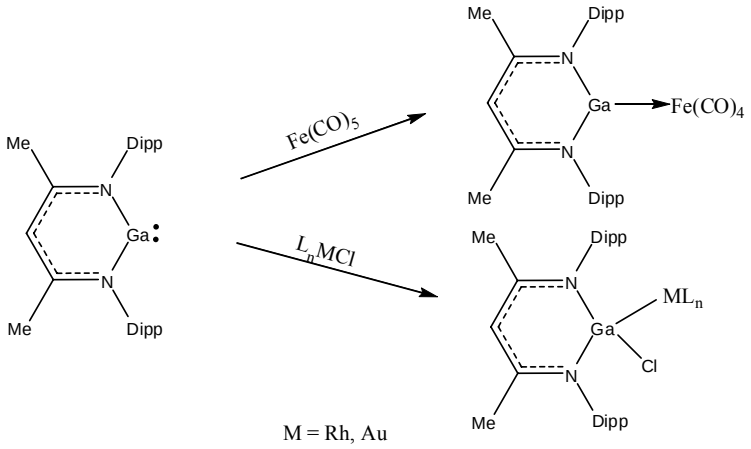

Scheme 2.3. β-diketiminato gallium organometallic complexes.

In the present chapter, the syntheses, spectroscopic characterization and, when possible, X-ray crystal structures of several new neutral group 13 compounds will be described. The first structurally characterized boron cation supported by a β-diketiminate ligand will be presented along with some other new boron cations. Finally, the synthesis and structural assay of a novel gallium complex will be described. In each case, a bulky β-diketiminate ligand with flanking 2,6-diisopropylphenyl substituents (L1 or L2) is employed to provide kinetic stabilization.

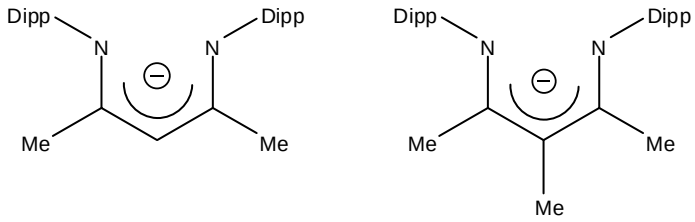

L1 L2

Dipp = 2,6-diisopropylphenyl

Results and Discussion

Some Neutral Group 13 Neutral Complexes Supported by β-Diketiminate Ligands

*Synthesis and Characterization of $[HC(CMe)_2(NDipp)_2]BF_2$ (**25**)*

The new difluoroborane **25** was prepared *via* the reaction of equimolar quantities of $[HC(CMe)_2(NDipp)_2]Li$ and $BF_3{\cdot}OEt_2$ in toluene solution at ambient temperature (Eq. 1).

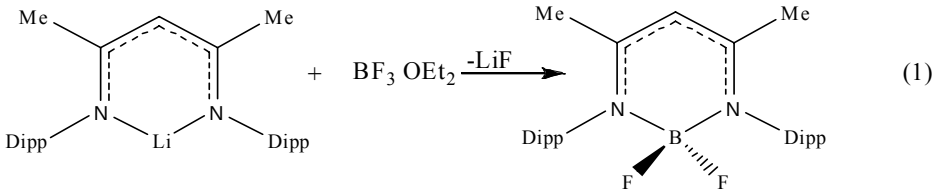

(1)

The equivalence of the pairs of methyl and Dipp groups in the ^1H NMR spectrum revealed that **25** possesses a symmetrical backbone. The detection of a triplet at 1.24 ($J_{B\text{-}F}$ = 28.7 Hz) in the $^{11}B\{^1H\}$ NMR spectrum confirmed the presence of a BF_2 moiety. This was corroborated by the ^{19}F NMR spectrum which exhibits a quartet at -128.48 with a similar $J_{B\text{-}F}$ coupling constant 28.4 Hz. Thus the NMR spectral data are consistent with the structure proposed in Eq. 1. Furthermore, these data are similar to those of previously reported β-diketiminato boron difluorides.[22] The low-resolution mass spectrum evidenced the M^+ peak at *m/z* 466 and the $[M\text{-}F]^+$ peak at *m/z* 448. The HRMS was consistent with

the proposed elemental composition. A crystal of **25** suitable for single-crystal X-ray diffraction study was obtained by cooling a saturated toluene solution to -40°C for one week. However, although the atom connectivity was clear (Figure 2.7), the X-ray data were not of sufficient quality to permit a detailed discussion of metrical parameters.

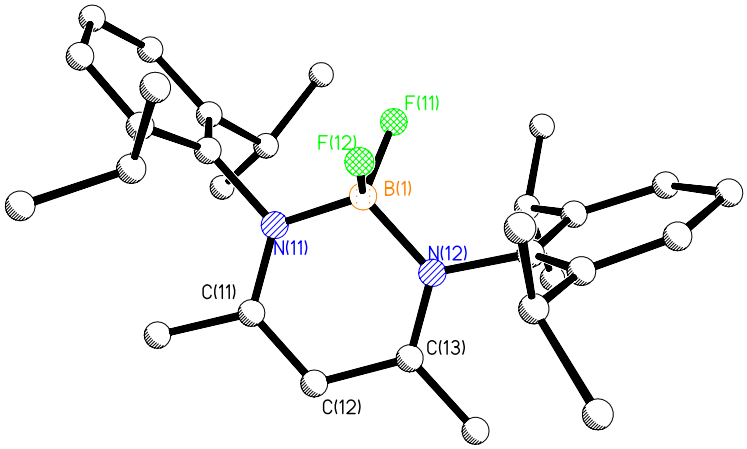

Figure 2.7. Atom connectivity of compound **25**.

*Synthesis and Characterization of [MeC(CMe)$_2$(NDipp)$_2$]AlMe$_2$ (**26**)*

The reaction of [MeC(CMe)$_2$(NDipp)$_2$]H with an equimolar quantity of AlMe$_3$ in hexane solution afforded, after workup of the reaction mixture, colorless crystalline compound **26** in high yield (90 %).

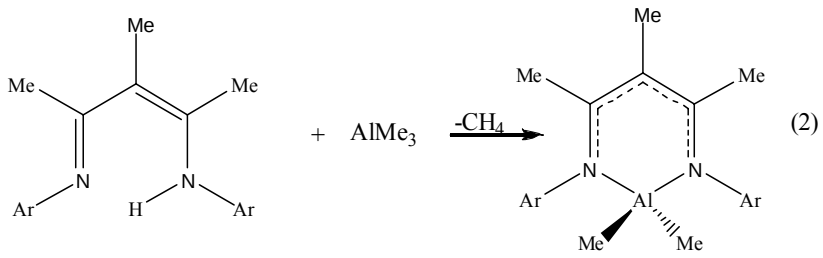

(2)

The ^{1}H NMR spectrum of **26** revealed the presence of methyl groups in 2:1 abundance. The characteristic $AlMe_2$ ^{1}H resonance was detected at δ -1.12 ppm. The parent peak was detected in the CI^{+} mass spectrum at *m/z* 489, and the $[M\text{-}Me]^{+}$ was recorded at *m/z* 473. High-resolution mass spectra confirmed the proposed elemental composition. The proposed structure of **26** was confirmed by a single-crystal X-ray diffraction study.

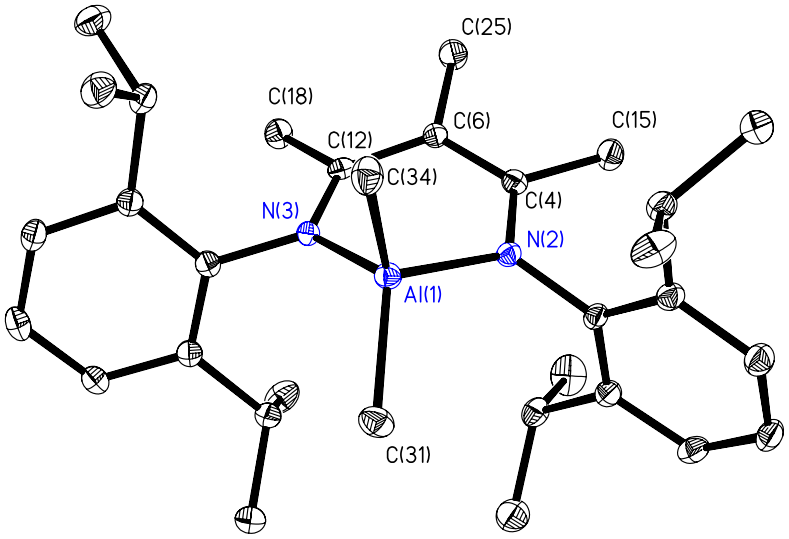

Figure 2.8. ORTEP view of compound **26**. Thermal ellipsoids drawn at 30% probability. All hydrogen atoms have been omitted for clarity.

Compound **26** crystallizes in the monoclinic space group $P2_1/a$ with Z = 4. The X-ray crystal structure revealed that the cyclic aluminum complex (Figure 2.8) consists of an $AlMe_2$ moiety which is N,N'-chelated by the β-diketiminate ligand. The geometry of **26** is somewhat similar to those previously published β-diketimintate-substituted $AlMe_2$ compounds.[13b] However, unlike the previous structures, the AlN_2C_3 ring of compound **26** is not a planar and adopts a boat shape. The atoms N(3), C(12), C(4), N(2) are almost coplanar but Al(1) and C(6) deviate from the said plane by 0.606(2) Å and by 0.170(3) Å, respectively. On the other hand, the Al-N and Al-C bond distances are similar to those of previously reported $L1AlMe_2$ complexes.[13b] The adoption of the boat shape is presumably a consequence of the presence of the *γ*-methyl substituent, which may have a very weak interaction with the $AlMe_2$ moiety.

*Synthesis and Characterization of $[MeC(CMe)_2(NDipp)_2]AlCl_2$ (**27**)*

The β-diketiminatoaluminum dichloride **27** was prepared by treatment $[MeC(CMe)_2(NDipp)_2]H$ with methylaluminum dichloride in hexane solution at ambient temperature. The white solid isolated from the reaction mixture was purified by sublimation. When pure, compound **27** is a colorless crystalline solid. The ^1H, $^{13}C\{^1H\}$ and $^{27}Al\{^1H\}$ NMR spectra are consistent with the structure proposed in Eq. 3, and are very similar to those for $[HC(CMe)_2(NDipp)_2]AlCl_2$.[13b] Confirmation was provided by a

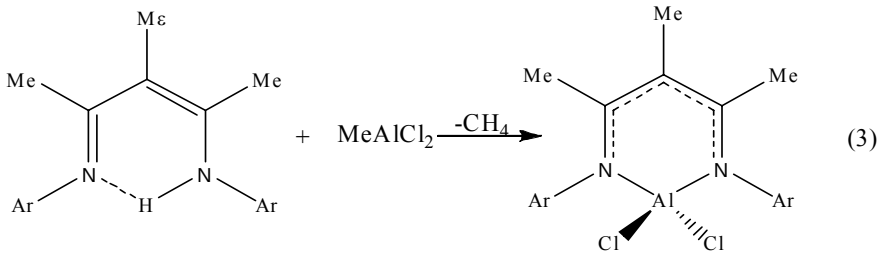

(3)

27

single-crystal X-ray diffraction study. Compound **27** crystallizes in the mono clinic space group $P2_1/c$ with Z = 4. The X-ray crystal structure of **27** revealed that all the bond distances and bond angles for the C_3N_2Al backbone are very similar to those of compound **26**. The average Al-Cl bond distance is 2.122(2) Å which falls within the range observed for this bond in the Cambridge Structural Data Base.

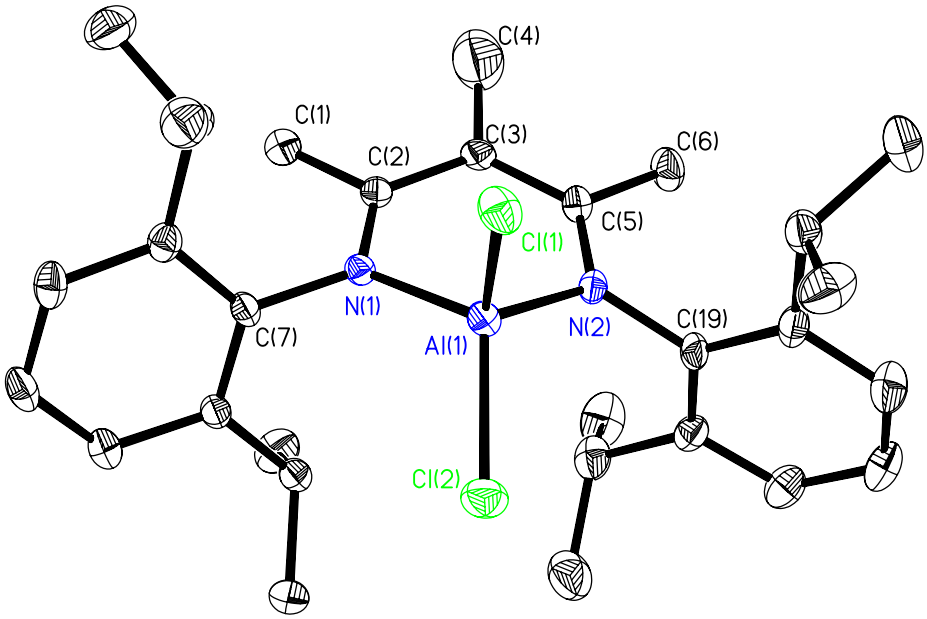

Figure 2.9. ORTEP view of compound **27**. Thermal ellipsoids drawn at 30% probability. All hydrogen atoms have been omitted for clarity.

Synthesis and Structural Characterization of a Monomeric Boron Cation Supported by a β-Diketiminate Ligand

The β-diketiminato boron monochloride derivative **28** was prepared by the metathetical reaction of $[HC(CMe)_2(NDipp)_2]K$ with $PhBCl_2$ in toluene solution at room temperature as summarized in Eq. 4. Unfortunately, however, it was not possible to isolate **28** in pure state because this compound undergoes facile hydrolysis (Eq. 5).

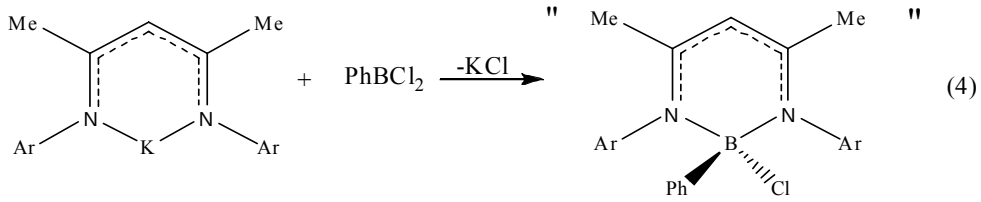

(4)

28

The $^{11}B\{^1H\}$ NMR spectrum of **28** evidenced a peak at δ 11.42 ppm which falls within the range anticipated for a four-coordinate boron center. The low-resolution mass spectrum showed a peak at *m/z* 505 which corresponds to the parent peak minus chloride. Several attempts were made to obtain crystals of **25** suitable for X-ray diffraction experiments by cooling saturated toluene solutions of **28** to -30°C for several days. However, in each case the hydrolysis product **29** was isolated in very small quantities. Since only a few crystals were collected, it was not possible to acquire spectroscopic data and therefore **29** was characterized exclusively by single-crystal X-ray diffraction (Figure 2.10).

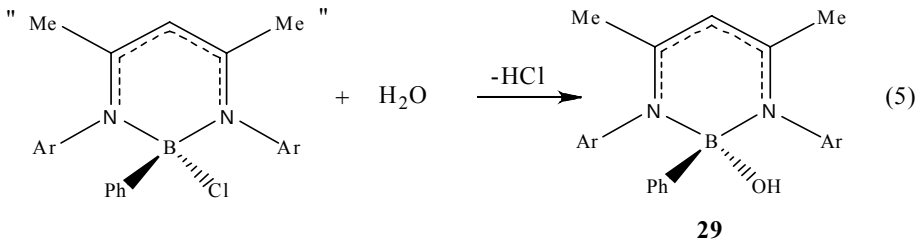

(5)

29

Compound **29** crystallizes in the monoclinic space group $P2_1/n$ with Z = 4. The X-ray analysis showed that the molecular structure comprises a closed six-membered C_3N_2B ring in which the boron atom is chelated by two nitrogen atoms with an average B-N bond distance of 1.605(7) Å. The four-coordinate boron center adopts an approximately tetrahedral geometry. The C_3N_2 part of the ring is planar within experimental error and the B(1) atom deviates from this planar by 0.331(4) Å. The similarity in the C-N and C-C bond distances implies some electron delocalization within the C_3N_2B ring. The N-B-N bond angle is 106.2(4)°. The phenyl substituent is almost orthogonal to the C_3N_2B backbone with the dihedral angle of 85.36(8)°.

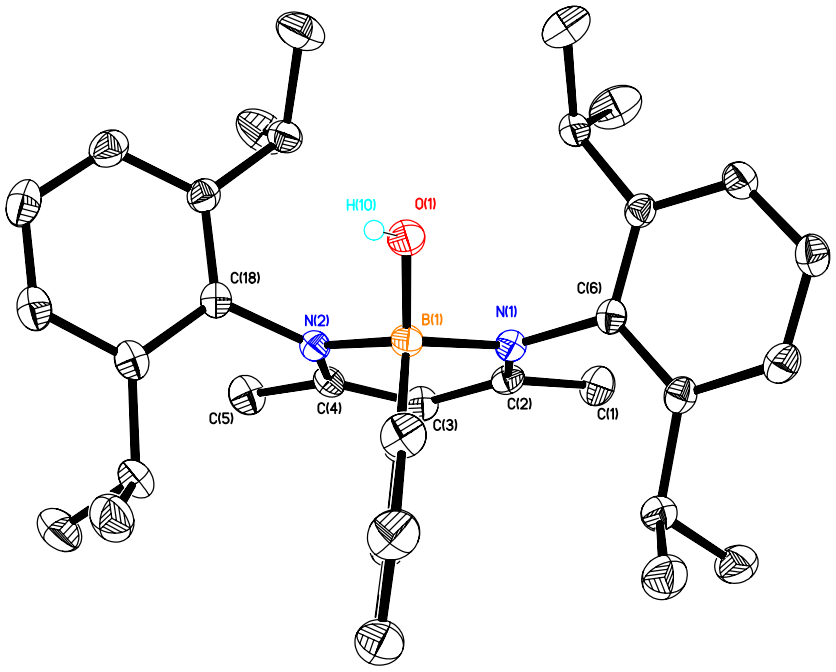

Figure 2.10. ORTEP view of compound **29**. Thermal ellipsoids drawn at 30% probability.

Treatment of **28** with $AlCl_3$ *in situ* in a toluene solution results in the formation of boron cation **30** as its $[Al_2Cl_7]^-$ salt. Compound **30** is a yellow crystalline solid that is thermally stable providing that it is stored in an inert atmosphere.

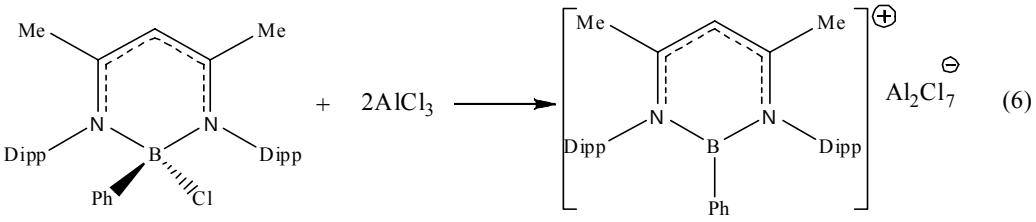

(6)

The ^{1}H and $^{13}C\{^{1}H\}$ NMR spectra of **30** provide evidence for a somewhat delocalized β-diketiminate backbone and for the presence of a phenyl substituent. The $^{11}B\{^{1}H\}$ NMR spectrum features a broad signal at δ 33.4 ppm, which falls within the range reported for three-coordinate boron centers[29]. The parent peak for the cation $\mathbf{30}^{+}$ was detected at *m/z* 505 and high resolution mass spectrum was consistent with the proposed elemental composition of $\mathbf{30}^{+}$.

Compound **30** crystallizes in the triclinic space group $P\bar{1}$ with Z = 2. The X-ray crystal structure confirmed that **30** is the $[Al_2Cl_7]^-$ salt of the targeted boron cation $\mathbf{30}^{+}$ and revealed that there are no close anion-cation contacts. The shortest distance between $\mathbf{30}^{+}$ and the $Al_2Cl_7^-$ anion exceeds 3.5 Å . The B-N(1)-C(83)-C(81)-C(84)-N(2) ring is planar (sum of bond angles = 719.2°) and each atom of the six-membered ring adopts a trigonal planar geometry within experimental error. The C-C and C-N bond distances in $\mathbf{30}^{+}$, which average 1.381(5) Å and 1.356(5) Å, respectively, are similar to those reported for the neutral β-diketiminate complex **13**[22] and compound **29**. The average B-N bond distance of 1.450(5) Å is shorter than that in compound **29** and therefore indicative of the existence of π-bonding. The existence of such π-bonding is expected because this ring is a 6π-electron system. The N-B-N bond angle is 114.6(3)°. The phenyl substituent is twisted by 53.3(3)° with respect to the C_3N_2B plane.

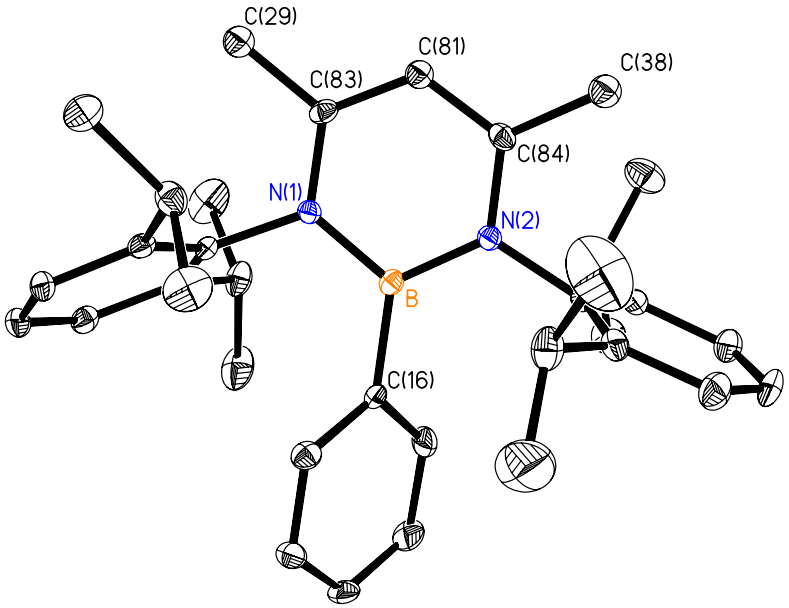

Figure 2.11. ORTEP view of the cation of compound **30**. Thermal ellipsoids drawn at 30% probability. All hydrogen atoms have been omitted for clarity.

To gain insight into the extent of π-delocalization in the C_3N_2B ring, DFT calculations were carried out on $\mathbf{30}^+$ at the B3LYP level of theory using the 3-21G* basis set. A summary of selected computed and experimental metrical parameters is provided in Table 2.1. The maximum differences between the computed and experimental bond distances and bond angles are 0.03 Å and 1.2°, respectively. The HOMO is largely phenyl ring-π in nature, while the LUMO evidences considerable N-C π* character within the BN_2C_3 ring; the HOMO-LUMO gap is 386 $kJ \cdot mol^{-1}$. The BN_2C_3 ring π-

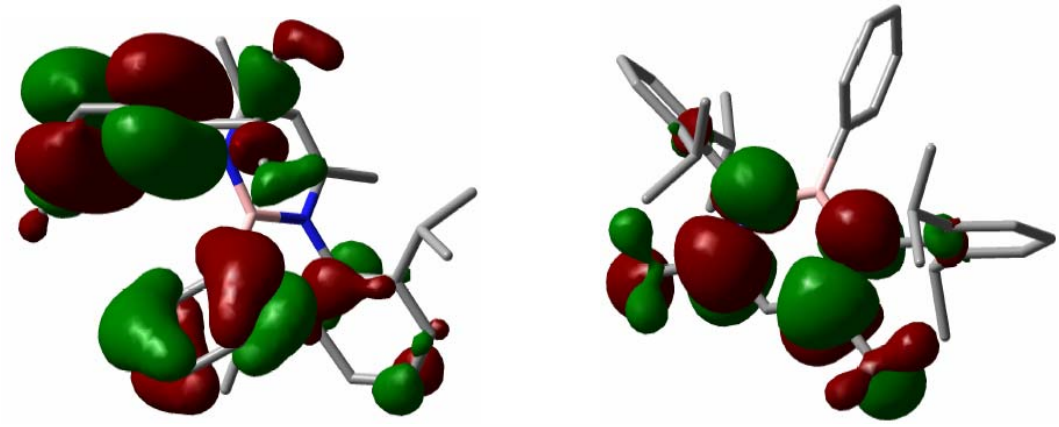

HOMO LUMO

Figure 2.12. HOMO and LUMO of the β-diketiminato boron cation **30**$^{+}$.

bonding character is found in the HOMO-6 and HOMO-7 orbitals. The HOMO-6 orbital comprises two π-allylic N-B-N and C-C-C fragments, while the HOMO-7 features two N-C π-bonds.

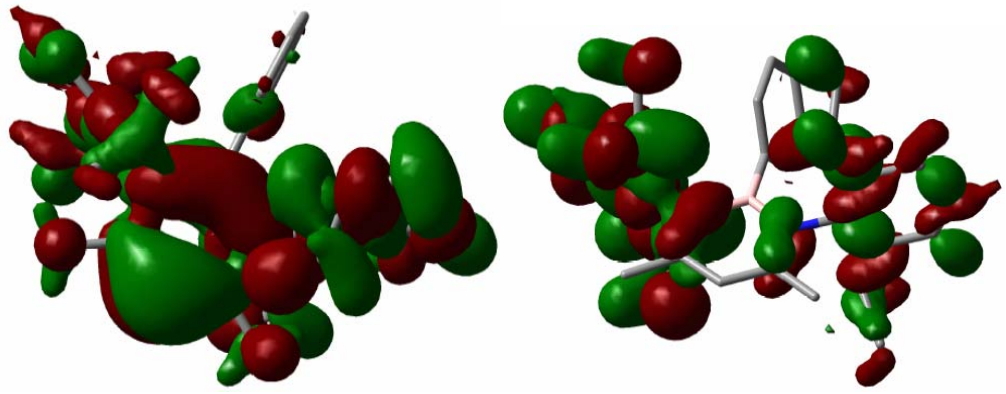

HOMO-6 HOMO-7

Figure 2.13. HOMO-6 and HOMO-7 of β-diketiminato boron cation **30**$^{+}$ showing the π-bond character.

Table 2.1. Computed and experimental metrical parameters for selected bond lengths (Å) and angles (°) for boron cation **30**$^{+}$.

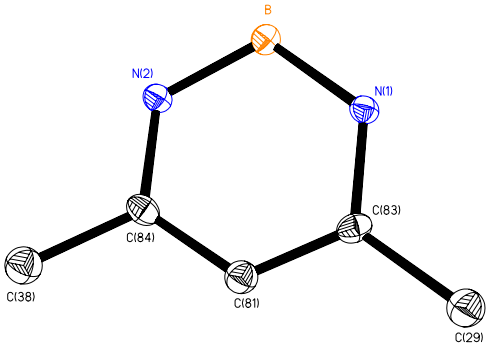

	Computed	Experimental
B-N(1)	1.48	1.45
N(1)-C(83)	1.37	1.35
C(83)-C(81)	1.39	1.38
C(81)-C(84)	1.39	1.38
N(2)-C(84)	1.37	1.36
B-N(2)	1.38	1.45
N(1)-B-N(2)	112.8	114.6
B-N(1)-C(83)	122.5	122.4
N(1)-C(83)-C(81)	119.9	118.7
C(83)-C(81)-C(84)	121.9	122.5
C(81)-C(84)-N(2)	119.9	119.1
C(84)-N(2)-B	122.5	121.8

Synthesis and Characterization of a Bulky, Acyclic Boron β-Diketiminate

Treatment of the bulky dichloroborane Cp*BCl_2 with [{$HC(CMe)_2(NDipp)_2$}Li] resulted, after workup, the isolation of the acyclic derivative **31**. Compound **31** is a yellow crystalline compound for which it was not possible to detect a ^{11}B NMR signal. The ^{1}H NMR spectrum evidenced three signals attributable to the Cp* ring protons, thus indicating that the Cp* ring is bonded to boron in an η^1 fashion. The low-resolution CI^{+}

mass spectrum exhibited the $[M+H]^+$ peak at *m/z* 599 and the elemental composition was confirmed by a satisfactory HRMS of the parent peak.

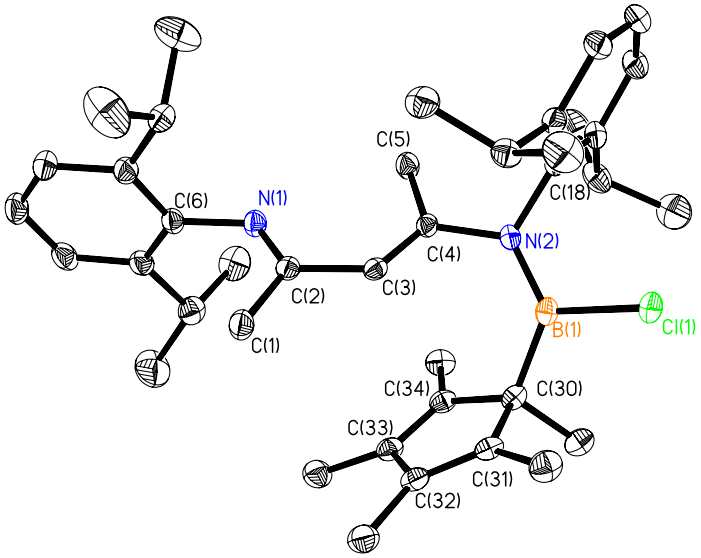

Figure 2.14. ORTEP view of compound **31**. Thermal ellipsoids drawn at 30% probability. All hydrogen atoms have been omitted for clarity.

A single-crystal X-ray diffraction study was undertaken to determine the structure of **31**. This compound crystallizes in the monoclinic space group $P2_1/c$ with Z = 4. The X-ray analysis revealed that compound **31** is acyclic and that the Cp*BCl moiety is bonded in a monodentate fashion to one of the β-diketiminate nitrogen atoms. The β-diketiminate backbone adopts a *trans*-iminoaminate structure. The atoms N(1), C(2), C(3), C(4) and N(2) are coplanar. However, the C(4)-N(2) bond distance is 1.442(3) Å longer than the C(2)-N(1) [1.274(3) Å] bond distance since the latter involves an imino rather than an amino nitrogen atom. The B-N bond distance of 1.407(3) Å is much shorter than those in the cyclic β-diketiminatoboron compounds **29** [1.618(4) Å] and **30**

[1.450 (5) Å] indicating a strong π-bond component in the B-N bond of **31**. The Cp* ring contains three C-C single bonds and two C-C double bonds, *i.e.* the typical pattern for an η^1-bonded Cp* ligand. The monodentate coordination mode is unusual for a β-diketiminate ligand. In fact, the only other example of this bonding mode was reported by Ding *et al*. for an Sn(II) compound in which the metal was bonded to two β-diketiminate ligands. Interestingly, in the latter compound one β-diketiminate ligand was bonded in a bidentate fashion while the other exhibits a bonding mode akin to that of **31**.[30] A survey of the Cambridge Structural Database shows that compound **31** represents the first example of monodentate coordinated group 13 β-diketiminate. The iminoamine skeletal structure of **31** also appears to be unprecedented.

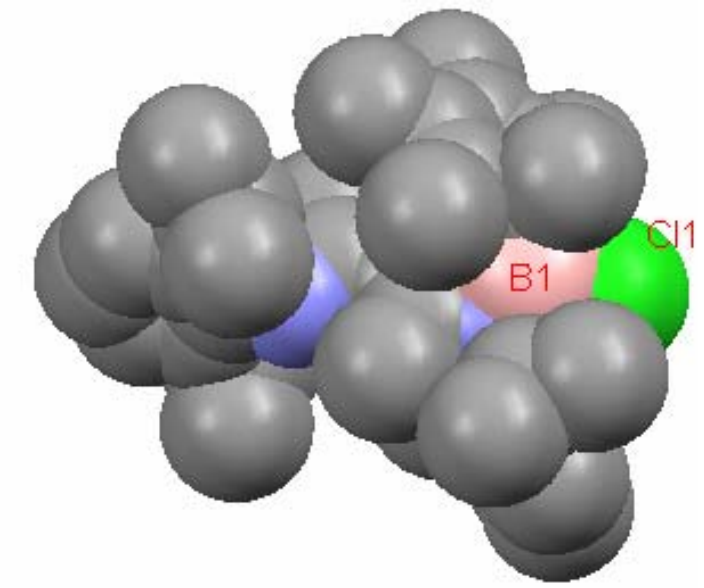

Figure 2.15. Space filling model of compound **31** showing the steric saturation around B(1).

Examination of a space-filling model of compound **31** (Figure 2.15) reveals that the presence of a bulky Cp* ring, a bulky Dipp ligand and a chlorine atom causes steric saturation at the B(1) center thus precluding the N,N'-chelated coordination mode.

*Synthesis and Characterization of a Cyclic Pentamethylcyclopentadienyl-Subsituted Boron Cation (**32**)*

Treatment **31** with one equivalent of $AlCl_3$ in toluene solution, followed by workup of the reaction mixture resulted in a 23% of yield of $[\{HC(CMe)_2(NDipp)_2\}B(\eta^1\text{-}C_5Me_5)][AlCl_4]$ (**32**). Compound **32** is a yellow crystalline material.

The evidence of a pair of equivalent Dipp groups in the ^1H NMR spectrum of **32** suggested that **32** possesses a symmetrical backbone, which implies that the boron atom is N,N'-chelated by the β-diketiminate ligand. Three signals attributable to the Cp* ring protons are indicative of an η^1 bonding mode it to the boron atom. The $^{11}B\{^1H\}$ NMR spectrum of **32** (δ 11.82 ppm) suggested that **32** does not feature a typical three-coordinate boron center, but, it is more likely a four-coordinate boron center. It is possible that in solution steric saturation around the boron center may cause a weak π-type interaction between the Cp* substituent and the boron atom.

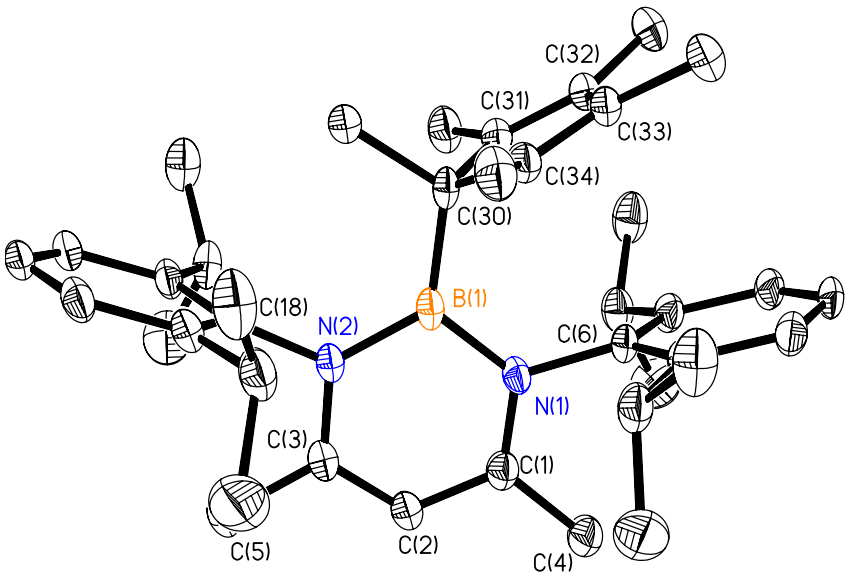

Figure 2.16. ORTEP view of compound **32**$^{+}$. Thermal ellipsoids drawn at 30% probability. All hydrogen atoms have been omitted for clarity.

The single-crystal X-ray diffraction study of **32** was undertaken. Compound **32** crystallizes in the monoclinic space group $P2_1/n$ with Z = 4. There are no short contacts between the cation and anion and the closest cation-anion distance between the cation and anion exceeds 3.5 Å. The C-N and C-C bond distances are similar on either side of the six-membered C_3N_2B ring thus indicating some delocalization in the β-diketiminate backbone. The C_3N_2B ring is coplanar (sum of angles = 720°), and the C(30) atom of the Cp* substituent lies in the same plane. The average B-N bond distance in **32** [1.487(4) Å] is similar to that in **32**, as is the N-B-N bond angle [112.3(3)°]. The fact that the torsion angles of N(1)-B(1)-C(30)-C(31) (-28.3°) and N(1)-B(1)-C(30)-C(34) (26.8°) are similar which indicates that the C_3N_2B ring bisects the Cp* ring from the C(30) atom to the midpoint of the C(32)-C(33) bond. The Cp* ring contains three C-C single bonds

[C(30)-C(31), C(30)-C(34), C(32)-C(33)] and two C-C double bonds [(C(31)-C(32) and C(33)-C(34))] showing that it is bonded in the localized η^1-bonding mode.

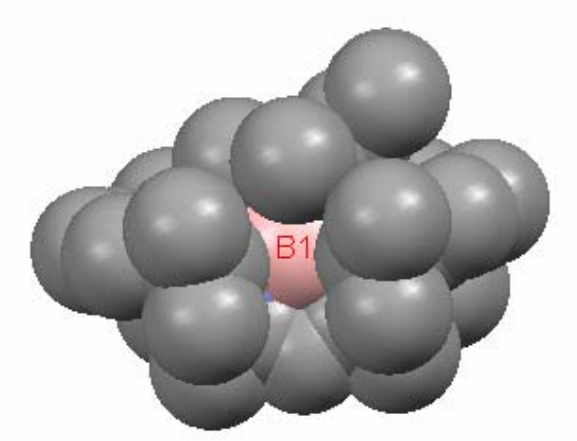

Figure 2.17. Space filling model of the β-diketiminatoboron cation $[\{HC(CMe)_2(NDipp)_2\}B(\eta^1\text{-}C_5Me_5)]^+$ (**32**$^+$).

The space filling for cation **32**$^+$ (Figure 2.17) shows that the boron center is sterically protected by the presence of three bulky substituents.

Preparation of a β-Diketiminate-Supported Boron Cation Salt by a Boron-Aluminum Exchange Process

The first step of this process involved the synthesis of $[MeC(CMe)_2(NDipp)_2]AlCl_2$ (**27**) by treatment of $[MeC(CMe)_2(NDipp)_2]H$ with $MeAlCl_2$ in toluene solution. In turn, treatment of **27** with an equimolar quantity of $PhBCl_2$ in toluene solution using the

method of Kuhn *et al.*[24] resulted in an 80% yield (per NMR) of the $[AlCl_4]^-$ salt β-diketiminatoboron cation **33** (Eq. 7).

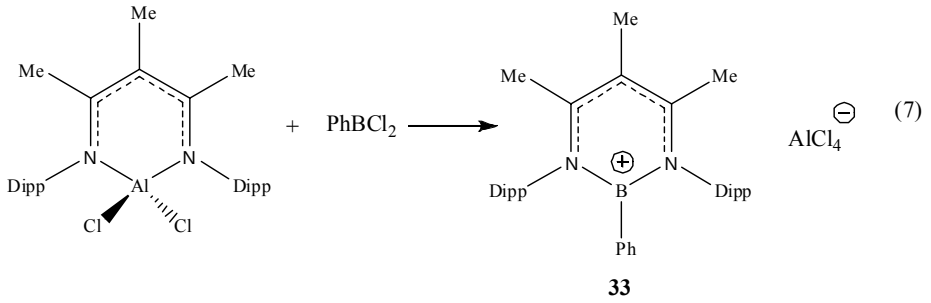

33 (7)

Confirmation of the proposed structure for **33** is based on ^1H, $^{13}C\{^1H\}$, $^{11}B\{^1H\}$ and $^{27}Al\{^1H\}$ NMR experiments, as well as high-resolution mass spectral data. The $^{27}Al\{^1H\}$ NMR spectrum shows a sharp signal at δ 103.2 ppm which is diagnostic of the $[AlCl_4]^-$ anion [31]. The $^{11}B\{^1H\}$ NMR chemical shift for **30** (δ 31.9 ppm) falls within the range established for N,N'-chelated three-coordinate boron cations. Furthermore, the $^{11}B\{^1H\}$ NMR chemical shift for $\mathbf{33}^+$ is similar to that of the analogous boron cation $\mathbf{30}^+$. The high-resolution mass spectral data for **33** are also consisted with the proposed elemental composition. The analogous salt $[\{HC(CMe)_2(NDipp)_2\}BPh][AlCl_4]$ is also accessible by this synthetic route.

Overall, the boron-aluminum exchange process represents the best synthetic method for these β-diketiminatoboron cations both from the standpoint of yields and also because the experimental procedure is straightforward.

Synthesis of a β-Diketiminatoboron Cation Salt by Salt Metathesis

The reaction of the β-diketiminate-supported boron difluoride **25** with an equimolar quantity of $Ag[B(C_6F_5)_4]$ in toluene solution at ambient temperature afforded the fluoro-substituted β-diketiminatoboron salt **34** in a yield of approximately 70% after workup of the reaction mixture.

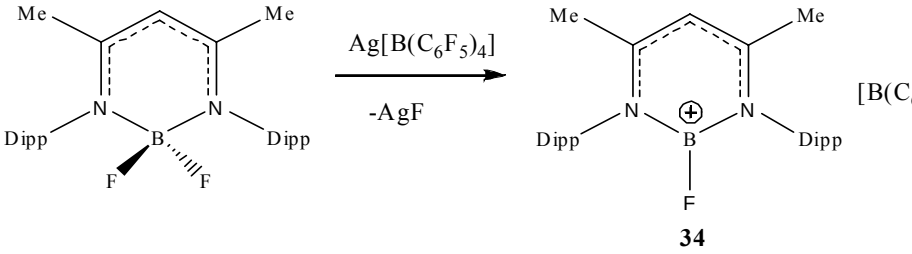

34 (8)

The $^{11}B\{^1H\}$ NMR spectrum of **34** evidenced signals at δ -16 and 21 ppm. The intense signal at δ -16 ppm corresponds to that reported in the literature for the $[B(C_6F_5)_4]^-$ anion[32], while the less intense peak at δ 21 ppm falls in the region appropriate for a β-diketiminatoboron cation. The ^{19}F NMR spectrum exhibits intense signals attributable to the $[B(C_6F_5)_4]^-$ anion. Due to the dominating intensity of the $[B(C_6F_5)_4]^-$ signals, it was not possible to detect the cationic B-F resonance. Likewise, the CI mass spectrum of the cation $\mathbf{34}^+$ was not detectable due to masking by the intense fragmentation peaks of the $[B(C_6F_5)_4]^-$ anion.

Given the above discussion, it was important to characterize the salt **34** by single-crystal X-ray diffraction. A suitable single crystal of **34** was obtained by cooling a saturated toluene solution to -30°C for 2 d. Compound **34** crystallizes in the monoclinic

space group $P2_1/c$ with Z = 4. The asymmetric unit contains four independent molecules of **34** (Figure 2.18). The C_3N_2B backbone of **34** is planar as evidenced by the sum of angles of 719.97(5)°. The delocalized nature of the backbone can be deduced from the

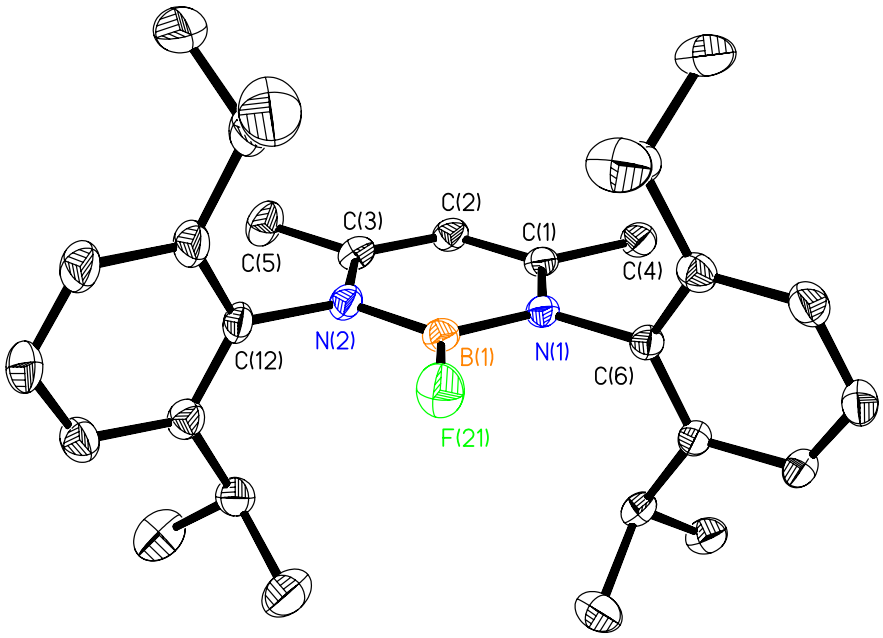

Figure 2.18. ORTEP view of the cation of compound **34**. Thermal ellipsoids drawn at 30% probability. All hydrogen atoms have been omitted for clarity.

fact that the pairs of B-N and C-N bond distances and the B-N-C and N-C-C bond angles are of similar magnitude. The fluorine atom is coplanar with the C_3N_2B backbone. The average B-N bond distance of 1.451(6) Å is very similar to that of compound $[\{HC(CMe)_2(NDipp)_2\}BPh][Al_2Cl_7]$ (**30**) but is shorter than that of compound $[HC(CMe)_2(N\textit{p}\text{-tolyl})_2]BF_2$ (**13**).[22] The B(1)-F(21) bond distance of 1.345(6) Å is shorter

than in the neutral difluoroborane compound **13** by approximately 0.05 Å.[22] The shorter B-F bond distance in **34** is due to a combination of the formal positive charge at B(1) and the possibility of enhanced B-F π-bonding. The bite angle of N(1)-B(1)-N(2) [116.3(4)°] is not unusual.

Attempted Preparation of a Dicationic β-Diketiminate-Supported Boron Complex

The bis(dibromoborane) derivative **35** was obtained according to the literature method[33]. Treatment of **35** with two equivalents of $[MeC(CMe)_2(NDipp)_2]Li$ in toluene solution at ambient temperature followed by workup of the reaction mixture afforded compound **36** as an intractable orange-yellow oil. However, all attempts to isolate com-

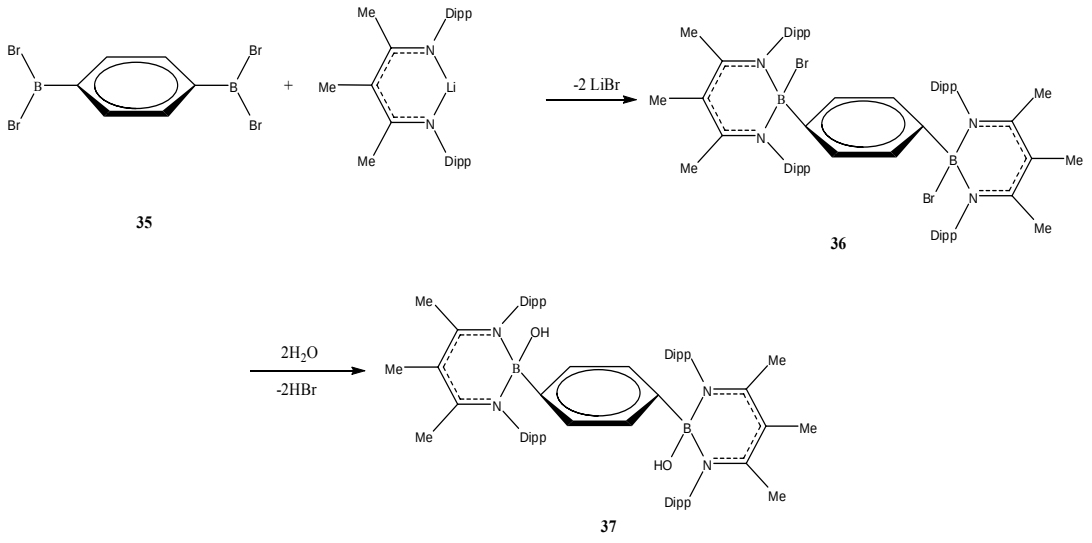

Scheme 2.4. Reactions of a bis(dibromoborane)benzene.

pound **36** in a pure state by recrystallization from a variety of solvents resulted in the formation of the hydrolysis product **37**. Crystals of **37** were obtained by cooling a saturated toluene solution to -30°C for one week.

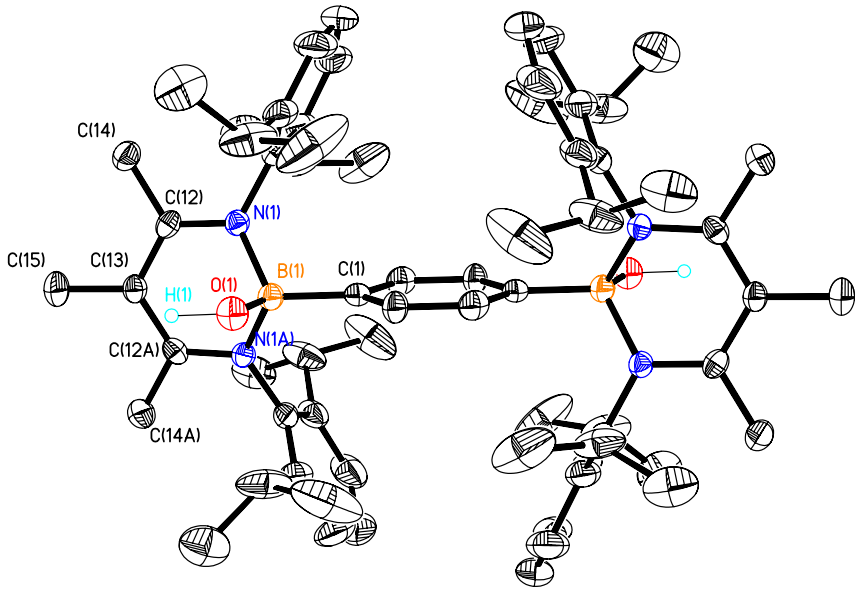

Figure 2.19. ORTEP view of compound **37**. Thermal ellipsoids drawn at 30% probability.

Compound **37** crystallizes in the monoclinic space group of C_2/m with Z = 2. The two [{MeC(CMe)$_2$(NDipp)$_2$}BOH] fragments lie on an inversion center and are linked to the *1* and *4* positions of the benzene ring. The C_3N_2 atoms of each β-diketiminate unit are coplanar, but the boron atom deviates from the C_3N_2 plane by 0.473(10) Å. The linking benzene ring is perpendicular to each C_3N_2 backbone. The B(1)-O(1) bond distance of 1.477(5) Å is longer than in the compound [HC(CMe)$_2$(NDipp)$_2$]B(Ph)OH (**29**) [1.431(3)

Å]. However, the average B-N bond distance in **37** [1.592(4) Å] is shorter than that in compound **29** [1.619(4) Å].

The *in situ* reaction of compound **36** with two equivalents of $AlBr_3$ was carried out in an effort to prepare the boron dication **38** (Scheme 2.5). Workup of the reaction mixture resulted in the formulation of an intractable yellow oil. Several unsuccessful attempts were made to crystallize this product.

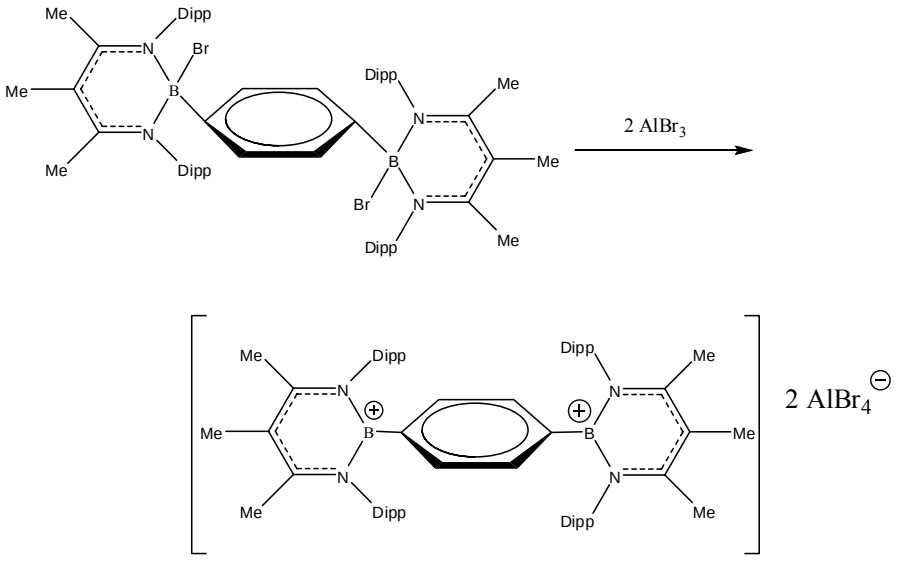

38

Scheme 2.5. Attempted preparation of a dinuclear boron dication.

Coordination Chemistry of a β-Diketiminatogallium Compound

The reaction of $[HC(CMe)_2(NDipp)_2]Li$ with $[Cp(CO)_2FeGaCl_2]_\infty$ (Cp = cyclopentadienyl) in THF solution at ambient temperature resulted, after workup of the

reaction mixture, in the isolation of the yellow crystalline compound **39** in 70% yield (Eq. 9).

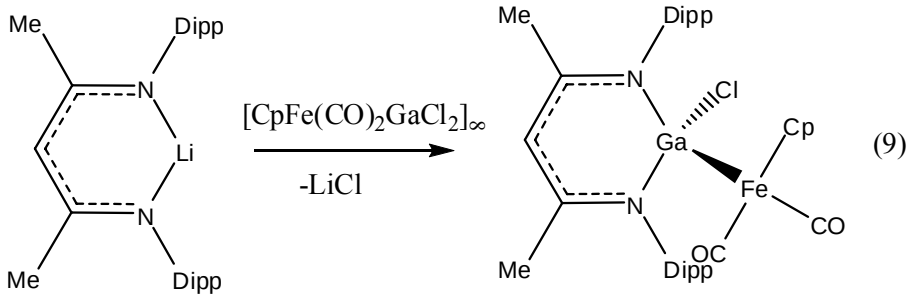

(9)

The ^{1}H NMR spectrum of **39** exhibits all the anticipated resonances for the diketiminate backbone and the Cp ring. Similarly, the $^{13}C\{^{1}H\}$ NMR spectrum evidences all the expected signals except that due to the CO groups. The CI^{+} mass spectral peak at *m/z* 700 is attributable to the $[M+H]^{+}$ ion while the peaks at *m/z* 663 and at *m/z* 521 are assignable to the $[M-Cl]^{+}$ and $[M-CpFe(CO)_2]^{+}$ ions, respectively. The high-resolution mass for the $[M-Cl]^{+}$ is consistent with the composition $C_{36}H_{46}N_2O_2FeGa$.

Single crystals of **39** suitable for X-ray analysis were grown by slow evaporation of a toluene solution. Compound **39** crystallizes in the triclinic space group $P1\bar{}$ with Z = 4. The X-ray crystal structure of **39** revealed that there are two independent molecules in the asymmetric unit. These molecules differ with respect to the orientation of the $CpFe(CO)_2$ substituents. In one form the geometry of the Cl-Ga-Fe-CO moiety is *trans* (**39a**) while in the other geometry of this fragment is *cis* (**39b**). Since the gallium atoms deviate from the C_3N_2 backbone in the same direction, the two molecules are not enantiomeric (Figure

2.20). There are, however, slight differences in the metrical parameters of the two molecules. For example, Ga(1) is displaced from the C_3N_2 backbone

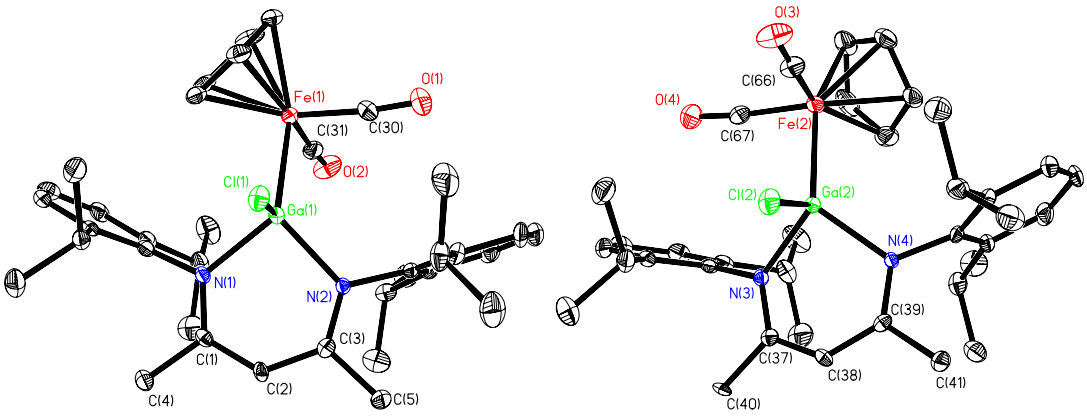

39a **39b**

Figure 2.20. ORTEP view of the two forms of compound **39**. Thermal ellipsoids drawn at 30% probability. All hydrogen atoms have been omitted for clarity.

by 0.741(4) Å while the displacement for Ga(2) is 0.578(3) Å. There is also a significant difference in the Cl-Ga-Fe bond angles. The Cl(1)-Ga(1)-Fe(1) angle is 109.96(4)° in **39a** while the Cl(2)-Ga(2)-Fe(2) angle is 113.92(5)° in **39b**. A superimposed view of **39a** and **39b** is presented in Figure 2.21. Since the geometries around the gallium atoms are similar for the two molecules, the following discussion will focus only on the *trans* form **39a**.

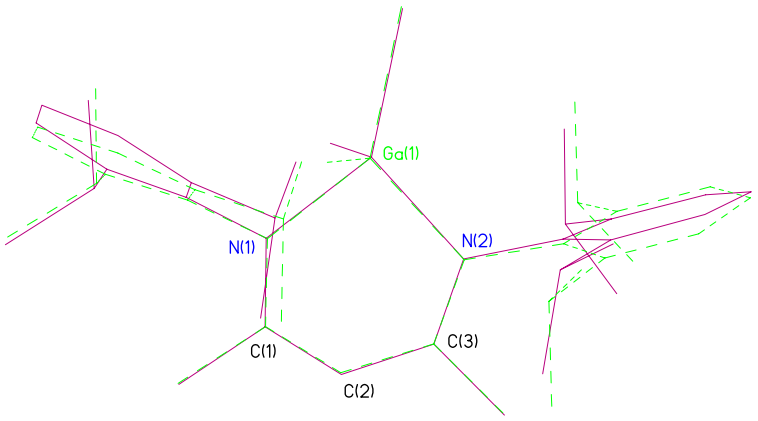

Figure 2.21. Superimposed view of **39a** (solid lines) and **39b** (dashed lines).

An amidinate analogue of this type of Ga-Fe compound (**40**) has been reported by Jones *et al*.[34] The Ga-Cl and Ga-N bond distances for **39a** are very similar to those for **40**. Thus for **39a** the Ga-Cl bond distance is 2.278(2) Å, while that for **40** is 2.2294(8) Å.

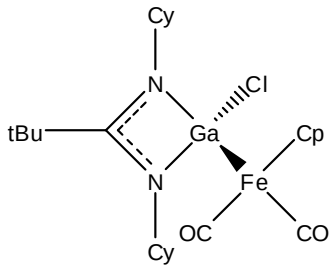

Cy = cyclohexyl

40

Likewise, the N-Ga-Fe and Fe-Ga-Cl bond angles for **39a** [124.5(1)° and 109.96(4)°, respectively] are very similar to those for **40** [127.27(8)° and 115.20(3)°, respectively]. As expected, the N(1)-Ga(1)-N(1) bond angle for **39a** [94.4(2)°] is larger than that for **40** [66.39(9)°] due to the smaller ring size of the latter compound. The fact that the Ga-Fe bond distance is longer in **39a** [2.393(1) Å] than that in **40** of [2.3540(6) Å] is

presumably due to the steric demands of the Dipp substituents. The geometry around the gallium center in **39a** is very similar to $[(Ph_3P)Au\{Ga(HC(CMe)_2(NDipp)_2)Cl\}]$[25c].

Attempted Preparation of a Cationic Ga-Fe Compound

Several attempts were made to abstract a chloride anion from $[\{HC(CMe)_2(NDipp)_2\}Ga(Cl)\{Fe(Cp)CO_2\}]$ (**39**) by treatment with $GaCl_3$, $Ag[B(C_6F_5)_4]$ or $[Et_3Si][B(C_6F_5)_4]$. However, even though color changes were observed on mixing the reagents, the products were too unstable to isolate (Scheme 2.6). All attempts to grow crystals resulted in formation of the protonated ligand $[\{HC(CMe)_2(NDipp)_2\}H_2][AlBr_4]$ (**42**). A similar outcome has been reported in the attempted preparation of the Rh complex $[(coe)Rh(C_6H_6)\{Ga(HC(CMe)_2(NDipp)_2)Cl\}]$ (coe = cyclooctene) [25b].

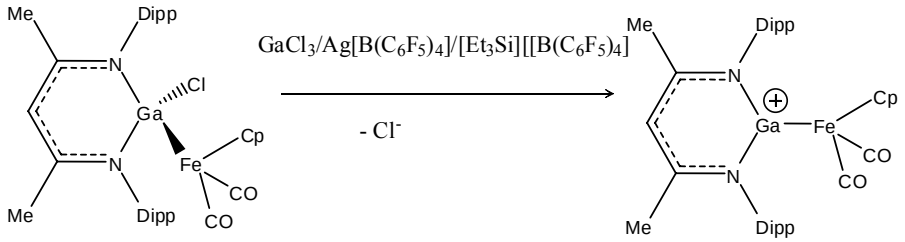

39 **41**

Scheme 2.6. Attempted preparation of a cationic gallium-iron compound.

The salt **42** is a colorless solid. The CI^+ mass spectrum shows a characteristic peak at *m/z* 420 that corresponds to the composition $[C_{29}H_{44}N_2]^+$. The single-crystal X-ray structure of **42** was determined (Figure 2.22). Compound **42** crystallizes in the

monoclinic space group C_2/c with Z = 4. There are no short contacts between the cation and the anion. The shortest such contact is approximately 2.55 Å between H(1N) and Cl(3). The structure of the cation is symmetrical, the two halves of the structure being related by a plane of symmetry that passes through C(10). The C(7)-N(5) and C(7)-C(10) bond distances of 1.337(5) Å and 1.383(4) Å, respectively, are shorter than those of typical single C-N and C-C bonds which suggests some delocalization within the C_3N_2 chain.

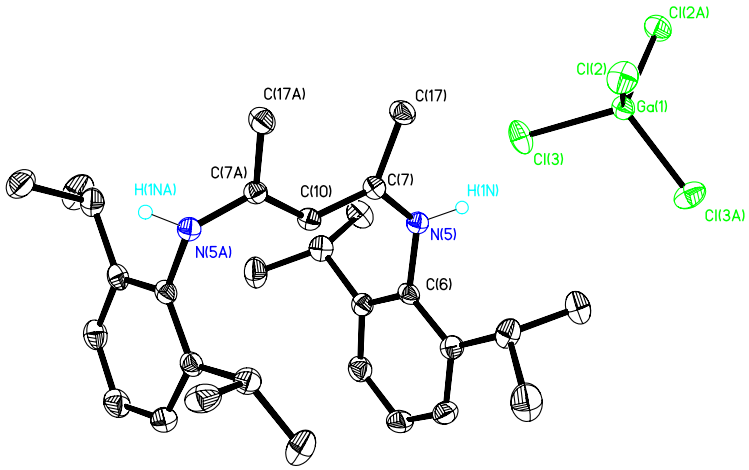

Figure 2.22. ORTEP view of compound **42**. Thermal ellipsoids drawn at 30% probability.

Conclusions

Two different methods have been employed for the preparation of three neutral β-diketiminate-supported group 13 complexes. The boron difluoride compound was prepared by salt metathesis and the aluminum dichloride and dimethyl aluminum complexes were synthesized via methane elimination reactions. All three complexes were fully characterized.

The first structurally authenticated β-diketiminatoboron cation was prepared by a halide abstraction reaction. DFT calculations revealed that the HOMO-6 and HOMO-7 orbitals of this compound feature the π-bonding character of the BN_3C_2 ring. The Cp*-substituted β-diketiminatoboron cation was also synthesized via a halide abstraction reaction. The precursor for the latter reaction possesses a monodentate β-diketiminate fragment which is rare for a group 13 element. The aluminum/boron exchange process and the salt metathesis reaction have also been employed for generating cationic β-diketiminatoboron complexes. However, the attempted preparation of a dinuclear β-diketiminatoboron dication resulted in hydrolyzed product.

A gallium-iron complex supported by a β-diketiminate ligand was synthesized via a salt metathesis reaction. The attempted preparation of a cationic gallium-iron complex by means of halide abstraction reaction resulted in formation of the protonated β-diketiminate ligand.

Part II

Diboron Complexes of Dinuclear Bis(amidinate) Ligands

Introduction

Amidinate anions are uninegative, N,N'-chelating ligands of the general formula $[RC(NR')_2]^-$ (**43**). They bear an obvious structural relationship to the β-diketiminate ligand class (**44**), but with the difference that, when N,N'-chelated, they afford four-membered rather than six-membered rings. On account of their readily tunable steric and electronic properties, amidinate anions have been widely used as ligands in main group, transition metal and *f*-block coordination chemistry[35].

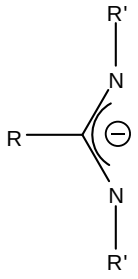

43

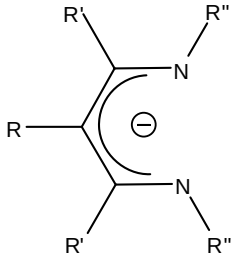

44

Early work in this field was focused on the benzamidinate derivative $[PhC\{NSiMe_3\}_2]^-$, which is readily synthesized *via* the reaction of $Li[N(SiMe_3)_2]$ with PhCN[36]. Several other synthetic routes to metal amidinate complexes have been developed subsequently, the most prevalent being the following:

(i) reaction of a metal halide with an N,N,N'-tris(trimethylsilyl)amidine;

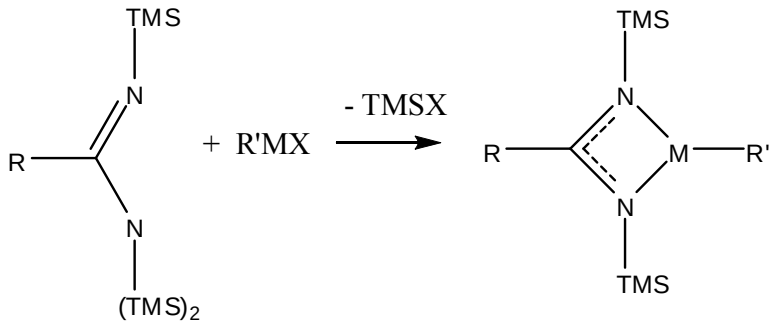

X = halide; TMS = Me_3Si

(ii) protonolysis of an amidine using a metal alkyl;

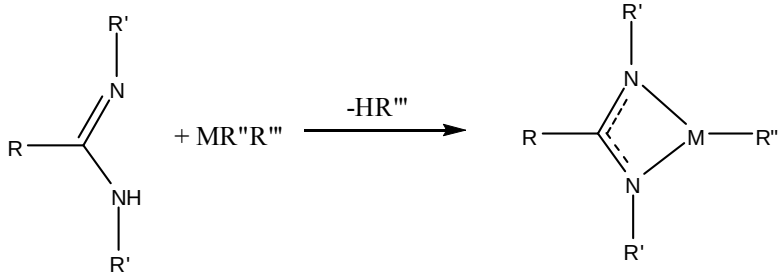

(iii) insertion of a carbodiimide into a metal-alkyl bond; and

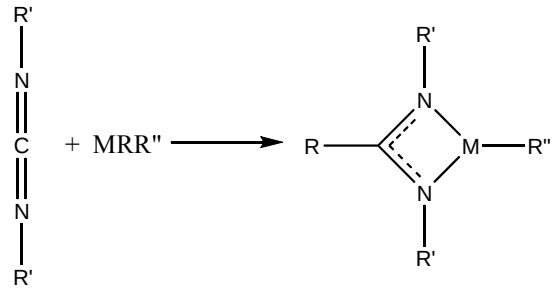

(iv) salt metathesis between a metal halide substrate and a lithium amidinate (generated *in situ* by route (ii) or (iii)).

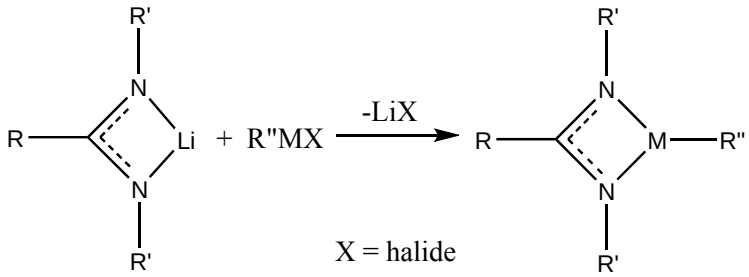

More recently, several binuclear amidinate ligands have been developed. For example, bimetallic complexes of bis(amidinates) based upon dibenzofuran (**45**)[37], 9,9-dimethylxanthene (**46**)[37], and 1,2-disubstituted cyclohexyl (**47**)[38] frameworks have been reported (Figure 2.23).

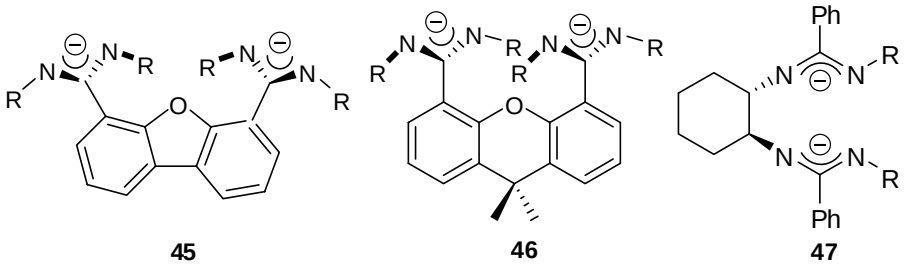

Figure 2.23. Bisamidinate ligand systems.

In these compounds, the proximity of the two metal fragments is governed by the nature of the structural unit linking the amidinate functional groups. Binuclear complexes of these types have been developed as bifunctional catalysts. However, in

comparison with the above systems, the chemistry of the related bis(benzene)amidinates 1,3- and 1,4-$C_6H_4[C(NR)_2]^-$ [N = $SiMe_3$ (**48**), Cy (**49**), Cy = cyclohexyl, Figure 2.24] is much less developed. These ligands are readily synthesized and, on account of their rigidity, have the ability to bridge two coordinated metal moieties. However, prior to the present work, their coordination chemistry was restricted to a bis(trichlorostannyl) derivatives[39], a bis(phosphenium) dication[40], a zwitterionic titanium compound[41], and a pair of neutral bimetallic aluminum complexes, 1,4-$C_6H_4[C(N\text{-}i\text{-}Pr)_2AlMeX]_2$ (X = Me, Cl)[42]. Compounds **48a** and **48b** have also been employed for the preparation of bifunctional 1,2,3,5-dithia- and diselena-diazolyl radicals, classes of compounds that have potential application as single component molecular semiconductors[43].

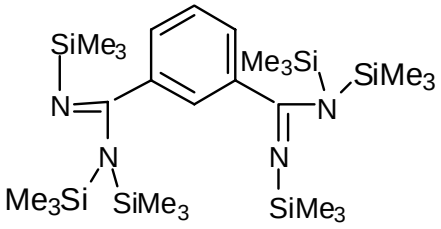

48a

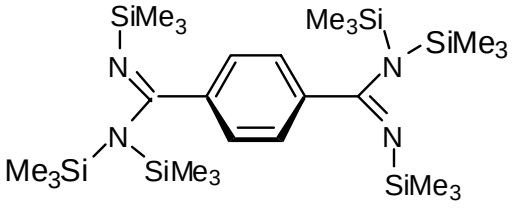

48b

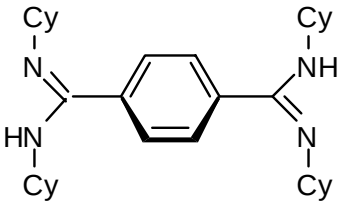

49

Figure 2.24. Bis(benzene)amidinate compounds.

Within the realm of *p*-block chemistry, amidinate complexes featuring group 13 metal-alkyl and metal-halide fragments have received sustained interest during the last decade due to the discovery of useful applications for such compounds in key technological areas. For example, amidinate-supported alkylaluminum cations have proved to be active catalysts for the polymerization of olefins, while gallium amidinate complexes have been employed as single-source precursors for the product of nitride materials[44].

The present work describes the synthetic and structural chemistry of a series of diboron amidinates derived from **48**, **49** and the bis(dibromoboron) complex **35**. Attempts to prepare boron dications and polymers using the new diboron amidinates will also be described.

Results and Discussion

*Synthesis and Characterization of Compound **48a***

Compound **48a** was prepared according to the literature method[43b]. Since the molecular structure of this compound had not been reported, it was decided to undertake a single-crystal X-ray diffraction study. Compound **48a** crystallizes in the monoclinic space group C_2/c with Z = 4. The molecular structure of amidine **48a** is shown in Figure 2.25. The two amidine groups that are attached to the 1 and 3 positions of the benzene ring are equivalent, being related by a C_2 rotation symmetry with respect to the C(1)-C(4) axis. The N(1)-C(5) and N(2)-C(5) bond distances of 1.402(4) and 1.279(4) Å, respectively, are indicative of localized C-N and C=N bonds. For comparison, the corresponding bond distances in the 5-*tert*-butyl analogue of **48b** are 1.410(5) and 1.264(5) Å, respectively [43c], while those in **49** are 1.413(3) and 1.271(3) Å, respectively[45].

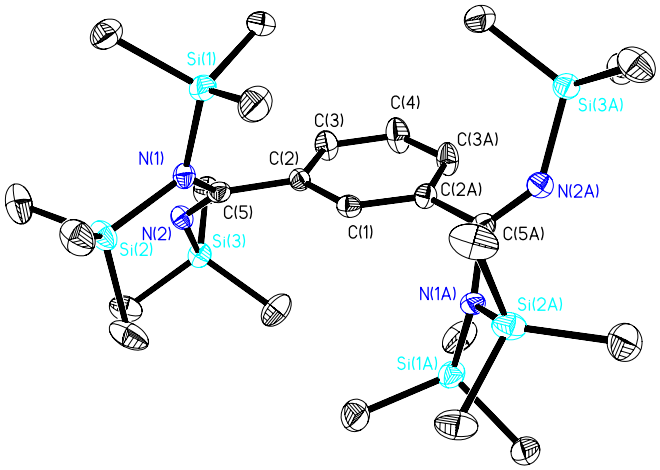

Figure 2.25. ORTEP diagram of **48a** with thermal ellipsoids at 30% probability. All hydrogen atoms have been omitted for clarity.

*Synthesis and Characterization of Compound **50***

The reaction of **48a** with two equivalents of BCl_3 in toluene solution at room temperature afforded, after workup of the reaction mixture, compound **50** as a colorless crystalline solid in high yield (Eq. 10). The ^{1}H and $^{13}C\{^{1}H\}$ NMR spectra of **50** show signals due to equivalent trimethylsilyl groups and the bridging phenyl group, along with a weak $^{13}C\{^{1}H\}$ resonance at δ 169 ppm attributable to electron delocalization within the N-C-N fragment. The $^{11}B\{^{1}H\}$ NMR spectrum features an intense singlet resonance at δ 5.73 ppm that falls in the typical range for four-coordinate boron atoms[29]. The detection of a CI^{+} mass spectral peak at *m/z* 612 corresponds to the $[M+H]^{+}$ ion and confirms the presence of two BCl_2 groups on the binuclear bis(amidinate) ligand. The proposed elemental composition was confirmed by a high-resolution mass spectrum.

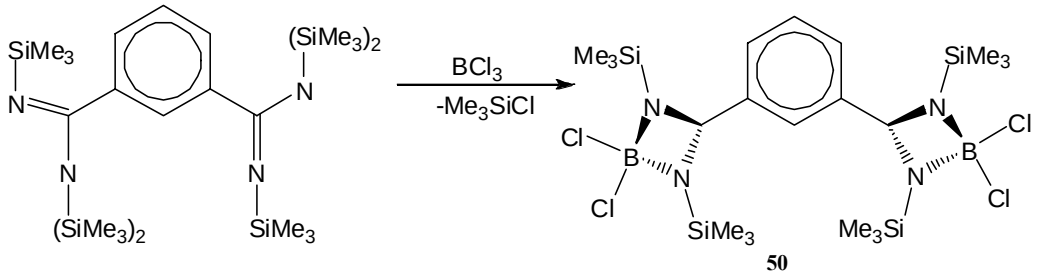

50 (10)

A crystalline sample of **50** suitable for X-ray diffraction study was obtained by recrystallization from dichloromethane solution. Compound **50** crystallizes in the orthorhombic space group Pca2/1 with Z = 4 and the molecular structure of **50** is shown in Figure 2.26. Compound **50** is monomeric in the solid state and features two planar,

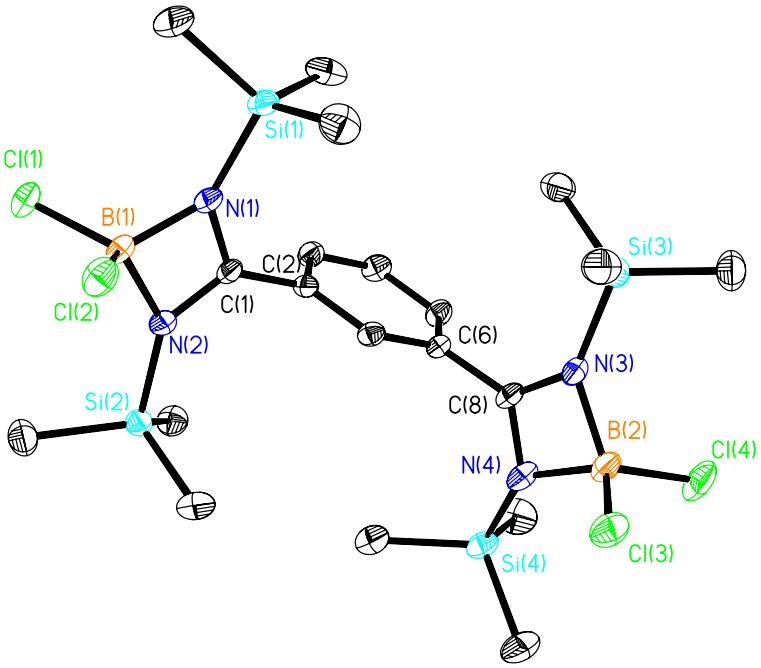

Figure 2.26. ORTEP diagram of **50** with thermal ellipsoids at 30% probability. All hydrogen atoms have been omitted for clarity.

four-membered B-N-C-N chelate rings linked by a phenyl group. The chelate rings are arranged in a perpendicular fashion with respect to the bridging phenyl group. The boron atoms are bound to two chlorine and two nitrogen atoms, giving rise to an overall distorted tetrahedral coordination environment. The B-N, B-Cl, and N-C bond distances and internal bond angles of the four-membered ring are very similar to those observed for the parent boron amidinate [PhC{NSiMe$_3$}$_2$BCl$_2$], and are indicative of electron delocalization within the N-C-N junction [46]

*Synthesis and Characterization of Compounds **51** and **52***

Compounds **51** and **52** were obtained in a similar fashion to that described for compound **50** by replacing **48a** with **48b** and using BCl_3 or $PhBCl_2$ (Eq. 11). Both new compounds were obtained as colorless crystalline solids in high yields. Analogously to **50**, the ^{1}H and $^{13}C\{^{1}H\}$ NMR spectra of **51** and **52** show resonances due to the trimethylsilyl groups and the bridging phenyl group, along with weak $^{13}C\{^{1}H\}$ resonances at δ 169 ppm and δ 179 ppm, respectively, that are indicative of electron delocalization within the N-C-N fragments. The $^{11}B\{^{1}H\}$ NMR spectra of **51** and **52** exhibit intense signals at δ 5.63 and δ 9.05 ppm, respectively. Both resonances fall within the typical range established for four-coordinate boron atoms[29]. The CI^{+} mass spectra of **51** and **52** evidence peaks at *m/z* 612 and 695, respectively, thus proving the attachment of BCl_2 and PhBCl fragments, respectively, to the binuclear bis(amidinate) framework. The elemental compositions of **51** and **52** were confirmed by high-resolution mass spectroscopy.

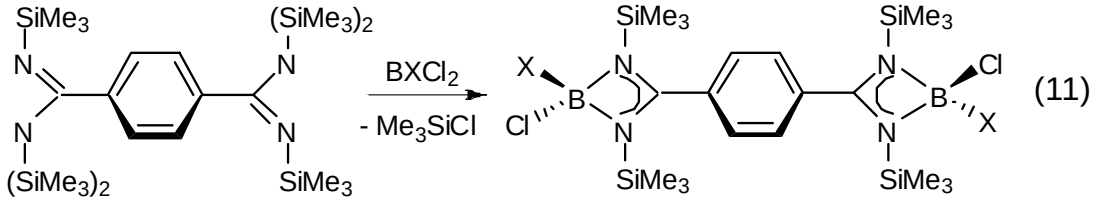

48b

51: X = Cl
52: X = Ph

(11)

A crystal of **52** suitable for single-crystal X-ray diffraction was obtained by cooling a toluene solution to -40°C overnight. Compound **52** crystallizes in the monoclinic space

group $P2_1/c$ with Z = 2. However, disorder of the phenyl and trimethylsilyl groups (Fig. 2.27) precluded a satisfactory refinement of the X-ray data thus preventing a detailed comparison of the metrical parameters with those of **52**. The atom connectivity of the molecule is shown in Figure 2.27.

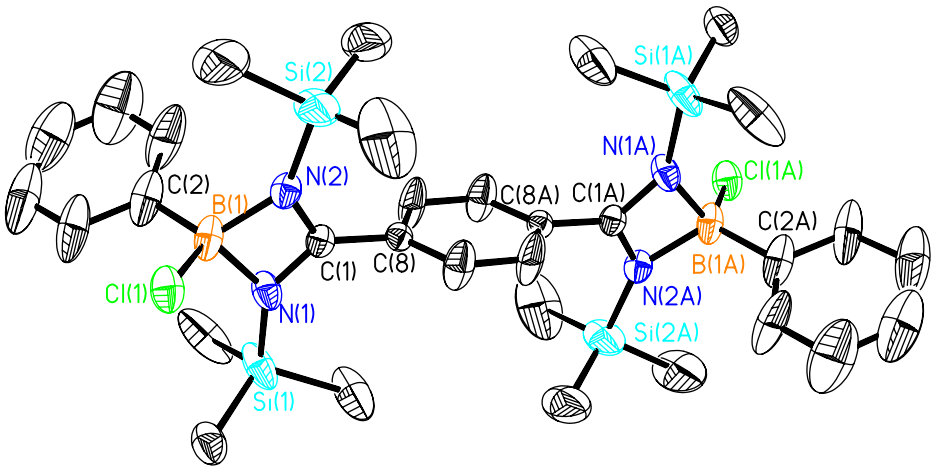

Figure 2.27. ORTEP diagram of **52** with thermal ellipsoids at 30% probability. All hydrogen atoms have been omitted for clarity.

*Synthesis and Characterization of Compound **53***

Treatment of **35** with two equivalents of a solution of N,N,N'-tris(trimethylsilyl)-benzamidine in toluene at room temperature resulted, after workup, in the isolation of compound **53** as colorless crystalline solid in high yield (Eq. 12). The ^{1}H and $^{13}C\{^{1}H\}$ NMR spectra of compound **53** exhibits signals due to equivalent trimethylsilyl groups, the phenyl groups on the amidinate ligands and the bridging phenyl group. A low-

intensity $^{13}C\{^1H\}$ resonance at δ 180 ppm is attributable to electron delocalization within the N-C-N fragment. The $^{11}B\{^1H\}$ NMR spectrum of **53** consists of an intense singlet resonance at δ 6.41 ppm that falls in the typical range established for four-coordinate boron atoms[29]. The CI^- mass spectral peak at *m/z* 784 is consistent with the binding of two amidinate ligands to the $C_6H_4(BBr)_2$ fragment. The CI^+ mass spectrum evidenced a peak corresponding to the $[M\text{-}Br]^+$ ion at *m/z* 705. The proposed elemental composition was confirmed by high-resolution mass spectroscopy.

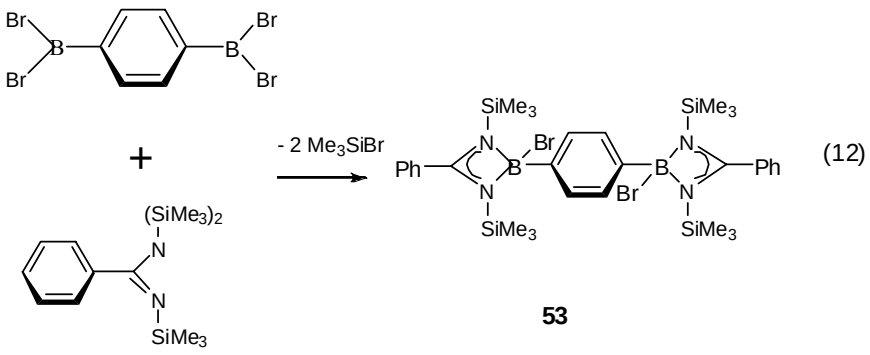

53 (12)

Confirmation of the proposed structure of **53** was provided by a single-crystal X-ray diffraction study. Compound **53** crystallizes in the triclinic space group $P\bar{1}$ with two independent molecules in the asymmetric unit. Each molecule features two boron amidinate moieties bridged in the 1, 4 position by a phenyl group. Each CNNB ring is a planar as indicated by the sums of angles of 359.74(4)° and 359.73(4)°, respectively. The two four-membered rings are not exactly perpendicular to the linking phenyl group, since

the dihedral angles are 87.7(2)° and 85.3(2)°. The two boron atoms deviate from the plane of the phenyl ring by -0.19(1) Å for B(1) and by -0.11(1) Å for B(2). The two bromine atoms deviate from the phenyl plane by 0.39(1) Å and -0.16(1) Å for Br(1) and Br(2), respectively. The torsion angle between the B(1)-Br(1) and B(2)-Br(2) bonds is 16.8°. The geometries of the two amidinate moieties are identical within experimental error. The average B-N bond distance is 1.582(3) Å and is very similar to that of compound **50** and other boron amidinates[46, 47].

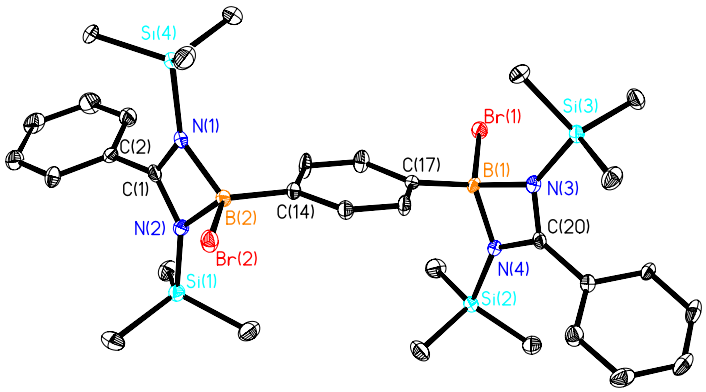

Figure 2.28. ORTEP diagram of **53** with thermal ellipsoids at 30% probability. All hydrogen atoms have been omitted for clarity.

*Syntheses of Compounds **54** and **55** by the Salt Metathesis Method*

Treatment of the bis(amidine) **49** with two equivalents of *n*-BuLi, followed by the addition of the requisite boron halide furnished, after workup, **54** and **55** as colorless crystalline solids in high yields (Eq. 13). The ^{1}H, $^{13}C\{^{1}H\}$ and $^{11}B\{^{1}H\}$ NMR data for both compounds are very similar to those of **51** and **52**, indicating the presence of

amidinate ligands linked by a benzene ring in the *1* and *4* positions. The mass spectral data were also consistent with this proposal and confirmation was provided by an X-ray

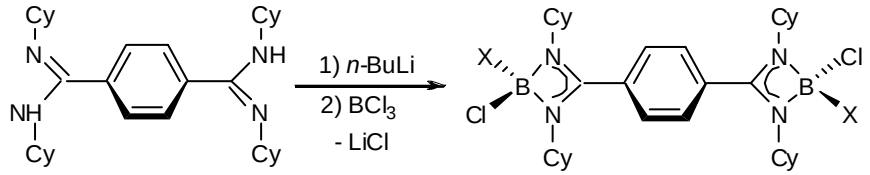

49 **54: X = Cl** **55: X = Ph** (13)

diffraction study of a single crystal of **54** (Figure 2.29). Compound **54** crystallizes in the orthorhombic space group Pbcn with Z = 4. The molecular structure of **54** is very similar to those of **50** and **52** in the sense that a BCl_2 fragment is bound by each of the two N-donors of the amidinate in a symmetrical bidentate fashion thereby resulting in a planar B-N-C-N ring. The B-Cl, B-N and C-N bond distances and bond angles in **54** are similar to those in **50** and the bulky boron amidinate [Mes*C{NCy}$_2$BCl$_2$] [Mes* = 2,4,6-tri(*tert*-butyl)phenyl] [46].

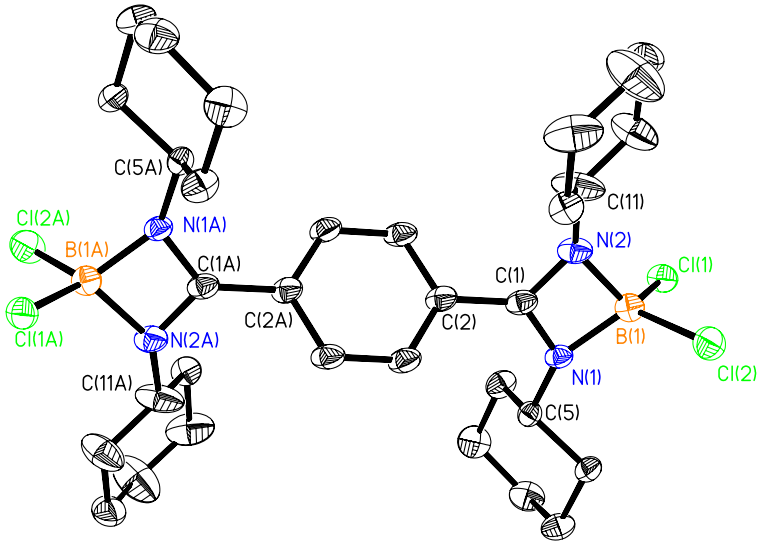

Figure 2.29. ORTEP diagram of **54** with thermal ellipsoids at 30% probability. All hydrogen atoms have been omitted for clarity.

Attempted Preparation of Dicationic Boron Bis(amidinates)

Several attempts were made to abstract the two halides from compound **52**, **53** and **55** by treatment of these compounds with $AlCl_3$ or $K[B(C_6F_5)_4]$ in toluene or methylene chloride solution at ambient temperature. The progress of each of these reactions was monitored by $^{11}B\{^1H\}$ NMR spectroscopy. In all cases, the characteristic signals for **52**, **53** and **55** disappeared, and in the case of the $AlCl_3$ reactions, broad weak signals around δ 30 ppm were detected. These observations are very similar to those made with the analogous cationic β-diketiminate cationic complexes that were described in **Part I** of this Chapter. However, although these $^{11}B\{^1H\}$ NMR observations are consistent with the formation of diboron dications (Scheme 2.7), the evidence is not conclusive.

Attempts to isolate such compounds were not successful due to facile hydrolysis of the reaction mixture.

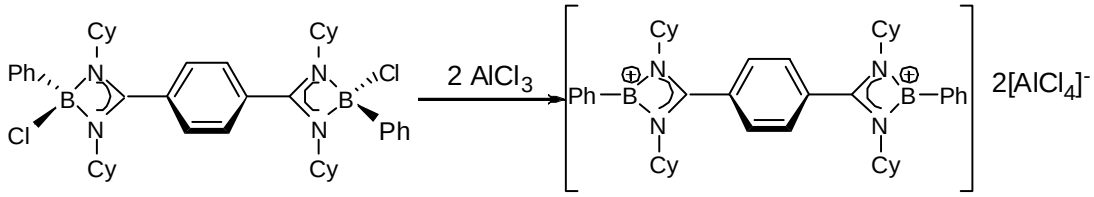

Scheme 2.7. Attempted preparation of a diboron dication.

Attempted Preparation of a Boron-Containing Polymer

The successful preparation of compounds **52** and **53** raised the possibility of preparing a novel boron-containing polymer (Scheme 2.8). The proposed polymer is potentially a conjugated system and could therefore exhibit conductivity. The reaction indicated in Scheme 2.8 was attempted in several different solvents. However, in each case, a pink material was precipitated within 5 minutes. Unfortunately, the extreme insolubility of this product precluded NMR measurements and several other attempted characterization methods such as MALDI-TOF mass spectroscopy were not successful. It is likely that extensive cross-linking of the chain took place via elimination of Me_3SiBr.

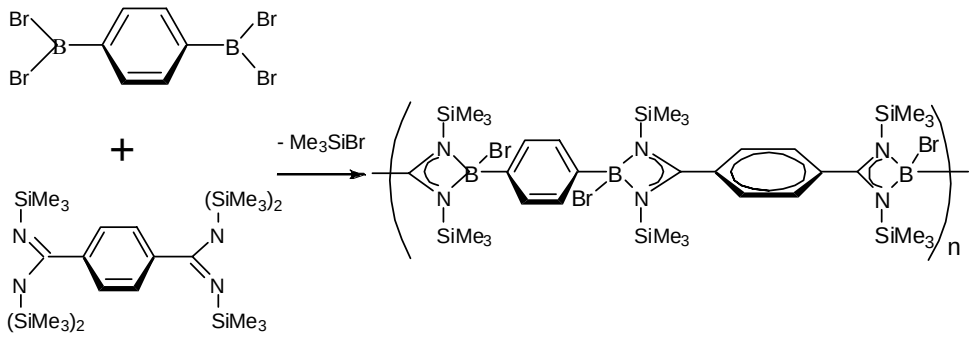

Scheme 2.8. Attempted preparation of an amidinate-based polymer.

Conclusions

In summary, the range of boron amidinates has been expanded to include binuclear complexes. On the basis of spectroscopic and X-ray structural data, the bonding in the four-membered B-N-C-N chelate rings in these compounds can be described in terms of equal contributions from two diaza-allyl resonance forms which results in electron delocalization at the N-C-N junctions. This structural feature is characteristic of the majority of group 13 amidinate compounds [44,46,47]. Bridged binuclear compounds such as **50-55** may find use as synthons for the construction of coordination networks and advanced materials.

Attempts to synthesize dinuclear boron dicationic bisamindinate complexes were not successful due to the difficulty of isolating the final products. However, $^{11}B\{^{1}H\}$ NMR spectroscopic evidence shows that proposed dications are present in the reaction mixture. Attempts to prepare a boron bis(amidinate) polymer were not successful due to the extreme insolubility of the resulting material.

Experimental Section

General Procedures

All reactions were performed under a dry, oxygen-free atmosphere utilizing Schlenk manifold techniques or a drybox. Diethyl ether and toluene were dried by storage over sodium benzophenone ketyl and freshly distilled prior to use. The starting materials $[\{HC(CMe)_2(NDipp)_2\}H]$,[48] Cp^*BCl_2,[49] 1,4-$C_6H_4(BBr_2)_2$,[32] $Ag[B(C_6F_5)_4]$[50] and $[CpFe(CO)_2GaCl_2]_\infty$[51] were prepared according to the literature procedures. Phenyldichloroborane, potassium hydride, aluminum trichloride, gallium tribromide and boron trifluoride monoetherate were obtained commercially and used without further purification.

Low-resolution CI mass spectra were measured on a Finnigan MAT TSQ-700 mass spectrometer and high-resolution CI mass spectra were recorded on a VG Analytical ZAB-VE sector instrument. ^1H, $^{13}C\{^1H\}$, $^{11}B\{^1H\}$ and $^{27}Al\{^1H\}$ NMR spectra were recorded at 295 K on a Varian Unity+ 300 instrument (^1H, 300 MHz; ^{13}C, 75 MHz; ^{11}B, 96 MHz; ^{27}Al, 78 MHz). The ^1H and $^{13}C\{^1H\}$ chemical shift values are reported in parts per million (ppm) relative to $SiMe_4$ (δ 0 ppm). The $^{11}B\{^1H\}$ and $^{27}Al\{^1H\}$ NMR data are referenced to $BF_3{\cdot}OEt_2$ (δ 0 ppm) and $AlCl_3/D_2O$ solution (δ 0 ppm), respectively.

X-ray Crystallography

Suitable single crystals were removed from a Schlenk flask under a positive pressure of argon, placed on a glass slide, covered immediately with degassed hydrocarbon oil and

mounted on a thin glass fiber. The X-ray diffraction data were collected at 153 K on a Nonius Kappa CCD diffractometer equipped with an Oxford Cryostream low-temperature device and a graphite-monochromated Mo Kα radiation source (λ = 0.71073 Å). Corrections were applied for Lorentz and polarization effects. All structures were solved by direct methods and refined by full-matrix least-squares cycles on F^2.[53] All non-hydrogen atoms were allowed anisotropic thermal motion, and hydrogen atoms were placed in fixed, calculated positions using a riding model (C-H 0.96 Å).

*Preparation of $[HC(CMe)_2(NDipp)_2]BF_2$ (**25**)*

A solution of *n*-BuLi (0.15 mL, 1.6 *M*) was added to a solution of $[HC(CMe)_2(NDipp)(NHDipp)]$ (0.1 g, 0.24 mmol) in 20 mL of toluene at ambient temperature. The reaction mixture was stirred for approximately 2 h, $BF_3{\cdot}OEt_2$ was added, and the reaction mixture was allowed to stir overnight. After workup of the reaction mixture, colorless crystalline **25** was isolated in 60% yield. Mass spectrum (CI^+) M^+ *m/z* 466, $[M\text{-}F]^+$ *m/z* 448. HRMS (CI^+, CH_4): Calcd. for $C_{29}H_{41}N_2BF_2$, 466.3331; found 466.3333. ^1H NMR (C_6D_6): δ 1.11-1.46 (m, 24H, $CH(CH_3)_2$), 1.67 (s, 6H, CH_3), 3.32 (septet, 4H, $CH(CH_3)_2$), 4.89 (s, 1H, CH), 7.10-7.18 (m, 6H, Ar). ^{13}C NMR (CD_2Cl_2): δ 146.64, 142.67, 125.73, 124.39, 123.48, 120.12, 94.15, 28.51, 24.60, 24.36, 23.32, 20.66. $^{11}B\{^1H\}$ NMR (C_6D_6): δ 1.24 (t, $J_{B\text{-}F}$ = 28.8 Hz). ^{19}F NMR (C_6D_6): δ -128.48 (quartet, $J_{B\text{-}F}$ = 28.4 Hz).

*Preparation of [MeC(CMe)$_2$(NDipp)$_2$]AlMe$_2$ (**26**)*

A hexane solution of $AlMe_3$ (1.2 mL, 1.0 *M*) was added to a vigorously stirred solution of 0.5 g of [{MeC(CMe)$_2$(NDipp)$_2$}H] (1.2 mmol) in 100 mL toluene solution at ambient temperature. The reaction mixture was allowed to stir for approximately 2 h. The precipitate that had formed was filtered off and the filtrate was concentrated to a volume of approximately 5 mL. Storage of this solution overnight at -40 °C resulted in the formation of 0.40 g (70%) of colorless crystalline **26**. ^{1}H NMR (C_6D_6) δ 7.18-7.15 (m, 6H, Ar), 3.43 (quartet, J = 6.9 Hz, 4H, C*H*Me$_2$), 1.78 (s, 3H, CH_3), 1.68 (s, 6H, CH_3), 1.38-1.11 (m, 24H, CH*Me$_2$*), -1.12 (s, 6H, Al*Me$_2$*). ^{13}C{^{1}H} NMR (C_6D_6) δ 169.19 (*C*N), 144.94, 125.91, 124.89, 123.95 (Ar), 99.96 (*C*Me), 28.75 (*C*HMe$_2$), 25.52, 25.13, 24.77, 23.97 (CH*Me$_2$*), 22.50 (*C*H_3), 19.08 (*C*H_3), 18.43 (*C*H_3). ^{27}Al{^{1}H} NMR (C_6D_6) δ 5.89. Mass Spectrum (CI^+, CH_4): M^+ *m/z* 489, $[M\text{-}CH_3]^+$ *m/z* 473. HRMS (CI, CH_4): calcd for $C_{32}H_{50}N_2Al$ 489.3789, found 489.3790.

*Preparation of [MeC(CMe)$_2$(NDipp)$_2$]AlCl$_2$ (**27**)*

A hexane solution of $MeAlCl_2$ (1.2 mL, 1.0 *M*) was added to a vigorously stirred solution of 0.5 g of [{MeC(CMe)$_2$(NDipp)$_2$}H] (1.2 mmol) in 100 mL of toluene at ambient temperature. The reaction mixture was allowed to stir for approximately 2 h. The precipitate that had formed was filtered off and the filtrate was concentrated to a volume of approximately 5 mL. Storage of this solution overnight at -40 °C resulted in the formation of 0.5 g (70%) of colorless crystalline **27**. ^{1}H NMR (CD_2Cl_2): δ 7.35-7.27 (m, 6H, Ar), 5.45 (s, 1H, γ-C*H*), 3.25 (quartet, J = 6.9Hz, 4H, C*H*Me$_2$), 2.09 (s, 3H, CH_3),

1.98 (s, 6H, CH_3), 1.32-1.14 (m, 24H, CH*Me*$_2$). $^{13}C\{^1H\}$ NMR (CD_2Cl_2) δ 172.08 (*C*N), 145.57, 128.46, 128.31, 125.26, 125.22 (Ar), 99.96 (*C*Me), 29.12 (*C*HMe_2), 29.03, 25.74, 25.61, 25.39, 25.07 (CH*Me*$_2$), 22.98 (*C*H_3), 18.68 (*C*H_3). $^{27}Al\{^1H\}$ NMR (CD_2Cl_2): δ 99.1. Mass Spectrum (CI^+, CH_4): $[M+H]^+$ *m/z* 530, $[M\text{-}Cl]^+$ *m/z* 493; HRMS (CI, CH_4): calcd for $C_{30}H_{43}N_2AlCl_2$ 528.2620, found 528.2619.

*Preparation of [{HC(CMe)$_2$(NDipp)$_2$}B(Ph)Cl] (**28**)*

A solution of [HC(CMe)$_2$(NDipp)$_2$]H (1 g, 2.38 mmol) in 20 mL of Et_2O was added to a rapidly stirred suspension of KH (0.11 g, 2.62 mmol) in Et_2O at room temperature. The reaction mixture was allowed to stir overnight. After filtration and solvent removal from the filtrate under reduced pressure, the resulting residue was redissolved in 30 mL of toluene. Neat $PhBCl_2$ (0.29 mL) was added to the [HC(CMe)$_2$(NDipp)$_2$]K solution and the reaction mixture was stirred rapidly for 2 h at room temperature. Following filtration, the volatiles were removed from the filtrate under reduced pressure leaving a yellow oil that was characterized by $^{11}B\{^1H\}$ NMR and low-resolution mass spectroscopy. $^{11}B\{^1H\}$ NMR δ 11.42 ppm. Mass Spectrum (CI^+): M^+ *m/z* 541, $[M\text{-}Cl]^+$ *m/z* 505.

*Preparation of [{HC(CMe)$_2$(NDipp)$_2$}B(Ph)OH] (**29**)*

Compound **29** was obtained by exposure of **28** to moist air. This compound was characterized solely on the basis of a single-crystal X-ray diffraction study.

*Preparation of [{HC(CMe)$_2$(NDipp)$_2$}BPh][Al$_2$Cl$_7$] (**30**)*

A toluene solution of [{HC(CMe)$_2$(NDipp)$_2$}B(Ph)Cl] (**28**) was prepared as described above. Following filtration, the filtrate was transferred via cannula on to 0.30 g (2.24 mmol) of $AlCl_3$ and the reaction mixture was stirred for 3 h at room temperature. Filtration followed by concentration and cooling of the filtrate to –40ºC afforded a crop of pale yellow crystals of **30** (0.41 g, 23 %). ^{1}H NMR ($CDCl_3$): δ 0.78 (d, 12H, J = 6.6 Hz, CH(CH_3)$_2$), 1.06 (d, 12H, J = 6.6 Hz, CH(CH_3)$_2$), 2.16 (s, 6H, CH_3), 2.50 (septet, 4H, J=6.6 Hz, CH(CH$_3$)$_2$), 6.33-7.42 (m, 12H, γ-CH + ArCH). ^{13}C{^{1}H} NMR (CD_2Cl_2): δ 172.5 (*C*N), 143.3, 135.7, 134.3,131.3, 130.7, 127.4, 126.0 (Ph ring C), 115.1 (γ-*C*H), 29.5 (*C*HMe), 24.9 (CH*Me*$_2$), 23.7 (CH*Me*$_2$), 23.4 (Me). ^{11}B{^{1}H} NMR ($CDCl_3$): δ 33.5 (s, br). HRMS (CI$^+$, CH_4): Calcd. for $C_{35}H_{46}BN_2$, 505.3754; found 505.3760.

Preparation of [(NDipp)C(Me)C(H)C(Me)(NDipp)B(Cp)Cl] (**31**)*

A hexane solution of *n*-BuLi (0.95 mL, 2.5 *M*, 2.38 mmol) was added to a rapidly stirred solution of [HC(CMe)$_2$(NDipp)$_2$]H (1.0 g, 2.38 mmol) in 20 mL of hexane at room temperature. The reaction mixture was allowed to stir overnight. Neat Cp*BCl_2 (0.52 g, 2.38 mmol) was added to the [HC(CMe)$_2$(NDipp)$_2$]Li solution and the reaction mixture was stirred rapidly for 2 h at room temperature. After filtration, the hexane was removed under reduced pressure. The crude product was recrystallized from toluene affording a crop of yellow crystals of **31** (1.0 g, 70 %). HRMS (CI$^+$, CH_4): Calcd. for $C_{39}H_{57}BN_2Cl$, 599.4303; found 599.4305. ^{1}H NMR (C_6D_6): δ 1.12-1.21 (m, 24H, CH(CH_3)$_2$), 1.46 (s, 3H, CH_3), 1.66 (s, 3H, CH_3), 1.77 (s, 6H, Cp*), 2.09 (s, 6H, Cp*),

2.24 (s, 3H, Cp*), 2.83 (septet, 2H, J = 6.6 Hz, C*H*$(CH_3)_2$), 3.33 (septet, 2H, J = 6.6 Hz, C*H*$(CH_3)_2$), 5.25 (s, 1H, γ-C*H*), 7.04-7.17 (m, 6H, Ar). A $^{11}B\{^1H\}$ NMR signal was not detected.

Preparation of [{HC(CMe)$_2$(NDipp)$_2$}BCp][AlCl$_4$] (**32**)*

The same procedure was employed as that described for the preparation of **31**. Following removal of the hexane solvent, the resulting residue was redissolved in 20 mL of toluene, and the solution was transferred via cannula on to 0.30 g (2.24 mmol) of solid $AlCl_3$. The reaction mixture was stirred for 3 h at room temperature. Following filtration and removal of the toluene under reduced pressure, the resulting solid was recrystallized by addition of a layer of hexane to a toluene solution of **32**. Yield 0.41 g (23.3 %). HRMS (CI^+, CH_4): Calcd. for $C_{39}H_{56}BN_2$, 563.4537; found 563.4536. ^1H NMR (CD_2Cl_2): δ 0.91-1.41 (m, 24H, CH(C*H*$_3$)$_2$), 1.60 (s, 3H,C*H*$_3$), 1.64 (s, 3H, C*H*$_3$), 1.86 (s, 6H, Cp*), 2.38 (s, 6H, Cp*), 2.75 (s, 3H, Cp*), 3.24 (septet, 4H, J = 6.6 Hz, C*H*$(CH_3)_2$), 4.46 (s, 1H, γ-C*H*), 7.07-7.31 (m, 6H, Ar). $^{11}B\{^1H\}$ NMR: δ 11.8. $^{27}Al\{^1H\}$ NMR: δ 103.2.

*Preparation of [{MeC(CMe)$_2$(NDipp)$_2$}BPh][AlCl$_4$] (**33**)*

An equimolar quantity of neat $PhBCl_2$ was added to a toluene solution of [{MeC(CMe)$_2$(NDipp)$_2$}$AlCl_2$] (**27**) and the reaction mixture was stirred at room temperature overnight. After removal of all the volatiles under reduced pressure, colorless solid **33** was obtained in *ca.* 80 % yield. ^1H NMR (CD_2Cl_2): δ 8.27-6.70 (m, 11H, Ar), 2.79-2.71 (m, 4H, C*H*Me_2), 2.54 (s, 3H, C*H*$_3$), 2.50 (s, 6H, C*H*$_3$), 1.26-0.93 (m,

24H, CH*Me*$_2$); ^{13}C{^{1}H} NMR (CD_2Cl_2) δ 170.69 (*C*N), 143.55, 135.94, 133.97,131.20, 130.26, 128.37, 127.28, 125.89 (Ph ring C), 29.48 (*C*HMe$_2$), 24.99 (CH*Me*$_2$), 23.25 (CH*Me*$_2$), 22.45, 16.51, 13.61 (*Me*). ^{11}B{^{1}H} NMR ($CDCl_3$): δ 31.9 (s, br). HRMS (CI, CH_4): Calcd. for $C_{36}H_{48}BN_2$, 519.3911; found 519.3914.

*Synthesis of [{HC(CMe)$_2$(NDipp)$_2$}BF][B(C$_6$F$_5$)$_4$] (**34**)*

Solid Ag[B(C_6F_5)$_4$] (1.1 equiv.) was added to a toluene solution of [HC(CMe)$_2$(NDipp)$_2$]BF_2 (**25**). The reaction mixture was allowed to stir overnight. Following removal of the precipitated material by filtration, the volatile material was removed from the filtrate under reduced pressure. Colorless solid **34** was obtained in *ca.* 60 % yield . LRMS (CI^-) [B(C_6F_5)$_4$]$^-$ *m/z* 679. ^{1}H NMR (CD_2Cl_2): δ 7.45-7.10 (m, 6H, Ar), 6.78 (s, 1H, C*H*), 4.02 (septet, 4H, C*H*(CH_3)$_2$), 2.34 (s, 6H, C*H*$_3$), 1.45-0.86 (m, 24H, CH(C*H*$_3$)$_2$). ^{11}B{^{1}H} NMR (CD_2Cl_2): δ 27.35 (*B*F), -16.89 [*B*(C_6F_5)$_4$]. ^{19}F NMR (CD_2Cl_2): δ -133.52, -164.02, -167.93 (B(C_6F_5)$_4$).

*Attempted syntheses of 1,4-C$_6$H$_4$[BBr{(NDipp)$_2$(CMe)$_2$CMe}]$_2$ (**36**) and 1,4-C$_6$H$_4$[B(OH){(NDipp)$_2$(CMe)$_2$CMe}]$_2$ (**37**)*

The compound 1,4-$C_6H_4(BBr_2)_2$ (**35**) was added to an equimolar quantity of [MeC(CMe)$_2$(NDipp)$_2$]Li in toluene solution at room temperature. The reaction mixture was allowed to stir overnight. After removal of all solid material by filtration, the volatiles were removed from the filtrate under reduced pressure. Compound **36** was isolated as a yellow oil. Cooling of the yellow oil **36** to -30°C for one week resulted in

the formation of a yellow crystal of **37**, which was characterized by single-crystal X-ray diffraction. No spectroscopic data were obtained because of the small size of the sample.

*Preparation of [{HC(CMe)$_2$(NDipp)$_2$}Ga(Cl)Fe(C$_5$H$_5$)(CO)$_2$] (**39**)*

A hexane solution of *n*-BuLi (0.14 mL, 1.6 M, 0.24 mmol) was added to a THF solution of [HC(CMe)$_2$(NDipp)$_2$]H (0.1 g, 0.24 mmol). The reaction mixture was stirred for 3 h, following which [CpFe(CO)$_2$GaCl$_2$]$_\infty$ (0.1 g, 0.31 mmol) in 10 mL THF was added. The resulting reaction mixture was allowed to stir overnight, after which all volatiles were removed under reduced pressure. The solid product was extracted with toluene. After recrystallization from toluene, 0.16 g (70 %) of compound **39** was isolated. ^{1}H NMR (C_6D_6): δ 7.18-7.08 (m, 6H, Ar), 5.18 (s, 1H, γ-C*H*), 3.99 (s, 5H, Cp), 3.43-3.26 (m, 4H, C*H*Me$_2$), 1.65 (s, 6H, C*H$_3$*), 1.43-1.08 (m, 24H, CH*Me$_2$*); ^{13}C{^{1}H} NMR (C_6D_6) δ 179.30 (*C*N), 161.40, 146.64, 143.15, 142.66, 141.14, 138.55, 124.75, 123.47 (Ar), 94.15 (γ-*C*H), 82.15 (Cp), 29.95 (*C*HMe$_2$), 28.50 (CH*Me$_2$*), 25.28 (CH*Me$_2$*), 24.65, 24.34, 23.31, 20.65 (*Me*). The CO resonance was not detected. HRMS (CI, CH_4): Calcd. for $C_{36}H_{46}N_2O_2FeGa$, 663.2164; found 663.2166.

Synthesis of 1,3-C$_6$H$_4$[C{N(SiMe$_3$)}$_2$BCl$_2$]$_2$ (**50**).

Boron trichloride (10 mL, 1.0 *M* in hexane, 10 mmol) was added to a stirred solution of **48a** (3.0 g, 5 mmol) in 20 mL of toluene at room temperature. After being stirred overnight, the reaction mixture was filtered through Celite® and the solvent was removed from the filtrate under reduced pressure to afford a white powder. Recrystallization of

this powder from dichloromethane solution afforded a crop of colorless crystals of **50** (91 % yield). ^{1}H NMR ($CDCl_3$): δ 7.69 (m, Ph, 3H), 7.50 (s, Ph, 1H), 0.170 (s, $SiMe_3$, 36H); $^{13}C\{^{1}H\}$ NMR (C_6D_6): δ 169.37 (N*C*N), 132.96, 129.72, 129.13, 124.12 (Ph), 0.35 ($SiMe_3$); $^{11}B\{^{1}H\}$ NMR ($CDCl_3$): δ 5.73. MS (CI^+): $[M+H]^+$ *m/z* 612, $[M-Cl]^+$ *m/z* 576. HRMS (CI, CH_4) calcd. for $C_{20}H_{40}N_4B_2Si_4Cl_4$, 610.1270; found 610.1278.

Synthesis of 1,4-$C_6H_4[C\{N(SiMe_3)\}_2BCl_2]_2$ (**51**).

Colorless crystalline **51** was prepared in 90 % yield from BCl_3 (10 mL, 1.0 *M* in hexane, 10 mmol) and **48b** (3.0 g, 5 mmol) using the procedure described for the preparation of **50**. ^{1}H NMR ($CDCl_3$): δ 7.47 (m, Ph, 4H), 0.15 (s, $SiMe_3$, 36H); $^{13}C\{^{1}H\}$ NMR (C_6D_6): δ 168.95 (NCN), 136.40, 122.20 (Ph), 0.32 ($SiMe_3$); $^{11}B\{^{1}H\}$ NMR ($CDCl_3$): δ 5.62. MS (CI^+): $[M+H]^+$ *m/z* 612, $[M-Cl]^+$ *m/z* 576. HRMS (CI, CH_4) calcd. for $C_{20}H_{40}N_4B_2Si_4Cl_4$, 610.1270; found 610.1280.

Synthesis of 1,4-$C_6H_4[C\{N(SiMe_3)\}_2B(Ph)Cl]_2$ (**52**).

Colorless crystalline **52** was prepared in 91 % yield from $PhBCl_2$ (1.6 g, 10 mmol) and **48b** (3.0 g, 5 mmol) in 20 mL of toluene using the procedure described for the preparation of **50**. ^{1}H NMR ($CDCl_3$): δ 7.45 (m, Ph, 14H), -0.05 (s, $SiMe_3$, 36H); $^{13}C\{^{1}H\}$ NMR ($CDCl_3$): δ 178.85 (NCN), 140.78, 136.11, 133.66, 132.14 (Ph), 0.42 ($SiMe_3$); $^{11}B\{^{1}H\}$ NMR ($CDCl_3$): δ 9.05. MS (CI^+): $[M+H]^+$ *m/z* 695, $[M-Cl]^+$ *m/z* 660, $[M-Ph]^+$ 617. HRMS (CI, CH_4) calcd. for $C_{32}H_{50}N_4B_2Si_4Cl_2$, 694.2676; found 694.2678.

Synthesis of 1,4-$C_6H_4[BrB\{N(SiMe_3)\}_2CPh]_2$ (**53**).

20 mL of a toluene solution of 1,4-$C_6H_4(BBr_2)_2$ (**35**) (4.2 g, 10 mmol) was added to a stirred solution of N,N,N'-tris(trimethylsilyl)-benzamidine (3.0 g, 5 mmol) in 20 mL of toluene at room temperature. After being stirred overnight, the reaction mixture was filtered through Celite® and the solvent was stripped from the filtrate to afford a white powder. Recrystallization of this powder from dichloromethane solution afforded a crop of colorless crystals of **53** (91 % yield). ^{1}H NMR ($CDCl_3$): δ 8.20 (d, Ph, 4H), 7.53-6.93 (m, Ph, 10H), 0.04 (s, $SiMe_3$, 36H); $^{13}C\{^1H\}$ NMR (C_6D_6): δ 180.39 (N*C*N), 146.65, 133.56, 132.24, 130.78, 126.91 (Ph), 0.29 ($SiMe_3$); $^{11}B\{^1H\}$ NMR ($CDCl_3$): δ 6.41. MS (CI^+): $[M\text{-}Br]^+$ *m/z* 705. (CI^-): M^- *m/z* 784. HRMS (CI, CH_4) calcd. for $C_{32}H_{50}N_4B_2Si_4Br_2$, 782.1665; found 782.1679.

Synthesis of 1,4-$C_6H_4[C\{NCy\}_2BCl_2]_2$ (**54**).

A 2.5 *M* solution of *n*-BuLi in hexane (4 mL, 10 mmol) was added dropwise to a solution of **49** (1.67 g, 5 mmol) in 30 mL of toluene at room temperature. The resulting slurry was stirred for 2 h, after which BCl_3 (10 mL, 1.0 *M* in hexane, 10 mmol) was added dropwise. After being stirred overnight, the reaction mixture was filtered through Celite® and the solvent was removed from the filtrate under reduced pressure to afford a white powder. Recrystallization of this powder from dichloromethane solution afforded a crop of colorless crystals of **54** (92% yield). ^{1}H NMR ($CDCl_3$): δ 7.71 (m, Ph, 4H), 3.44 (m, NC*H*, 4H), 1.76-1.12 (m, Cy, 40H); $^{13}C\{^1H\}$ NMR (C_6D_6): δ 173.25 (NCN), 138.60, 120.19 (Ph), 54.87 (Cy-C1), 33.45 (Cy), 25.49, 25.25 (Cy); $^{11}B\{^1H\}$ NMR ($CDCl_3$): δ

5.97. MS (CI^+): $[M+H]^+$ *m/z* 652, $[M-Cl]^+$ *m/z* 617. HRMS (CI, CH_4) calcd. for $C_{32}H_{48}N_4B_2Cl_4$, 650.2819; found 650.2822.

Synthesis of 1,4-C_6H_4[C{NCy}$_2$B(Ph)Cl]$_2$ (**55**).

Colorless crystalline **55** was prepared in 93% yield from *n*-BuLi (4.0 mL, 2.5 *M* in hexanes, 10 mmol), $PhBCl_2$ (1.6 g, 10 mmol) and **49** (1.67 g, 5 mmol) in 30 mL of toluene using the procedure described for the preparation of **55**. ^1H NMR ($CDCl_3$): δ 8.17 (d, Ph, 4H), 7.49-7.25 (m, Ph, 10H), 3.29 (m, NCH, 4H), 1.90-0.74 (m, Cy, 40H); $^{13}C\{^1H\}$ NMR ($CDCl_3$): δ 169.54 (NCN), 146.74, 138.62, 135.49, 133.20, 130.19 (Ph), 54.83 (Cy-C1), 34.51, 33.95, 25.49, 25.23 (Cy); $^{11}B\{^1H\}$ NMR ($CDCl_3$): δ 9.69. MS (CI^+): $[M+H]^+$ *m/z* 736, $[M-Cl]^+$ *m/z* 698. HRMS (CI, CH_4) calcd. for $C_{44}H_{58}N_4B_2Cl_2$, 734.4225; found 734.4222.

Table of Crystallographic Data

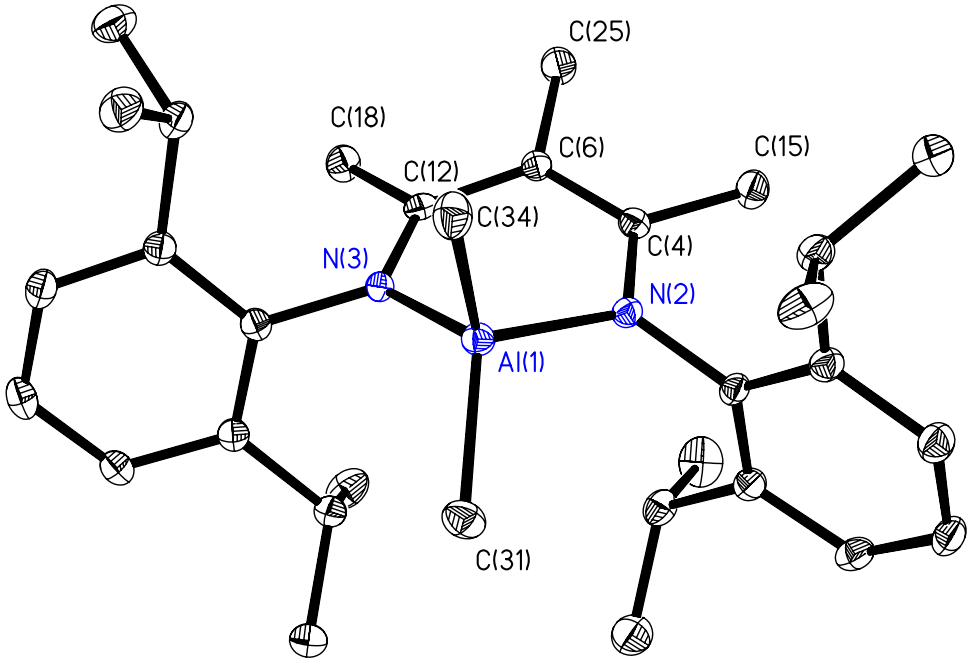

ORTEP diagram of compound **26** at 30% probability. All hydrogen atoms have been omitted for clarity.

Table 2.2. Crystal data and structure refinement for **26**.

Identification code	**26**	
Empirical formula	C32 H49 Al N2	
Formula weight	488.71	
Temperature	153(2) K	
Wavelength	0.71069 Å	
Crystal system	monoclinic	
Space group	p21/a	
Unit cell dimensions	a = 17.362(5) Å	α= 90.000(5)°.
	b = 9.961(5) Å	β= 109.939(5)°.
	c = 18.265(5) Å	γ = 90.000(5)°.
Volume	2969.5(19) $Å^3$	
Z	4	
Density (calculated)	1.093 Mg/m^3	
Absorption coefficient	0.090 mm^{-1}	
F(000)	1072	
Crystal size	0.2 x 0.2 x 0.2 mm^3	
Theta range for data collection	3.06 to 27.50°.	
Index ranges	-22<=h<=20, -12<=k<=12, -23<=l<=23	
Reflections collected	20427	
Independent reflections	6780 [R(int) = 0.0933]	
Completeness to theta = 27.50°	99.6 %	
Absorption correction	None	
Refinement method	Full-matrix least-squares on F^2	
Data / restraints / parameters	6780 / 0 / 513	
Goodness-of-fit on F^2	1.098	
Final R indices [I>2sigma(I)]	R1 = 0.0509, wR2 = 0.0800	
R indices (all data)	R1 = 0.1407, wR2 = 0.1020	
Extinction coefficient	0.0038(5)	
Largest diff. peak and hole	0.346 and -0.424 $e.Å^{-3}$	

Table 2.3. Selected Bond lengths [Å] and angles [°] for **26**.

Al(1)-N(2)	1.9086(16)
Al(1)-N(3)	1.9202(16)
Al(1)-C(31)	1.957(2)
Al(1)-C(34)	1.963(2)
N(2)-C(4)	1.346(2)
N(2)-C(7)	1.450(2)
N(3)-C(12)	1.343(2)
N(3)-C(10)	1.455(2)
C(4)-C(6)	1.403(3)
C(6)-C(12)	1.420(3)
N(2)-Al(1)-N(3)	94.29(7)
N(2)-Al(1)-C(31)	109.98(10)
N(3)-Al(1)-C(31)	116.68(9)
N(2)-Al(1)-C(34)	112.83(9)
N(3)-Al(1)-C(34)	108.21(10)
C(31)-Al(1)-C(34)	113.44(12)
C(4)-N(2)-C(7)	118.30(15)
C(4)-N(2)-Al(1)	121.07(13)
C(7)-N(2)-Al(1)	120.58(12)
C(12)-N(3)-Al(1)	120.60(12)
C(10)-N(3)-Al(1)	119.64(12)
N(2)-C(4)-C(6)	122.99(17)
C(4)-C(6)-C(12)	124.30(18)
N(3)-C(12)-C(6)	123.77(17)

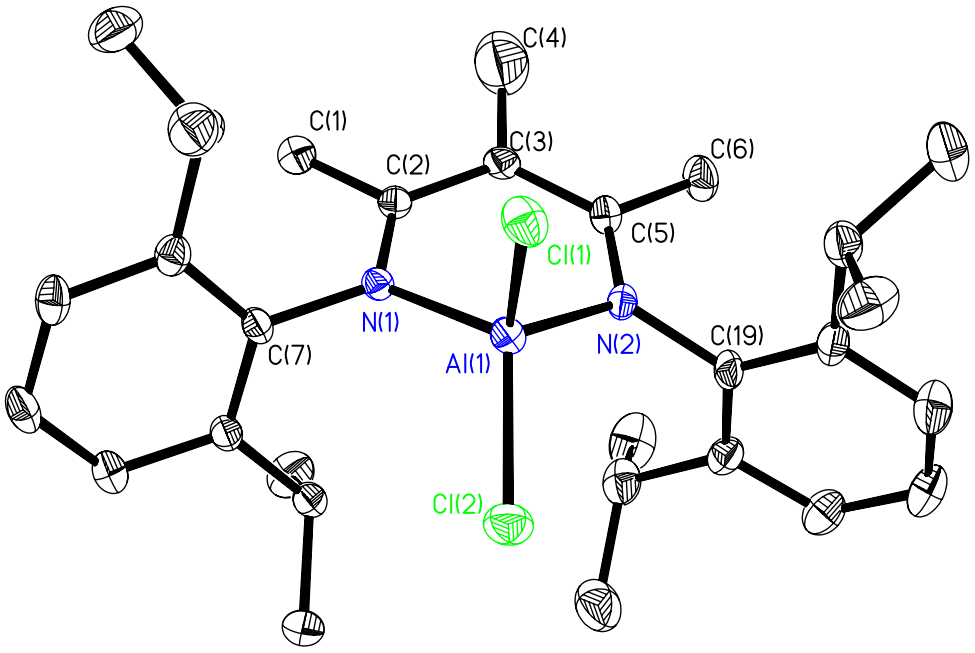

ORTEP diagram of compound **27** at 30% probability. All hydrogen atoms have been omitted for clarity.

Table 2.4. Crystal data and structure refinement for **27**.

Identification code	**27**	
Empirical formula	C30 H43 Al Cl2 N2	
Formula weight	529.54	
Temperature	153(2) K	
Wavelength	0.71069 Å	
Crystal system	monoclinic	
Space group	p21/c	
Unit cell dimensions	a = 18.065(5) Å	α= 90.000(5)°.
	b = 10.024(5) Å	β= 109.702(5)°.
	c = 17.308(5) Å	γ = 90.000(5)°.
Volume	2950.7(19) $Å^3$	
Z	4	
Density (calculated)	1.192 Mg/m^3	
Absorption coefficient	0.271 mm^{-1}	
F(000)	1136	
Crystal size	0.2 x 0.2 x 0.2 mm^3	
Theta range for data collection	3.07 to 25.00°.	
Index ranges	-21<=h<=21, -11<=k<=11, -19<=l<=20	
Reflections collected	16947	
Independent reflections	5179 [R(int) = 0.1530]	
Completeness to theta = 25.00°	99.7 %	
Absorption correction	None	
Refinement method	Full-matrix least-squares on F^2	
Data / restraints / parameters	5179 / 0 / 311	
Goodness-of-fit on F^2	1.015	
Final R indices [I>2sigma(I)]	R1 = 0.0673, wR2 = 0.1502	
R indices (all data)	R1 = 0.1786, wR2 = 0.2007	
Largest diff. peak and hole	0.494 and -0.575 $e.Å^{-3}$	

Table 2.5. Bond lengths [Å] and angles [°] for **27**.

C(2)-N(1)	1.344(6)
C(2)-C(3)	1.413(6)
C(3)-C(5)	1.399(6)
C(5)-N(2)	1.347(6)
C(7)-N(1)	1.461(5)
C(19)-N(2)	1.467(6)
N(1)-Al(1)	1.873(4)
N(2)-Al(1)	1.854(4)
Al(1)-Cl(2)	2.109(2)
Al(1)-Cl(1)	2.1357(19)
N(1)-C(2)-C(3)	123.3(4)
N(1)-C(2)-C(1)	119.7(4)
C(3)-C(2)-C(1)	117.0(4)
C(5)-C(3)-C(2)	126.0(4)
C(5)-C(3)-C(4)	117.3(5)
C(2)-C(3)-C(4)	116.4(5)
N(2)-C(5)-C(3)	122.7(4)
N(2)-C(5)-C(6)	119.1(4)
C(3)-C(5)-C(6)	118.1(4)
C(2)-N(1)-C(7)	119.3(4)
C(2)-N(1)-Al(1)	119.4(3)
C(7)-N(1)-Al(1)	121.0(3)
C(5)-N(2)-C(19)	117.4(4)
C(5)-N(2)-Al(1)	119.9(3)
C(19)-N(2)-Al(1)	122.6(3)
N(2)-Al(1)-N(1)	98.49(17)
N(2)-Al(1)-Cl(2)	111.87(14)
N(1)-Al(1)-Cl(2)	116.00(13)
N(2)-Al(1)-Cl(1)	112.82(13)
N(1)-Al(1)-Cl(1)	108.95(13)
Cl(2)-Al(1)-Cl(1)	108.53(8)

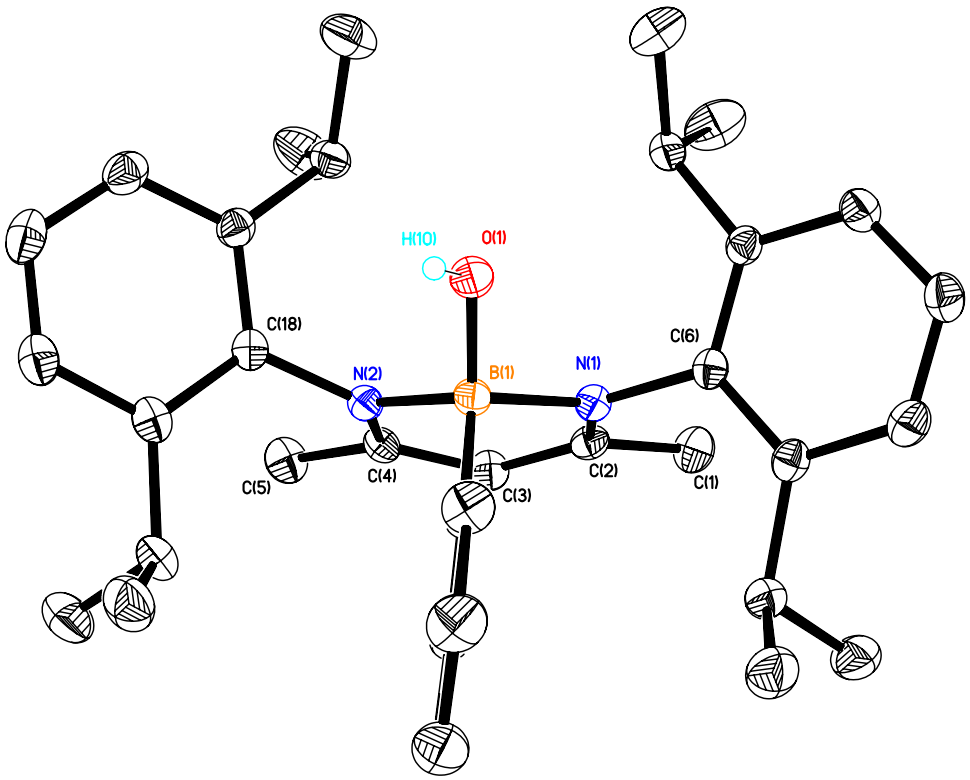

ORTEP diagram of compound **29** at 30% probability.

Table 2.6. Crystal data and structure refinement for **29**.

Identification code	**29**	
Empirical formula	C35 H47 B N2 O	
Formula weight	522.56	
Temperature	153(2) K	
Wavelength	0.71073 Å	
Crystal system	monoclinic	
Space group	p21/n	
Unit cell dimensions	a = 11.9633(3) Å	α= 90°.
	b = 16.2307(4) Å	β= 92.8690(10)°.
	c = 15.8214(4) Å	γ = 90°.
Volume	3068.23(13) $Å^3$	
Z	4	
Density (calculated)	1.131 Mg/m^3	
Absorption coefficient	0.067 mm^{-1}	
F(000)	1136	
Crystal size	0.36 x 0.23 x 0.19 mm^3	
Theta range for data collection	3.03 to 27.49°.	
Index ranges	-15<=h<=15, -16<=k<=20, -20<=l<=20	
Reflections collected	11498	
Independent reflections	7000 [R(int) = 0.0754]	
Completeness to theta = 27.49°	99.3 %	
Absorption correction	None	
Max. and min. transmission	0.9875 and 0.9765	
Refinement method	Full-matrix least-squares on F^2	
Data / restraints / parameters	7000 / 0 / 357	
Goodness-of-fit on F^2	0.916	
Final R indices [I>2sigma(I)]	R1 = 0.0620, wR2 = 0.1348	
R indices (all data)	R1 = 0.2084, wR2 = 0.1819	
Extinction coefficient	0.0091(15)	
Largest diff. peak and hole	0.275 and -0.210 $e.Å^{-3}$	

Table 2.7. Selected Bond lengths [Å] and angles [°] for **29**.

O(1)-B(1)	1.431(3)
O(1)-H(1O)	0.87(4)
N(1)-C(2)	1.334(3)
N(1)-C(6)	1.463(3)
N(1)-B(1)	1.624(4)
N(2)-C(4)	1.338(3)
N(2)-C(18)	1.453(3)
N(2)-B(1)	1.613(4)
B(1)-C(30)	1.626(4)
C(2)-C(3)	1.384(3)
C(3)-C(4)	1.394(3)
B(1)-O(1)-H(1O)	118(3)
C(2)-N(1)-C(6)	119.4(2)
C(2)-N(1)-B(1)	122.4(2)
C(6)-N(1)-B(1)	118.1(2)
C(4)-N(2)-C(18)	119.1(2)
C(4)-N(2)-B(1)	122.9(2)
C(18)-N(2)-B(1)	117.90(19)
O(1)-B(1)-N(2)	109.5(2)
O(1)-B(1)-N(1)	106.7(2)
N(2)-B(1)-N(1)	105.5(2)
O(1)-B(1)-C(30)	114.1(2)
N(2)-B(1)-C(30)	109.8(2)
N(1)-B(1)-C(30)	110.8(2)
N(1)-C(2)-C(3)	121.1(2)
N(1)-C(2)-C(1)	121.0(2)
C(3)-C(2)-C(1)	117.9(2)
C(2)-C(3)-C(4)	123.4(2)

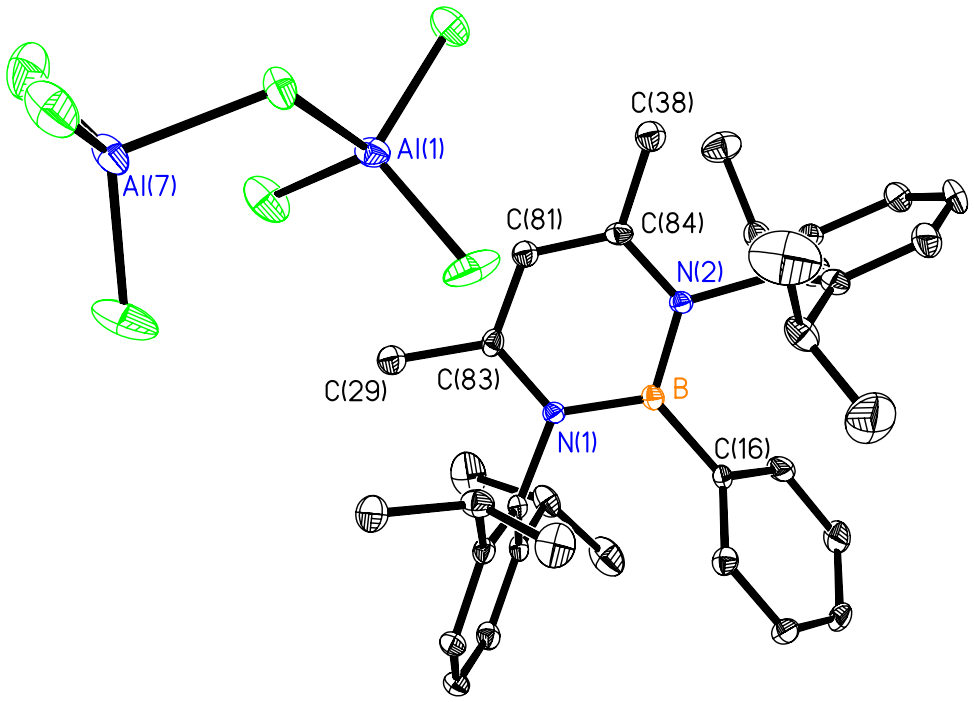

ORTEP diagram of compound **30** at 30% probability. All hydrogen atoms have been omitted for clarity.

Table 2.8. Crystal data and structure refinement for **30**.

Identification code	**30**	
Empirical formula	C35 H46 Al2 B Cl7 N2	
Formula weight	807.66	
Temperature	153(2) K	
Wavelength	0.71069 Å	
Crystal system	triclinic	
Space group	p-1	
Unit cell dimensions	a = 10.371(5) Å	α= 97.258(5)°.
	b = 12.220(5) Å	β= 102.094(5)°.
	c = 17.297(5) Å	γ = 101.856(5)°.
Volume	2064.6(14) $Å^3$	
Z	2	
Density (calculated)	1.299 Mg/m^3	
Absorption coefficient	0.550 mm^{-1}	
F(000)	840	
Crystal size	0.30 x 0.30 x 0.20 mm^3	
Theta range for data collection	3.24 to 27.57°.	
Index ranges	-13<=h<=11, -15<=k<=15, -22<=l<=21	
Reflections collected	16043	
Independent reflections	9325 [R(int) = 0.0397]	
Completeness to theta = 27.57°	97.5 %	
Absorption correction	None	
Max. and min. transmission	0.8979 and 0.8523	
Refinement method	Full-matrix least-squares on F^2	
Data / restraints / parameters	9325 / 0 / 571	
Goodness-of-fit on F^2	1.308	
Final R indices [I>2sigma(I)]	R1 = 0.1009, wR2 = 0.1618	
R indices (all data)	R1 = 0.1258, wR2 = 0.1696	
Largest diff. peak and hole	0.605 and -0.474 $e.Å^{-3}$	

Table 2.9. Selected Bond lengths [Å] and angles [°] for **30**.

N(2)-C(84)	1.359(5)
N(2)-B	1.449(5)
N(1)-C(83)	1.354(5)
N(1)-B	1.451(5)
C(83)-C(81)	1.382(5)
C(16)-B	1.571(5)
C(81)-C(84)	1.382(5)
C(84)-N(2)-B	121.9(3)
C(84)-N(2)-C(15)	115.7(3)
B-N(2)-C(15)	122.2(3)
C(83)-N(1)-B	122.4(3)
C(83)-N(1)-C(17)	117.7(3)
B-N(1)-C(17)	119.9(3)
N(1)-C(83)-C(81)	118.7(3)
N(1)-C(83)-C(29)	121.0(3)
C(33)-C(16)-B	120.8(3)
C(34)-C(16)-B	122.6(3)
C(83)-C(81)-C(84)	122.5(4)
N(2)-C(84)-C(81)	119.0(3)
N(2)-B-N(1)	114.6(3)
N(2)-B-C(16)	123.0(3)
N(1)-B-C(16)	122.4(3)

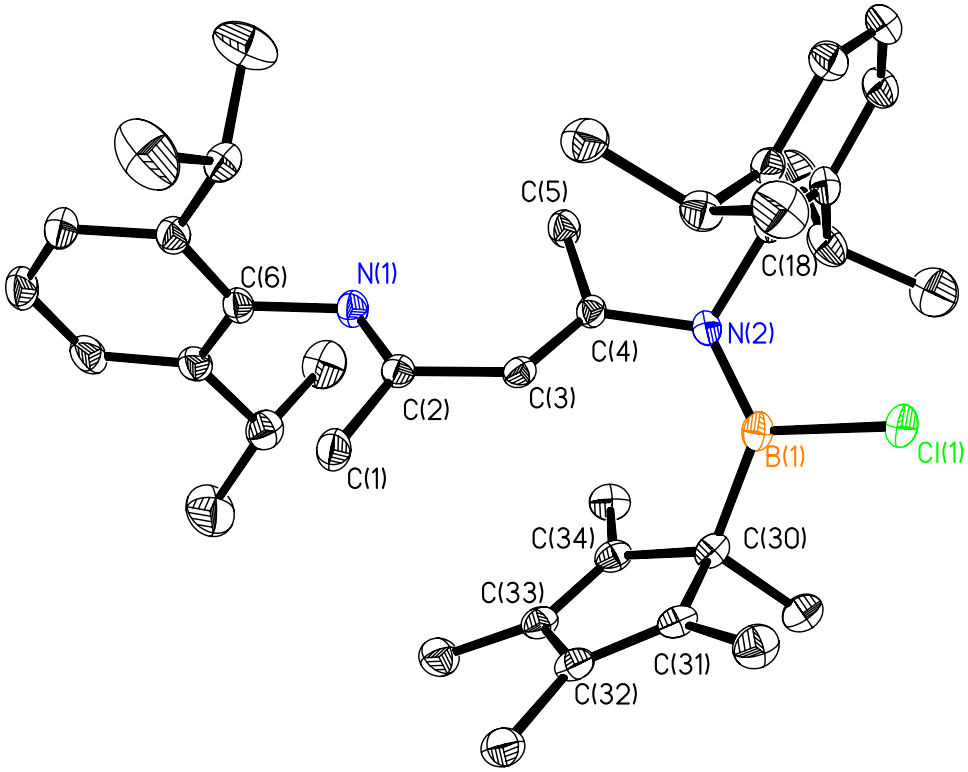

ORTEP diagram of compound **31** at 30% probability. All hydrogen atoms have been omitted for clarity.

Table 2.10. Crystal data and structure refinement for **31**.

Identification code	**31**	
Empirical formula	C39 H56 B Cl N2	
Formula weight	599.12	
Temperature	153(2) K	
Wavelength	0.71073 Å	
Crystal system	Monoclinic	
Space group	p21/c	
Unit cell dimensions	a = 11.884(2) Å	α= 90°.
	b = 18.676(4) Å	β= 96.80(3)°.
	c = 17.086(3) Å	γ = 90°.
Volume	3765.5(12) $Å^3$	
Z	4	
Density (calculated)	1.057 Mg/m^3	
Absorption coefficient	0.128 mm^{-1}	
F(000)	1304	
Crystal size	0.25 x 0.15 x 0.10 mm^3	
Theta range for data collection	2.04 to 27.44°.	
Index ranges	-13<=h<=15, -22<=k<=24, -22<=l<=19	
Reflections collected	25670	
Independent reflections	8585 [R(int) = 0.1097]	
Completeness to theta = 27.44°	99.8 %	
Absorption correction	Semi-empirical from equivalents	
Max. and min. transmission	0.987 and 0.977	
Refinement method	Full-matrix least-squares on F^2	
Data / restraints / parameters	8585 / 0 / 403	
Goodness-of-fit on F^2	0.998	
Final R indices [I>2sigma(I)]	R1 = 0.0650, wR2 = 0.1390	
R indices (all data)	R1 = 0.1576, wR2 = 0.1761	
Largest diff. peak and hole	0.293 and -0.347 $e.Å^{-3}$	

Table 2.11. Selected Bond lengths [Å] and angles [°] for **31**.

C(1)-C(2)	1.504(3)
C(2)-N(1)	1.274(3)
C(2)-C(3)	1.473(3)
C(3)-C(4)	1.338(3)
C(4)-N(2)	1.442(3)
C(4)-C(5)	1.492(3)
B(1)-N(2)	1.407(3)
B(1)-C(30)	1.601(4)
B(1)-Cl(1)	1.804(3)
C(30)-C(34)	1.520(3)
C(30)-C(31)	1.526(3)
C(31)-C(32)	1.348(3)
C(32)-C(33)	1.468(4)
C(33)-C(34)	1.343(3)
N(1)-C(2)-C(3)	121.8(2)
N(1)-C(2)-C(1)	123.3(2)
C(3)-C(2)-C(1)	114.9(2)
C(4)-C(3)-C(2)	128.2(2)
C(4)-C(3)-H(3)	115.9
C(2)-C(3)-H(3)	115.9
C(3)-C(4)-N(2)	117.5(2)
C(3)-C(4)-C(5)	126.2(2)
N(2)-C(4)-C(5)	116.31(18)
N(2)-B(1)-C(30)	130.2(2)
N(2)-B(1)-Cl(1)	114.38(18)
C(30)-B(1)-Cl(1)	115.42(19)
C(34)-C(30)-C(31)	102.09(18)
C(34)-C(30)-C(39)	106.2(2)
C(31)-C(30)-C(39)	108.4(2)
C(34)-C(30)-B(1)	118.0(2)
C(31)-C(30)-B(1)	112.6(2)
C(39)-C(30)-B(1)	108.94(18)
C(32)-C(31)-C(35)	127.4(2)
C(32)-C(31)-C(30)	109.2(2)
C(35)-C(31)-C(30)	123.3(2)
C(31)-C(32)-C(33)	109.4(2)
C(31)-C(32)-C(36)	127.7(2)
C(33)-C(32)-C(36)	122.9(2)
C(34)-C(33)-C(32)	109.7(2)
C(34)-C(33)-C(37)	127.6(2)
C(32)-C(33)-C(37)	122.7(2)
C(33)-C(34)-C(38)	128.2(2)
C(33)-C(34)-C(30)	109.4(2)
C(38)-C(34)-C(30)	122.3(2)
C(2)-N(1)-C(6)	120.66(19)
B(1)-N(2)-C(4)	125.07(18)
B(1)-N(2)-C(18)	121.05(18)
C(4)-N(2)-C(18)	113.33(18)

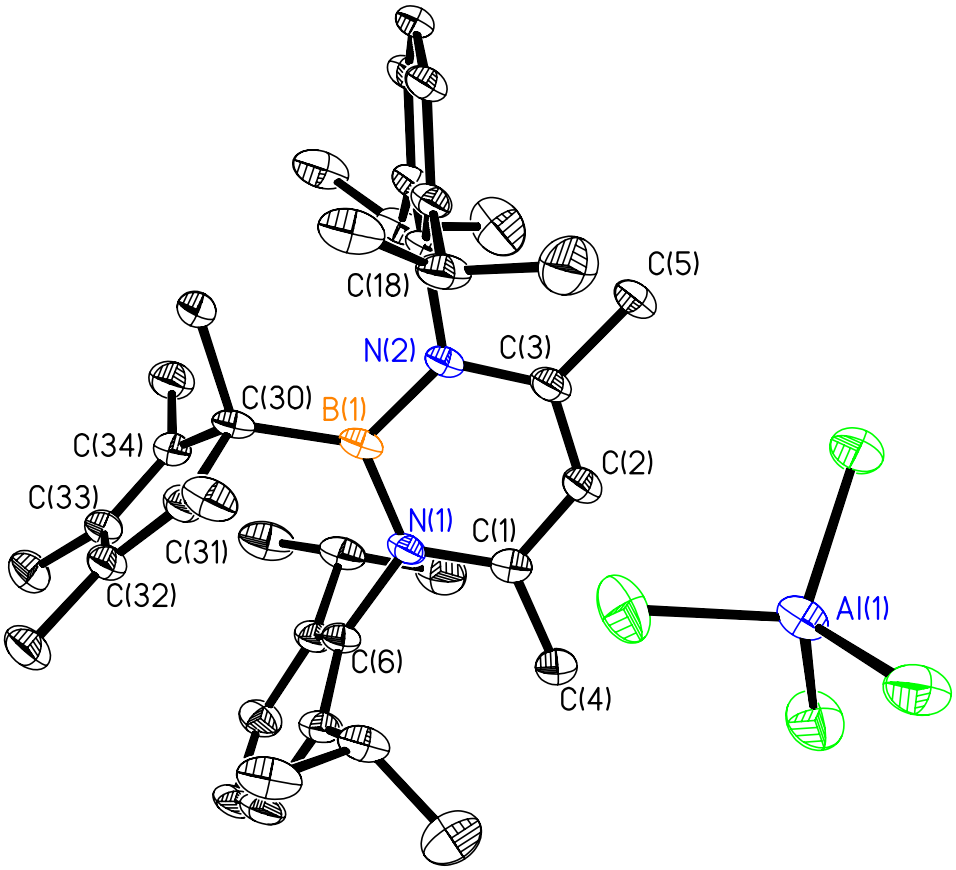

ORTEP diagram of compound **32** at 30% probability. All hydrogen atoms have been omitted for clarity.

Table 2.12. Crystal data and structure refinement for **32**.

Identification code	**32**	
Empirical formula	C39 H56 Al B Cl4 N2	
Formula weight	732.45	
Temperature	153(2) K	
Wavelength	0.71073 Å	
Crystal system	Monoclinic	
Space group	p21/n	
Unit cell dimensions	a = 11.354(2) Å	α= 90°.
	b = 19.607(4) Å	β= 105.66(3)°.
	c = 18.683(4) Å	γ = 90°.
Volume	4004.8(15) $Å^3$	
Z	4	
Density (calculated)	1.215 Mg/m^3	
Absorption coefficient	0.347 mm^{-1}	
F(000)	1560	
Crystal size	0.20 x 0.19 x 0.19 mm^3	
Theta range for data collection	2.26 to 27.49°.	
Index ranges	-14<=h<=14, -25<=k<=23, -24<=l<=24	
Reflections collected	14904	
Independent reflections	9050 [R(int) = 0.0562]	
Completeness to theta = 27.49°	98.4 %	
Absorption correction	Semi-empirical from equivalents	
Max. and min. transmission	0.936 and 0.933	
Refinement method	Full-matrix least-squares on F^2	
Data / restraints / parameters	9050 / 0 / 439	
Goodness-of-fit on F^2	1.004	
Final R indices [I>2sigma(I)]	R1 = 0.0595, wR2 = 0.1184	
R indices (all data)	R1 = 0.1661, wR2 = 0.1562	
Largest diff. peak and hole	0.271 and -0.251 $e.Å^{-3}$	

Table 2.13. Selected Bond lengths [Å] and angles [°] for **32**.

C(1)-N(1)	1.353(3)
C(1)-C(2)	1.384(4)
C(2)-C(3)	1.359(4)
C(3)-N(2)	1.365(4)
C(30)-C(31)	1.520(4)
C(30)-C(34)	1.527(4)
C(30)-B(1)	1.616(4)
C(31)-C(32)	1.347(4)
C(32)-C(33)	1.454(4)
C(33)-C(34)	1.349(4)
B(1)-N(2)	1.481(4)
B(1)-N(1)	1.493(4)
N(1)-C(1)-C(2)	119.7(3)
N(1)-C(1)-C(4)	123.7(3)
C(2)-C(1)-C(4)	116.6(3)
C(3)-C(2)-C(1)	122.4(3)
C(2)-C(3)-N(2)	120.7(3)
C(2)-C(3)-C(5)	117.8(3)
N(2)-C(3)-C(5)	121.5(3)
C(31)-C(30)-B(1)	109.3(2)
C(34)-C(30)-B(1)	115.8(2)
C(35)-C(30)-B(1)	116.5(2)
N(2)-B(1)-N(1)	112.3(3)
N(2)-B(1)-C(30)	125.0(2)
N(1)-B(1)-C(30)	122.7(2)
C(1)-N(1)-C(6)	114.2(2)
C(1)-N(1)-B(1)	122.8(2)
C(6)-N(1)-B(1)	123.0(2)
C(3)-N(2)-B(1)	122.1(2)
C(3)-N(2)-C(18)	112.7(2)
B(1)-N(2)-C(18)	125.2(2)

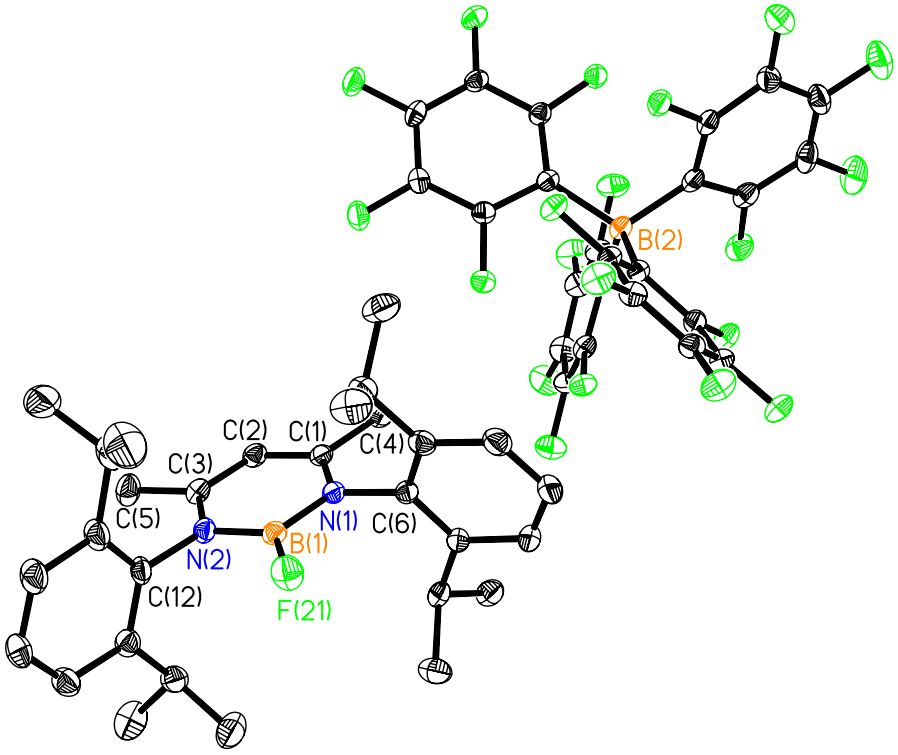

ORTEP diagram of compound **34** at 30% probability. All hydrogen atoms have been omitted for clarity.

Table 2.14. Crystal data and structure refinement for **34·C_7H_8**.

Identification code	**34·C_7H_8**	
Empirical formula	C60 H49 B2 F21 N2	
Formula weight	1218.63	
Temperature	293(2) K	
Wavelength	0.71069 Å	
Crystal system	monoclinic	
Space group	p21/c	
Unit cell dimensions	a = 11.628(5) Å	α= 90.000(5)°.
	b = 30.125(5) Å	β= 105.106(5)°.
	c = 17.307(5) Å	γ = 90.000(5)°.
Volume	5853(3) $Å^3$	
Z	4	
Density (calculated)	1.383 Mg/m^3	
Absorption coefficient	0.127 mm^{-1}	
F(000)	2488	
Crystal size	0.15 x 0.2 x 0.3 mm^3	
Theta range for data collection	2.96 to 27.50°.	
Index ranges	-13<=h<=15, -39<=k<=37, -21<=l<=22	
Reflections collected	35565	
Independent reflections	13367 [R(int) = 0.0577]	
Completeness to theta = 27.50°	99.4 %	
Absorption correction	None	
Refinement method	Full-matrix least-squares on F^2	
Data / restraints / parameters	13367 / 0 / 767	
Goodness-of-fit on F^2	0.988	
Final R indices [I>2sigma(I)]	R1 = 0.0954, wR2 = 0.2819	
R indices (all data)	R1 = 0.1553, wR2 = 0.3267	
Extinction coefficient	0.0067(10)	
Largest diff. peak and hole	2.748 and -0.421 $e.Å^{-3}$	

Table 2.15. Bond lengths [Å] and angles [°] for **34·C_7H_8**.

C(1)-N(1)	1.352(6)
C(1)-C(2)	1.387(6)
C(1)-C(4)	1.505(6)
C(2)-C(3)	1.372(7)
C(3)-N(2)	1.349(6)
N(1)-B(1)	1.450(6)
N(2)-B(1)	1.452(6)
F(21)-B(1)	1.345(6)
N(1)-C(1)-C(2)	119.9(4)
N(1)-C(1)-C(4)	120.0(4)
C(2)-C(1)-C(4)	120.2(4)
C(3)-C(2)-C(1)	122.0(4)
C(3)-C(2)-H(2)	119.0
C(1)-C(2)-H(2)	119.0
N(2)-C(3)-C(2)	120.3(4)
N(2)-C(3)-C(5)	119.3(4)
C(2)-C(3)-C(5)	120.4(4)
C(1)-N(1)-B(1)	120.8(4)
C(1)-N(1)-C(6)	120.3(4)
B(1)-N(1)-C(6)	118.9(4)
C(3)-N(2)-B(1)	120.7(4)
C(3)-N(2)-C(12)	122.1(4)
B(1)-N(2)-C(12)	117.1(4)
F(21)-B(1)-N(1)	119.6(4)
F(21)-B(1)-N(2)	124.1(4)
N(1)-B(1)-N(2)	116.3(4)

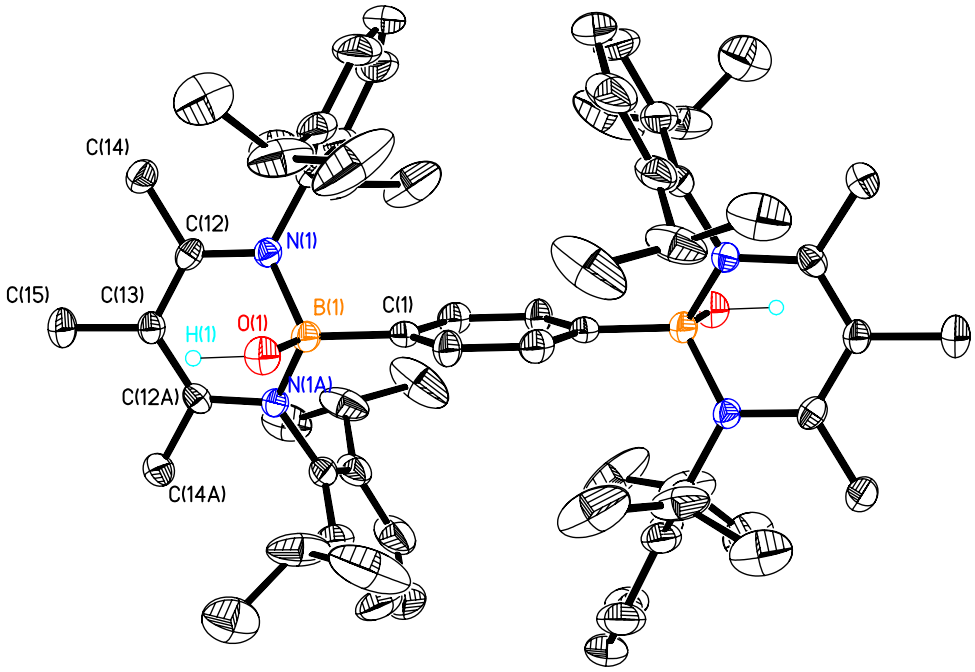

ORTEP diagram of compound **37** at 30% probability.

Table 2.16. Crystal data and structure refinement for **37·C_7H_8**.

Identification code	**37·C_7H_8**	
Empirical formula	C80 H108 B2 N4 O2	
Formula weight	1179.32	
Temperature	293(2) K	
Wavelength	0.71073 Å	
Crystal system	monoclinic	
Space group	c2/m	
Unit cell dimensions	a = 19.785(4) Å	α= 90°.
	b = 16.474(3) Å	β= 123.58(3)°.
	c = 13.929(3) Å	γ = 90°.
Volume	3782.1(13) $Å^3$	
Z	2	
Density (calculated)	1.036 Mg/m^3	
Absorption coefficient	0.060 mm^{-1}	
F(000)	1284	
Crystal size	0.2 x 0.2 x 0.2 mm^3	
Theta range for data collection	1.75 to 27.49°.	
Index ranges	-25<=h<=25, -21<=k<=21, -18<=l<=17	
Reflections collected	13428	
Independent reflections	4463 [R(int) = 0.0802]	
Completeness to theta = 27.49°	99.4 %	
Absorption correction	Sphere	
Refinement method	Full-matrix least-squares on F^2	
Data / restraints / parameters	4463 / 0 / 231	
Goodness-of-fit on F^2	0.973	
Final R indices [I>2sigma(I)]	R1 = 0.0810, wR2 = 0.1927	
R indices (all data)	R1 = 0.1920, wR2 = 0.2311	
Extinction coefficient	0.0018(6)	
Largest diff. peak and hole	0.212 and -0.216 $e.Å^{-3}$	

Table 2.17. Selected Bond lengths [Å] and angles [°] for **37·C_7H_8**.

N(1)-C(12)	1.346(3)
N(1)-C(4)	1.465(3)
N(1)-B(1)	1.595(3)
O(1)-B(1)	1.477(5)
O(1)-H(1)	1.07(8)
C(12)-C(13)	1.403(3)
C(12)-C(14)	1.498(3)
C(2)-C(3)#1	1.392(5)
C(2)-C(1)	1.399(5)
C(13)-C(12)#2	1.403(3)
C(1)-C(3)	1.382(5)
C(1)-B(1)	1.589(5)
C(3)-C(2)#1	1.392(5)
C(4)-C(9)	1.389(4)
C(4)-C(5)	1.408(4)
C(5)-C(6)	1.389(5)
B(1)-N(1)#2	1.595(3)
C(12)-N(1)-C(4)	119.00(19)
C(12)-N(1)-B(1)	117.2(2)
C(4)-N(1)-B(1)	123.1(2)
B(1)-O(1)-H(1)	116(4)
N(1)-C(12)-C(13)	121.2(2)
N(1)-C(12)-C(14)	119.7(2)
C(13)-C(12)-C(14)	119.0(2)
C(12)-C(13)-C(12)#2	120.2(3)
C(12)-C(13)-C(15)	119.78(15)
C(12)#2-C(13)-C(15)	119.78(15)
C(3)-C(1)-B(1)	121.7(3)
C(2)-C(1)-B(1)	123.4(3)
C(9)-C(4)-N(1)	119.0(2)
C(5)-C(4)-N(1)	119.7(2)
O(1)-B(1)-C(1)	112.4(3)
O(1)-B(1)-N(1)#2	106.4(2)
C(1)-B(1)-N(1)#2	113.4(2)
O(1)-B(1)-N(1)	106.4(2)
C(1)-B(1)-N(1)	113.4(2)
N(1)#2-B(1)-N(1)	104.2(3)

Symmetry transformations used to generate equivalent atoms:
#1 -x+1,-y,-z+1 #2 x,-y,z

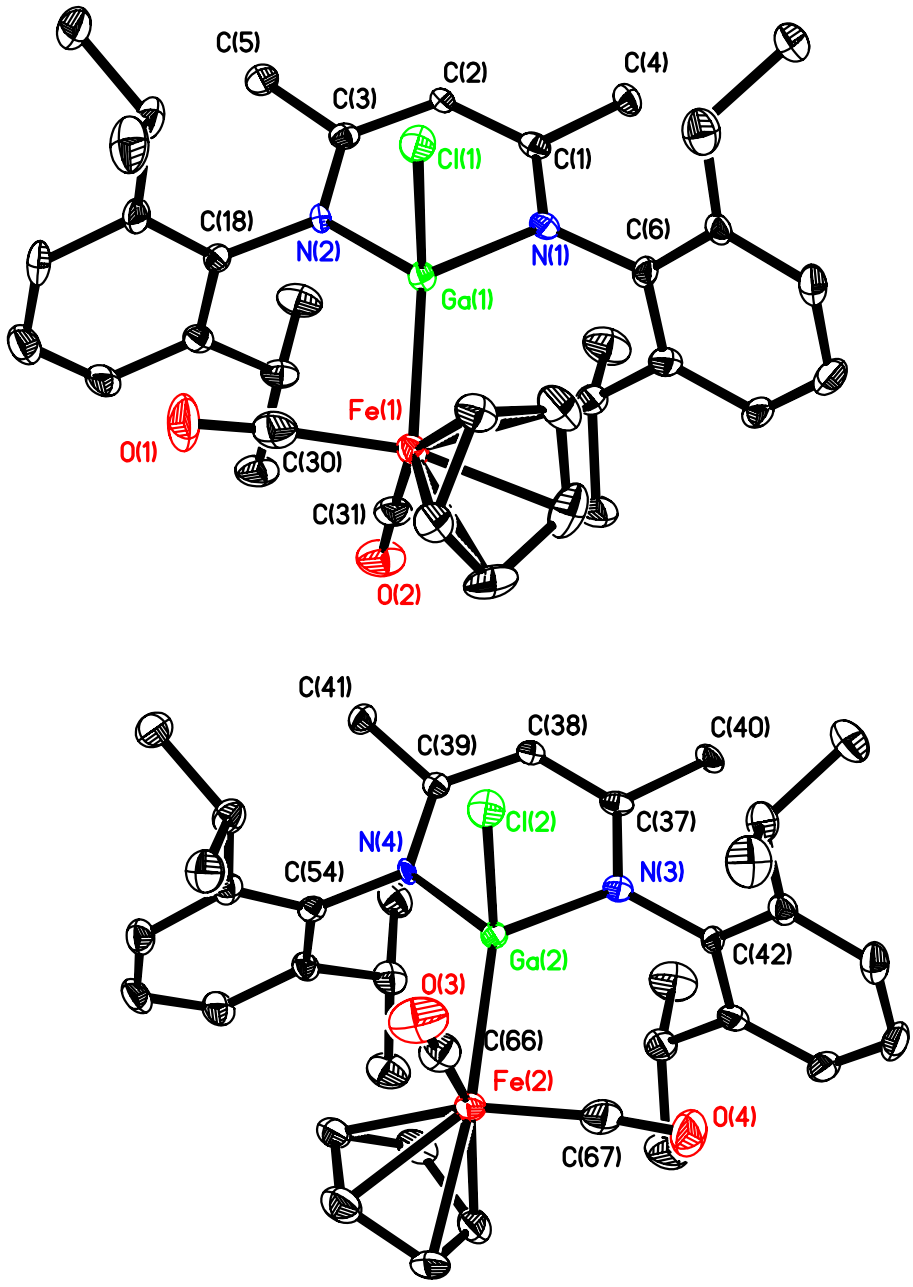

ORTEP diagram of compound **39** at 30% probability. All hydrogen atoms have been omitted for clarity.

Table 2.18. Crystal data and structure refinement for **39**.

Identification code	**39**	
Empirical formula	C36 H46 Cl Fe Ga N2 O2	
Formula weight	699.77	
Temperature	153(2) K	
Wavelength	0.71069 Å	
Crystal system	Triclinic	
Space group	p-1	
Unit cell dimensions	a = 10.633(5) Å	α= 89.617(5)°.
	b = 15.703(5) Å	β= 89.013(5)°.
	c = 20.556(5) Å	γ = 83.742(5)°.
Volume	3411(2) $Å^3$	
Z	4	
Density (calculated)	1.363 Mg/m^3	
Absorption coefficient	1.327 mm^{-1}	
F(000)	1464	
Crystal size	0.13 x 0.12 x 0.12 mm^3	
Theta range for data collection	2.18 to 27.49°.	
Index ranges	-11<=h<=13, -20<=k<=20, -26<=l<=26	
Reflections collected	23364	
Independent reflections	15499 [R(int) = 0.0503]	
Completeness to theta = 27.49°	98.8 %	
Absorption correction	Semi-empirical from equivalents	
Max. and min. transmission	0.853 and 0.842	
Refinement method	Full-matrix least-squares on F^2	
Data / restraints / parameters	15499 / 0 / 795	
Goodness-of-fit on F^2	1.000	
Final R indices [I>2sigma(I)]	R1 = 0.0565, wR2 = 0.1180	
R indices (all data)	R1 = 0.1563, wR2 = 0.1859	
Largest diff. peak and hole	1.170 and -1.422 $e.Å^{-3}$	

Table 2.19. Selected Bond lengths [Å] and angles [°] for **39**.

C(1)-N(1)	1.328(6)
C(1)-C(2)	1.403(7)
C(2)-C(3)	1.394(7)
C(3)-N(2)	1.334(6)
C(30)-O(1)	1.152(7)
C(30)-Fe(1)	1.747(7)
C(31)-O(2)	1.167(6)
C(31)-Fe(1)	1.738(5)
C(37)-N(3)	1.330(6)
C(37)-C(38)	1.409(7)
C(38)-C(39)	1.376(7)
C(39)-N(4)	1.341(6)
C(66)-O(3)	1.177(6)
C(66)-Fe(2)	1.730(6)
C(67)-O(4)	1.161(7)
C(67)-Fe(2)	1.734(7)
N(1)-Ga(1)	1.999(4)
N(2)-Ga(1)	1.983(4)
N(3)-Ga(2)	1.988(4)
N(4)-Ga(2)	1.995(4)
Cl(1)-Ga(1)	2.2782(15)
Cl(2)-Ga(2)	2.2772(14)
Fe(1)-Ga(1)	2.3933(12)
Fe(2)-Ga(2)	2.3921(11)
N(1)-C(1)-C(2)	124.6(5)
N(1)-C(1)-C(4)	120.0(5)
C(2)-C(1)-C(4)	115.4(4)
C(3)-C(2)-C(1)	128.0(5)
N(2)-C(3)-C(2)	124.5(4)
N(2)-C(3)-C(5)	119.3(5)
C(2)-C(3)-C(5)	116.1(4)
N(3)-C(37)-C(38)	123.4(5)
N(3)-C(37)-C(40)	120.4(4)
C(38)-C(37)-C(40)	116.2(4)
C(39)-C(38)-C(37)	128.2(5)
N(4)-C(39)-C(38)	124.4(4)
N(4)-C(39)-C(41)	119.4(4)
C(38)-C(39)-C(41)	116.1(4)
C(1)-N(1)-C(6)	119.9(4)
C(1)-N(1)-Ga(1)	120.4(3)
C(6)-N(1)-Ga(1)	119.4(3)
C(3)-N(2)-C(18)	119.5(4)
C(3)-N(2)-Ga(1)	120.0(3)
C(18)-N(2)-Ga(1)	119.9(3)
C(37)-N(3)-C(42)	118.7(4)
C(37)-N(3)-Ga(2)	119.6(3)
C(42)-N(3)-Ga(2)	121.1(3)
C(39)-N(4)-C(54)	119.8(4)
C(39)-N(4)-Ga(2)	117.3(3)

C(54)-N(4)-Ga(2)	122.2(3)
C(31)-Fe(1)-Ga(1)	95.29(17)
C(30)-Fe(1)-Ga(1)	88.30(19)
C(66)-Fe(2)-Ga(2)	86.29(19)
C(67)-Fe(2)-Ga(2)	90.59(19)
N(2)-Ga(1)-N(1)	94.44(16)
N(2)-Ga(1)-Cl(1)	99.65(10)
N(1)-Ga(1)-Cl(1)	98.50(11)
N(2)-Ga(1)-Fe(1)	125.46(11)
N(1)-Ga(1)-Fe(1)	123.62(11)
Cl(1)-Ga(1)-Fe(1)	109.96(4)
N(4)-Ga(2)-N(3)	93.36(16)
N(4)-Ga(2)-Cl(2)	98.32(11)
N(3)-Ga(2)-Cl(2)	97.20(11)
N(4)-Ga(2)-Fe(2)	124.23(11)
N(3)-Ga(2)-Fe(2)	123.89(11)
Cl(2)-Ga(2)-Fe(2)	113.92(5)

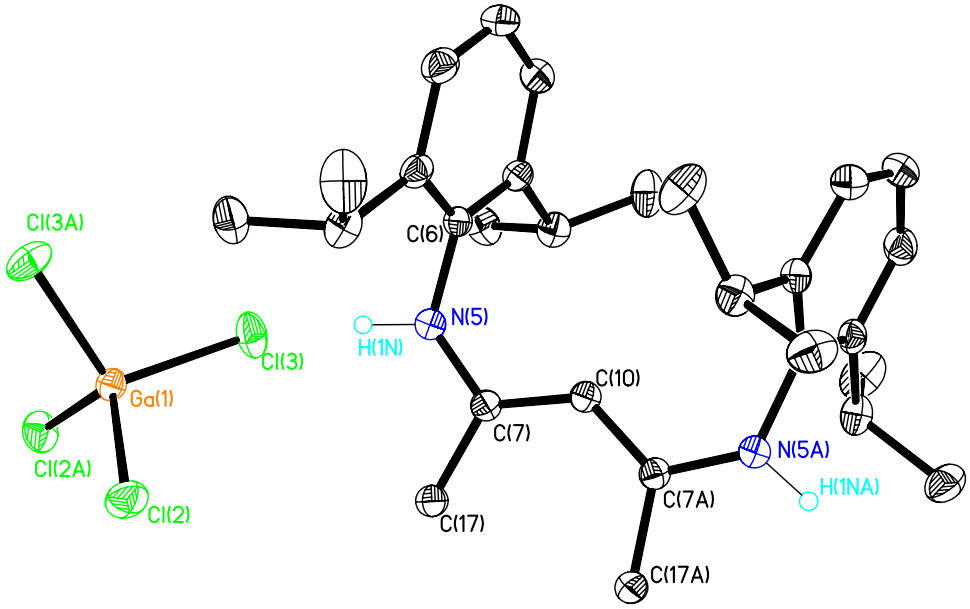

ORTEP diagram of compound **42** at 30% probability.

Table 2.20. Crystal data and structure refinement for **42·CH_2Cl_2**.

Identification code	**42·CH_2Cl_2**	
Empirical formula	C30 H41 Cl6 Ga N2	
Formula weight	712.07	
Temperature	153(2) K	
Wavelength	0.71069 Å	
Crystal system	monoclinic	
Space group	c2/c	
Unit cell dimensions	a = 12.858(5) Å	α= 90.000(5)°.
	b = 28.881(5) Å	β= 106.857(5)°.
	c = 10.121(5) Å	γ = 90.000(5)°.
Volume	3597(2) $Å^3$	
Z	4	
Density (calculated)	1.315 Mg/m^3	
Absorption coefficient	1.232 mm^{-1}	
F(000)	1472	
Crystal size	0.15 x 0.2 x 0.18 mm^3	
Theta range for data collection	1.80 to 27.50°.	
Index ranges	-16<=h<=16, -37<=k<=37, -13<=l<=10	
Reflections collected	11820	
Independent reflections	4119 [R(int) = 0.0604]	
Completeness to theta = 27.50°	99.5 %	
Absorption correction	None	
Refinement method	Full-matrix least-squares on F^2	
Data / restraints / parameters	4119 / 0 / 183	
Goodness-of-fit on F^2	1.039	
Final R indices [I>2sigma(I)]	R1 = 0.0571, wR2 = 0.1414	
R indices (all data)	R1 = 0.1041, wR2 = 0.1701	
Extinction coefficient	0.0000(4)	
Largest diff. peak and hole	0.959 and -0.989 $e.Å^{-3}$	

Table 2.21. Selected Bond lengths [Å] and angles [°] for **42·CH_2Cl_2**.

N(5)-C(7)	1.337(5)
N(5)-C(6)	1.446(4)
N(5)-H(1N)	0.94(5)
C(6)-C(8)	1.396(5)
C(6)-C(9)	1.404(5)
C(7)-C(10)	1.383(4)
C(10)-C(7)#2	1.383(4)
C(7)-N(5)-C(6)	126.5(3)
C(7)-N(5)-H(1N)	125(3)
C(6)-N(5)-H(1N)	107(3)
N(5)-C(7)-C(10)	120.5(3)
C(7)#2-C(10)-C(7)	128.7(5)

Symmetry transformations used to generate equivalent atoms:
#1 -x+1,y,-z+1/2 #2 -x,y,-z+1/2

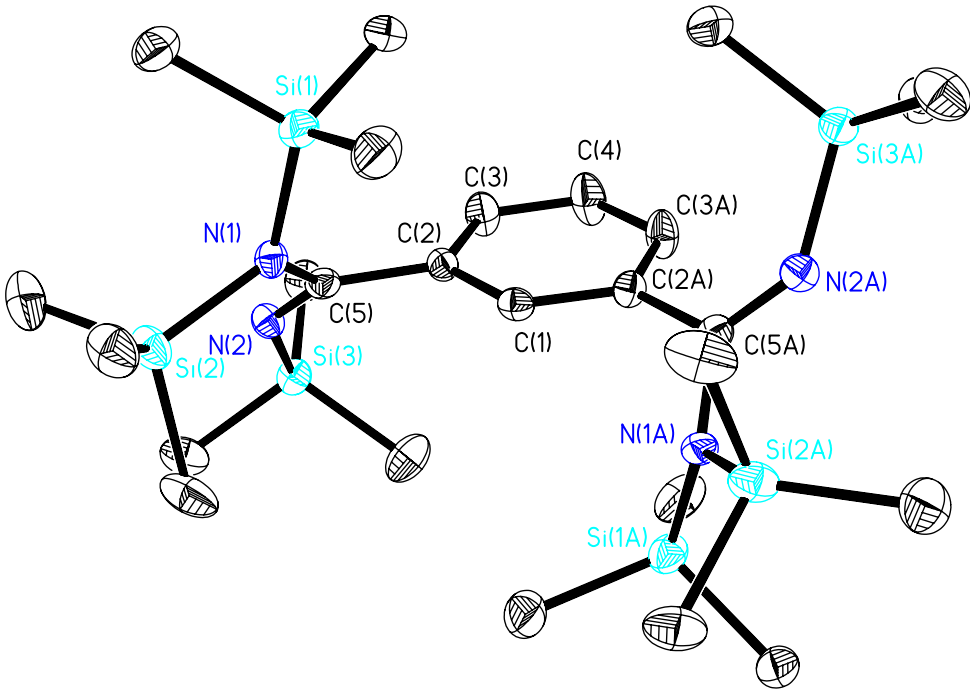

ORTEP diagram of compound **48a** at 30% probability. All hydrogen atoms have been omitted for clarity.

Table 2.22. Crystal data and structure refinement for **48a**.

Identification code	**48a**	
Empirical formula	C26 H58 N4 Si6	
Formula weight	595.30	
Temperature	293(2) K	
Wavelength	0.71069 Å	
Crystal system	monoclinic	
Space group	c2/c	
Unit cell dimensions	a = 27.732(5) Å	α= 90.000(5)°.
	b = 9.515(5) Å	β= 124.245(5)°.
	c = 17.665(5) Å	γ = 90.000(5)°.
Volume	3853(2) $Å^3$	
Z	4	
Density (calculated)	1.026 Mg/m^3	
Absorption coefficient	0.236 mm^{-1}	
F(000)	1304	
Crystal size	0.30 x 0.30 x 0.30 mm^3	
Theta range for data collection	1.78 to 27.51°.	
Index ranges	-35<=h<=36, -12<=k<=10, -22<=l<=22	
Reflections collected	6793	
Independent reflections	4331 [R(int) = 0.0695]	
Completeness to theta = 27.51°	97.9 %	
Absorption correction	None	
Max. and min. transmission	0.9326 and 0.9326	
Refinement method	Full-matrix least-squares on F^2	
Data / restraints / parameters	4331 / 0 / 164	
Goodness-of-fit on F^2	0.907	
Final R indices [I>2sigma(I)]	R1 = 0.0633, wR2 = 0.1337	
R indices (all data)	R1 = 0.2164, wR2 = 0.1900	
Largest diff. peak and hole	0.365 and -0.322 $e.Å^{-3}$	

Table 2.23. Selected Bond lengths [Å] and angles [°] for **48a**.

C(2)-C(5)	1.503(5)
C(5)-N(2)	1.279(4)
C(5)-N(1)	1.402(4)
N(1)-Si(2)	1.769(3)
N(1)-Si(1)	1.774(3)
N(2)-Si(3)	1.729(3)
N(2)-C(5)-N(1)	119.8(3)
N(2)-C(5)-C(2)	123.6(3)
N(1)-C(5)-C(2)	116.6(3)
C(5)-N(1)-Si(2)	113.1(2)
C(5)-N(1)-Si(1)	122.1(2)
Si(2)-N(1)-Si(1)	123.07(17)
C(5)-N(2)-Si(3)	136.6(3)
N(1)-Si(1)-C(6)	111.94(18)
N(1)-Si(1)-C(8)	108.32(17)
N(1)-Si(1)-C(7)	111.81(18)
N(1)-Si(2)-C(10)	113.36(19)
N(1)-Si(2)-C(11)	109.93(18)
N(1)-Si(2)-C(9)	107.97(18)
C(10)-Si(2)-C(9)	108.7(2)
N(2)-Si(3)-C(12)	105.73(18)
N(2)-Si(3)-C(14)	113.31(17)
N(2)-Si(3)-C(13)	110.29(18)

Symmetry transformations used to generate equivalent atoms:
#1 -x,y,-z+1/2

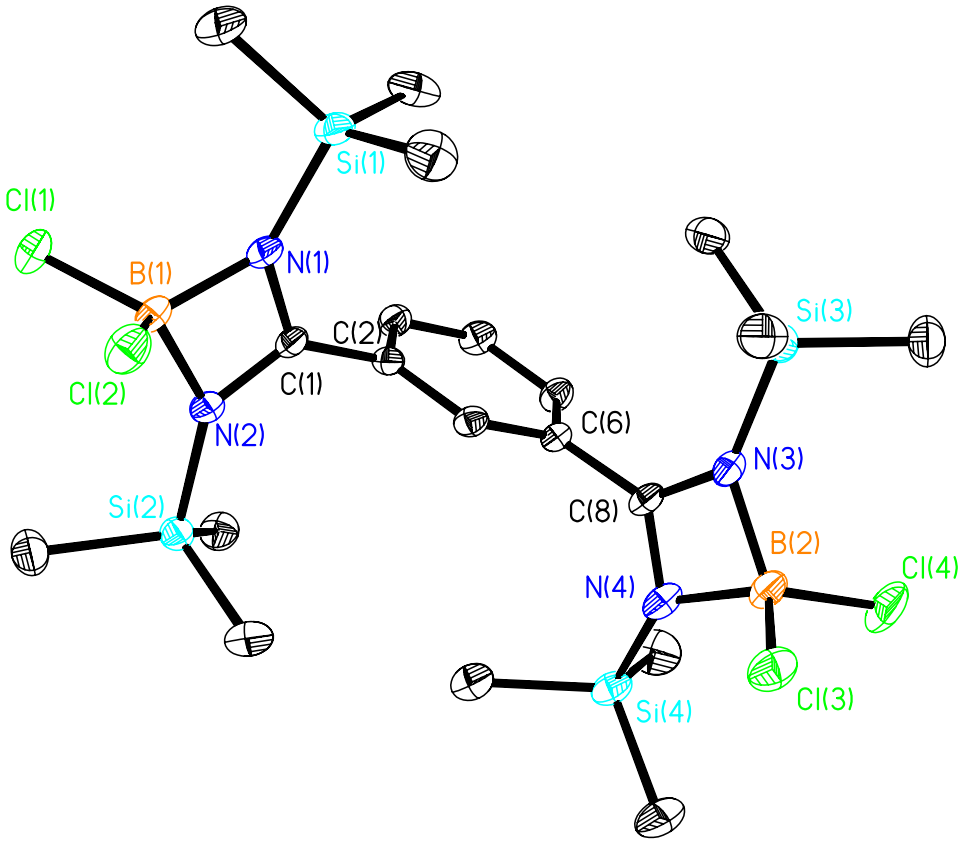

ORTEP diagram of compound **50** at 30% probability. All hydrogen atoms have been omitted for clarity.

Table 2.24. Crystal data and structure refinement for **50**.

Identification code	**50**	
Empirical formula	C20 H40 B2 Cl4 N4 Si4	
Formula weight	612.34	
Temperature	153(2) K	
Wavelength	0.71069 Å	
Crystal system	orthorhombic	
Space group	pca2/1	
Unit cell dimensions	a = 21.111(5) Å	α= 90.000(5)°.
	b = 12.901(5) Å	β= 90.132(5)°.
	c = 12.380(5) Å	γ = 90.000(5)°.
Volume	3372(2) $Å^3$	
Z	4	
Density (calculated)	1.206 Mg/m^3	
Absorption coefficient	0.510 mm^{-1}	
F(000)	1288	
Crystal size	0.20 x 0.15 x 0.10 mm^3	
Theta range for data collection	1.93 to 27.41°.	
Index ranges	-27<=h<=27, -16<=k<=15, -16<=l<=16	
Reflections collected	12923	
Independent reflections	7169 [R(int) = 0.0662]	
Completeness to theta = 27.41°	99.9 %	
Absorption correction	None	
Max. and min. transmission	0.9508 and 0.9049	
Refinement method	Full-matrix least-squares on F^2	
Data / restraints / parameters	7169 / 1 / 320	
Goodness-of-fit on F^2	0.996	
Final R indices [I>2sigma(I)]	R1 = 0.0545, wR2 = 0.1187	
R indices (all data)	R1 = 0.0862, wR2 = 0.1347	
Absolute structure parameter	0.51(7)	
Largest diff. peak and hole	0.493 and -0.431 $e.Å^{-3}$	

Table 2.25. Selected Bond lengths [Å] and angles [°] for **50**.

C(1)-N(2)	1.335(5)
C(1)-N(1)	1.343(5)
C(8)-N(3)	1.319(5)
C(8)-N(4)	1.346(5)
B(1)-N(2)	1.568(5)
B(1)-N(1)	1.577(6)
B(1)-Cl(1)	1.835(4)
B(1)-Cl(2)	1.839(5)
B(2)-N(4)	1.583(6)
B(2)-N(3)	1.588(6)
B(2)-Cl(4)	1.820(5)
B(2)-Cl(3)	1.826(5)
N(1)-Si(1)	1.765(3)
N(2)-Si(2)	1.767(3)
N(3)-Si(3)	1.772(4)
N(4)-Si(4)	1.756(4)
N(2)-C(1)-N(1)	104.2(3)
N(3)-C(8)-N(4)	105.2(3)
N(2)-B(1)-N(1)	84.4(3)
N(2)-B(1)-Cl(1)	114.3(3)
N(1)-B(1)-Cl(1)	114.1(3)
N(2)-B(1)-Cl(2)	114.8(3)
N(1)-B(1)-Cl(2)	113.9(3)
Cl(1)-B(1)-Cl(2)	112.5(2)
N(4)-B(2)-N(3)	83.7(3)
N(4)-B(2)-Cl(4)	114.4(3)
N(3)-B(2)-Cl(4)	115.2(3)
N(4)-B(2)-Cl(3)	114.2(3)
N(3)-B(2)-Cl(3)	113.7(3)
Cl(4)-B(2)-Cl(3)	112.7(2)
C(1)-N(1)-B(1)	85.4(3)
C(1)-N(2)-B(1)	86.0(3)
C(8)-N(3)-B(2)	85.9(3)
C(8)-N(4)-B(2)	85.2(3)

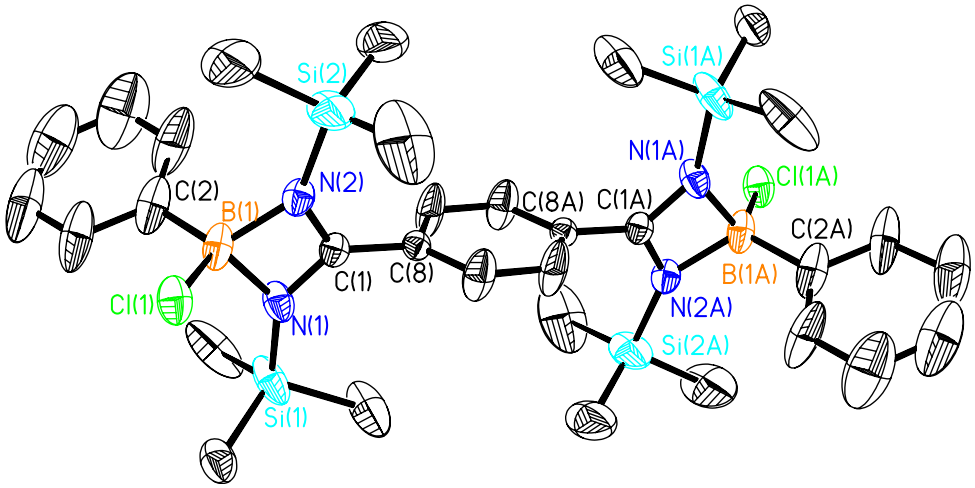

ORTEP diagram of compound **52** at 30% probability. All hydrogen atoms have been omitted for clarity.

Table 2.26. Crystal data and structure refinement for **52**.

Identification code	**52**	
Empirical formula	$C_{32}\ H_{50}\ B_2\ Cl_2\ N_4\ Si_4$	
Formula weight	695.64 $gmol^{-1}$	
Temperature	153(2) K	
Wavelength	0.71069 Å	
Crystal system	Monoclinic	
Space group	P21/c	
Unit cell dimensions	a = 10.293(5) Å	α= 90°.
	b = 12.988(5) Å	β= 115.973(5)°.
	c = 16.781(5) Å	γ = 90°.
Volume	2016.8(14) $Å^3$	
Z	2	
Density (calculated)	1.146 Mg/m^3	
Absorption coefficient	0.306 mm^{-1}	
F(000)	740	
Crystal size	0.20 x 0.20 x 0.20 mm^3	
Theta range for data collection	2.63 to 27.52°.	
Index ranges	-10<=h<=13, -16<=k<=16, -21<=l<=21	
Reflections collected	14344	
Independent reflections	4593 [R(int) = 0.1002]	
Completeness to theta = 27.52°	98.8 %	
Absorption correction	None	
Max. and min. transmission	0.9413 and 0.9413	
Refinement method	Full-matrix least-squares on F^2	
Data / restraints / parameters	4593 / 0 / 199	
Goodness-of-fit on F^2	1.064	
Final R indices [I>2sigma(I)]	R1 = 0.0972, wR2 = 0.2467	
R indices (all data)	R1 = 0.2447, wR2 = 0.3215	
Largest diff. peak and hole	0.580 and -0.724 $e.Å^{-3}$	

Table 2.27. Selected Bond lengths [Å] and angles [°] for **52**.

C(1)-N(1)	1.326(6)
C(1)-N(2)	1.331(6)
C(1)-C(8)	1.482(7)
C(2)-B(1)	1.580(10)
B(1)-N(2)	1.573(8)
B(1)-N(1)	1.613(8)
B(1)-Cl(1)	1.869(8)
N(1)-Si(1)	1.760(5)
N(2)-Si(2)	1.731(5)
N(1)-C(1)-N(2)	104.8(4)
N(2)-B(1)-C(2)	117.6(7)
N(2)-B(1)-N(1)	82.7(4)
C(2)-B(1)-N(1)	113.4(5)
N(2)-B(1)-Cl(1)	112.2(4)
C(2)-B(1)-Cl(1)	114.5(5)
N(1)-B(1)-Cl(1)	112.5(5)
C(1)-N(1)-B(1)	85.4(4)
C(1)-N(2)-B(1)	86.9(4)

Symmetry transformations used to generate equivalent atoms:
#1 -x+1,-y+1,-z

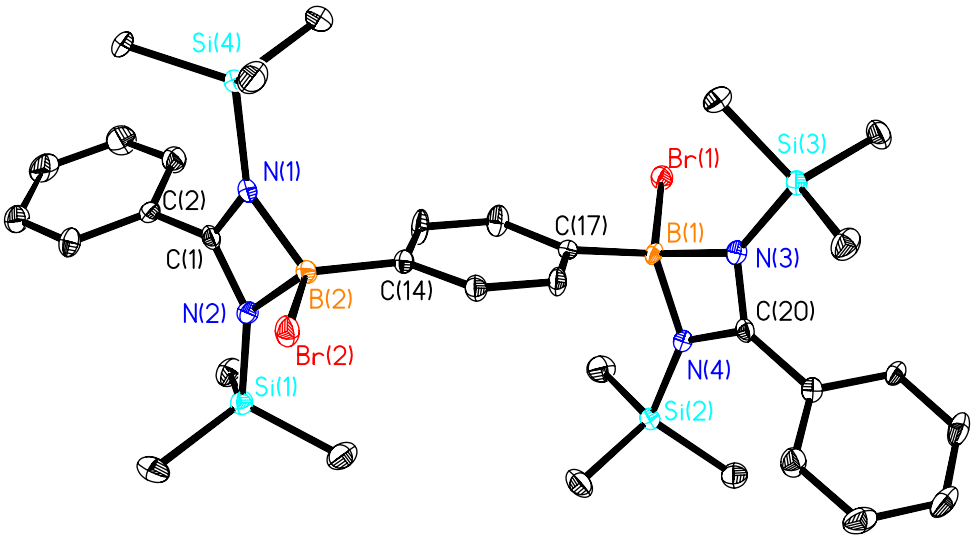

ORTEP diagram of compound **53** at 30% probability. All hydrogen atoms have been omitted for clarity.

Table 2.28. Crystal data and structure refinement for **53**.

Identification code	**53**	
Empirical formula	C32 H50 B2 Br2 N4 Si4	
Formula weight	784.56	
Temperature	153(2) K	
Wavelength	0.71069 Å	
Crystal system	Triclinic	
Space group	P-1	
Unit cell dimensions	a = 10.850(5) Å	α= 110.600(5)°.
	b = 12.470(5) Å	β= 90.050(5)°.
	c = 15.766(5) Å	γ = 90.833(5)°.
Volume	1996.5(14) $Å^3$	
Z	2	
Density (calculated)	1.305 Mg/m^3	
Absorption coefficient	2.177 mm^{-1}	
F(000)	812	
Crystal size	0.20 x 0.20 x 0.17 mm^3	
Theta range for data collection	1.74 to 27.49°.	
Index ranges	-14<=h<=14, -13<=k<=16, -20<=l<=19	
Reflections collected	14177	
Independent reflections	9102 [R(int) = 0.0395]	
Completeness to theta = 27.49°	99.4 %	
Absorption correction	None	
Max. and min. transmission	0.7085 and 0.6700	
Refinement method	Full-matrix least-squares on F^2	
Data / restraints / parameters	9102 / 0 / 409	
Goodness-of-fit on F^2	1.173	
Final R indices [I>2sigma(I)]	R1 = 0.0741, wR2 = 0.1944	
R indices (all data)	R1 = 0.0973, wR2 = 0.2086	
Largest diff. peak and hole	1.679 and -1.075 e.$Å^{-3}$	

Table 2.29. Selected Bond lengths [Å] and angles [°] for **53**.

C(1)-N(1)	1.338(8)
C(1)-N(2)	1.339(8)
C(1)-C(2)	1.475(9)
C(1)-B(2)	2.000(9)
C(20)-N(4)	1.331(8)
C(20)-N(3)	1.333(8)
C(20)-C(21)	1.480(9)
C(20)-B(1)	1.996(9)
B(1)-N(3)	1.584(8)
B(1)-N(4)	1.583(9)
B(1)-Br(1)	2.044(7)
B(2)-N(2)	1.582(8)
B(2)-N(1)	1.583(9)
B(2)-Br(2)	2.031(7)
N(4)-Si(2)	1.765(5)
N(3)-Si(3)	1.759(6)
N(1)-Si(4)	1.768(6)
N(2)-Si(1)	1.755(6)
N(1)-C(1)-N(2)	104.1(5)
N(1)-C(1)-C(2)	128.7(6)
N(2)-C(1)-C(2)	127.1(6)
N(1)-C(1)-B(2)	52.2(4)
N(2)-C(1)-B(2)	52.1(4)
C(2)-C(1)-B(2)	174.9(5)
N(4)-C(20)-N(3)	104.5(5)
N(4)-C(20)-C(21)	128.8(6)
N(3)-C(20)-C(21)	126.7(6)
N(4)-C(20)-B(1)	52.3(4)
N(3)-C(20)-B(1)	52.3(4)
C(21)-C(20)-B(1)	176.2(5)
N(3)-B(1)-N(4)	83.4(4)
N(3)-B(1)-C(20)	41.8(3)
N(4)-B(1)-C(20)	41.7(3)
C(17)-B(1)-C(20)	123.7(5)
N(3)-B(1)-Br(1)	111.2(4)
N(4)-B(1)-Br(1)	112.8(4)
C(17)-B(1)-Br(1)	113.8(4)
C(20)-B(1)-Br(1)	122.4(4)
N(2)-B(2)-N(1)	83.7(4)
N(2)-B(2)-C(14)	115.0(5)
N(1)-B(2)-C(14)	116.0(5)
N(2)-B(2)-C(1)	41.9(3)
N(1)-B(2)-C(1)	41.9(3)
N(2)-B(2)-Br(2)	110.9(4)
N(1)-B(2)-Br(2)	112.7(4)
C(14)-B(2)-Br(2)	114.8(4)
C(1)-B(2)-Br(2)	122.3(4)
C(20)-N(4)-B(1)	86.0(5)
C(20)-N(3)-B(1)	85.9(5)

C(20)-N(3)-Si(3)	134.8(5)
B(1)-N(3)-Si(3)	139.3(4)
C(1)-N(1)-B(2)	86.0(5)
C(1)-N(2)-B(2)	86.0(5)
C(1)-N(2)-Si(1)	134.5(5)

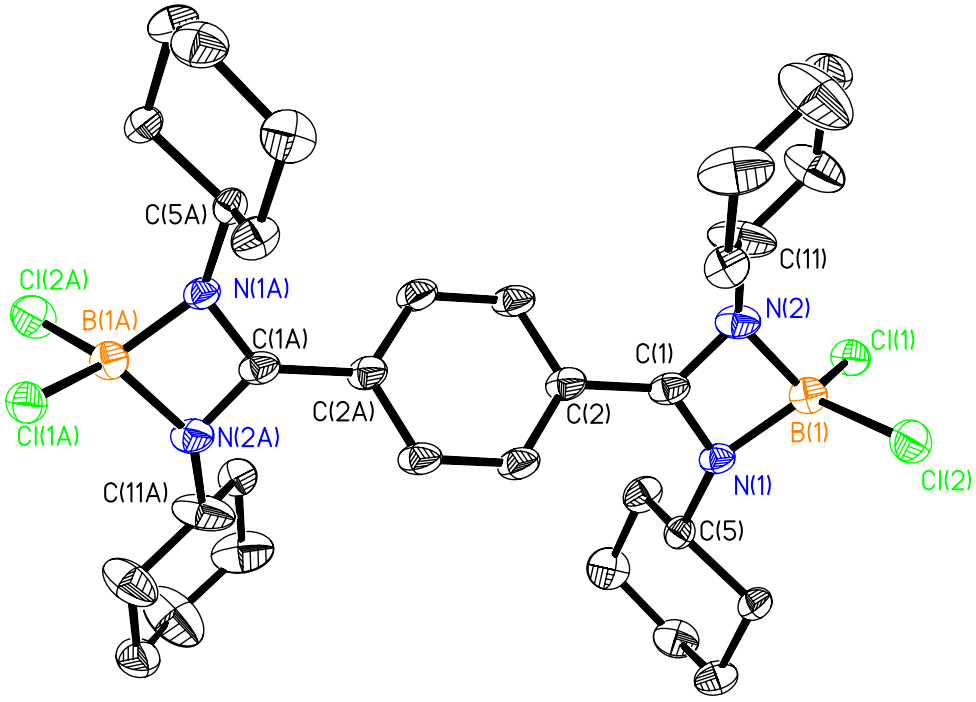

ORTEP diagram of compound **54** at 30% probability. All hydrogen atoms have been omitted for clarity.

Table 2.30. Crystal data and structure refinement for **54**.

Identification code	**54**	
Empirical formula	C_{32} H_{48} B_2 Cl_4 N_4	
Formula weight	652.16 g/mol	
Temperature	153(2) K	
Wavelength	0.71073 Å	
Crystal system	Orthorhombic	
Space group	Pbcn	
Unit cell dimensions	a = 13.870(3) Å	α= 90°.
	b = 14.466(3) Å	β= 90°.
	c = 19.406(4) Å	γ = 90°.
Volume	3893.6(14) $Å^3$	
Z	4	
Density (calculated)	1.113 Mg/m^3	
Absorption coefficient	0.329 mm^{-1}	
F(000)	1384	
Crystal size	0.20 x 0.20 x 0.15 mm^3	
Theta range for data collection	2.29 to 27.49°.	
Index ranges	-17<=h<=18, -18<=k<=18, -25<=l<=25	
Reflections collected	8409	
Independent reflections	4452 [R(int) = 0.0610]	
Completeness to theta = 27.49°	99.8 %	
Absorption correction	None	
Max. and min. transmission	0.9513 and 0.9274	
Refinement method	Full-matrix least-squares on F^2	
Data / restraints / parameters	4452 / 0 / 190	
Goodness-of-fit on F^2	0.968	
Final R indices [I>2sigma(I)]	R1 = 0.0656, wR2 = 0.1645	
R indices (all data)	R1 = 0.1464, wR2 = 0.1864	
Largest diff. peak and hole	0.443 and -0.488 $e.Å^{-3}$	

Table 2.31. Selected Bond lengths [Å] and angles [°] for **54**.

C(1)-N(1)	1.331(4)
C(1)-N(2)	1.332(4)
C(1)-C(2)	1.466(4)
C(5)-N(1)	1.473(4)
C(11)-N(2)	1.459(4)
B(1)-N(1)	1.552(4)
B(1)-N(2)	1.567(4)
B(1)-Cl(2)	1.828(4)
B(1)-Cl(1)	1.843(4)
N(1)-C(1)-N(2)	101.9(3)
N(1)-B(1)-N(2)	83.1(2)
N(1)-B(1)-Cl(2)	115.4(2)
N(2)-B(1)-Cl(2)	115.0(2)
N(1)-B(1)-Cl(1)	115.4(2)
N(2)-B(1)-Cl(1)	114.5(2)
Cl(2)-B(1)-Cl(1)	110.98(19)
C(1)-N(1)-B(1)	87.8(2)
C(5)-N(1)-B(1)	138.7(2)
C(1)-N(2)-B(1)	87.2(2)
C(11)-N(2)-B(1)	138.6(3)

Symmetry transformations used to generate equivalent atoms:
#1 -x,-y,-z+1

References

(1). Burkhardt, E. R.; Matos, K. *Chem. Rev.* **2006**, *106*, 2617

(2). Eisch, J. J. In *Comprehensive Organometallic Chemistry II*; Abel, E. W.; Stone, D. G. A.; Wilkinson, G. Eds.; Elsevier: Oxford, UK, **1995**; Vol 1, Chapter 10

(3). Atwood, D. A. *Coord. Chem. Rev.* **1998**, *176*, 407

(4). (a) Atwood, D. A.; Jegier, J. A.; Rutherford, D. *J. Am. Chem. Soc.* **1995**, *117*, 6779; (b) Atwood, D. A.; Jegier, J. A.; Rutherford, D. *Inorg. Chem.* **1996**, *35*, 63; (c) Jegier, J. A.; Muñoz-Hernández, M.-A.; Atwood, D. A. *J. Chem. Soc., Dalton Trans.* **1999**, 2583

(5). Coles, M. P.; Jordan, R. F. *J. Am. Chem. Soc.* **1997**, *119*, 8125

(6). (a) Piers, W. E.; Bourke, S. C.; Conroy, K. D. *Angew. Chem., Int. Ed. Engl.* **2005**, *44*, 5016; (b) Kölle, P.; Nöth, H. *Chem. Rev.* **1985**, *85*, 399

(7). Nöth, H.; Staudigl, R.; Wagner, H.-U. *Inorg. Chem.* **1982**, *21*, 706

(8). Courtenay, S.; Mutus, J. Y.; Schurko, R. W.; Stephan, D. W. *Angew. Chem. Int. Ed.* **2002**, *41*, 498

(9). (a) Narula, C. K.; Nöth, H. *J. Chem. Soc., Chem. Commun.* **1984**, 1023; (b) Narula, C. K.; Nöth, H. *Inorg. Chem.* **1984**, *23*, 4147; (c) Narula, C. K.; Nöth, H. *Inorg. Chem.* **1985**, *24*, 2532

(10). Jutzi, P.; Karato, M.; Hursthouse, M.; Howers, A. J. *Chem. Ber.* **1987**, *120*, 1091

(11). Gates, D. P.; McWilliams, A. R.; Ziembinski, R.; Liable-Sands, L. M.; Guzei, I. A.; Yap, G. P. A.; Rheingold, A. L.; Manners, I. *Chem. Eur. J.* **1998**, *4*, 1489

(12). Ghesner, I.; Piers, W. E.; McDonald, R. *Chem. Commun.* **2005**, 2480

(13). (a) Cui, C.; Roesky, H. W.; Schmidt, H.-G.; Noltemeyer, M.; Hao, H.; Cimpoesu, F. *Angew. Chem. Int. Ed.* **2000**, *39*, 4274; (b) Stender, M.; Eichler, B. E.; Hardaman, N. J.; Power, J. J.; Prust, J.; Noltemeyer, M.; Roesky, H. W. *Inorg. Chem.* **2001**, *40*, 2794

(14). Singh, S.; Ahn, H.-J.; Stasch, A.; Jancik, V.; Roesky, H.W.; Pal, A.; Biadene, M.; Herbst-Irmer, R.; Noltemeyer, M.; Schmidt, H.-G. *Inorg. Chem.* **2006**, *45*, 1853

(15). Kuhn, N.; Fahl, J.; Fuchs, S.; Steimann, M.; Henkel, G.; Maulitz, A. H. Z. *Anorg. Allg. Chem.* **1999**, *625*, 2108

(16). Hardman, N. J.; Eichler, B. E.; Power, J. J. *Chem. Commun.* **2000**, 1991

(17). Hill, M. S.; Hitchcock, P. B. *Chem. Commun.* **2004**, 1818

(18). Cheng, Y.; Hitchcock, P. B.; Lappert, M. F.; Zhou, M. *Chem. Commun.* **2005**, 752

(19). Kuhn, N.; Kuhn, A.; Boese, R.; Augart, N.; *J. Chem. Soc., Chem. Commun.* **1989**, 975.

(20). Yalpani, M.; Köster, R.; Boese, R.; *Chem. Ber.* **1992**, *125*, 15.

(21). Kuhn, N.; Kuhn, A.; Speis, M.; Bläser, D.; Boese, R. *Chem Ber.* **1990**, *123*, 1301

(22). Qian, B.; Ward, D. L; Smith, III, M. R. *Organometallics* **1998**, *17*, 3070

(23). Park, K.-H.; Marshall, W. J. *J. Org. Chem.* **2005**, *70*, 2075

(24). Kuhn, N.; Kuhn, A.; Lewandowski, J.; Speis, M. *Chem. Ber.* **1991**, *124*, 2197

(25). (a) Hardman, N. J.; Wright, R. J.; Phillips, A. D.; Power, P. P. *J. Am. Chem. Soc.* **2003**, *125*, 2667; (b) Kempter, A.; Gemel, C.; Hardman, N. J.; Fischer, R. A. *Inorg. Chem.* **2006**, *45*, 3133; (c) Kempter, A.; Gemel, C.; Fischer, R. A. *Inorg. Chem.* **2005**, *44*, 163

(26). Kempter, A.; Gemel, C.; Fischer, R. A. *Chem. Commun.* **2006**, 1551

(27). Steinke, T.; Gemel, C.; Winter, M.; Fischer, R. A. *Chem.-Eur. J.* **2005**, *11*, 1636

(28). (a) Steinke, T.; Gemel, C.; Cokoja, M.; Winter, M.; Fischer, R. A. *Angew. Chem.* **2004**, *116*, 2349; (b) Steinke, T.; Gemel, C.; Cokoja, M.; Kempter, A.; Krapp, A.; Frenking, G.; Zenneck, U.; Fischer, R. A. *Angew. Chem.* **2005**, *117*, 3003; (c) Cadenbach, T.; Gemel, C.; Schmid, R.; Fischer, R. A. *J. Am. Chem. Soc.* **2005**, *127*, 17068

(29). Nöth, H.; Wrackmeyer, B. *Nuclear Magnetic Resonance Spectroscopy of Boron Compounds*; Springer Verlag: Berlin, **1978**; ch. 7, p. 74-101.

(30). Ding, Y.; Roesky, H. W.; Noltemeyer, M.; Schmidt H.-G.; Power, P. P. *Organometallics* **2001**, *20*, 1190.

(31). Mason, J. Ed. *Multinuclear NMR*, Plenum Press, New York, USA, **1987**

(32). Ishida, Y.; Donnadieu, B.; Bertrand, G. *Proc. Natl. Acad. Sci. USA* **2006**, *103*, 13585

(33). Jutzi, P.; Krato, B.; Hursthouse, M.; Howes, A. J. *Chem. Ber.* **1987**, *120*, 565

(34). Jones, C.; Aldridge, Simon; Gans-Eichler, T.; Stasch, A. *Dalton Trans.* **2006**, *45*, 5357

(35). (a) Edelmann, F. T. *Coord. Chem. Rev.* **1994**, *137*, 403; (b) Barker, J.; Kilner, M. *Coord. Chem. Rev.* **1994**, *133*, 219.

(36). Sanger, A. R. *Inorg. Nucl. Chem. Lett.* **1973**, *9*, 351.

(37). (a) Hagadorn, J. R. *Chem. Commun.* **2001**, 2144; (b) Hagadorn, J. R.; McNevin, M.J.; Wiedenfied, G.; Shoemaker, R. *Organometallics* **2003**, *22*, 4818; (c) McNevin,

M. J.; Hagadorn, J. R. *Inorg. Chem.* **2004**, *43*, 8547; (d) Clare, B.; Sarker, N.; Shoemaker, R.; Hagadorn, J. R. *Inorg. Chem.* **2004**, *43*,1159.

(38). (a) Hagadorn, J. R.; Arnold, J.; *Angew. Chem., Int. Ed.* **1998**, *37*, 1729; (b) Li, J. F.; Weng, L. H.; Wei, X. H.; Liu, D. S. *Dalton Trans.* **2002**, 1401; (c) Kawaguchi, H.; Matsuo, T. *Chem. Commun.* **2002**, 958.

(39). Appel, S.; Weller, F.; Dehnicke, K. *Z. Anorg. Allg. Chem.* **1990**, *583*, 7.

(40). Rouques, C.; Mazières, M.-R.; Majoral, J.-P.; Sanchez, M. *Inorg. Chem.* **1989**, *28*, 3932.

(41). Grundy, J.; Coles, M. P.; Hitchcock, P. B. *New. J. Chem.* **2004**, *28*,1195.

(42). Grundy, J.; Coles, M. P.; Hitchcock, P. B. *J. Organomet. Chem.* **2002**, *662*, 178.

(43). (a) Cordes, A.W.; Haddon, R. C.; Oakley, R. T.; Scheemeyer, L. F.; Waszczak, J. V. Young, K. M.; Zimmerman, N. M. *J. Am. Chem. Soc.* **1991**, *113*, 582; (b) Andrews, M. P.; Cordes, A. W.; Douglas, D. C.; Fleming, R. M.; Glarum, S. H.; Haddon, R. C.; Marsh, P.; Oakley, R. T.; Palstra, T. T. M.; Scheemeyer, L. F.; Trucks, G. W.; Tycko, R.; Waszczak, J. V.; Young, K. M.; Zimmerman, N. M. *J. Am. Chem. Soc.* **1991**, *113*, 3559; (c) Beekman, R. A.; Boeré, R. T.; Moock, K. M.; Parvez, M. *Can. J. Chem.* **1998**, *76*, 85.

(44). (a) Cole, M. L.; Jones, C.; Junk, P. C.; Kloth, M.; Stasch, A. *Chem. Eur. J.* **2005**, *11*, 4482; (b) Amo, V.; Andres, R.; de Jesus, E.; de la Mata, F. J.; Flores, J. C.; Gomez, R.; Gomez- Sal, M. P.; Turner, J. F. C. *Organometallics* **2005**, *29*, 2331; (c) Boeré, R. T.; Cole, M. L.; Junk, P. C. *New J. Chem.* **2005**, *29*, 128; (d) Jenkins, H. A.; Abeysekara, D.; Dickie, D. A.; Clyburne, J. A. C. *Dalton Trans.* **2002**, 3919; (e)

Abeysekara, D.; Robertson, K. N.; Cameron, T. S.; Clyburne, J. A. C. *Organometallics* **2001**, *20*, 5532; (f) Kincaid, K.; Gerlach, C. P.; Giesbrecht, G. R.; Hagadorn, J. R.; Wheeler, G. D.; Shafir, A.; Arnold, J.; *Organometallics* **1999**, *18*, 5360; (g) Chang, C. C.; Hsiung, C. S.; Su, H. L.; Srinivas, B.; Chiang, M. Y.; Lee, G. H.; Wang, Y. *Organometallics* **1998**, *17*, 1595; (h) Coles, M. P.; Swenson, D. C.; Jordan, R. F.; Young, V. G. *Organometallics* **1998**, *17*, 4042; (i) Coles, M. P.; Swenson, D. C.; Jordan, R. F.; Young, V. G. *Organometallics* **1997**, *16*, 5183; (j) Patton, J. T.; Bokota, M. M.; Abboud, K. A. *Organometallics* **2002**, *21*, 2145; (k) Dagorne, S.; Jordan, R. F.; Young, V. G. *Organometallics* **1999**, *18*, 4619; (l) Barker, J.; Blacker, N.C.; Phillips, P. R.; Alcock, N. W.; Errington, W. W.; Wallbridge, M. G. H. *J. Chem. Soc. Dalton Trans.* **1996**, 431; (m) Zhou, Y.; Richeson, D. S. *Inorg. Chem.* **1996**, *35*, 2448; (n) Zhou, Y.; Richeson, D. S. *Inorg. Chem.* **1996**, *35*, 1423.

(45). Weller, F.; Schmick, F.; Dehnicke, K. *Z. Natrurforsch. B* **1999**, *44*, 548.

(46). Nöth, H.; Wrackmeyer, B. *Nuclear Magnetic Resonance Spectroscopy of Boron Compounds*; Springer Verlag: Berlin, **1978**; ch. 7, p. 74-101.

(47). Hill, N. J.; Findlater, M.; Cowley, A. H.; *Dalton Trans.* **2005**, 3229;

(48). (a) Hill, N. J.; Moore, J. A.; Findlater, M.; Cowley, A. H. *Chem. Commun.* **2005**, 5462; (b) Findlater, M.; Hill, N. J.; Cowley, A. H. *Polyhedron* **2006**, *25*, 983.

(49). Stender, M.; Wright, R. J.; Eichler, B. E.; Prust, J.; Olmstead, M. M.; Roesky, H. W.; Power, P. P. *J. Chem. Soc., Dalton Trans.* **2001**, *23*, 3465

(50). Kaufmann, D. *Chem. Ber.* **1987**, *120*, 901

(51). Tanaka, S.; Takashina, M.; Tokimoto, H.; Fujimoto, Y.; Tanaka, K.; Fukase, K. *Synlett* **2005** , *15*, 2325

(52). Borovik, A. S.; Bott, S. G.; Barron, A. R. *Organometallics* **1999**, *18*, 2668

(53). Sheldrick, G. M. SHELL-PC Version 5;03, Siemens Analytical X-ray Instruments, Inc., Madison, WI, USA, 1994

VITA

Zheng Lu was born in Zhenze, Wujiang, Jiangsu Province, P.R. China on February 10, 1973, the son of Shixing Lu and Xianming Zheng. After completing his work at Zhenze High School, Jiangsu Province, P. R. China, in 1990, he entered Beijing Institute of Technology in Beijing, China. He received the degree of Bachelor of Engineering from Beijing Institute of Technology in June 1994. During the following five years, he was employed as a research and teaching assistant at the same university. In July 1999, he entered The National University of Singapore, Singapore and received his degree of Master of Science from there in October 2001. In January 2002, he entered the Graduate School of The University of Texas at Austin.

Permanent Address: Sanguantangnong 8-1,
Zhenze, Wujiang, Jiangsu, P. R. China, 215231

The dissertation was typed by the author.